AVANCES EN LAS PROPIEDADES DE BIOCATALIZADORES: DISEÑO Y OBTENCIÓN DE MATERIALES MESOPOROSOS ORDENADOS COMO SOPORTES PARA LA INMOVILIZACIÓN NO COVALENTE DE ENZIMAS

MEMORIA

para optar al grado de Doctora en *Química: Ciencia Interdisciplinar* por la Universidad Autónoma de Madrid presentada por:

VICTORIA GASCÓN PÉREZ

Directores:

Dra. Rosa María Blanco Martín y Dr. Carlos Márquez-Álvarez

Instituto de Catálisis y Petroleoquímica (ICP),

Consejo Superior de Investigaciones Científicas

Tutor:

Dr. Felix Pariente Alonso

Departamento de Química Analítica, Facultad de Ciencias

Universidad Autónoma de Madrid

MADRID, 2014

El presente trabajo de investigación titulado "**Avances en las propiedades de biocatalizadores: Diseño y obtención de Materiales Mesoporosos Ordenados como soportes para la inmovilización no covalente de enzimas**" constituye la Memoria que presenta Dña. Victoria Gascón Pérez para optar al grado de doctora en Química: Ciencia Interdisciplinar por la Facultad de Ciencias de la Universidad Autónoma de Madrid. Ha sido realizado en los Laboratorios del Grupo de Tamices Moleculares del Instituto de Catálisis y Petroleoquímica (ICP-CSIC.) bajo la dirección del Dr. Carlos Márquez Álvarez y la Dra. Rosa María Blanco Martín.

Y para que así conste, firmamos el presente certificado en Cantoblanco, a 5 de Septiembre de 2014.

Fdo: Dr. Carlos Márquez Álvarez

Fdo: Dra. Rosa María Blanco Martín

AGRADECIMIENTOS

En primer lugar, agradecer al Ministerio de Economía y Competitividad (MINECO) por concederme una ayuda predoctoral de formación de personal investigador (FPI-BES-2010-040839), que me ha permitido costearme mis gastos durante el curso académico del Máster en Química Aplicada, y el primer año de tesis doctoral. También al Ministerio de Educación (MECD) por la concesión de una ayuda predoctoral de formación personal universitario (FPU-AP-2010-2145) con la que he podido dedicarme a la investigación los dos años restantes, aunque debo criticar que sin darme la posibilidad de hacer una estancia predoctoral en el extranjero.

También agradecer a mis directores, Rosa y Carlos, por todo lo que me enseñan, por sus valiosos comentarios, consejos, por su constante ayuda, disponibilidad y paciencia cada vez que surgen problemas en el laboratorio o fuera de él. Por supuesto agradecer a Isabel, que desde la lejanía siempre ha estado pendiente de los avances conseguidos. Espero seguir trabajando a vuestro lado.

Cómo no, agradecer a todos los integrantes del grupo de Tamices Moleculares, en especial a Joaquín Pérez Pariente por darme la oportunidad de trabajar en su grupo de investigación; a Enrique Sastre por estar siempre pendiente de las gestiones del grupo; a Manuel Sánchez por tener siempre la puerta de su despacho abierta para hablar de investigación o de MOF (otro gran campo de investigación por descubrir y en el que aún sólo hemos dado pequeñas pinceladas con las enzimas); a Marisol, a Luis, y a "las chicas": Isa, Teresa, Almudena, Ana, Irene, Bea, Claudia, Pilar,... Igualmente quiero dar las gracias a Vicente Cortés que siempre está dispuesto a ayudar, y a pasar un rato para charlar de ciencia, noticias, o de la vida misma; y a Álvaro Mayoral por el manejo tan maravilloso de los microscopios. También a todos los compañeros/as que han pasado por el laboratorio 107 (Óscar, Elsa,…). Y en especial a mi amigo Manuel "*El Mexicano*", porque no hay día que no hablemos de México o de comida rica, y a Nacho, el historiador del grupo, y mi compañero de adicción al té. Así como a todo el personal de apoyo a la investigación (Javi, Conchi, Rosa, Mercedes,…), de mantenimiento (Eduardo, Jose, Armando,…), a Paloma de almacén, a Adrián y Jesús de informática, así como a todo el personal de secretaría (Rosa, Nuria,…), de limpieza (Pili, Mari Angeles,…).

También tengo que darle las gracias a las amigas que he hecho en el instituto, sobre todo a Cris por ser tan sutil y delicada (cuanto voy a echar de menos nuestras profundas conversaciones sobre gatos), a Idoia "mi súper-bióloga" por el buen equipo que hicimos durante los 6 meses que estuviste haciendo tu proyecto, a Andreina y a su "beba" Carolina (esta niña va a acabar siendo científica seguro, sólo con oírnos durante los 9 meses de embarazo…), y a Marina por su positivismo y alegría. Claramente, sin vosotras este trabajo habría sido mucho más duro, por no decir imposible.

I would like to pass my gratitude also to my friends in Ethiopia who have been here in our institute for visiting and scientific discussion. Specially, Negash by naming his new daughter "Victoriya", and for his reinforcement in the scientific

work and social life. Also Solomon, Mamo, Alemnew, Mark, Kiros, Taju and Lijalem for their cooperation during their stay here in Spain and impressed me to visit Ethiopia: "Bekirbu Ethiopiayanina inanten indemigobegn tesfa adergalew".

En esta tesis no me puedo olvidar de mis antiguos directores de la Universidad Rey Juan Carlos, Jesús Mª Arsuaga y Amaya Arencibia, gracias a vosotros entré en este apasionante y arduo mundo de la investigación, y vosotros habéis sentado las bases de lo que soy ahora, *investigadora*, y a lo que deseo dedicarme el resto de mi vida.

Y a mis amigos/as de siempre que aunque nos veamos poco siempre estáis ahí. En especial a Laura Torres y a Natalia por preocuparse por mí y escucharme (qué sepáis que sois las protagonistas de mi novela literaria, sí o sí). A mi querido Victor por sus conversaciones políticas (en menudos líos que me metes siempre); a Darío que un día me enseño que "*La vida no es estabilidad; es saber andar en equilibrio*"; a Manolo por coincidir conmigo en tantas cosas, y sobre todo por introducirme en el mundo de los "deportes de alto riesgo": si ahora toca parapente motorizado, ¿qué será lo siguiente?; a Miguel por su arsenal de proteínas y vitaminas, y sus conversaciones sobre la eterna juventud (¿en serio que no duermes en formol?); a mis amigas de Toledo: Ruth (y a su familia) y Celia; a mi "*teacher*" de equitación Curro Bedoya (aunque nunca paso de la doma vaquera…); y a mis queridos vecinos de Alcorcón, Laura y Dani por cuidarme tanto.

Ante todo agradecer a mis padres, su inestimable ayuda, por apoyar mis decisiones, enseñarme a no rendirme cuando las cosas se ponen difíciles, a levantar la cabeza, coger aire y seguir adelante. Además, gracias a mi hermano Jorge, súper doctor en Informática Gráfica, Juegos y Realidad Virtual, mi ejemplo a seguir, aunque últimamente es al contrario (aún nos queda pendiente bucear en aguas tropicales…, no se me ha olvidado!). Y al resto de mi familia, en especial a mi tía Mila y a mi tío Paco, por tener siempre la puerta de su casa abierta; a mi tía favorita, Carmen, por sus sabios consejos. También a las que ya han dejado este mundo, a mi tía Ele, y a mi tía Rosi, una parte de vosotras siempre permanecerá en mi corazón.

Pero, sobre todo, tengo que darle las gracias a Fran, gracias por ser, por estar y por existir, desde hoy entiendo que si cruzaste o estas en mi vida es porque eres parte de mí. Todo este trabajo y esfuerzo te lo dedico a ti.

Agradezco todo lo que he recibido y todo lo que aún está por venir.

Victoria

A Fran

"Nunca te rindas, a veces la última llave es la que abre la puerta"

Anónimo

Bajo el cielo, cuando algo se concibe como bello,
aparece lo feo.
Cuando todos reconocen algo como bueno,
surge lo malo.

Por lo tanto, ser y no-ser se engendran uno al otro,
Tener y no tener se originan juntos,
Difícil y fácil se producen mutuamente,
Largo y corto se contrastan uno al otro,
Alto y bajo se apoyan uno al otro,
Palabra y sentido se armonizan uno al otro,
Adelante y atrás se siguen uno al otro.
Esta es la ley de la naturaleza.

Por eso el sabio va de un lado al otro
sin hacer nada, enseñando sin hablar.
Las Diez Mil Cosas se elevan y caen sin cesar.
Pero él crea, sin buscar posesión;
Trabaja, sin esperar reconocimiento;
Hecho el trabajo, pronto lo olvida.
Porque no lo reclama,
Su mérito perdura para siempre.

Lao-Tse (Tao Te Ching)

INDICE

ÍNDICE DE CONTENIDOS

RESUMEN

RESUMEN

En este trabajo se han diseñado novedosos materiales de naturaleza silícea de tipo MMO (Materiales Mesoporosos Ordenados) con distintas características como soportes de: lacasa de *Myceliophthora thermophila*, una oxidoreductasa multicobre que cataliza la oxidación de diferentes compuestos fenólicos, aminas y ligninas, de lipasa de *Candida antarctica* B encargada de la hidrólisis de triglicéridos a ácidos grasos libres y glicerol, y de β-glucosidasa de *Aspergillus niger*, enzima encargada de realizar la hidrólisis del enlace o-glicosil de los hidratos de carbono, liberando moléculas de glucosa.

En la primera parte de la tesis doctoral se han sintetizado materiales silíceos mesoporosos ordenados avanzados para optimizar la inmovilización post-síntesis y estabilización de lacasa. Estos materiales poseen una elevada superficie específica y estrecha distribución de tamaño de poro, que resultan de un sistema ordenado de mesoporos de simetría definida. El tamaño de poro se ha adaptado a las dimensiones moleculares de la enzima lacasa adecuando las condiciones de síntesis y mediante la adición de moléculas orgánicas que actúan de expansores de las micelas de surfactante que actúan de plantilla de la estructura porosa. Para la inmovilización de lacasa, la superficie de estos materiales se ha modificado incorporando cadenas orgánicas que contienen grupos funcionales de tipo amino, capaces de interaccionar electrostáticamente con la enzima en unas condiciones de pH adecuadas. Esta funcionalización orgánica se ha realizado tanto por anclaje (posterior a la síntesis de la estructura de sílice) como por cocondensación (incorporación directa durante la síntesis). Además, se han sintetizado novedosas organosílices periódicas mesoporosas que incorporan dentro de la propia pared del soporte tanto el grupo etileno para la inmovilización de lipasa, como grupos amino para la inmovilización de lacasa, y con un diámetro de poro suficientemente grande para inmovilizar las enzimas. Se han obtenido biocatalizadores heterogéneos con altas cargas enzimáticas y elevada actividad catalítica. Además, mediante estudios avanzados de microscopía electrónica de transmisión (STEM-HAADF) se ha conseguido localizar por primera vez, mediante método directos a las enzimas en el interior de los poros del material. La inmovilización mejora la estabilidad de las enzimas lacasa y lipasa en presencia de etanol y metanol,

respectivamente y a alta temperatura. A pesar de su carácter no covalente, la fuerte interacción de la enzima con los grupos activos del soporte junto con un tamaño de poro ajustado a las dimensiones moleculares de la enzima, impide la lixiviación de la misma en medio acuoso.

En la segunda parte de la tesis, se ha desarrollado una estrategia para inmovilizar la enzima en el interior del material mesoporoso durante la propia etapa de síntesis (inmovilización in-situ). Esto permite encapsular la enzima lacasa en sistemas caja-ventana, evitando cambios estructurales de las enzimas y protegiéndola del medio externo. Esta estrategia se ha aplicado también para encapsular in-situ β-glucosidasa; debido a sus grandes dimensiones moleculares (~12.3 nm x ~10.7 nm x ~ 8.1 nm) las cargas enzimáticas que se consiguen mediante inmovilización post-síntesis son bajas y limitadas. En cambio, mediante la encapsulación in-situ de la enzima en el interior de la estructura mesoporosa del soporte inorgánico se consiguen mayores cargas, y se evita la pérdida de actividad enzimática, y el lixiviado de la misma.

Para la encapsulación in-situ de enzimas dentro de materiales silíceos mesoporosos se ha requerido un profundo estudio del uso de diferentes surfactantes, aditivos y condiciones de síntesis para obtener la encapsulación de las enzimas lacasa y β-glucosidasa. La adecuada selección de los surfactantes y aditivos ha sido un factor clave para obtener micelas diferentes alrededor de las moléculas de enzimas que actúan como plantillas del sistema, y que permiten obtener materiales silíceos estructurados que contienen moléculas de enzima en su interior.

Todos los biocatalizadores obtenidos presentan alta estabilidad en medio orgánico, y en particular los de lacasa se han utilizado en estudios de reacción de oxidación de un compuesto fenólico, ácido cafeico, presente en vinos. Se ha obtenido una oxidación suave y controlada que permite el mantenimiento de una alta capacidad antioxidante en la mezcla de reacción. En muestras de vino, estas características podrían permitir la reducción de la adición de sulfitos como reductores en el proceso de maduración del vino.

ESTRUCTURA GENERAL

ESTRUCTURA GENERAL

La presente Tesis Doctoral consta de los siguientes apartados

1. **Introducción**
2. **Objetivos**
3. **Publicaciones**. Recoge los trabajos de investigación que han dado lugar a esta Memoria de Tesis y se ordenan en cinco capítulos. El contenido de estos artículos se ha mantenido en el idioma en que fueron publicados y constan de: Resumen, Materiales y Métodos, Resultados, Discusión, Conclusiones, Material Suplementario y Referencias Bibliográficas.

Capítulo 1: **V. Gascón**, I. Díaz, C. Márquez-Alvarez, R.M. Blanco, "Mesoporous silica with tunable morphology for the immobilization of lacase", *Molecules*, 19 (**2014**) 7057-7071.

Capítulo 2: **V. Gascón**, C. Márquez-Álvarez, R.M. Blanco, "Efficient retention of laccase by non-covalent immobilization on amino-functionalized ordered mesoporous silica", *Appl. Catal. A-Gen.*, 482 (**2014**) 116-126.

Capítulo 3: **V. Gascón**, I. Díaz, R.M. Blanco, C. Márquez-Alvarez, "Hybrid periodic mesoporous organosilica designed to improve properties of immobilized enzymes", *RCS Adv.*, 4 (**2014**) 34356-34368.

Capítulo 4: A. Mayoral, R. Arenal, **V. Gascon**, C. Marquez-Alvarez, R.M. Blanco, I. Diaz, "Designing Functionalized Mesoporous Materials for Enzyme Immobilization: Locating Enzymes by Using Advanced TEM Techniques", *ChemCatChem*, 5 (**2013**) 903-909.

Capítulo 5: A. Mayoral, **V. Gascón**, R.M. Blanco, C. Márquez-Alvarez, I. Díaz, "Location of laccase in ordered mesoporous materials", *APL Materials*, (**2014**). Accepted.

Los siguientes capítulos aún no han sido enviados para su publicación, por lo que no se incluyen en la presente memoria:

[6] **V. Gascón**, C. Márquez-Álvarez, R.M. Blanco, "In-Situ encapsulation of laccase and β-glucosidase in mesoporous silicas", *Paper under preparation*, (**2014**).

[7] **V. Gascón**, I. Martín de Lucía, C. Márquez-Alvarez, R.M. Blanco, "Optimization of enzyme immobilization in ordered mesoporous materials as an approach to polyphenols oxidation processes", *Paper under preparation*, (**2014**).

4. **Resumen de resultados**, que muestra un hilo conductor entre todos los trabajos presentados.
5. **Conclusiones** globales de la tesis.

INTRODUCCION

1. INTRODUCCIÓN

1.1. AVANCES EN LA INMOVILIZACIÓN DE ENZIMAS EN MATERIALES MESOPOROSOS ORDENADOS

Uno de los campos más apasionantes de la de la ciencia y de la tecnología actuales es la de aprovechar las posibilidades del mundo de lo más pequeño (átomos y moléculas), para crear y construir nuevos dispositivos o instrumentos con potenciales y novedosas aplicaciones, tal es el caso de la **nanociencia,** que permite obtener materiales en la nanoescala. Si además, unimos otro campo de investigación altamente novedoso como es la **biotecnología** que emplea moléculas biológicas como las enzimas, tendremos en nuestras manos dos líneas de investigación altamente innovadoras, que con sólidos conocimientos de cada una de las materias por separado podrán converger en una única línea de investigación siendo esta última una potentísima herramienta integrando las ventajas de cada una de ellas (Figura 1).

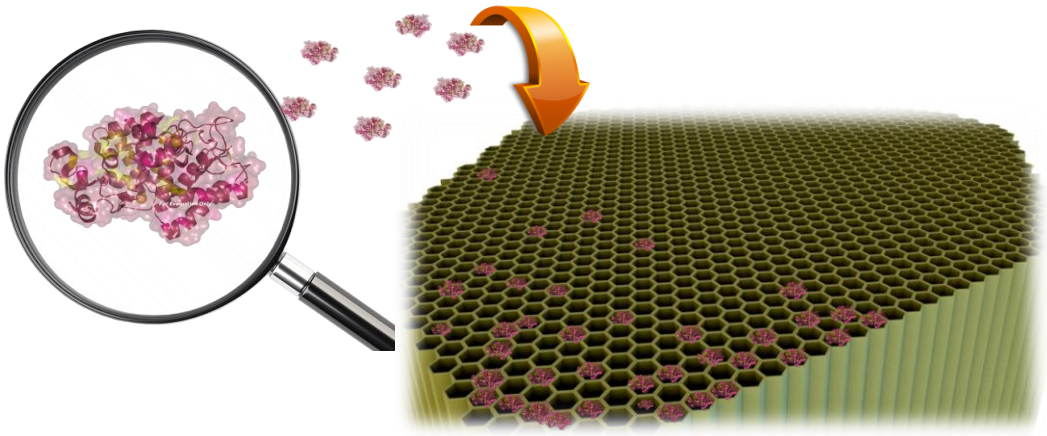

Figura 1. Esquema de inmovilización de la enzima lacasa en un nanomaterial mediante la estrategia postsíntesis.

El continuo desarrollo de la **biotecnología** y sus numerosas aplicaciones ofrecen soluciones en diversos campos en los que se demanda una química verde y sostenible, tales como: obtención de productos farmacéuticos, síntesis de química fina, desarrollo de biosensores, análisis proteómicos y celdas de biocombustible, entre otros. La mayoría de los procesos biotecnológicos son realizados por la presencia de enzimas. En comparación con los catalizadores químicos tradicionales, en general, el uso de enzimas es más respetuoso con el medioambiente y más económico debido al bajo coste energético que se

requiere, a la alta eficacia, alta quimio-, regio-, y estéreo-selectividad y a rutas sintéticas más cortas [1]. Sin embargo, en muchos casos la aplicación industrial de las enzimas de forma libre se ve obstaculizada por su baja estabilidad operacional, y por las dificultades para su recuperación y reutilización [2].

Los avances actuales en biotecnología han promovido el uso de enzimas inmovilizadas para una amplia variedad de aplicaciones [3-5]. La inmovilización de enzimas en materiales sólidos proporciona un método para superar estos inconvenientes, es decir, mejora la estabilidad de las enzimas, la facilidad de separación y la capacidad de utilizar la enzima en disoluciones en las que la enzima permanece insoluble, también mediante un adecuado diseño puede permitir su uso en reactores que operan de forma discontinua o continua.

Por otra parte, la inmovilización sobre soportes sólidos permite el uso de enzimas en diferentes procesos en cascada evitando interacciones negativas entre enzimas distintas y catalizadores químicos. Aunque la inmovilización de enzimas también tiene desventajas que incluyen la pérdida de actividad, y los costes adicionales asociados con el proceso de inmovilización.

Hasta ahora, los soportes más empleados para preparar biocatalizadores a escala industrial han sido; el gel de sílice, materiales de vidrio de poro controlado, polímeros impresos, y perlas de polímero [2, 6, 7].

Estudios previos sobre inmovilización de enzimas en diferentes soportes muestran que el confinamiento de la enzima en un espacio adecuado puede aumentar su estabilidad y reducir la desnaturalización por desplegamiento de la proteína [3]. Por lo tanto, con el fin de aumentar la eficacia de las enzimas inmovilizadas, es altamente conveniente desarrollar nuevos materiales que posean elevadas áreas superficiales, alta porosidad, un tamaño de poro uniforme y diseñado a medida, y estructuras de poro ordenadas para favorecer un microambiente adecuado a la enzima [8, 9].

De acuerdo con la definición de la IUPAC, los materiales porosos se pueden dividir en tres clases: **microporosos** (tamaño de poro inferior a 2 nm), **mesoporosos** (entre 2 y 50 nm) y **macroporosos** (superior a 50 nm). Durante los últimos años se ha producido la expansión del campo de los materiales mesoporosos debido al elevado interés tecnológico que despiertan sus potenciales aplicaciones como soportes de fases activas, catalizadores heterogéneos o adsorbentes [10]. Los materiales mesoporosos son excelentes candidatos

para la inmovilización de enzimas cuando el tamaño de los mesoporos coincide con el tamaño de la enzima [9].

De hecho, el desarrollo de materiales mesoporosos se inició hace poco más de dos décadas con el deseo de desarrollar aplicaciones relacionadas con el tratamiento de moléculas de gran volumen, para superar la limitación por el relativamente reducido tamaño de poro de las zeolitas y materiales microporosos relacionados [11].

Sin embargo, durante mucho tiempo, no existía un método eficiente para controlar el tamaño y la disposición ordenada de mesoporos. Los primeros materiales mesoporosos se sintetizaron mediante el método sol-gel que permitía obtener materiales con grandes áreas superficiales (~ 900 m^2/g) y tamaño de poro mesoporoso (entre 2 y 4 nm), pero con distribuciones de tamaño de poro muy amplias. A estos materiales se los denominó **FSM** (*Folded Sheet Mesoporous Materials*) [12].

En 1992, investigadores de la *Mobil Research and Development Corporation* publicaron la síntesis de un grupo de materiales mesoestructurados silíceos sintetizados con surfactantes (agregados de moléculas anfifílicas que actúan como agentes directores de la estructura). Estos materiales con una matriz regular uniforme constituyen la familia M41S [13, 14]. Se caracterizan por poseer distribuciones de tamaño de poro estrechas, entre 1,5 nm y 4 nm, y elevadas superficies específicas. Los principales grupos de esta familia son el MCM-48, el MCM-41, y el MCM-50.

Desde entonces, se han realizado numerosas síntesis de materiales mesoporosos, óxidos simples o mixtos cuya característica común es el empleo de surfactantes como agentes directores de la estructura porosa [15-18]. De este modo, se han obtenido con éxito estructuras bidimensionales y tridimensionales, es decir, formadas por canales unidireccionales o bien por sistemas de cavidades interconectadas, dando lugar a numerosos materiales mesoporosos diferentes. A diferencia de las zeolitas, los materiales mesoporosos no presentan cristalinidad en las paredes de su estructura, sino que sus paredes están formadas por sílice amorfa que presentan numerosos defectos estructurales, debido a una condensación silanol-siloxano incompleta tras la hidrólisis, lo que provoca la presencia de grupos silanol (Si–OH) terminales que pueden servir para funcionalizar su superficie con grupos orgánicos. No obstante, estos sólidos sí presentan cierto ordenamiento mesoscópico debido al ordenamiento de sus poros.

En la Tabla 1 se recogen algunos de los principales materiales mesoporosos silíceos con estructuras con ordenamiento mesoscópico [17, 19-23].

Tabla 1. Características de diferentes estructuras mesoporosas.

Material	Estructura	Mecanismo*	Tipo de poro
FSM-16	hexagonal plana	a partir de kanemita	canales
MCM-41	hexagonal plana	S^+I^-	canales
MCM-48	cúbica bicontinua	S^+I^-	canales
MCM-50	laminar	S^+I^-	bicapa
HMS	hexagonal desordenada	S^0I^0	canales
MSU	hexagonal desordenada	N^0I^0	canales
KIT-1	3D desordenada	S^+I^-	canales
SBA-1	cúbica	$S^+X^-I^+$	2 cavidades
SBA-2	hexagonal 3D	S^+I^- geminal	cavidades/canales
SBA-3	hexagonal plana	$S^+X^-I^+$	canales
SBA-6	hexagonal 3D	S^+I^-	2 cavidades
SBA-8	rómbica	S^+I^- geminal	?
SBA-11	cúbica	$N^0H^+X^-I^+$	?
SBA-12	hexagonal 3D	$N^0H^+X^-I^+$	cavidades/canales
SBA-14	cúbica	$N^0H^+X^-I^+$	?
SBA-15	hexagonal plana	$N^0H^+X^-I^+$	canales
SBA-16	cúbica 3D	$N^0H^+X^-I^+$	cavidades/canales
FDU-1	cúbica 3D	$N^0H^+X^-I^+$	cavidades/canales
FDU-2	cúbica 3D	$N^0H^+X^-I^+$	cavidades/canales
FDU-12	cúbica 3D	$N^0H^+X^-I^+$	cavidades/canales
FDU-5	cúbica bicontinua	$N^0H^+X^-I^+$	cavidades/canales
AMS	varias	S^-I^+	varias cavidades

* Mecanismos de formación: *iónicos* (S^+I^-; S^-I^+; $S^+X^-I^+$; $S^-X^+I^-$), *neutros* (S^0I^0; N^0I^0; SI), *electrostático débil* ($N^0H^+X^-I^+$).

En una primera etapa, los trabajos se centraron principalmente en el desarrollo de adsorbentes de cationes metálicos o moléculas orgánicas, y catalizadores heterogéneos basados en estos materiales [24].

Hasta 1996 no se intentó por primera vez la inmovilización de enzimas en materiales mesoporosos silíceos ordenados (MMSO). El primer trabajo publicado por Díaz & Balkus

trataba sobre la inmovilización de enzimas globulares pequeñas, como las proteasas tripsina y papaína, así como la proteína citocromo c que contiene el grupo hemo c, en MCM-41 con un diámetro de poro de 4 nm [25]. Este grupo también probó a inmovilizar peroxidasa pero el diámetro molecular esférico de esta enzima es de 4,6 nm y no se inmovilizaba de forma significativa en los mesoporos de la MCM-41 (sólo 0,4 mg/g_{MCM-41}). Hasta que no se desarrollaron materiales silíceos mesoporosos con mayores diámetros de poro (como la SBA-15 y las espumas mesocelulares silíceas (MCFs, *mesostructured cellular foams*) no se pudieron inmovilizar enzimas de mayor tamaño en este tipo de materiales.

Desde entonces, la evolución de la inmovilización de enzimas sobre MMSO ha ido en paralelo a los avances en la síntesis de nuevos materiales mesoporosos ordenados, aunque con un retardo en el tiempo de unos cuatro años [9]. Este desarrollo ha sido promovido en parte por la introducción de nuevas técnicas de inmovilización, por la demanda de nuevas aplicaciones y sistemas enzimáticos complejos, y por el descubrimiento de técnicas de caracterización avanzadas.

1.2. ESTRATEGIAS PARA LA INMOVILIZACIÓN DE ENZIMAS SOBRE MATERIALES MESOPOROSOS ORDENADOS

Los soportes mesoporosos poseen gran área superficial, siendo este un requisito importante para la adsorción de enzimas. También se pueden diseñar poros con un tamaño y una disposición estructural adecuada, lo que limita las restricciones difusionales de la enzima. Además, se deben considerar las interacciones que se establecen entre la enzima y el soporte; de esta manera la superficie de las enzimas puede ser polar o apolar, dependiendo de las propiedades de sus grupos superficiales, y la superficie de los MMOs se puede funcionalizar con grupos que potencien las interacciones y la afinidad hacia la enzima. Por lo tanto, existe la posibilidad de diseñar las propiedades superficiales de los MMO para que sean afines a la enzima específica que se quiera inmovilizar [26].

Los materiales mesoporosos ordenados se pueden preparar con diferentes composiciones químicas que incluyen sílices, organosílices [27], óxidos metálicos (óxidos de aluminio, titanio, hierro y circonio) [28-30], sulfuros metálicos, como por

ejemplo de germanio [31], metales, carbones [32], y polímeros [2, 33], los cuales se pueden diseñar con las propiedades superficiales específicas que se requieran [34].

Además de seleccionar un soporte que cumpla todos los requisitos necesarios para la enzima objetivo, se debe emplear la técnica de inmovilización más adecuada. Los métodos de inmovilización utilizados con mayor frecuencia para la incorporación de enzimas en materiales mesoporosos son [6, 8, 35, 36]: **1**) Adsorción física, a través de fuerzas de van der Waals, interacciones hidrofóbicas, enlace de hidrógeno e interacciones iónicas; **2**) unión covalente; **3**) la reticulación o entrecruzamiento (*cross-linking*) de las enzimas en el poro del soporte; y **4**) la encapsulación.

En general, cada una de estas técnicas tiene sus propias ventajas y desventajas que se enumeran en la Tabla 2, no existiendo por tanto, un método genérico para la inmovilización de enzimas en materiales mesoporosos [5, 35]. Se debe elegir cuidadosamente el método y las condiciones que se requieren para la adecuada inmovilización con el fin de preservar la actividad intrínseca y la selectividad de las enzimas, y evitar la desnaturalización e inactivación de las mismas. Un protocolo de inmovilización eficaz sólo puede ser desarrollado a partir de una serie de experimentos dirigidos a establecer un equilibrio entre actividad, selectividad, estabilidad y coste. Además, el proceso de inmovilización utilizado para cada enzima es único y depende de cada enzima específica y del soporte empleado [11, 37]. La unión a soportes mediante adsorción o enlace químico no covalente, y la encapsulación física son las estrategias de inmovilización empleadas en la presente Tesis Doctoral.

Tabla 2. Métodos aplicados para la inmovilización de enzimas en MMO.

Métodos	Interacción	Propiedades	Parámetros a considerar
Adsorción física	Fuerzas de Van der Waals, interacción hidrofóbica, enlace de hidrógeno, interacción iónica	Simple, interacción débil	Hidrofobicidad o hidrofilidad, punto isoelectrico, cargas superficiales
Unión covalente	Unión química	Unión fuerte	Grupos funcionales superficiales, desactivación irreversible, cambios

			conformacionales
Entrecruzamiento	Unión química entre la enzimas; agregación de las enzimas dentro de los poros	Unión fuerte, agregados grandes	Estructura del soporte, limitaciones difusionales
Encapsulación	Retención física	Unión física	Condiciones de síntesis, presencia de aditivos, temperatura, pH, empleo de surfactantes

1.3. MATERIALES MESOPOROSOS ORDENADOS

1.3.1. Materiales mesoporosos silíceos

Los materiales mesoporosos silíceos ordenados (MMSO) son los materiales más estudiados y utilizados de entre los materiales mesoporosos debido a sus aplicaciones diversas. Los precursores silíceos son baratos, y debido a la flexibilidad del ángulo de enlace Si-O-Si permite sintetizarlos de forma más sencilla y controlada en comparación con otros óxidos metálicos como TiO_2 o Al_2O_3, además los materiales silíceos presentan una alta estabilidad química y mecánica debido a que las paredes de sílice son robustas.

Desde su descubrimiento se han desarrollado numerosos materiales distintos con diferentes aplicaciones. La síntesis de los MMSO se produce mediante el autoensamblaje cooperativo de las especies de sílice y los agentes directores de estructura como los surfactantes anfifílicos y biomacromoléculas), de esta manera se forma la estructura ordenada del material con una simetría definida, y mediante la posterior eliminación del agente director se consigue el soporte con los poros vacíos [38-40]. Basados en esta estrategia de síntesis, se han obtenido una gran variedad de mesoestructuras en dos dimensiones (hexagonal, *p*6*mm*) y en tres dimensiones (hexagonal, cúbica, cúbica bicontinua, etc.) con diferentes tamaños de poro entre 2 y 50 nm.

Debido a las grandes dimensiones de las biomoléculas, de todos los posibles MMSO sólo unos pocos han sido utilizados hasta la actualidad como soportes de proteínas o enzimas. Los materiales preferentemente empleados para la inmovilización de enzimas son FSM-16, MCM-41, SBA-15 y MCF, principalmente debido a que los protocolos de

síntesis son más simples y reproducibles. Otros MMSO que también se han empleado son MCM-48, FSM-7, HMS, SBA-16, KIT-6, FDU-5, FDU-12, HMMS y MSU [9, 41]. Una comparación entre las dimensiones de las enzimas inmovilizadas y el tamaño de poro de los MMSO se muestra en la Figura 2 tomada del trabajo [9].

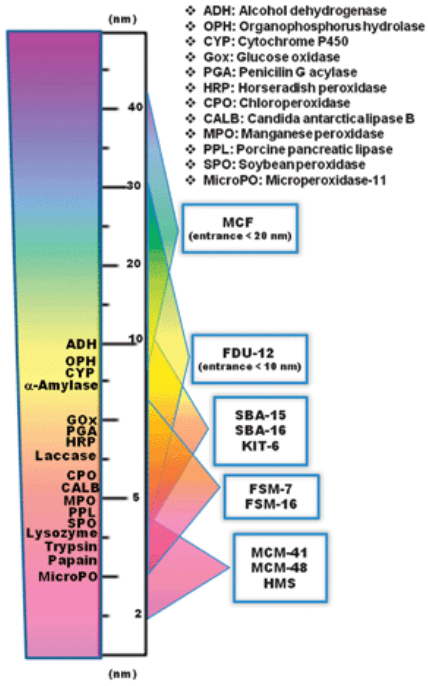

Figura 2. Comparación entre el tamaño de poro de diferentes materiales silíceos mesoporosos y el tamaño de enzima inmovilizadas.

A continuación se comentará brevemente las características más importantes de algunos de los materiales empleados como soportes de enzimas:

FSM-16 y **FSM-7** pertenecen a la familia de materiales **FSM** (*Folded Sheet Materials*) que fueron desarrollados por Kuroda y colaboradores en 1990 [12] a partir de un precursor de polisilicato laminado denominado kanemita, en presencia de surfactantes catiónicos (como el catión hexadecil-trimetilamonio). En 1993, Inagaki y col. [42] propusieron un mecanismo de formación de este material mesoporoso ordenado en dos etapas. En la primera etapa, los iones de sodio de las intercapas de kanemita son intercambiados por cationes del alquiltrimetilamonio, en la segunda etapa, las capas de kanemita se pliegan y se entrecruzan formando una estructura inorgánica [42]. El diámetro de poro de estos materiales se puede ajustar entre 2 y 4 nm mediante la variación de la longitud de cadena del alquilo del surfactante.

En 1992, científicos de *Mobil Oil Research and Development Corporation* sintetizaron de forma satisfactoria materiales mesoestructurados silíceos. Estos materiales, a los que se denominó familia **M41S**, se caracterizan por poseer un sistema poroso ordenado con una estrecha distribución de diámetros, acompañados de una elevada área superficial (> 700 m^2/g) y volumen de poro [13, 14, 17]. En la estrategia de síntesis se emplearon agregados moleculares o surfactantes iónicos también de tipo alquiltrimetilamonio que actúan como moldes o agentes directores de la estructura para formar los canales porosos que caracterizan a estos materiales. Las tres mesoestructuras más importantes de la familia M41S son la **MCM-41**, con una estructura porosa hexagonal *p*6*mm* formada por poros unidireccionales no conectados entre sí (Figura 3), el **MCM-48**, que tiene una estructura porosa cúbica tridimensional *Ia*3*d* formada por dos sistemas de canales tridimensionales (Figura 3), y el **MCM-50**, con estructura laminar *p*2. La estructura del sistema de poros hexagonal del material MCM-41 hace que sea el más destacado de la familia M41S debido a su mayor estabilidad y tamaño de poro (~ 4 nm) que hace que sea muy atractivo para aplicaciones como soportes de catalizadores, adsorbentes, detectores, etc. [17].

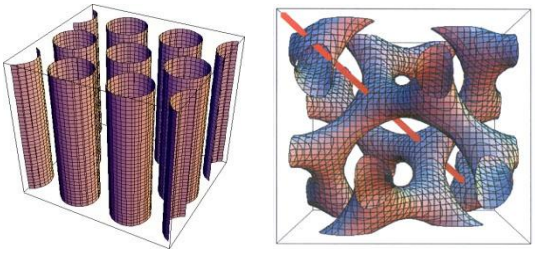

p6mm **MCM-41** ***Ia3d*** **MCM-48**

Figura 3. Representación esquemática de los materiales MCM-41 y MCM-48 correspondiente a la familia M41S [21, 43].

En lugar de los surfactantes iónicos, en 1995, Tanev y Pinnavaia [44] utilizaron aminas primarias como plantillas (principalmente docecilamina) y precursores inorgánicos neutros para preparar la síntesis del soporte mesoporoso **HMS** (*Hexagonal Mesoporous Silica*) que presenta una estructura hexagonal desordenada conocida como "agujeros de gusano", con canales mesoporosos pequeños de un tamaño de unos 2 nm. Ese mismo año, Bagshaw y col. publicaron la síntesis de **MSU-1** también con estructura hexagonal desordenada [45].

Desde entonces se ha realizado una intensa investigación en la síntesis de MMSO con mayores diámetros de poro en todo el mundo.

Dentro del campo de la sílice mesoestructurada, uno de los materiales más destacados ha sido el **SBA-15** (*Santa Barbara Amorphous*-15) desarrollado en 1998 por el grupo de Zhao y colaboradores [46, 47]. Este material presenta un sistema hexagonal de poros altamente ordenados y los **mayores tamaños de poro** encontrados en los materiales silíceos mesoestructurados. Además posee unas propiedades texturales y estructurales que son posiblemente las más deseables en este campo.

Este material se sintetiza mediante el **mecanismo electrostático débil** [44, 46, 47] utilizando como director de la estructura un **surfactante no iónico**, del tipo copolímero en bloques de polietileno y polipropileno, como por ejemplo el Pluronic P123 ($EO_{20}PO_{70}EO_{20}$). Con el empleo de este surfactante se obtiene una estructura porosa de simetría hexagonal altamente ordenada y bidimensional, *p6mm*, un tamaño de poro muy uniforme que puede alcanzar teóricamente 300 Å, y volúmenes de poro de hasta 2,5 cm^3/g. En general, se trata de materiales con paredes de óxido de silicio muy gruesas (de hasta 3 nm) lo que les confiere mayor estabilidad térmica e hidrotérmica que la MCM-41 [47]. Otra ventaja muy importante en nuestro caso se debe a que las interacciones que gobiernan la formación de estos materiales son débiles, por lo que la eliminación del surfactante mediante extracción a reflujo con etanol o calcinación es más sencilla [16], dando lugar a una estructura libre de surfactante y con gran volumen de poro, útil para la inmovilización de enzimas (Figura 4).

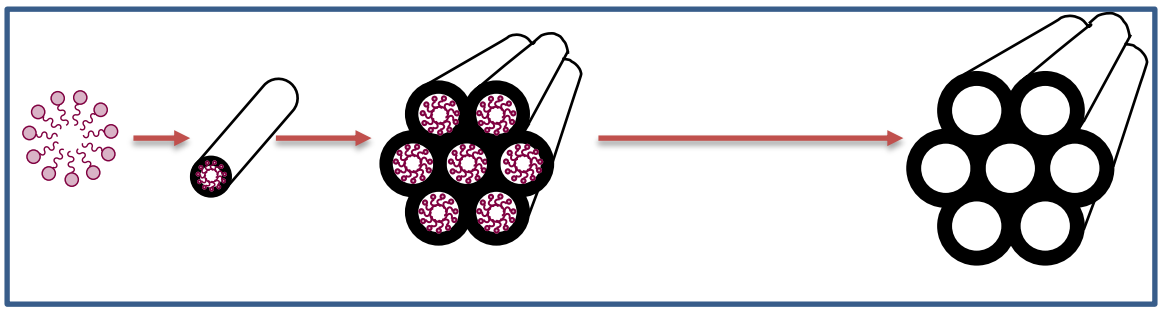

Figura 4. Proceso de síntesis de un material mesoestructurado, tipo SBA-15, con simetría de poros hexagonal.

Las posibles **fuentes de sílice** que se emplean en la preparación del material SBA-15 son tetraetilortosilicato (TEOS), tetrametilortosilicato (TMOS) o tetrapropilortosilicato (TPOS). Los canales hexagonales mesoporosos se forman en **medio ácido** (pH < 1) con

diferentes ácidos inorgánicos (HCl, HBr, HI, HNO_3, H_2SO_4 o H_3PO_4) de manera que las especies silíceas se encuentran protonadas. Las temperaturas de síntesis están comprendidas generalmente entre 35 ºC y 80 ºC [46, 47]. En la Figura 5 se esquematiza el procedimiento de síntesis y eliminación del surfactante del material SBA-15.

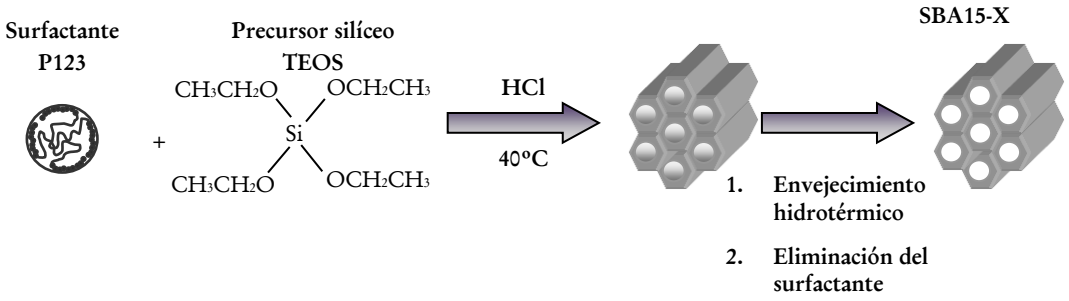

Figura 5. Esquema del mecanismo de síntesis para obtener el material silíceo de tipo SBA-15, utilizando como surfactante P123 y TEOS (tetraetilortosilicato) como fuente de sílice en medio ácido.

En la Figura 6 se representa la estructura porosa de este material. Como se observa, además de los canales de **mesoporos**, el SBA-15 presenta **microporos** que, en función de las condiciones de síntesis, pueden llegar a conectar los canales mesoporosos entre sí de forma aleatoria [20].

La presencia de estos microporos se atribuye al carácter hidrofílico de las cadenas de los bloques de poli(óxido de etileno) (PO), que penetran dentro de las paredes silíceas de la SBA-15 durante las etapas de condensación de las especias de sílice y que, al eliminar el surfactante, generan una microporosidad adicional. Como resultado de esta doble porosidad, los canales no presentan una superficie uniforme, sino más bien una superficie de textura irregular [48].

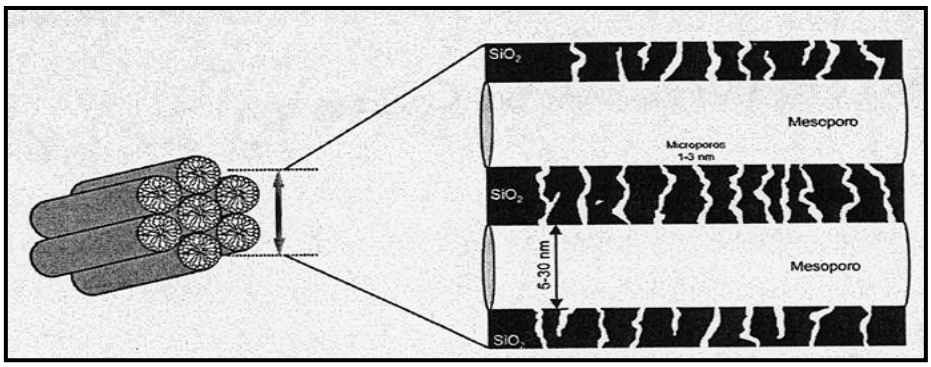

Figura 6. Esquema de canales de mesoporos y microporos que conforman el material SBA-15.

SBA-16 es una sílice mesoporosa que tiene la particularidad de presentar un sistema de poros del tipo caja y ventana dispuestas en una simetría tridimensional cúbica centrada en el cuerpo *Im*3*m* (Figura 7) [46]. Las cavidades, con un diámetro ~ 5-15 nm, están conectadas entre sí por aberturas o ventanas de menos diámetro [49]. Al igual que la SBA-15 se sintetiza en condiciones ácidas usando un surfactante no iónico de tipo Pluronic. La mesofase se puede crear utilizando mezclas de Pluronic P123 y Pluronic F127 ($EO_{106}PO_{70}EO_{106}$) o en un sistema ternario compuesto por agua, butanol y Pluronic F127. Según lo sugerido por estudios de cristalografía de rayos X [21, 38], cada uno de los mesoporos de la SBA-16 se conecta a ocho mesoporos vecinos. De este modo el tamaño de poro de una entrada o ventana de mesoporos a otra es, por lo general, significativamente menor que el tamaño de mesoporos de la caja o cavidad, siendo por tanto el tamaño de las ventanas el factor limitante para inmovilizar una enzima en el interior de las cavidades. Por ello, estos soportes se sintetizarán en presencia de la propia enzima (síntesis in-situ).

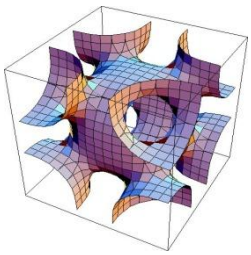

Im m

SBA-16

Figura 7. Modelización de la estructura de SBA-16 utilizando como surfactante F127 [21, 43].

1.3.2. Expansores de micelas: SBA-15

Para intentar sintetizar materiales mesoporosos con estructura hexagonal con mayores diámetros de poro y de forma controlada se han estudiado diferentes estrategias [39]: ***1***) variación de la longitud de cadena del surfactante, principalmente aumentando el tamaño de la parte hidrofóbica del copolímero de tres bloques del surfactante [13, 46, 47, 50]; ***2***) modificando la temperatura y tiempo de síntesis (de la hidrólisis, condensación y tratamiento hidrotermal) [49, 51-53]; ***3***) añadiendo cosolventes orgánicos, co-surfactantes [54] y/o agentes expansores de micela; ***4***) añadiendo sales al medio de síntesis [53, 55]; o

bien, **5**) sustituyendo o mezclando el precursor silíceo TEOS con metasilicato de sodio [56].

A continuación, se comentará cómo influye la adición de agentes expansores de micela sobre el diámetro de poro final por su importancia en la presente memoria.

Agentes expansores de micelas

Un agente expansor es un reactivo orgánico no polar que se solubiliza en el núcleo hidrofóbico de las micelas de surfactante y las expande, aumentando así el tamaño de poro del material final [57]. Estos compuestos se añaden en el medio de síntesis a la disolución micelar antes de la adición del precursor de sílice, como puede observarse esquemáticamente en la Figura 8:

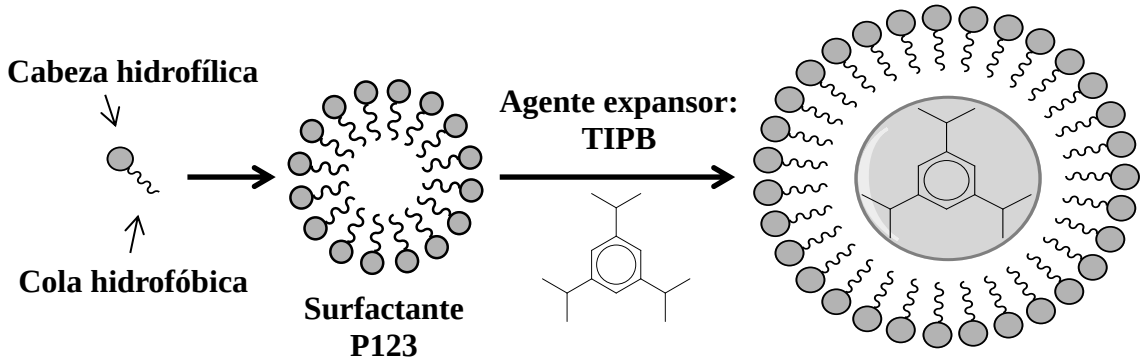

Figura 8. Interacción del agente expansor TIPB (1,3,5-triisopropilbenceno) con las micelas de surfactante P123.

Cuando Zhao y col., [47] publicaron su primer artículo sobre SBA-15 indicaron que utilizando 1,3,5-trimetilbenceno (**TMB**) como agente expansor de micelas se podría incrementar el diámetro de poro entre 5 y 30 nm. El grupo de Schmidt-Winkel y col. [58] adicionaron al medio de síntesis de la SBA-15 cantidades suficientemente grandes de (TMB), pero la adición del agente orgánico de hinchamiento derivó en la formación de estructuras amorfas, es decir, estructuras mesoporosas tridimensionales ultra-grandes formadas por grandes cavidades esféricas interconectadas por ventanas. Mediante estudios se observó que el TMB inducía una transformación de la fase altamente ordenada de la mesoestructura tipo SBA-15 a espumas mesocelulares silíceas que se denominaron MCFs [59]. Además, se ha demostrado que cuando la relación másica TMB/ P123 es superior a ~ 0,2, es cuando las micelas cambian su disposición de cilindros para dar la espuma mesocelular silícea [60]. El tamaño de las cavidades esféricas variaba

de 22 a 42 nm y el diámetro de las ventanas estaba en torno a ~ 10 nm [60]. El diámetro de cavidad y tamaño de la ventana de las MCF se pueden controlar cambiando la cantidad del agente expansor y la temperatura de síntesis.

Una alternativa, pero no tan eficiente, es mediante la adición de polímeros de tipo óxido de polipropileno (PPO), idéntico al que forma parte del bloque hidrofóbico del surfactante. La adición de este agente expansor puede aumentar el diámetro de poro de 4 nm a unos 5-6 nm dependiendo del peso molecular del polímero [61].

También se han utilizado alcanos (entre 8-20 carbonos) y benceno sustituido por grupos metil o isopropil como agentes expansores. En el caso de los alcanos, se obtienen estructuras de tipo MCF utilizando octano y nonano, pero con alcanos con 10 o más átomos de carbono se pueden obtener estructuras con ordenamiento hexagonal; en el caso concreto de decano el tamaño de poro de la SBA-15 se aumentó a 10-12 nm [62]. De forma general, el tamaño de poro se incrementa a medida que disminuye la longitud de la cadena del alcano empleado en una serie de C10 a C5, este comportamiento se debe a la solubilidad de dichos compuestos en las micelas de Pluronic P123. Al utilizar benceno sustituido, el tamaño de poro podría ser teóricamente diseñado entre 7-43 nm, aunque en la mayoría de los casos sólo se obtienen MCF.

Agentes expansores de micelas a baja temperatura y en presencia de sales

Alcanos más cortos, entre 6 y 9 átomos de carbono, también se pueden utilizar como agentes expansores si las primeras etapas de síntesis se realizan a bajas temperaturas (20-30 ºC) antes del envejecimiento hidrotérmico, y se adiciona la sal inorgánica, NH_4F [63]. Mediante la combinación de los efectos anteriores (bajas temperaturas, presencia de sales y del alcano de cadena corta) se puede sintetizar SBA-15 con poros que varían entre 13,4 nm (nonano) a 15,7 nm (hexano) y con diferentes morfologías [63, 64]. Además, los mesoporos se pueden incrementar gradualmente alargando el tiempo del tratamiento o envejecimiento hidrotérmico a una temperatura dada o fijando temperaturas más altas durante dicho tratamiento, de esta forma ha sido posible ajustar el tamaño de los poros entre 9,4 y 18,2 nm cuando se utilizó hexano como agente expansor [65].

Una alternativa a los alcanos es la utilización de 1,3,5-triisopropilbenceno (TIPB) en una síntesis similar (a bajas temperaturas y añadiendo NH_4F), pero la temperatura del gel inicial se debe disminuir más aún (entre 12 – 20 ºC) [66-69]. Una vez más, la solubilidad del agente expansor en el núcleo micelar es la clave para la formación de poros

suficientemente grandes. El grupo de Cao y col., consigue SBA-15 con una porosidad ordenada utilizando temperaturas de síntesis inferiores a 14 ºC, estas condiciones dieron lugar a poros de hasta 26 nm (el cálculo del diámetro se obtiene utilizando una ecuación geométrica para materiales con estructura 2D hexagonal de poros cilíndricos que están separadas por paredes microporosas [70, 71], que es el mayor tamaño de poro de la SBA-15 obtenido hasta la fecha [66, 69].

La disponibilidad del material SBA-15 con grandes diámetros de poro y con sus poros cilíndricos bien definidos y ordenados mejora significativamente las oportunidades en el uso de este importante material para confinar enzimas voluminosas en el mismo. Por ello, en la presente tesis se ha tratado de obtener sílices mesoporosas ordenadas con un diámetro de poro adaptado a las dimensiones moleculares de las enzimas objeto de estudio, utilizando en la síntesis expansores de micelas que interaccionan con el surfactante (TIPB), bajas temperaturas de síntesis y mediante la adición de sales, como NH_4F. Para ello se deben seleccionar agentes expansores de micelas con una capacidad de hinchamiento moderada para lograr una ampliación de diámetro de poro apreciable, pero evitando al mismo tiempo la formación de una mesoestructura heterogénea y / o mal definida de tipo MCF.

1.3.3. Funcionalización orgánica de los materiales silíceos mesoestructurados

Un aspecto importante de los materiales mesoporosos ordenados es la posibilidad de incorporar **funcionalidades orgánicas** en la superficie de los canales o dentro de la estructura silícea. De esta forma, el soporte silíceo proporciona estabilidad térmica, mecánica o estructural, mientras que los grupos orgánicos confieren al material múltiples e importantes propiedades ampliando su campo de aplicación [72-76].

Para llevar a cabo la funcionalización orgánica de los materiales mesoporosos existen dos métodos diferentes [75, 77, 78]: **anclaje** (posterior a la síntesis de la estructura de sílice) y **co-condensación** (incorporación directa durante la síntesis). En ambos métodos se producen uniones covalentes entre la estructura inorgánica de la sílice y los grupos funcionales.

Método de Anclaje

En el método de anclaje se parte del material mesoestructurado silíceo del cual se ha eliminado previamente el surfactante por **calcinación** o por **extracción**. El procedimiento

de anclaje está basado en la reacción de los grupos silanol superficiales (Si-OH) situados en la pared del material mesoporoso, con los grupos metoxi (CH_3-O-) o etoxi (CH_3-CH_2-O-) de las moléculas precursoras de grupos funcionales orgánicos (organoalcoxisilano que contiene el grupo funcional, por ejemplo, aminopropilo) mediante **reacciones de silanización** [73, 79]. Tras la reacción de anclaje, la estructura silícea se suele mantener sin alterar, salvo por una ligera disminución del volumen y del diámetro de poro debida a la presencia de nuevas especies en el interior del mismo [80, 81]. Por lo tanto, se necesita un material de poro suficientemente grande para anclar los grupos funcionales, y posteriormente poder inmovilizar las enzimas.

Si se desea un alto grado de funcionalización del material es necesario mantener una elevada concentración superficial de grupos silanol tras la eliminación del surfactante. Si esta se lleva a cabo mediante **extracción** con disolventes (alcoholes en el caso de utilizar surfactantes no iónicos), se minimiza la pérdida de grupos silanol superficiales. Pero cuando se elimina el surfactante por **calcinación** se produce una condensación de grupos silanol y tiene lugar una deshidroxilación de la estructura y, por tanto, se reduce el número de puntos de anclaje. Esta situación es reversible mediante un tratamiento posterior de **hidratación** del soporte por ebullición en agua, que debe continuar con un tratamiento de **deshidratación** para eliminar el exceso de agua no adecuada para la funcionalización posterior. De esta manera se consigue suministrar un número adecuado de grupos silanol para unir el grupo orgánico funcional [72, 82].

Este método se puede emplear para aumentar la hidrofobicidad de la superficie del soporte (incorporando cadenas de grupos fenilo o alquilo), introducir grupos funcionales reactivos (haluros, epóxidos, olefinas, etc.) que posteriormente reaccionen con otras moléculas de interés o bien, para funcionalizar selectivamente las superficies internas y externas. En el presente trabajo se han incorporado grupos amino que aportan hidrofilicidad a los soportes, por ejemplo, la funcionalización del material silíceo amorfo MS-3030 utilizado en la presente tesis, se lleva a cabo mediante el **método de anclaje** [82, 83] por reacción de silanización de los grupos silanol superficiales con el organosilano 3-(aminopropil)-trietoxisilano, APTE, de acuerdo con el esquema mostrado en la Figura 9.

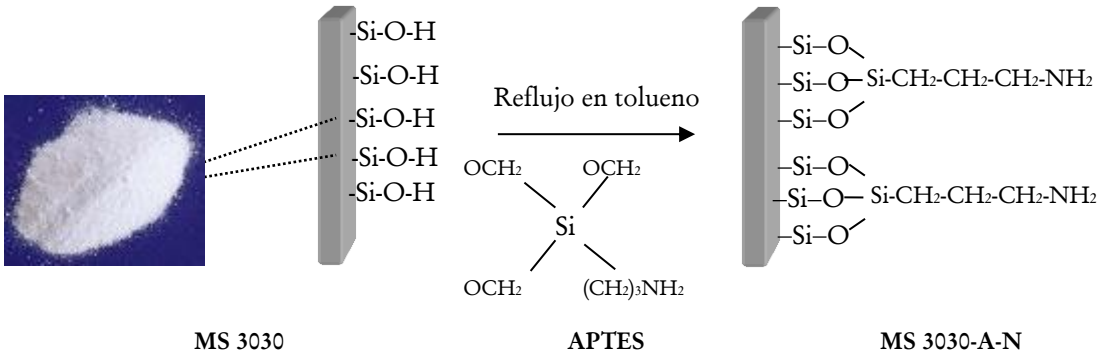

Figura 9. Funcionalización del material silíceo amorfo comercial MS-3030 mediante anclaje. El grupo orgánico incorporado es el aminopropilo (N).

Método de cocondensación

Este método, también denominado **síntesis directa** o de un solo paso, se basa en la condensación conjunta de las especies silíceas tipo tetraalcoxisilano (fuente precursora inorgánica) y los correspondientes precursores tipo organoalcoxisilano (incorpora el grupo orgánico) que contienen al menos un enlace Si-C, en presencia del surfactante [73, 77, 79]. El material mesoestructurado se obtiene ya funcionalizado tras la extracción del surfactante (Fig. 10).

La principal ventaja de este método frente al anclaje es que no se necesitan varias etapas; además la distribución de grupos orgánicos incorporados es más homogénea a lo largo de la superficie del material mesoporoso y se produce una menor disminución de la porosidad. Desgraciadamente, no todos los tipos de funcionalidades orgánicas pueden ser incorporadas de esta forma, ya que las condiciones de síntesis pueden no ser las adecuadas, además, el diámetro de poro es difícilmente controlable y la mesoestructura final no es tan ordenada, ya que el grado de ordenamiento mesoscópico disminuye al aumentar la concentración del organosilano en la mezcla de síntesis [73].

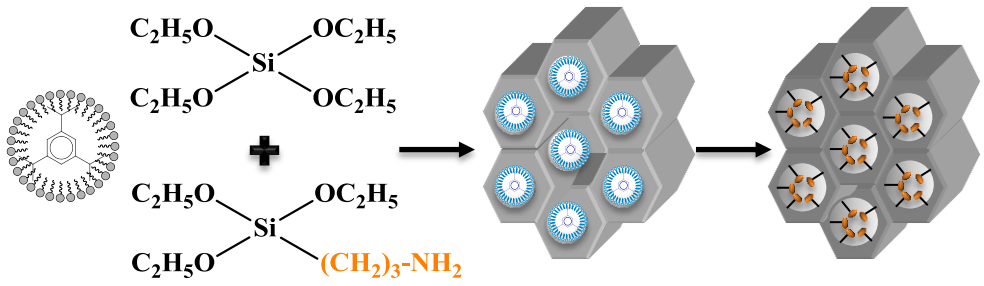

Figura 10. Funcionalización del material silíceo SBA-15 mediante cocondensación en presencia del agente expansor de micelas TIPB.

1.3.4. Materiales mesoestructurados híbridos organosilíceos (PMO)

En 1999 tres grupos de investigación descubrieron de forma simultánea e independiente una nueva clase de materiales mesoestructurados silíceos que incorporan especies orgánicas de diferente naturaleza *dentro* de las pareces silíceas denominados PMOs (*Periodic Mesoporous Organosilicas*) [84-86].

La síntesis de estos materiales es similar a la de las sílices mesoporosas ordenadas descritas en el apartado anterior, pero reemplazando el alcóxido de silicio por un alcoxisilano del tipo $(R'O)_3Si\text{-}R\text{-}Si(OR')_3$ (donde R es un grupo orgánico puente y R' metilo o etilo), que polimeriza y condensa alrededor de las plantillas de surfactante. Los primeros PMOs tenían diámetros de poro comprendidos entre 2 y 3 nm.

Estos materiales novedosos combinan las características estructurales de la sílice mesoporosa ordenada con la funcionalización química de los polímeros orgánicos [78, 87]. La principal diferencia entre los PMO y los procedimientos de funcionalización anteriores es que en los PMOs el grupo orgánico está integrado en la estructura tridimensional de la matriz de sílice a través de dos enlaces covalentes, y está distribuido de forma homogénea en las paredes de los poros, siendo la carga incorporada de grupos orgánicos mayor, además, se obtiene un sistema de poros totalmente desocupado y completamente accesibles para inmovilizar enzimas. El procedimiento de síntesis seguido queda esquematizado en la Figura 11.

El número de grupos orgánicos puente (R) que se pueden emplear en el diseño de PMO ha aumentado constantemente desde 1999 [87-90]. En las primeras investigaciones el grupo R estaba limitado a puentes orgánicos relativamente simples, tales como alcanos y alquenos de cadena corta. Por ejemplo, en este trabajo se ha empleado **etileno** como grupo funcional orgánico dentro de la matriz mesoporosa ordenada, obteniendo un soporte de naturaleza **hidrofóbica**. Mediante el control de la composición y naturaleza de los componentes orgánicos de las paredes silíceas se ha podido modular el carácter hidrofílico/hidrofóbico de las estructuras de PMO sintetizadas. De este modo se ha inmovilizado **lipasa** por adsorción no covalente sobre estos soportes, ya que estas enzimas tienen alta afinidad hacia superficies hidrofóbicas (Figura 12).

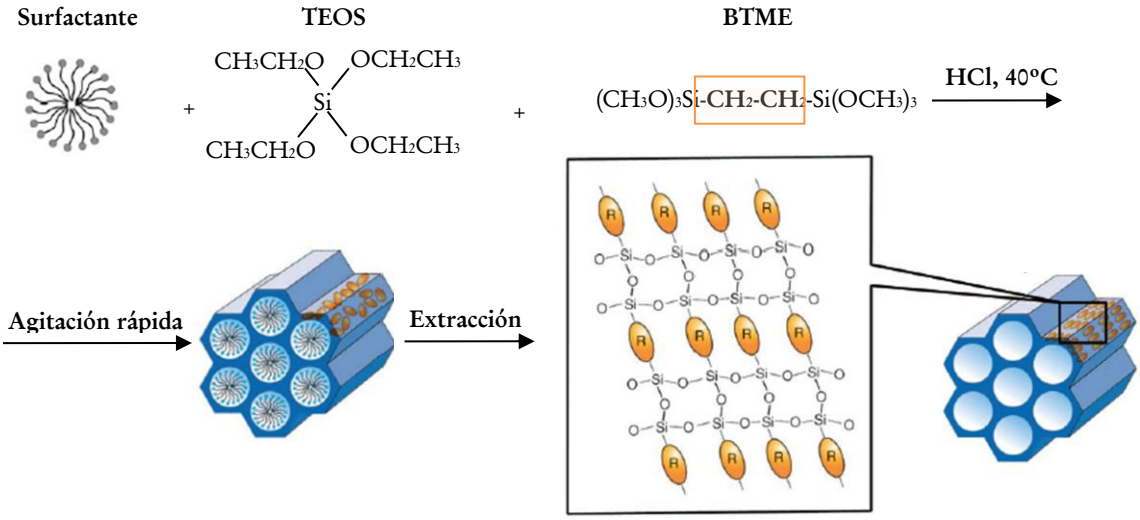

Figura 11. Esquema del procedimiento de síntesis de PMOs donde las unidades orgánicas R, correspondientes al etileno (-CH_2-CH_2-), se anclan dentro de las paredes del poro.

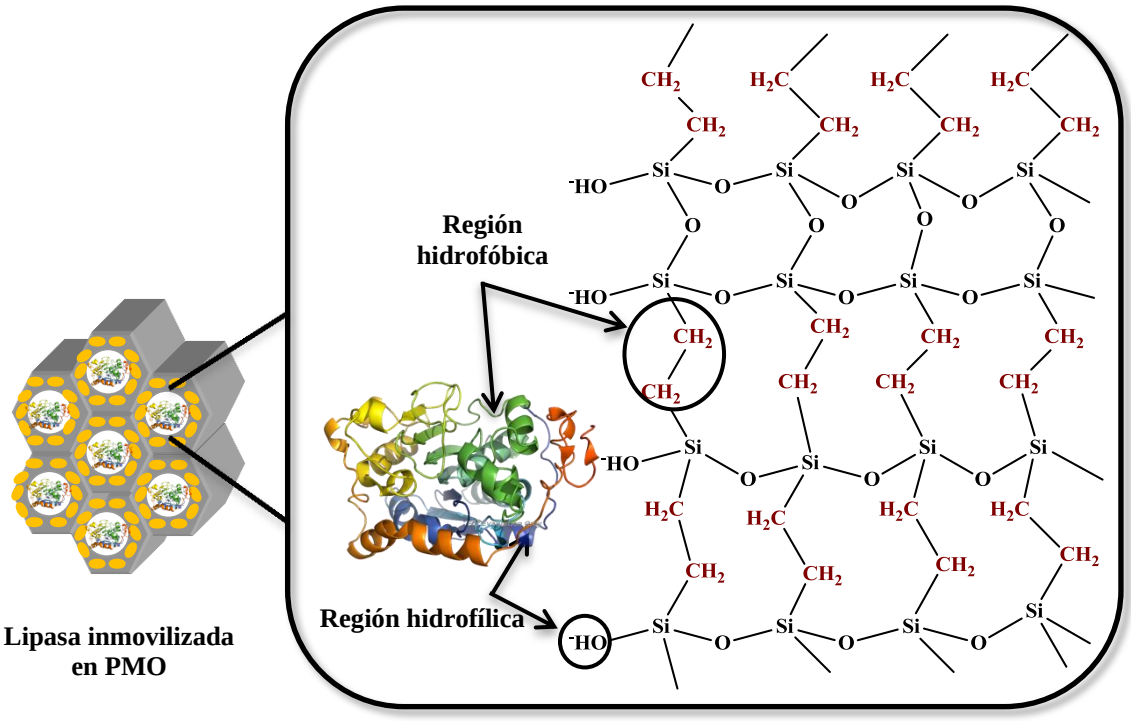

Figura 12. Inmovilización de lipasa de *Candida antarctica B* en PMO que incorpora grupos etileno.

En principio puede parecer que el uso de PMOs hará posible incorporar cualquier tipo de grupo orgánico en las paredes del material mesoporoso, en cualquier concentración

deseada, y ajustando las propiedades fisicoquímicas del material final. Sin embargo, la realidad de la situación no es tan simple. Hay algunas limitaciones estrictas en cuanto a los tipos de grupos orgánicos que se pueden utilizar que parecen estar relacionados con su flexibilidad, y solubilidad. En cuanto a la **flexibilidad**, cuanto más rígido sea el grupo orgánico puente, más probable es que el precursor será capaz de auto-ensamblar. Por ejemplo, cuando el grupo puente es o bien un grupo metileno o etileno el auto-ensamblaje se produce y se obtienen materiales con estructuras ordenadas. Sin embargo, si la cadena de alquilo se alarga en un átomo de carbono a un grupo propilo, el material resultante es un gel completamente amorfo. El fracaso del precursor de propilo a auto-ensamblar se debe más a su flexibilidad que a su tamaño, ya que se han publicado trabajos que utilizan precursores más grandes y más rígidos que pueden auto-ensamblar. Por ejemplo, si el benceno se utiliza como el grupo orgánico puente los materiales resultantes son ordenados, a pesar de que el benceno es más grande que el grupo propilo [91].

Esto limita la síntesis de PMOs ya que la mayoría de los precursores disponibles en el mercado son bastante largos y flexibles, que los hace inadecuados para su uso en la síntesis de PMOs. Actualmente, se han desarrollado nuevos procedimientos sintéticos para desarrollar precursores organosilanos que permiten la incorporación en la pared de los PMO de una gran variedad de grupos orgánicos, que van desde compuestos aromáticos e hidrocarburos a complejos metálicos y dendrímeros pequeños [92, 93], aunque los procedimientos de síntesis son complejos y difíciles de reproducir. Aquí radica la dificultad que se ha superado con éxito en esta Tesis, y es la síntesis de un material altamente ordenado de tipo PMA donde el grupo puente incorpora un grupo amino, y además tiene un diámetro de poro suficientemente grande (10 nm) como para poder retener en su interior a la enzima lacasa, como se muestra posteriormente en el Capítulo 3.

Los métodos previos mencionados que derivan en materiales híbridos orgánicos-inorgánicos mesoporosos ordenados ofrecen nuevas posibilidades de inmovilización de enzimas a través de diferentes interacciones tales como unión covalente, interacciones hidrofóbicas, enlaces de hidrógeno e interacciones electrostáticas. Precisamente la presente Tesis Doctoral trata de desarrollar avanzados materiales con diferentes funcionalidades orgánicas que sirvan como soportes adecuados para la inmovilización de enzimas mediante interacciones no covalentes.

1.4. INMOVILIZACIÓN DE ENZIMAS

1.4.1. Factores que afectan a la inmovilización de enzimas

Para llevar a cabo una inmovilización de enzimas con éxito sobre soportes de sílice porosa se deben tener en cuenta varios factores que influyen en gran medida en el biocatalizador final. Estos incluyen las condiciones de experimentación tales como el pH, la concentración del tampón y la temperatura de inmovilización; las propiedades fisicoquímicas del material, su morfología, tamaño de partícula, tamaño de poro, y su composición química; además de las propiedades de la propia enzima, como su tamaño, la presencia de grupos polares (por ejemplo grupos amino de la lisina, arginina e histidina y/o grupos ácidos de los residuos de aminoácidos glutámico y aspártico), así como la presencia de regiones superficiales apolares, o glicosilación (residuos de azúcares).

A continuación se va a explicar el efecto del tamaño de poro, el tamaño de partícula, y la morfología en la inmovilización de enzimas:

Tamaño de poro

Existen numerosos estudios que indican que la carga y la actividad enzimática son claramente dependientes de tamaño de poro del soporte silíceo [94, 95]. Por lo tanto, no todos los materiales de sílice porosos se pueden utilizar para la inmovilización de enzimas. Los materiales con diámetros de poro demasiado pequeños para acomodar moléculas de enzima no proporcionan un soporte adecuado, porque en este caso las moléculas de enzima se adsorben en la superficie externa y, no van a estar protegidas del medio externo [96]. Si por el contrario, los poros son mucho más grandes que las moléculas de enzima, esta última tampoco va a estar protegida (afectando a su actividad enzimática), ni retenida por el soporte pudiendo lixiviar de los poros si está adsorbida físicamente [97].

Por tanto, a la hora de diseñar un soporte se debe tener un compromiso entre el tamaño de poro del material y el tamaño de la enzima para obtener una alta carga enzimática y alta retención. Algunos estudios han demostrado que haciendo coincidir el diámetro de poro con el tamaño de la enzima, se mejora la estabilidad de la enzima inmovilizada [27, 95, 98] y se reduce su lixiviado [9, 99], ya que cuando los poros tienen un diámetro adecuado y adaptado a la enzima específica que se quiere inmovilizar no es necesario

emplear la inmovilización covalente [100]. En la Figura 13 se muestra un ejemplo del efecto del diámetro de poro sobre la inmovilización de la enzima lacasa.

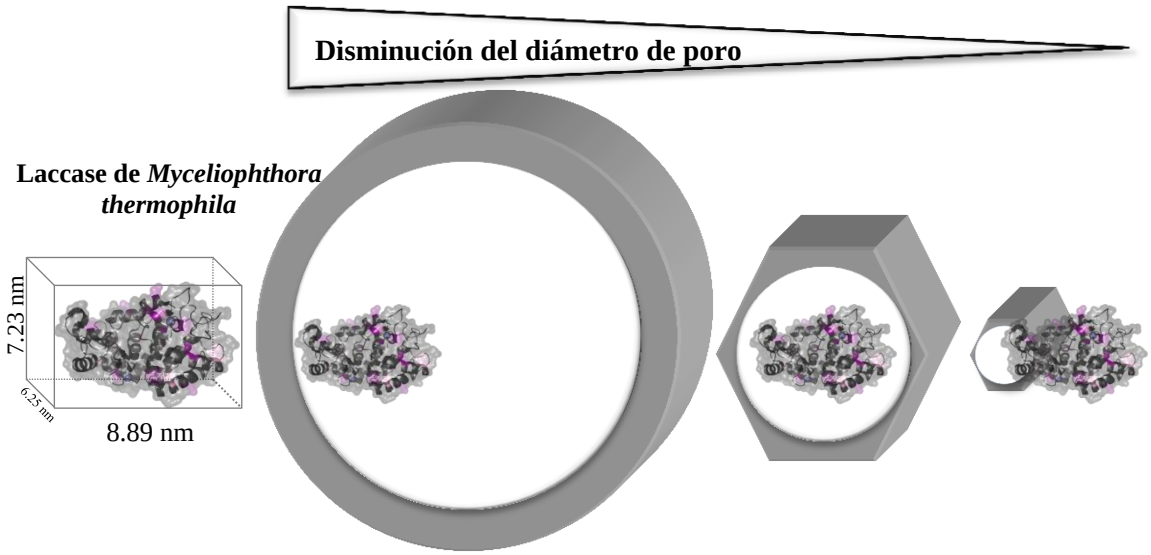

Figura 13. Efecto del diámetro de poro sobre la inmovilización de la enzima lacasa *Mt*L.

En bibliografía se pueden consultar algunos trabajos que estudian de forma destacada el efecto del diámetro de poro en la inmovilización de enzimas. Por ejemplo, Ikemoto y col. han inmovilizado HRP en SBA-15 con un diámetro de poro de 7,6 nm, y han observado que tanto la estabilidad térmica, cómo la estabilidad frente a determinados inhibidores de la enzima como cloruro de guanidinio y urea, mejoraron significativamente en comparación con HRP libre [101]. Recientemente, Sang y Coppens [102] utilizaron espectroscopia ATR-FTIR con el fin de analizar la estructura secundaria de dos proteínas globulares en los poros cilíndricos de SBA-15 con diferente tamaño, y demostraron una fuerte correlación entre la conformación de la molécula y la geometría local de los mesoporos. La proteína conserva su conformación nativa cuando se adsorbe en un poro con un tamaño cercano a las dimensiones moleculares de la proteína.

Estructura, tamaño de partícula y morfología

Además del tamaño de los poros del soporte, la **estructura** de los MMSO juega un papel importante con respecto a la carga y actividad de las enzimas inmovilizadas. Los materiales como MCM-41, FSM-16 y SBA-15 tienen una estructura de poros de una dimensión, donde la difusión de la enzima hacia el interior de la partícula puede estar limitada debido al bloqueo de los poros en la boca de los mismos.

Por el contrario, materiales como MCM-48, SBA-16, FDU-12, y los MCFs poseen una estructura tridimensional de poros interconectados que debería reducir potencialmente las limitaciones difusionales, siempre y cuando la enzima sea capaz de entrar a través de las ventanas. Por ejemplo, para el caso de una proteína pequeña, citocromo c, Balkus y col., [25, 103] demostraron que la carga enzimática depende de la estructura del soporte basándose en un estudio comparativo entre MCM-41, MCM-48 y SBA-15, consiguiendo mayores cargas con el material MCM-48.

La **morfología** y el **tamaño de partícula** del material también tienen un efecto importante en la inmovilización de enzimas. En 2003, Fan y col., [104, 105] estudiaron la adsorción de lisozima en SBA-15 convencional y en SBA-15 con canales más cortos y demostraron que el material con menor tamaño de partícula mejoraba la capacidad de absorción de la enzima, y se disminuía el tiempo para llegar al equilibrio de adsorción. Además, en esos estudios demostraron que el número de entradas o aperturas de los poros aumenta con la disminución del tamaño de partícula en las sílices mesoporosas, lo que lleva a una evidente mejora de la absorción de la enzima.

Recientemente, Gustafsson y col. [106] estudiaron la influencia del tamaño de partícula en la inmovilización, para ello utilizaron tres tipos de soportes silíceos mesoporosos (dos SBA-15 y una HMM (*Hiroshima Mesoporosus Materials*)) con diferentes tamaños de partículas (40 nm, 300 nm y 1000 nm, respectivamente), pero el mismo diámetro de poro de 9 nm, para la inmovilización de lipasas de *Mucor miehei* (*MM*L) y *Rhizopus oryzae* (*RO*L). Las lipasas utilizadas tienen el mismo tamaño molecular, pero difieren en gran medida en sus puntos eléctricos (pI (*MM*L) = 3,8; pI (*RO*L) = 7,6). Aunque la carga enzimática fue similar para las muestras utilizadas, se demostró que ambas lipasas presentan más actividad específica cuando se inmovilizan sobre el material con tamaños de partícula de 300 nm.

1.4.2. Enzimas objeto de estudio

El trabajo de investigación que aquí se presenta, se centra en la inmovilización de lacasa, lipasa y β-glucosidasa. Un estudio profundo de las inmovilizaciones de lacasa [107-109], lipasa [110-113] y β-glucosidasa servirían para incrementar el potencial y las aplicaciones de estas enzimas. El avance en la obtención de soportes silíceos mesoporosos, con grandes superficies y diámetros de poro superiores a 5 nm, como se ha

comentado anteriormente, ha abierto nuevos campos en la investigación de la inmovilización de diferentes enzimas (proteasas, lipasas, peroxidasas, etc).

Lacasas

Las lacasas son oxidasas multicobre (EC 1.10.3.1; p-difenol:dioxígeno:óxido-reductasa) que reducen el oxígeno molecular formando dos moléculas de agua y simultáneamente oxidan un amplio rango de polifenoles y sustratos aromáticos mediante la abstracción de cuatro electrones [114-117]. Las lacasas son producidas por una amplia variedad de microorganismos, especialmente por plantas, hongos y algunas bacterias [107], siendo las extraídas de hongos las más estudiadas [118].

Esta enzima ha sido empleada en forma inmovilizada para degradar compuestos xenobióticos en residuos acuosos, en la detoxificación de compuestos fenólicos en vinos, y en la obtención de hidrolizados de lignocelulosa antes de ser usados para la fermentación alcohólica por *Saccharomyces cerevisiae*, encontrándose también la participación de esta enzima en la decoloración de melazas y colorantes [109, 117, 119-127].

La mayoría de las lacasas son monoméricas, con tres dominios globulares conectados consecutivamente, contienen cuatro átomos de cobre que se distribuyen en diferentes centros de la estructura, y tienen un importante papel en el mecanismo de la catálisis enzimática. El centro de cobre mononuclear T1 es el sitio de oxidación de sustratos, desde el cual los electrones son transferidos al centro trinuclear compuesto por un cobre tipo 2 (T2) y dos tipo 3 (T3), en donde tiene lugar la reducción del oxígeno molecular.

Las lacasas de hongo tienen un peso molecular de 60-110 kDa, un punto isoeléctrico (pI) cercano a 4,0, en el caso de la lacasa de *Myceliophthora thermophila* (*Mt*L) [128], utilizada en este trabajo su peso molecular es de 110 kDa y su pI es de 4,2 [129, 130]. La Figura 14 muestra una lacasa homóloga a *Mt*L, la lacasa de *Melanocarpus albomyces* (1GWO, chain *a*) [131] con un 97,6 % de homología, ya que la enzima *Mt*L no está aún cristalizada, por lo que no está disponible su PDB.

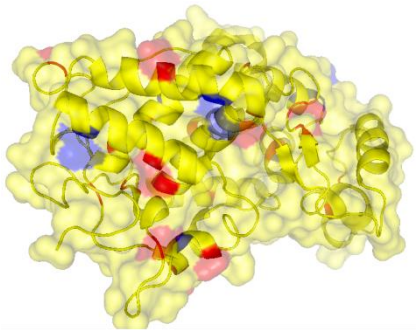

Figura 14. Estructura modelizada de lacasa de *Melanocarpus albomyces*. Los aminoácidos aspártico y glutámico están resaltados en rojo y azul. Sus dimensiones moleculares son 6,3 x 7,2 x 8,9 nm.

Lipasas

Las lipasas (EC. 3.1.1.3) son un tipo de enzimas hidrolíticas producidas por plantas, animales y microorganismos. En condiciones fisiológicas, estas enzimas catalizan la hidrólisis de triglicéridos de aceites y grasas para dar glicerol y ácidos grasos libres, mono y diglicéridos, puesto que su función biológica es la del metabolismo de los lípidos.

En condiciones controladas, las lipasas pueden catalizar otras reacciones además de la hidrólisis. Esta capacidad hace que las lipasas sean muy utilizadas como biocatalizadores en la modificación de grasas y aceites y otras reacciones de síntesis química [132-134]. La acción de las lipasas es reversible, es decir, catalizan la hidrólisis en sistemas acuosos, pero también catalizan la esterificación (reacción inversa a la hidrólisis) en sistemas con reducido contenido en agua.

Las lipasas poseen un dominio hidrofóbico sobre su superficie constituido por una serie de aminoácidos con cadenas laterales hidrofóbicas [135], que constituye una especie de tapadera, de modo que cuando la enzima se encuentra en medio acuoso, estos grupos interaccionan entre sí impidiendo el acceso de sustratos al centro activo. Sólo cuando en el medio existe una interfase hidrofóbica, la tapadera se abre para permitir el acceso de los triglicéridos al centro activo.

La lipasa que se utiliza en la presente tesis es la procedente de *Candida antárctica* B (CALB) [136]. Se trata de una variedad que carece de esta tapadera, y su centro activo es más accesible al encontrarse más cerca de la superficie [112, 137, 138]. Aunque como todas las lipasas posee un dominio hidrofóbico en su superficie lo que permite la inmovilización sobre superficies hidrofóbicas [139, 140]. Su peso molecular es de unos

32 kDa, su punto isoeléctrico es de 6,0 y sus dimensiones son aproximadamente de 3 x 4 x 5 nm (Fig. 15).

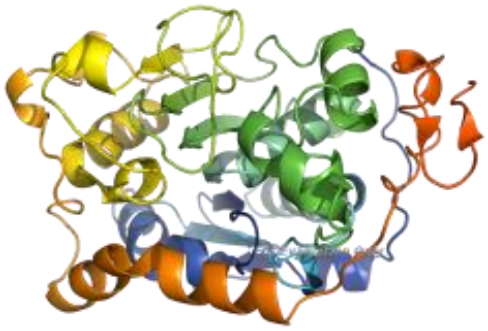

Figura 15. Estructura modelizada de la lipasa de *Candida antartica* B.

B-Glucosidasas

La B-glucosidasa (EC 3.2.1.21) utilizada en la presente Tesis puede recibir diferentes nombres entre ellos: β-D-glucosidasa, β-1,6-glucosidasa, Novozyme 188, celobiasa, etc [141]. Se encarga de catabolizar la hidrólisis del enlace O-glicosil de los hidratos de carbono: liberando moléculas de glucosa. Su origen es principalmente de hongos; la que se emplea en este trabajo es producida por el organismo *Aspergillus niger* [142]. Esta enzima no está aún cristalizada por lo que no aparece en la base de datos del *Protein Data Bank* (PDB), por ello se ha modelizado utilizando β-Glucosidasa de *Aspergillus aculeatus* (4IIB .pdb) que tiene una secuencia de 841 aminoácidos (aa.) frente a 860 aa. de la β-Glucosidasa de *Aspergillus niger*. En la Figura 16 se muestra su estructura modelizada, como se observa se trata de una enzima dimérica, siendo, sus dimensiones aproximadas de ~ 12.3 nm x ~10.7 nm x ~ 8.1 nm, su peso molecular es de unos 240 KDa y su punto isoeléctrico de 4,0 [143].

Como posibles aplicaciones, destaca que esta enzima es útil durante las etapas finales de las fermentaciones alcohólicas; para incrementar la liberación de aromas en el vino (hidrolizar precursores del aroma), así como en la hidrólisis de oleuropeína (fenol esterificado) para obtener hidroxitirosol (con importantes propiedades antioxidantes) [144].

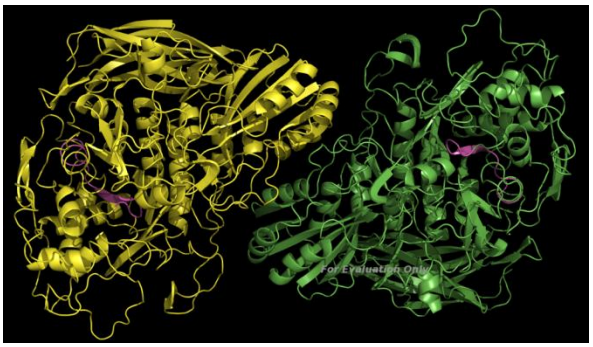

Figura 16. Estructura modelizada de la β-Glucosidasa de *Aspergillus niger*.

1.4.3. Estrategias de inmovilización en MMSO

Las estrategias de inmovilización utilizadas en la presente Tesis Doctoral han sido: ***1***) incorporación de la enzima sobre un soporte ya existente (inmovilización post-síntesis), y ***2***) mediante la inmovilización in-situ o encapsulación en el interior de un material poroso durante el propio proceso de síntesis. A continuación se va a mostrar las característivas principales de la encapsulación.

Encapsulación In-situ

La encapsulación de la enzima es un método atractivo entre las diferentes estrategias de inmovilización para mejorar la reutilización y la estabilidad de las enzimas, ya que puede evitar cambios estructurales de las enzimas y se pueden separar o proteger a las mismas de un entorno externo agresivo. Sin embargo, los métodos de encapsulación actuales tienen limitaciones incluyendo la lixiviación de la enzima.

El atrapamiento en sílice sol-gel es la técnica más utilizada para la encapsulación de la enzima. Pero sin el empleo de surfactantes (o agentes directores de estructura) se forma una red porosa en la que la enzima está atrapada al azar, existiendo limitaciones difusionales de sustratos y productos, debido a la tortuosidad de la estructura [145, 146].

En apartados anteriores se ha destacado que mediante el empleo de surfactantes es posible obtener materiales mesoporosos silíceos ordenados (MMSO) con alta área superficial, diámetro de poro controlable, red porosa altamente ordenada y volumen de poro grande. Para ello se requiere usar condiciones de pH muy ácidas, procesos de alta temperatura y etapas de síntesis hidrotermal a altas presiones y temperatura, que obviamente no son compatibles con la presencia “in-situ” de la mayoría de las enzimas, ya que estas se desnaturalizan en condiciones drásticas. Por ello, el objetivo en la presente

Tesis es encapsular las enzimas en MMSO en condiciones suaves y que además se evite el lixiviado. De tal manera que la enzima esté atrapada en una estructura de "cáscara", siendo la cáscara una capa de encapsulación de sílice robusta y estable para proteger a las enzimas, y que a la misma vez sea porosa para permitir la difusión de sustratos y productos.

Actualmente existen pocos trabajos que han apostado por esta vía de inmovilización in-situ o en un solo paso [147-150]. Los primeros estudios para alcanzar este objetivo se realizaron en el grupo de investigación donde se ha desarrollado la presente tesis [151]. Primeramente se partió de un material tipo SBA-16 (caja-ventana) y se realizó una inmovilización post-síntesis con lipasa mediante interacciones electrostáticas. Como se observa en la Figura 17 el tamaño de las cajas es lo suficientemente amplio para albergar a la enzima, pero no así el diámetro de las ventanas que es muy similar a las dimensiones de la lipasa. La carga enzimática que se consiguió sólo era 5 mg /g de sílice. Esto significa que probablemente sólo puede entrar en el interior, la enzima que está orientada de modo que su dimensión más pequeña se enfrente a la ventana. Aunque la carga enzimática es baja, es importante resaltar que sólo el 2 % de la enzima que había conseguido entrar lixivió tras 2 horas, siendo un resultado muy prometedor.

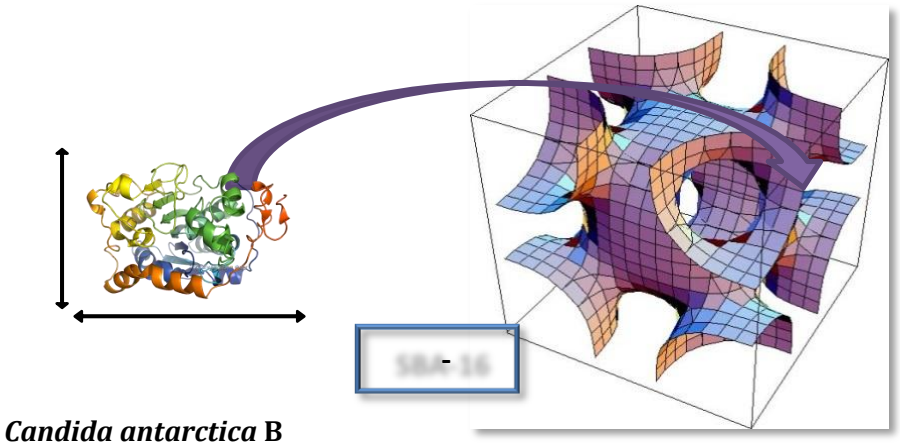

Figura 17. Inmovilización de la enzima lipasa en SBA-16 mediante la estrategia post-síntesis.

Para solucionar este inconveniente y conseguir mayores cargas enzimáticas y que no lixivie la enzima se requiere sintetizar el propio soporte caja-ventana alrededor de las moléculas de enzima. Para lograr este objetivo se requirió de un profundo estudio sobre la naturaleza del surfactante (de tipo Pluronic) y de las condiciones de síntesis (presencia de

sales, baja temperatura, pH 3,5). La naturaleza dual hidrofílica/fóbica de la lipasa, con marcada afinidad por las interfases hidrofóbicas, indujo a pensar que en la fase micelar previa a la adición de la fuente de silicio se incluiría la enzima en el interior de las micelas de surfactante, en íntimo contacto con su núcleo hidrófobico. La posterior adición de un alcóxido de silicio daría lugar a un material mesoporoso ordenado con un sistema de canales rellenos de surfactante, en el interior del cual está alojada la lipasa. Finalmente, el surfactante se eliminó en condiciones suaves para no afectar a las enzimas encapsuladas.

Después de estos brillantes resultados se trató de extrapolar el mismo protocolo para encapsular diferentes enzimas: Peroxidasa de rábano (HRP) y tirosinasa (PPO, polifenol oxidasa). En el caso de la HRP, la enzima quedó atrapada, pero la estructura resultante no fue ordenada sino una espuma mesocelular (MCF). Para la PPO (polifenol oxidasa) se obtiene una estructura regular pero la enzima no está atrapada en ella [152].

Si se analizan estos resultados atendiendo a las diferentes características de las enzimas: hidrofobicidad y punto isoeléctrico observamos que el punto isoeléctrico de la lipasa es 6,0, por lo tanto, está cargado positivamente al pH de la síntesis (3,5). Además, la hidrofobicidad de la superficie externa ayuda a las micelas a organizarse alrededor de la molécula de enzima, colocándose la lipasa en el interior del núcleo hidrofóbico mientras que las cabezas polares o hidrófilas quedarían orientadas hacia la disolución acuosa externa. Como consecuencia de esto las micelas se forman correctamente alrededor de la enzima y el biocatalizador final es altamente ordenado con enzima atrapada en su interior.

En el caso de la HRP su punto isoeléctrico es de 7,2, por lo que la enzima tiene también una carga neta positiva a pH 3,5 que impulsa la formación de las micelas. Pero la ausencia de una superficie hidrofóbica en esta enzima impide la correcta organización de las micelas a diferencia de los que sucede con lipasa. El resultado es un material que contiene enzima desordenada.

La enzima PPO tiene un punto isoeléctrico mucho menor, de 4,75, por lo que en el pH de la síntesis de (3,5) la carga neta es cercana a cero. No hay ninguna fuerza que ayude a la formación de micelas, y la enzima carece de una superficie hidrófoba. Por lo tanto, la enzima y el agente surfactante funcionan por separado, y las micelas se forman

independientemente de la enzima. Así que en este caso se obtiene un material ordenado que no contiene la enzima.

Para lacasa, una de las enzimas utilizadas en este trabajo, y que carece de superficie hidrofóbica se probará a encapsular la enzima en presencia de aditivos que provean a la enzima de suficiente hidrofobicidad para ayudar a dirigir la formación de un material silíceo quedando la enzima previsiblemente atrapada en su interior (Figura 18).

En el caso de la β-glucosidasa, una enzima con grandes dimensiones moleculares, lo que se intentará es sintetizar materiales caja-ventana pero de tipo FDU-12 y en presencia tanto de sales, como de agentes expansores de micelas y a baja temperatura.

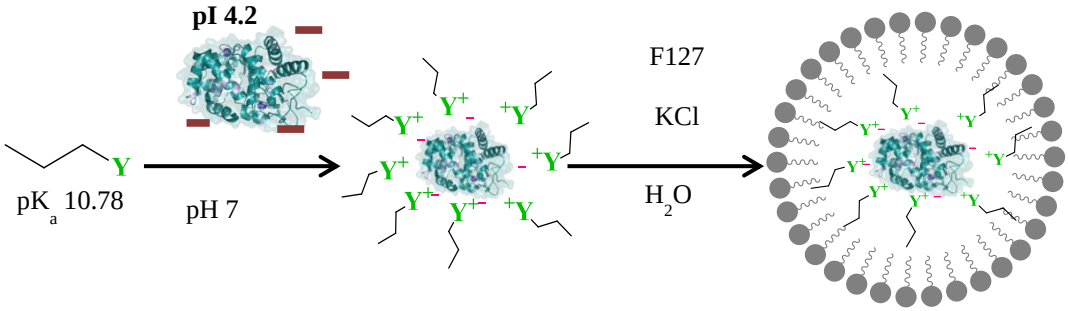

Figura 18. Estrategia de inmovilización in-situ de lacasa, mediante la adición de aditivos.

REFERENCIAS BIBLIOGRÁFICAS

[1] F. Secundo, Conformational changes of enzymes upon immobilisation, *Chem Soc Rev*, 42 (**2013**) 6250-6261.

[2] N. Miletic, A. Nastasovic, K. Loos, Immobilization of biocatalysts for enzymatic polymerizations: Possibilities, advantages, applications, *Bioresource Technol.*, 115 (**2012**) 126-135.

[3] M. Hartmann, Ordered mesoporous materials for bioadsorption and biocatalysis, *Chem. Mater.*, 17 (**2005**) 4577-4593.

[4] C. Spahn, S.D. Minteer, Enzyme Immobilization in Biotechnology, *Recent Pat. Eng.*, 2 (**2008**) 195-200.

[5] R.A. Sheldon, S. van Pelt, Enzyme immobilisation in biocatalysis: why, what and how, *Chem. Soc. Rev.*, 42 (**2013**) 6223-6235.

[6] W. Tischer, F. Wedekind, Immobilized enzymes: Methods and applications, *Biocatalysis - from Discovery to Application*, 200 (**1999**) 95-126.

[7] W. Tischer, V. Kasche, Immobilized enzymes: crystals or carriers?, *Trends Biotechnol.*, 17 (**1999**) 326-335.

[8] D.N. Tran, K.J. Balkus, Perspective of Recent Progress in Immobilization of Enzymes, *ACS Catal.*, 1 (**2011**) 956-968.

[9] Z. Zhou, M. Hartmann, Progress in enzyme immobilization in ordered mesoporous materials and related applications, *Chem. Soc. Rev.*, 42 (**2013**) 3894-3912.

[10] X.S. Zhao, X.Y. Bao, W. Guo, F.Y. Lee, Immobilizing catalysts on porous materials, *MATER TODAY*, 9 (**2006**) 32-39.

[11] E. Magner, Immobilisation of enzymes on mesoporous silicate materials, *Chem. Soc. Rev.*, 42 (**2013**) 6213-6222.

[12] T. Yanagisawa, T. Shimizu, K. Kuroda, C. Kato, THE PREPARATION OF ALKYLTRIMETHYLAMMONIUM-KANEMITE COMPLEXES AND THEIR CONVERSION TO MICROPOROUS MATERIALS, *Bull. Chem. Soc. Jpn.*, 63 (**1990**) 988-992.

[13] J.S. Beck, J.C. Vartuli, W.J. Roth, M.E. Leonowicz, C.T. Kresge, K.D. Schmitt, C.T.W. Chu, D.H. Olson, E.W. Sheppard, A new family of mesoporous molecular sieves prepared with liquid crystal templates, *J. Am. Chem. Soc.*, 114 (**1992**) 10834-10843.

[14] C.T. Kresge, M.E. Leonowicz, W.J. Roth, J.C. Vartuli, J.S. Beck, Ordered mesoporous molecular sieves synthesized by a liquid-crystal template mechanism, *Nature*, 359 (**1992**) 710-712.

[15] A. Sayari, P. Liu, Non-silica periodic mesostructured materials: recent progress, *Microporous Mater.*, 12 (**1997**) 149-177.

[16] U. Ciesla, F. Schuth, Ordered mesoporous materials, *Microporous Mesoporous Mat.*, 27 (**1999**) 131-149.

[17] G. Oye, J. Sjoblom, M. Stocker, Synthesis, characterization and potential applications of new materials in the mesoporous range, *Adv. Colloid Interface Sci.*, 89 (**2001**) 439-466.

[18] D. Trong On, D. Desplantier-Giscard, C. Danumah, S. Kaliaguine, Perspectives in catalytic applications of mesostructured materials, *Appl. Catal., A.*, 222 (**2001**) 299-357.

[19] S. Biz, M.L. Occelli, Synthesis and characterization of mesostructured materials, *Catalysis Reviews-Science and Engineering*, 40 (**1998**) 329-407.

[20] M. Kruk, M. Jaroniec, C.H. Ko, R. Ryoo, Characterization of the porous structure of SBA-15, *Chem. Mater.*, 12 (**2000**) 1961-1968.

[21] Y. Sakamoto, M. Kaneda, O. Terasaki, D.Y. Zhao, J.M. Kim, G. Stucky, H.J. Shim, R. Ryoo, Direct imaging of the pores and cages of three-dimensional mesoporous materials, *Nature*, 408 (**2000**) 449-453.

[22] V. Meynen, P. Cool, E.F. Vansant, Verified syntheses of mesoporous materials, *Microporous Mesoporous Mater.*, 125 (**2009**) 170-223.

[23] Y. Han, D. Zhang, Ordered mesoporous silica materials with complicated structures, *Curr. Opin. Chem. Eng.*, 1 (**2012**) 129-137.

[24] A. Taguchi, F. Schüth, Ordered mesoporous materials in catalysis, *Microporous Mesoporous Mater.*, 77 (**2005**) 1-45.

[25] J.F. Diaz, K.J. Balkus, Enzyme immobilization in MCM-41 molecular sieve, *J. Mol. Catal. B: Enzym.*, 2 (**1996**) 115-126.

[26] N. Carlsson, H. Gustafsson, C. Thorn, L. Olsson, K. Holmberg, B. Akerman, Enzymes immobilized in mesoporous silica: A physical-chemical perspective, *Adv. Colloid Interface Sci.*, 205 (**2014**) 339-360.

[27] H.H.P. Yiu, P.A. Wright, Enzymes supported on ordered mesoporous solids: a special case of an inorganic-organic hybrid, *J. Mater. Chem.*, 15 (**2005**) 3690-3700.

[28] Q. Huo, D.I. Margolese, U. Ciesla, P. Feng, T.E. Gier, P. Sieger, R. Leon, P.M. Petroff, F. Schüth, G.D. Stucky, Generalized synthesis of periodic surfactant/inorganic composite materials, *Nature*, 368 (**1994**) 317-321.

[29] F. Schuth, Non-siliceous mesostructured and mesoporous materials, *Chem. Mater.*, 13 (**2001**) 3184-3195.

[30] L. Treccani, T.Y. Klein, F. Meder, K. Pardun, K. Rezwan, Functionalized ceramics for biomedical, biotechnological and environmental applications, *Acta Biomaterialia*, 9 (**2013**) 7115-7150.

[31] G.A. Ozin, M.J. MacLachlan, N. Coombs, Non-aqueous supramolecular assembly of mesostructured metal germanium sulphides from $(Ge_4S_{10})^{4-}$ clusters, *Nature*, 397 (**1999**) 681-684.

[32] R. Ryoo, S.H. Joo, S. Jun, Synthesis of Highly Ordered Carbon Molecular Sieves via Template-Mediated Structural Transformation, *J. Phys. Chem. B.*, 103 (**1999**) 7743-7746.

[33] Y. Meng, D. Gu, F. Zhang, Y. Shi, H. Yang, Z. Li, C. Yu, B. Tu, D. Zhao, Ordered mesoporous polymers and homologous carbon frameworks: amphiphilic surfactant templating and direct transformation, *Angew. Chem. Int. Ed.*, 44 (**2005**) 7053-7059.

[34] K. Ariga, A. Vinu, Y. Yamauchi, Q. Ji, J.P. Hill, Nanoarchitectonics for Mesoporous Materials, *Bull. Chem. Soc. Jpn.*, 85 (**2012**) 1-32.

[35] R.A. Sheldon, Enzyme immobilization: The quest for optimum performance, *Adv. Synth. Catal.*, 349 (**2007**) 1289-1307.

[36] C. Garcia-Galan, A. Berenguer-Murcia, R. Fernandez-Lafuente, R.C. Rodrigues, Potential of Different Enzyme Immobilization Strategies to Improve Enzyme Performance, *Adv. Synth. Catal.*, 353 (**2011**) 2885-2904.

[37] A.S. Bommarius, M.F. Paye, Stabilizing biocatalysts, *Chem. Soc. Rev.*, 42 (**2013**) 6534-6565.

[38] M.W. Anderson, T. Ohsuna, Y. Sakamoto, Z. Liu, A. Carlsson, O. Terasaki, Modern microscopy methods for the structural study of porous materials, *Chem. Commun.*, (**2004**) 907-916.

[39] Y. Wan, D. Zhao, On the controllable soft-templating approach to mesoporous silicates, *Chem. Rev.*, 107 (**2007**) 2821-2860.

[40] V.L. Zholobenko, A.Y. Khodakov, M. Imperor-Clerc, D. Durand, I. Grillo, Initial stages of SBA-15 synthesis: An overview, *Adv. Colloid Interface Sci.*, 142 (**2008**) 67-74.

[41] L. Bayne, R.V. Ulijn, P.J. Halling, Effect of pore size on the performance of immobilised enzymes, *Chem. Soc. Rev.*, 42 (**2013**) 9000-9010.

[42] S. Inagaki, Y. Fukushima, K. Kuroda, Synthesis of highly ordered mesoporous materials from a layered polysilicate, *J. Chem. Soc., Chem. Commun.*, (**1993**) 680.

[43] E. Serra, A. Mayoral, Y. Sakamoto, R.M. Blanco, I. Diaz, Immobilization of lipase in ordered mesoporous materials: Effect of textural and structural parameters, *Microporous Mesoporous Mater.*, 114 (**2008**) 201-213.

[44] P.T. Tanev, T.J. Pinnavaia, A neutral templating route to mesoporous molecular sieves, *Science*, 267 (**1995**) 865-867.

[45] S.A. Bagshaw, E. Prouzet, T.J. Pinnavaia, Templating of mesoporous molecular sieves by nonionic polyethylene oxide surfactants, *Science*, 269 (**1995**) 1242-1244.

[46] D.Y. Zhao, Q.S. Huo, J.L. Feng, B.F. Chmelka, G.D. Stucky, Nonionic triblock and star diblock copolymer and oligomeric surfactant syntheses of highly ordered, hydrothermally stable, mesoporous silica structures, *J. Am. Chem. Soc.*, 120 (**1998**) 6024-6036.

[47] D.Y. Zhao, J.L. Feng, Q.S. Huo, N. Melosh, G.H. Fredrickson, B.F. Chmelka, G.D. Stucky, Triblock copolymer syntheses of mesoporous silica with periodic 50 to 300 angstrom pores, *Science*, 279 (**1998**) 548-552.

[48] C.-M. Yang, B. Zibrowius, W. Schmidt, F. Schüth, Consecutive Generation of Mesopores and Micropores in SBA-15, *Chem. Mat.*, 15 (**2003**) 3739-3741.

[49] T. Yamada, H.S. Zhou, K. Asai, I. Honma, Pore size controlled mesoporous silicate powder prepared by triblock copolymer templates, *Mater. Lett.*, 56 (**2002**) 93-96.

[50] Q.S. Huo, R. Leon, P.M. Petroff, G.D. Stucky, Mesostructure design with gemini surfactants - supercage formation in a 3-dimensional hexagonal array, *Science*, 268 (**1995**) 1324-1327.

[51] K. Kosuge, T. Sato, N. Kikukawa, M. Takemori, Morphological control of rod- and fiberlike SBA-15 type mesoporous silica using water-soluble sodium silicate, *Chem. Mater.*, 16 (**2004**) 899-905.

[52] T. Klimova, A. Esquivel, J. Reyes, M. Rubio, X. Bokhimi, J. Aracil, Factorial design for the evaluation of the influence of synthesis parameters upon the textural and structural properties of SBA-15 ordered materials, *Microporous Mesoporous Mater.*, 93 (**2006**) 331-343.

[53] Z.W. Jin, X.D. Wang, X.G. Cui, Synthesis and morphological investigation of ordered SBA-15-type mesoporous silica with an amphiphilic triblock copolymer template under various conditions, *Colloids Surf., A*, 316 (**2008**) 27-36.

[54] W.H. Zhang, L. Zhang, J.H. Xiu, Z.Q. Shen, Y. Li, P.L. Ying, C. Li, Pore size design of ordered mesoporous silicas by controlling micellar properties of triblock copolymer EO(20)PO(70)EO(20), *Microporous Mesoporous Mater.*, 89 (**2006**) 179-185.

[55] C.V. Teixeira, H. Amenitsch, P. Linton, M. Linden, V. Alfredsson, The Role Played by Salts in the Formation of SBA-15, an in Situ Small-Angle X-ray Scattering/Diffraction Study, *Langmuir*, 27 (**2011**) 7121-7131.

[56] P.F. Fulvio, S. Pikus, M. Jaroniec, Tailoring properties of SBA-15 materials by controlling conditions of hydrothermal synthesis, *Journal of Materials Chemistry*, 15 (**2005**) 5049-5053.

[57] J.L. Ruggles, E.P. Gilbert, S.A. Holt, P.A. Reynolds, J.W. White, Expanded mesoporous silicate films grown at the air-water interface by addition of hydrocarbons, *Langmuir*, 19 (**2003**) 793-800.

[58] P. Schmidt-Winkel, W.W. Lukens, D.Y. Zhao, P.D. Yang, B.F. Chmelka, G.D. Stucky, Mesocellular siliceous foams with uniformly sized cells and windows, *J. Am. Chem. Soc.*, 121 (**1999**) 254-255.

[59] P. Schmidt-Winkel, C.J. Glinka, G.D. Stucky, Microemulsion templates for mesoporous silica, *Langmuir*, 16 (**2000**) 356-361.

[60] J.S. Lettow, Y.J. Han, P. Schmidt-Winkel, P.D. Yang, D.Y. Zhao, G.D. Stucky, J.Y. Ying, Hexagonal to mesocellular foam phase transition in polymer-templated mesoporous silicas, *Langmuir*, 16 (**2000**) 8291-8295.

[61] J.C. Park, J.H. Lee, P. Kim, J. Yi, in: S.E. Park, R. Ryoo, W.S. Ahn, C.W. Lee, J.S. Chang (Eds.) Nanotechnology in Mesostructured Materials**2003**, pp. 109-112.

[62] H. Zhang, J.M. Sun, D. Ma, X.H. Bao, A. Klein-Hoffmann, G. Weinberg, D.S. Su, R. Schlogl, Unusual mesoporous SBA-15 with parallel channels running along the short axis, *J. Am. Chem. Soc.*, 126 (**2004**) 7440-7441.

[63] J.M. Sun, H. Zhang, D. Ma, Y.Y. Chen, X.H. Bao, A. Klein-Hoffmann, N. Pfander, D.S. Su, Alkanes-assisted low temperature formation of highly ordered SBA-15 with large cylindrical mesopores, *Chem. Comm.*, (**2005**) 5343-5345.

[64] H. Zhang, J.M. Sun, D. Ma, G. Weinberg, D.S. Su, X.H. Bao, Engineered complex emulsion system: Toward modulating the pore length and

morphological architecture of mesoporous silicas, *J. Phys. Chem. B*, 110 (**2006**) 25908-25915.

[65] M. Kruk, L. Cao, Pore size tailoring in large-pore SBA-15 silica synthesized in the presence of hexane, *Langmuir*, 23 (**2007**) 7247-7254.

[66] L. Cao, T. Man, M. Kruk, Synthesis of Ultra-Large-Pore SBA-15 Silica with Two-Dimensional Hexagonal Structure Using Triisopropylbenzene As Micelle Expander, *Chem. Mater.*, 21 (**2009**) 1144-1153.

[67] L. Cao, M. Kruk, Synthesis of large-pore SBA-15 silica from tetramethyl orthosilicate using triisopropylbenzene as micelle expander, *Colloids Surf., A*, 357 (**2010**) 91-96.

[68] L. Cao, M. Kruk, Facile method to synthesize platelet SBA-15 silica with highly ordered large mesopores, *J. Colloid Interf. Sci.*, 361 (**2011**) 472-476.

[69] M. Kruk, Access to ultralarge-pore ordered mesoporous materials through selection of surfactant/swelling-agent micellar templates, *Acc. Chem. Res.*, 45 (**2012**) 1678-1687.

[70] A. Sayari, M. Kruk, M. Jaroniec, Characterization of microporous-mesoporous MCM-41 silicates prepared in the presence of octyltrimethylammonium bromide, *Catal. Lett.*, 49 (**1997**) 147-153.

[71] M. Kruk, M. Jaroniec, A. Sayari, Relations between pore structure parameters and their implications for characterization of MCM-41 using gas adsorption and X-ray diffraction, *Chem. Mater.*, 11 (**1999**) 492-500.

[72] J. Liu, X.D. Feng, G.E. Fryxell, L.Q. Wang, A.Y. Kim, M. Gong, Hybrid mesoporous materials with functionalized monolayers, *Chemical Engineering & Technology*, 21 (**1998**) 97-100.

[73] A. Stein, B.J. Melde, R.C. Schroden, Hybrid inorganic-organic mesoporous silicates - Nanoscopic reactors coming of age, *Adv. Mater.*, 12 (**2000**) 1403-1419.

[74] A.S.M. Chong, X.S. Zhao, Functionalization of SBA-15 with APTES and characterization of functionalized materials, *J. Phys. Chem. B*, 107 (**2003**) 12650-12657.

[75] A.S.M. Chong, X.S. Zhao, A.T. Kustedjo, S.Z. Qiao, Functionalization of large-pore mesoporous silicas with organosilanes by direct synthesis, *Microporous and Mesoporous Materials*, 72 (**2004**) 33-42.

[76] S.S. Park, C.S. Ha, Organic-inorganic hybrid meseporous silicas: Functionalization, pore size, and morphology control, *Chemical Record*, 6 (**2006**) 32-42.

[77] M.H. Lim, A. Stein, Comparative studies of grafting and direct syntheses of inorganic-organic hybrid mesoporous materials, *Chemistry of Materials*, 11 (**1999**) 3285-3295.

[78] F. Hoffmann, M. Cornelius, J. Morell, M. Froeba, Silica-based mesoporous organic-inorganic hybrid materials, *Angew. Chem. Int. Ed.*, 45 (**2006**) 3216-3251.

[79] A. Vinu, K.Z. Hossain, K. Ariga, Recent advances in functionalization of mesoporous silica, *J. Nanosci. Nanotechnol.*, 5 (**2005**) 347-371.

[80] A. Walcarius, M. Etienne, J. Bessière, Rate of Access to the Binding Sites in Organically Modified Silicates. 1. Amorphous Silica Gels Grafted with Amine or Thiol Groups, *Chemistry of Materials*, 14 (**2002**) 2757-2766.

[81] A. Walcarius, M. Etienne, B. Lebeau, Rate of access to the binding sites in organically modified silicates. 2. Ordered mesoporous silicas grafted with amine or thiol groups, *Chemistry of Materials*, 15 (**2003**) 2161-2173.

[82] X. Feng, G.E. Fryxell, L.Q. Wang, A.Y. Kim, J. Liu, K.M. Kemner, Functionalized monolayers on ordered mesoporous supports, *Science*, 276 (**1997**) 923-926.

[83] J. Aguado, J.M. Arsuaga, A. Arencibia, M. Lindo, V. Gascon, Aqueous heavy metals removal by adsorption on amine-functionalized mesoporous silica, *J. Hazard. Mater.*, 163 (**2009**) 213-221.

[84] T. Asefa, M.J. MacLachlan, N. Coombs, G.A. Ozin, Periodic mesoporous organosilicas with organic groups inside the channel walls, *Nature*, 402 (**1999**) 867-871.

[85] S. Inagaki, S. Guan, Y. Fukushima, T. Ohsuna, O. Terasaki, Novel mesoporous materials with a uniform distribution of organic groups and inorganic oxide in their frameworks, *J. Am. Chem. Soc.*, 121 (**1999**) 9611-9614.

[86] B.J. Melde, B.T. Holland, C.F. Blanford, A. Stein, Mesoporous sieves with unified hybrid inorganic/organic frameworks, *Chem. Mat.*, 11 (**1999**) 3302-3308.

[87] F. Hoffmann, M. Cornelius, J. Morell, M. Froba, Periodic mesoporous organosilicas (PMOs): Past, present, and future, *J. Nanosci. Nanotechnol.*, 6 (**2006**) 265-288.

[88] W.J. Hunks, G.A. Ozin, Challenges and advances in the chemistry of periodic mesoporous organosilicas (PMOs), *J. Mater. Chem.*, 15 (**2005**) 3716-3724.

[89] M. Mandal, M. Kruk, Versatile approach to synthesis of 2-D hexagonal ultra-large-pore periodic mesoporous organosilicas, *J. Mater. Chem.*, 20 (**2010**) 7506-7516.

[90] H.-S. Xia, C.-H. Zhou, D.S. Tong, C.X. Lin, Synthesis chemistry and application development of periodic mesoporous organosilicas, *Journal of Porous Materials*, 17 (**2010**) 225-252.

[91] M. Kuroki, T. Asefa, W. Whitnal, M. Kruk, C. Yoshina-Ishii, M. Jaroniec, G.A. Ozin, Synthesis and properties of 1,3,5-benzene periodic mesoporous organosilica (PMO): Novel aromatic PMO with three point attachments and unique thermal transformations, *Journal of the American Chemical Society*, 124 (**2002**) 13886-13895.

[92] N. Mizoshita, T. Tani, S. Inagaki, Syntheses, properties and applications of periodic mesoporous organosilicas prepared from bridged organosilane precursors, *Chem. Soc. Rev.*, 40 (**2011**) 789-800.

[93] P. Van der Voort, D. Esquivel, E. De Canck, F. Goethals, I. Van Driessche, F.J. Romero-Salguero, Periodic Mesoporous Organosilicas: from simple to complex bridges; a comprehensive overview of functions, morphologies and applications, *Chem. Soc. Rev.*, 42 (**2013**) 3913-3955.

[94] M.E. Gimon-Kinsel, V.L. Jimenez, L. Washmon, K.J. Balkus, in: L. Bonneviot, F. Beland, C. Danumah, S. Giasson, S. Kaliaguine (Eds.) Mesoporous Molecular Sieves 1998**1998**, pp. 373-380.

[95] H. Takahashi, B. Li, T. Sasaki, C. Miyazaki, T. Kajino, S. Inagaki, Catalytic activity in organic solvents and stability of immobilized enzymes depend on the pore size and surface characteristics of mesoporous silica, *Chemistry of Materials*, 12 (**2000**) 3301-3305.

[96] Y.J. Han, J.T. Watson, G.D. Stucky, A. Butler, Catalytic activity of mesoporous silicate-immobilized chloroperoxidase, *Journal of Molecular Catalysis B-Enzymatic*, 17 (**2002**) 1-8.

[97] E. Weber, D. Sirim, T. Schreiber, B. Thomas, J. Pleiss, M. Hunger, R. Glaser, V.B. Urlacher, Immobilization of P450 BM-3 monooxygenase on mesoporous molecular sieves with different pore diameters, *J. Mol. Catal. B: Enzym.*, 64 (**2010**) 29-37.

[98] H.H.P. Yiu, P.A. Wright, N.P. Botting, Enzyme immobilisation using siliceous mesoporous molecular sieves, *Microporous and Mesoporous Materials*, 44 (**2001**) 763-768.

[99] M. Hartmann, X. Kostrov, Immobilization of enzymes on porous silicas--benefits and challenges, *Chem. Soc. Rev.*, 42 (**2013**) 6277-6289.

[100] H. Gustafsson, C. Thorn, K. Holmberg, A comparison of lipase and trypsin encapsulated in mesoporous materials with varying pore sizes and pH conditions, *Colloids and Surfaces B-Biointerfaces*, 87 (**2011**) 464-471.

[101] H. Ikemoto, Q. Chi, J. Ulstrup, Stability and Catalytic Kinetics of Horseradish Peroxidase Confined in Nanoporous SBA-15, *J. Phys. Chem. C*, 114 (**2010**) 16174-16180.

[102] L.C. Sang, M.O. Coppens, Effects of surface curvature and surface chemistry on the structure and activity of proteins adsorbed in nanopores, *Physical Chemistry Chemical Physics*, 13 (**2011**) 6689-6698.

[103] L. Washmon-Kriel, V.L. Jimenez, K.J. Balkus, Cytochrome c immobilization into mesoporous molecular sieves, *Journal of Molecular Catalysis B-Enzymatic*, 10 (**2000**) 453-469.

[104] J. Fan, J. Lei, L.M. Wang, C.Z. Yu, B. Tu, D.Y. Zhao, Rapid and high-capacity immobilization of enzymes based on mesoporous silicas with controlled morphologies, *Chem. Commun.*, (**2003**) 2140-2141.

[105] J. Lei, J. Fan, C.Z. Yu, L.Y. Zhang, S.Y. Jiang, B. Tu, D.Y. Zhao, Immobilization of enzymes in mesoporous materials: controlling the entrance to nanospace, *Microporous and Mesoporous Materials*, 73 (**2004**) 121-128.

[106] H. Gustafsson, E.M. Johansson, A. Barrabino, M. Oden, K. Holmberg, Immobilization of lipase from Mucor miehei and Rhizopus oryzae into mesoporous silica-The effect of varied particle size and morphology, *Colloids Surf., B.*, 100 (**2012**) 22-30.

[107] N. Duran, M.A. Rosa, A. D'Annibale, L. Gianfreda, Applications of laccases and tyrosinases (phenoloxidases) immobilized on different supports: a review, *Enzyme Microb. Technol.*, 31 (**2002**) 907-931.

[108] L. Fernando Bautista, G. Morales, R. Sanz, Immobilization strategies for laccase from Trametes versicolor on mesostructured silica materials and the application to the degradation of naphthalene, *Bioresour. Technol.*, 101 (**2010**) 8541-8548.

[109] M. Fernandez-Fernandez, M.A. Sanroman, D. Moldes, Recent developments and applications of immobilized laccase, *Biotechnol Adv*, 31 (**2013**) 1808-1825.

[110] M. Arroyo, J.M. Sanchez-Montero, J.V. Sinisterra, Thermal stabilization of immobilized lipase B from Candida antarctica on different supports: Effect of water activity on enzymatic activity in organic media, *Enzyme Microb. Tech.*, 24 (**1999**) 3-12.

[111] R. Fernandez-Lafuente, P. Armisen, P. Sabuquillo, G. Fernandez-Lorente, J.M. Guisan, Immobilization of lipases by selective adsorption on hydrophobic supports, *Chem. Phys. Lipids*, 93 (**1998**) 185-197.

[112] R.M. Blanco, P. Terreros, M. Fernandez-Perez, C. Otero, G. Diaz-Gonzalez, Functionalization of mesoporous silica for lipase immobilization - Characterization of the support and the catalysts, *J. Mol. Catal. B: Enzym.*, 30 (**2004**) 83-93.

[113] R.M. Blanco, P. Terreros, N. Munoz, E. Serra, Ethanol improves lipase immobilization on a hydrophobic support, *J. Mol. Catal. B: Enzym.*, 47 (**2007**) 13-20.

[114] A. Leonowicz, K. Grzywnowicz, Quantitative estimation of laccase forms in some white-rot fungi using syringaldazine as a substrate, *Enzyme Microb. Technol.*, 3 (**1981**) 55-58.

[115] R. Bourbonnais, D. Leech, M.G. Paice, Electrochemical analysis of the interactions of laccase mediators with lignin model compounds, *Biochimica Et Biophysica Acta-General Subjects*, 1379 (**1998**) 381-390.

[116] A. Leonowicz, N.S. Cho, J. Luterek, A. Wilkolazka, M. Wojtas-Wasilewska, A. Matuszewska, M. Hofrichter, D. Wesenberg, J. Rogalski, Fungal laccase: properties and activity on lignin, *J. Basic Microbiol.*, 41 (**2001**) 185-227.

[117] S. Rodriguez Couto, J.L. Toca Herrera, Industrial and biotechnological applications of laccases: a review, *Biotechnol Adv*, 24 (**2006**) 500-513.

[118] P. Baldrian, Fungal laccases - occurrence and properties, *FEMS Microbiol. Rev.*, 30 (**2006**) 215-242.

[119] A.I. Yaropolov, O.V. Skorobogatko, S.S. Vartanov, S.D. Varfolomeyev, LACCASE - PROPERTIES, CATALYTIC MECHANISM, AND APPLICABILITY, *Applied Biochemistry and Biotechnology*, 49 (**1994**) 257-280.

[120] R.C. Minussi, G.M. Pastore, N. Duran, Potential applications of laccase in the food industry, *Trends Food Sci. Tech.*, 13 (**2002**) 205-216.

[121] E. Chiacchierini, D. Restuccia, G. Vinci, Bioremediation of food industry effluents: Recent applications of free and immobilised polyphenoloxidases, *Food Sci. Technol. Int.*, 10 (**2004**) 373-382.

[122] S. Riva, Laccases: blue enzymes for green chemistry, *Trends Biotechnol.*, 24 (**2006**) 219-226.

[123] O.V. Morozova, G.P. Shumakovich, S.V. Shleev, Y.I. Yaropolov, Laccase-mediator systems and their applications: A review, *Appl. Biochem. Microbiol.*, 43 (**2007**) 523-535.

[124] A. Kunamneni, F.J. Plou, A. Ballesteros, M. Alcalde, Laccases and their applications: a patent review, *Recent Pat. Biotechnol.*, 2 (**2008**) 10-24.

[125] K. Brijwani, A. Rigdon, P.V. Vadlani, Fungal laccases: production, function, and applications in food processing, *Enzyme Res.*, 2010 (**2010**) 149748.

[126] T. Kudanga, G.S. Nyanhongo, G.M. Guebitz, S. Burton, Potential applications of laccase-mediated coupling and grafting reactions: a review, *Enzyme Microb. Technol.*, 48 (**2011**) 195-208.

[127] J.-R. Jeon, P. Baldrian, K. Murugesan, Y.-S. Chang, Laccase-catalysed oxidations of naturally occurring phenols: from in vivo biosynthetic pathways to green synthetic applications, *Microbial Biotech.*, 5 (**2012**) 318-332.

[128] R.M. Berka, I.V. Grigoriev, R. Otillar, A. Salamov, J. Grimwood, I. Reid, N. Ishmael, T. John, C. Darmond, M.C. Moisan, B. Henrissat, P.M. Coutinho, V. Lombard, D.O. Natvig, E. Lindquist, J. Schmutz, S. Lucas, P. Harris, J. Powlowski, A. Bellemare, D. Taylor, G. Butler, R.P. de Vries, I.E. Allijn, J. van den Brink, S. Ushinsky, R. Storms, A.J. Powell, I.T. Paulsen, L.D. Elbourne, S.E. Baker, J. Magnuson, S. Laboissiere, A.J. Clutterbuck, D. Martinez, M. Wogulis, A.L. de Leon, M.W. Rey, A. Tsang, Comparative genomic analysis of the thermophilic biomass-degrading fungi Myceliophthora thermophila and Thielavia terrestris, *Nat. Biotechnol.*, 29 (**2011**) 922-929.

[129] R.M. Berka, P. Schneider, E.J. Golightly, S.H. Brown, M. Madden, K.M. Brown, T. Halkier, K. Mondorf, F. Xu, Characterization of the gene encoding an extracellular laccase of Myceliophthora thermophila and analysis of the recombinant enzyme expressed in Aspergillus oryzae, *Appl. Environ. Microbiol.*, 63 (**1997**) 3151-3157.

[130] J.I. Lopez-Cruz, G. Viniegra-Gonzalez, A. Hernandez-Arana, Thermostability of native and pegylated Myceliophthora thermophila laccase in aqueous and mixed solvents, *Bioconjug. Chem.*, 17 (**2006**) 1093-1098.

[131] N. Hakulinen, L.L. Kiiskinen, K. Kruus, M. Saloheimo, A. Paananen, A. Koivula, J. Rouvinen, Crystal structure of a laccase from Melanocarpus albomyces with an intact trinuclear copper site, *Nature Structural Biology*, 9 (**2002**) 601-605.

[132] K. Nie, F. Xie, F. Wang, T. Tan, Lipase catalyzed methanolysis to produce biodiesel: Optimization of the biodiesel production, *J. Mol. Catal. B: Enzym.*, 43 (**2006**) 142-147.

[133] B.D. Ribeiro, A.M. de Castro, M.A. Coelho, D.M. Freire, Production and use of lipases in bioenergy: a review from the feedstocks to biodiesel production, *Enzyme Res.*, 2011 (**2011**) 615803.

[134] C. Jose, G.B. Austic, R.D. Bonetto, R.M. Burton, L.E. Briand, Investigation of the stability of Novozym (R) 435 in the production of biodiesel, *Catal. Today*, 213 (**2013**) 73-80.

[135] P. Trodler, J. Pleiss, Modeling structure and flexibility of Candida antarctica lipase B in organic solvents, *BMC Struct. Biol.*, 8 (**2008**) 9.

[136] J. Uppenberg, M.T. Hansen, S. Patkar, T.A. Jones, The sequence, crystal structure determination and refinement of two crystal forms of lipase B from Candida antarctica, *Structure*, 2 (**1994**) 293-308.

[137] M. Martinelle, M. Holmquist, K. Hult, On the interfacial activation of Candida antarctica lipase A and B as compared with Humicola lanuginosa lipase, *Biochim. Biophys. Acta, Lipids Lipid Metab.*, 1258 (**1995**) 272-276.

[138] C.H. Kwon, D.Y. Shin, J.H. Lee, S.W. Kim, J.W. Kang, Molecular Modeling and its experimental verification for the catalytic mechanism of Candida antarctica lipase B, *J. Microbiol. Biotechn.*, 17 (**2007**) 1098-1105.

[139] B.C. Koops, E. Papadimou, H.M. Verheij, A.J. Slotboom, M.R. Egmond, Activity and stability of chemically modified Candida antarctica lipase B adsorbed on solid supports, *Appl. Microbiol. Biot.*, 52 (**1999**) 791-796.

[140] S. Volden, A.R. Moen, W.R. Glomm, T. Anthonsen, J. Sjoeblom, Immobilization of Lipases from Candida antarctica. Influence of Surface Polarity on Adsorption and Transesterification Activity, *J. Disper. Sci. Technol.*, 30 (**2009**) 865-872.

[141] L.P.V. Calsavara, F.F. De Moraes, G.M. Zanin, Comparison of catalytic properties of free and immobilized cellobiase Novozym 188, *Applied Biochemistry and Biotechnology*, 91-3 (**2001**) 615-626.

[142] T. Watanabe, T. Sato, S. Yoshioka, T. Koshijima, M. Kuwahara, PURIFICATION AND PROPERTIES OF ASPERGILLUS-NIGER BETA-GLUCOSIDASE, *European Journal of Biochemistry*, 209 (**1992**) 651-659.

[143] Y.R. Jung, H.Y. Shin, Y.S. Song, S.B. Kim, S.W. Kim, Enhancement of immobilized enzyme activity by pretreatment of β-glucosidase with cellobiose and glucose, *Journal of Industrial and Engineering Chemistry*, 18 (**2012**) 702-706.

[144] R. Mazzei, L. Giorno, E. Piacentini, S. Mazzuca, E. Drioli, Kinetic study of a biocatalytic membrane reactor containing immobilized β-glucosidase for the hydrolysis of oleuropein, *Journal of Membrane Science*, 339 (**2009**) 215-223.

[145] M.T. Reetz, Entrapment of biocatalysts in hydrophobic sol-gel materials for use in organic chemistry, *Advanced Materials*, 9 (**1997**) 943-&.

[146] I. Gill, A. Ballesteros, Encapsulation of biologicals within silicate, siloxane, and hybrid sol-gel polymers: An efficient and generic approach, *Journal of the American Chemical Society*, 120 (**1998**) 8587-8598.

[147] M. Mureseanu, A. Galarneau, G. Renard, F. Fajula, A new mesoporous micelle-templated silica route for enzyme encapsulation, *Langmuir*, 21 (**2005**) 4648-4655.

[148] Y. Wei, H. Dong, J.G. Xu, Q.W. Feng, Simultaneous immobilization of horseradish peroxidase and glucose oxidase in mesoporous sol-gel host materials, *Chemphyschem*, 3 (**2002**) 802-+.

[149] J.L. Blin, C. Gerardin, C. Carteret, L. Rodehuser, C. Selve, M.J. Stebe, Direct one-step immobilization of glucose oxidase in well-ordered mesostructured silica using a nonionic fluorinated surfactant, *Chemistry of Materials*, 17 (**2005**) 1479-1486.

[150] A. Macario, M. Moliner, A. Corma, G. Giordano, Increasing stability and productivity of lipase enzyme by encapsulation in a porous organic-inorganic system, *Microporous and Mesoporous Materials*, 118 (**2009**) 334-340.

[151] S. Urrego, E. Serra, V. Alfredsson, R.M. Blanco, I. Díaz, Bottle-around-the-ship: A method to encapsulate enzymes in ordered mesoporous materials, *Microporous Mesoporous Mater.*, 129 (**2010**) 173-178.

[152] E. Santalla, E. Serra, A. Mayoral, J. Losada, R.M. Blanco, I. Díaz, In-situ immobilization of enzymes in mesoporous silicas, *Solid State Sciences*, 13 (**2011**) 691-697.

OBJETIVOS

2. OBJETIVOS

Este trabajo de investigación se enmarca en el ámbito del desarrollo de estrategias adecuadas para optimizar la **inmovilización y estabilización de enzimas de marcado interés industrial en materiales silíceos mesoporosos**. Concretamente, el objetivo fundamental es el estudio de las características de distintos materiales sintetizados como soportes para la inmovilización de enzimas, dado el interés en las posibilidades de aplicación de estos biocatalizadores. El proyecto de Tesis se ha planteado desde el punto de vista del diseño de materiales silíceos mesoporosos ordenados (MMO), y el estudio de las interacciones de las enzimas con estos soportes de distintas estructuras y distinta naturaleza química de sus superficies.

Los objetivos globales planteados al inicio de la tesis doctoral han sido:

1. **Inmovilización en MMO mediante el método post-síntesis**: Para el desarrollo de este objetivo se han sintetizado materiales MMO con diferentes morfologías de partícula y tamaños de poro, y se han utilizado como soportes para tres enzimas distintas: lacasa, lipasa y β-glucosidasa, para utilizarlos en ensayos de actividad catalíticos.

2. **Encapsulación "*in situ*" de las enzimas dentro de materiales mesoporosos ordenados**. Para abordar este propósito se han utilizado surfactantes y condiciones de síntesis adecuadas para la encapsulación de lacasa y β-glucosidasa. Mediante la correcta selección de los surfactantes y aditivos (n-butilamina, agentes expansores de micelas, sales inorgánicas) se han obtenido micelas diferentes alrededor de las moléculas de enzimas actuando estas como plantillas del sistema y obteniendo diferentes cavidades con distinto tamaño.

3. **Caracterización**. Se han empleado técnicas de caracterización de materiales con el objetivo de optimizar el proceso de síntesis, para ello se ha realizado una detallada caracterización fisicoquímica de los biocatalizadores obtenidos, principalmente mediante técnicas de difracción de rayos X, adsorción-desorción de nitrógeno, microscopía electrónica de barrido y de transmisión, análisis químico y análisis termogravimétrico. También técnicas de bioquímica: como ensayos de actividad catalítica, cuantificación e identificación de las moléculas proteicas (por Bradford y electroforesis, respectivamente).

4. **Evaluación de las propiedades catalíticas**. Todos los biocatalizadores se han ensayado para evaluar su estabilidad en frente a disolventes orgánicos y temperatura. Además se ha evaluado la resistencia de las enzimas al lixiviado, y el efecto del pH en la actividad enzimática. Los biocatalizadores de lacasa se han evaluado preliminarmente en reacciones de oxidación de fenoles, de gran interés en la industria del vino, donde la oxidación de fenoles es necesaria para su polimerización y obtención de taninos (presentan actividad antioxidante que conduce a la protección contra enfermedades cardiovasculares, trastornos inmunes y enfermedades neurodegenerativas).

PUBLICACIONES CIENTIFICAS

CAPÍTULO 1

Mesoporous silicas with tunable morphology for the immobilization of laccase

Victoria Gascón, Isabel Díaz, Carlos Márquez-Álvarez and Rosa M. Blanco

Published in *Molecules*, 2014, vol. 19, pp. 7057-7071.
DOI: 10.3390/molecules19067057

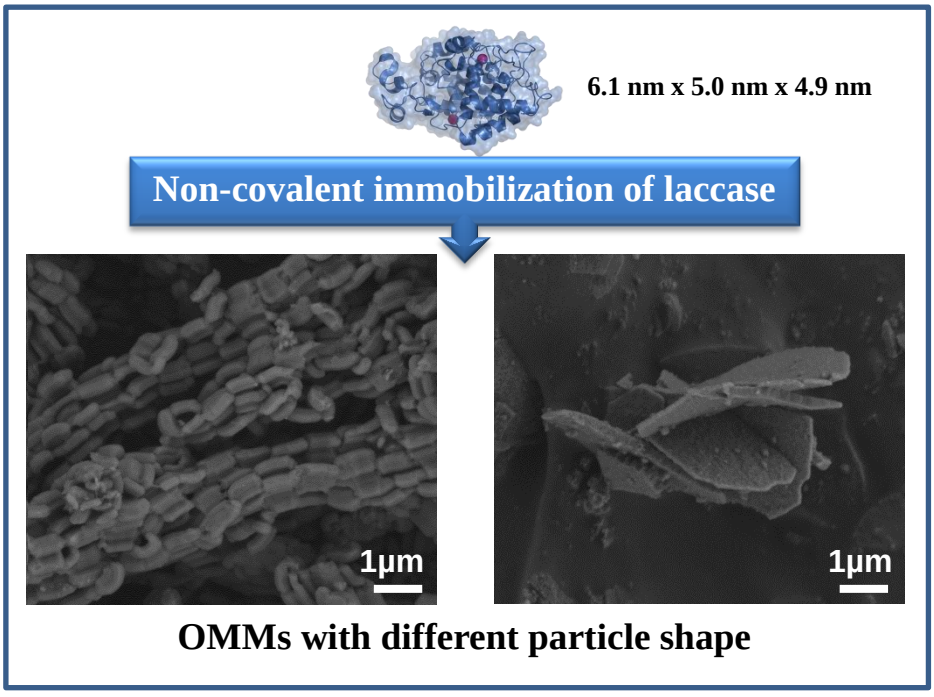

V. Gascón, Dra. I. Diaz, Dr. C. Márquez-Álvarez y Dra. R. M. Blanco. Instituto de Catálisis y Petroleoquímica. ICP-CSIC. C/ Marie Curie 2, 28049 Madrid, Spain.

ABSTRACT

Siliceous ordered mesoporous materials (OMM) are gaining interest as supports for enzyme immobilization due to their uniform pore size, large surface area, tunable pore network and the introduction of organic components to mesoporous structure. We used SBA-15 type silica materials, which exhibit a regular 2D hexagonal packing of cylindrical mesopores of uniform size, for non-covalent immobilization of laccase. Synthesis conditions were adjusted in order to obtain supports with different particle shape, where those with shorter channels had higher loading capacity. Despite the similar isoelectric points of silica and laccase and the close match between the size of laccase and the pore dimensions of these SBA-15 materials, immobilization was achieved with very low leaching. Surface modification of macro-/mesoporous amorphous silica by grafting of amine moieties was proved to significantly increase the isoelectric point of this support and improve the immobilization yield.

Keywords: amorphous silica; biocatalysts; enzyme immobilization; functionalization; grafting; laccase; MS-3030; ordered mesoporous materials; SBA-15; support.

1. INTRODUCTION

Siliceous ordered mesoporous materials (OMMs) are gaining interest as supports for enzyme immobilization because of their uniform and tunable pore size and large surface area, which make them excellent hosts for the adsorption of bulky molecules like enzymes [1-5]. OMMs are thermally, mechanically and chemically stable and insoluble in the solution used for the immobilization process and their surface can be grafted with different functionalities [6-10]. The immobilization of enzymes in functionalized OMMs can increase the operational stability, durability and importantly, the catalyst particles can be easily separated and reused without loss of catalytic activity [11, 12].

To evaluate the suitability of a mesoporous material for enzyme immobilization the following factors are to be considered: pore diameter, surface area, pore volume, particle size, morphology, as well as surface modification. The effects of pore size and enzyme-support material interactions have demonstrated to have significant roles in the enzyme loading and activity. Surface chemical modification of the support could further enhance interactions between the pore walls and the enzyme [12]. In addition, the diffusion phenomena related to particle size are greatly affected by the support morphology [4, 13].

Enzymes can be immobilized in mesoporous materials by different methods: adsorption, covalent attachment or encapsulation [4]. Covalent attachment is not advisable when pore size is close to enzyme dimension because of a “stopper” effect which may result in low immobilization yield, and always requires chemical modification of the enzyme which may result in catalytic activity decay. Adsorption seems more suitable because both drawbacks are avoided. However the driving forces of non-covalent immobilization are relatively weak interactions and, therefore, a careful design of the mesoporous support is necessary.

Laccases (E.C. 1.10.3.2) are a group of multicopper enzymes of industrial interest that catalyze the oxidation of phenolic compounds such as ortho- and para-diphenols to their corresponding quinones with the concomitant reduction of oxygen to water [14-18]. Their potential as biocatalysts for use in several biotechnological processes, in nanobiotechnology applications, in food processing and in green chemistry [19-26] is

limited by their low operational stability, mostly due to their rapid inactivation by different factors [12].

In this article we deal with the synthesis of SBA-15 type mesoporous silica supports with different particle morphology offering improved diffusional properties. SBA-15 with conventional rod type of particles, showing long channels (SBA-15-L) is compared with hexagonal particles formed by short mesochannels (SBA-15-S). Finally, we evaluate the incorporation of amine groups in large pore-size amorphous silica via grafting method (MS-3030-N). The morphology of SBA-15 structure, the effect of aminopropyl surface groups on the laccase immobilization behavior and detailed characterization results will be discussed in order to shed some light on the immobilization of enzymes. The laccase immobilization yields on pure silicas and the functionalized amorphous silica, specific activity measurements as well as enzyme leaching tests of immobilized laccase are also reported.

2. EXPERIMENTAL SECTION

2.1. Synthesis of the supports

Synthesis of SBA-15-L. Pure silica SBA-15 with elongated rod particles was synthesized by using Pluronic P123 triblock copolymer according to the bibliography [27]. First, Pluronic P123 (4 g) was dissolved at room temperature in 1.9 M aqueous HCl solution (125 mL). The resulting solution was slowly stirred at 25 °C until the solution became clear. TEOS (9.25 mL) was then added to the solution and the resulting mixture was vigorously stirred at 40 °C for 20 h. Aging was then performed at 110 °C under static conditions for 24 h in a closed Teflon container. Finally, the white solid product was recovered by filtration, washed with water, air dried at room temperature and calcined at 550 °C in air for 5 h in a furnace for removal of the surfactant.

Synthesis of SBA-15-S. Pure silica SBA-15 with dish-shaped particles was synthesized using Pluronic PE-10400 as structure directing agent and with tetramethylorthosilicate (TMOS) as the silica source. This material has prepared according to the method reported by Linton *et al.* [28, 29]. PE-10400 (2.5 g) was dissolved in 1.6 M aqueous HCl solution (97.5 g). The mixture was stirred at room

temperature in a closed Teflon container until a homogeneous clear solution was obtained. Then, the solution was heated at 55 °C for 1 h, after which TMOS (3.8 g) was added and stirred vigorously at 55 °C for 24 h. Subsequently, the container was transferred to an oven and kept at 80 °C for 24 h under static conditions. The resultant product was filtered, washed thoroughly with dry ethanol and air-dried at room temperature overnight. Finally, the surfactant template was removed by calcination at 550 °C for 5 h in air.

Functionalization of MS-3030 by grafting with aminopropyl groups (MS-3030-N). Commercial mesoporous amorphous silica material, MS-3030 manufactured by PQ Corporation (Conshohocken, PA, USA), was functionalized with aminopropyl groups by silanization reaction of surface silanol groups with aminopropyltriethoxysilane (APTES) [8, 30]. Silica powder (5 g) was placed in a round bottom flask and degassed at 80 °C under vacuum for 20 h to remove adsorbed water [7]. This dried material was dispersed in dry toluene (100 mL), and APTES (25 g) was added under constant stirring. The reaction mixture was refluxed under stirring at atmospheric pressure in a nitrogen atmosphere for 24 h. After a slow cooling of the reaction mixture, the resulting amino-functionalized material was recovered by filtration, washed twice with dry toluene for removal of unreacted reagent, followed by three times with acetone, and finally dried under vacuum for 24 h.

2.2. Characterization techniques

X-ray diffraction (XRD) patterns were acquired with a X'PERT diffractometer (PANalytical, Almelo, The Netherlands) using the Cu-K_α (λ = 1.5406 Å) radiation. The data were registered with two theta step size 0.02° and accumulation time 20 s. Transmission electron micrographs (TEM) were obtained on a JEM-2100 electron microscope (JEOL, Akishima, Japan) operated at 200 kV. A small amount of sample powder was dispersed in ethanol and dropped on a holey carbon coated copper grid. Scanning electron microscopy (SEM) images were collected with a Nova NanoSEM 230 FE-SEM microscope (FEI, Eindhoven, The Netherlands) with vCD detector. The samples were prepared by placing material powder on double-sided graphite adhesive tape mounted on the sample holder. Nitrogen adsorption-desorption isotherms were measured at −196 °C on an ASAP 2420 device (Micromeritics, Norcross, GA, USA). All calcined silicas before enzyme immobilization were outgassed at 350 °C for 16 h

under high vacuum prior to the measurements. The specific surface area, S_{BET}, was calculated from nitrogen adsorption data in the relative pressure range from 0.04 to 0.2 using the BET (Brunauer-Emmett-Teller) method. The total pore volume, V_p, was determined from the amount of nitrogen adsorbed at a relative pressure of 0.97. Pore size distributions were determined from the adsorption branch of the N_2 isotherms using the BJH (Barrett-Joyner-Halenda) model with cylindrical geometry of the pores. The BJH pore diameter, $D_{p\ BJH}$, is defined as the position of the maximum of the pore size distribution. Quantitative determination of the nitrogen content of organo-functionalized support was performed using a CHNS-932 Elemental Analyser (LECO Corporation, St. Joseph, MI, USA) with an AD-4 autobalance (Perkin Elmer, Shelton, CT, USA). Thermogravimetric analyses were carried out using a TGA 7 instrument (Perkin Elmer). Samples were heated in air atmosphere from 25 to 900 °C at a rate of 20 °C/min (*see Supplementary Information* SI 1).

2.3. Protein determination and activity assay

Protein content of commercial laccase extract was determined with the Bio-Rad Protein Assay (Bio-Rad, München, Germany), based on the Bradford assay [31], using bovine serum albumin (BSA) as protein standard. This extract was found to contain a protein concentration of 1.3 mg/mL. Electrophoresis (lane 2 in Figure 9) showed a unique band, so all protein was assigned to laccase.

Enzymatic activity of free and immobilized laccase was determined spectrophotometrically by measuring the increase in absorbance at 530 nm caused by the oxidation of syringaldazine in the presence of atmospheric oxygen to tetramethoxyazobis(methylene) quinone [32, 33], using an 8453 UV-Vis spectrophotometer (Agilent Technologies, Waldbronn, Germany) equipped with a stirring device and temperature control. The reaction mixture consisted of 2200 µL of potassium dihydrogen phosphate/disodium hydrogen phosphate buffer (pH 6.5, 100 mM), 60 µL of 1 mM syringaldazine solution dissolved in ethanol. 100 µL of enzyme solution, suspension or supernatant, were added to the cuvette containing the above substrate solution under stirring and the reaction was monitored continuously for 5 min by measuring the absorption at 530 nm at 30 °C. One laccase activity unit (*U*) is defined as the amount of enzyme required to oxidize 1 µmol of syringaldazine per

minute at 30 °C (ε_{530} nm = 65,000 M^{-1} cm^{-1}). Each sample was measured three times, and the average value was used.

2.4. Immobilization of laccase on mesoporous silicates

Immobilization of laccase on purely siliceous supports, namely SBA-15-L, SBA-15-S and MS-3030, was performed by suspending the materials in enzyme solutions at pH 3.5 (50 mM citric acid/trisodium citrate buffer). Amino-functionalized material, MS-3030-N, was suspended in laccase solutions in 50 mM acetic acid/sodium acetate buffer at pH 5.5.

To 10 mL enzyme solutions (containing 2.5 mg laccase), the support (50 mg) was added and left in suspension under slow rotation at room temperature to allow immobilization to occur by adsorption. Aliquots were withdrawn at given times, and the enzymatic activity of the suspension and supernatant were analyzed by the syringaldazine oxidation assay. The decrease in activity of the supernatant to a minimum and constant value indicated the end point of the immobilization process. At this equilibrium point, the solid was filtered off and washed with 50 mM buffer (at the same pH as used for immobilization, pH 3.5 or 5.5). The solid samples were first dried under vacuum and afterwards under dry nitrogen stream, and then stored at 4 °C in the refrigerator for later analysis. A mass balance was applied to calculate the amount of enzyme immobilized on the supports.

To evaluate the enzymatic activity of laccase immobilized on mesoporous silicas, 10 mg of the respective dried biocatalysts were resuspended in 1 mL of 50 mM buffer (pH 3.5 for biocatalysts prepared with purely siliceous supports or pH 5.5 for those on amino-silica supports) and analyzed for remaining laccase activity by the syringaldazine oxidation assay.

2.5. Immobilized laccase leaching tests

To measure the leaching of laccase from the supports, samples of the solid containing the enzyme were suspended in 50 mM acetic acid/sodium acetate at pH 4.5 and the solid/liquid ratio was 1.25 mg/mL. At different times aliquots of the suspensions were withdrawn and centrifuged, and the protein content of the supernatants was measured according to Bradford assay [31].

2.6. SDS-PAGE electrophoresis

An attempt to verify the location of laccase inside the porous network of the materials was made. Since solid samples are not suitable for electrophoresis, the enzyme was forced to exit the pores. First, the laccase immobilized on different materials was suspended in buffered solutions for 24 h at pH 4.5 as described above to desorb all protein molecules adsorbed on the external surface of support particles. The filtered solids were suspended in electrophoresis sample buffer (containing sodium dodecyl sulfate, mercaptoethanol, bromophenol blue, Tris/HCl buffer pH 6.8 and glycerol) in the same amounts as in electrophoresis samples, and boiled for 5 min. In such denaturing conditions, the tertiary structure of the protein should be lost and the lineal peptide chain should then be easily released from the pores. The supernatants of these suspensions after centrifuging were withdrawn and analyzed by SDS-PAGE electrophoresis [34].

3. RESULTS AND DISCUSSION

3.1. Characterization of supports

The SBA-15 materials were characterized by X-ray diffraction, scanning and transmission electron microscopy to evaluate the morphology and internal structure of the particles, and nitrogen adsorption, to obtain the textural properties of the supports.

X-ray diffraction patterns of the SBA-15 materials synthesized with different surfactants, conditions and silica sources corroborated the 2D *p6mm* mesostructure with a unit cell parameter a_o of 11.1 nm (*Supplementary Information* SI 2). The desired effect of morphology modification was observed by scanning electron microscopy. SEM images of SBA-15-L and SBA-15-S are shown in Figure 1. The structure of SBA-15-L particles is fiber-like or elongated rod, formed by aggregates of rods connected into ropelike macrostructures (Figure 1 A). The average particle size is 0.75–1 μm in length and about 2 μm in width (Figure 1 B, C). SBA-15-S particles exhibit hexagonal dish-shaped morphology or short rod (Figure 1 D–F). The average particle size is 5 μm in diameter and 0.2 μm width. Moreover, the alignment of channels with the axial direction of the rod-like particles on SBA-15-L and SBA-15-S could be corroborated by transmission electron microscopy (TEM).

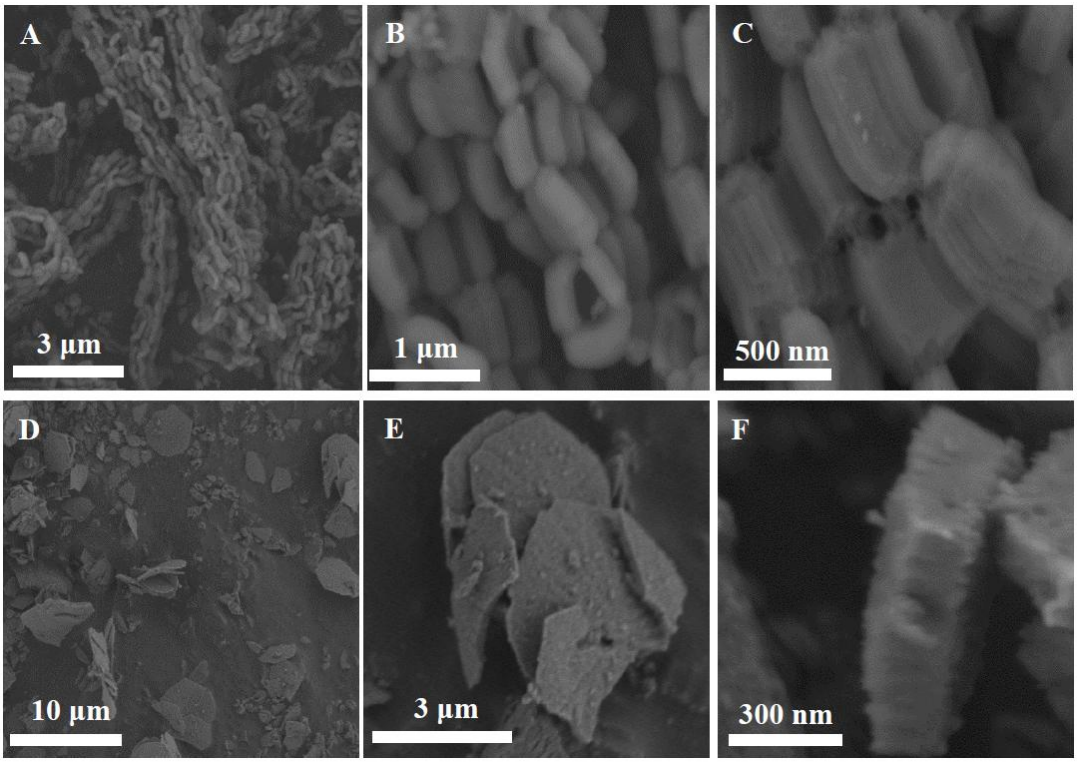

Figure 1. SEM micrographs of mesoporous silicas: SBA-15-L (**A**–**C**), SBA-15-S (**D**–**F**).

Figure 2 displays representative TEM images of these materials showing the projection in the direction perpendicular to the channels in the longitudinal axis of sample SBA-15-L (Figure 2 A). The hexagonal symmetry of the pores, like a honeycomb, characteristic of this kind of symmetry is also observed when the image is taken in the direction parallel to the mesochannels and along the short axis of the dish in sample SBA-15-S (Figure 2 B). In both cases, the images allow observing the respective morphology, long rods in SBA-15-L and hexagonal dishes in SBA-15-S.

XRD patterns of commercial amorphous silica, MS-3030, and amino-functionalized sample, MS-3030-N, show disordered structure with no reflections at low diffraction angles (*data not shown*). These materials were used to compare the effect of the structure and pore diameter with OMMs. Figure 3 shows the SEM images of MS-3030 (Figure 3 A) and MS-3030-N (Figure 3 B) revealing fragmented spherical particles with diameter around 74 µm, indicating that there is no alteration in silica morphology after amine-functionalization with aminopropyltriethoxysilane (APTS).

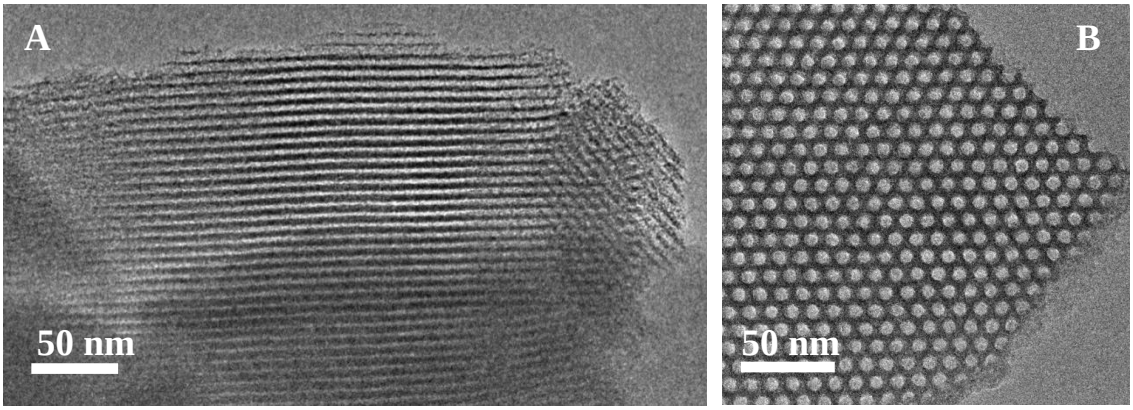

Figure 2. TEM images of calcined SBA-15-L in the direction perpendicular to the pore axis (**A**) and SBA-15-S in the direction of the pore axis (**B**).

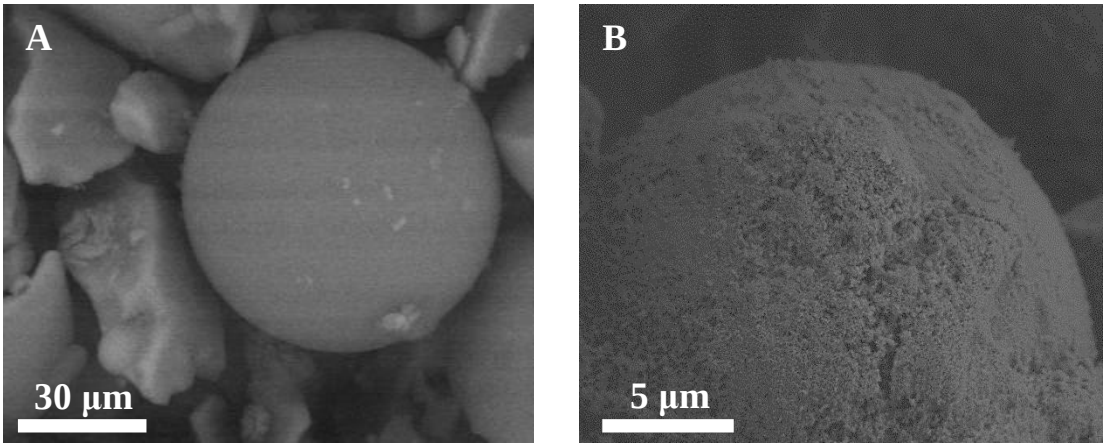

Figure 3. SEM micrographs of amorphous silicas: MS-3030 (**A**) and MS-3030-N (**B**).

SBA-15-L and SBA-15-S exhibit type IV nitrogen adsorption-desorption isotherms with hysteresis loops of H1 type associated with capillarity condensation at high relative pressure (P/P_o 0.7–0.8), which is characteristic of mesoporous materials with hexagonal arrangement of cylindrical pore channels (Figure 4 A). Pore size distribution curves calculated from the adsorption branch of the isotherms are shown in the inset of Figure 4 A. The curves show very narrow pore size distribution with 7.8 and 6.4 nm mean pore size, respectively. SBA-15-L has a surface are of 609 m^2/g and pore volume of 1.0 cm^3/g and SBA-15-S has 550 m^2/g and 0.7 cm^3/g, respectively.

The N_2 isotherms of amorphous silica before and after functionalization (MS-3030 and MS-3030-N) are shown in Figure 4 B. Both materials exhibited type IV isotherms, corresponding to mesoporous materials. The pore size distribution curves of amorphous materials show a wider range, indicating heterogeneity in the porous

structure with average pore diameter of 30 nm. As compared to MS-3030, MS-3030-N exhibited an expected slight decrease in BET surface area (from 296 to 236 m^2/g) and pore volume (from 2.5 to 2.1 cm^3/g) due to grafting of aminopropyl organic chains. The incorporation of the amine functional groups by grafting has been confirmed by elemental analysis yielding a 1.81 mmol N per gram of SiO_2 in MS-3030-N material.

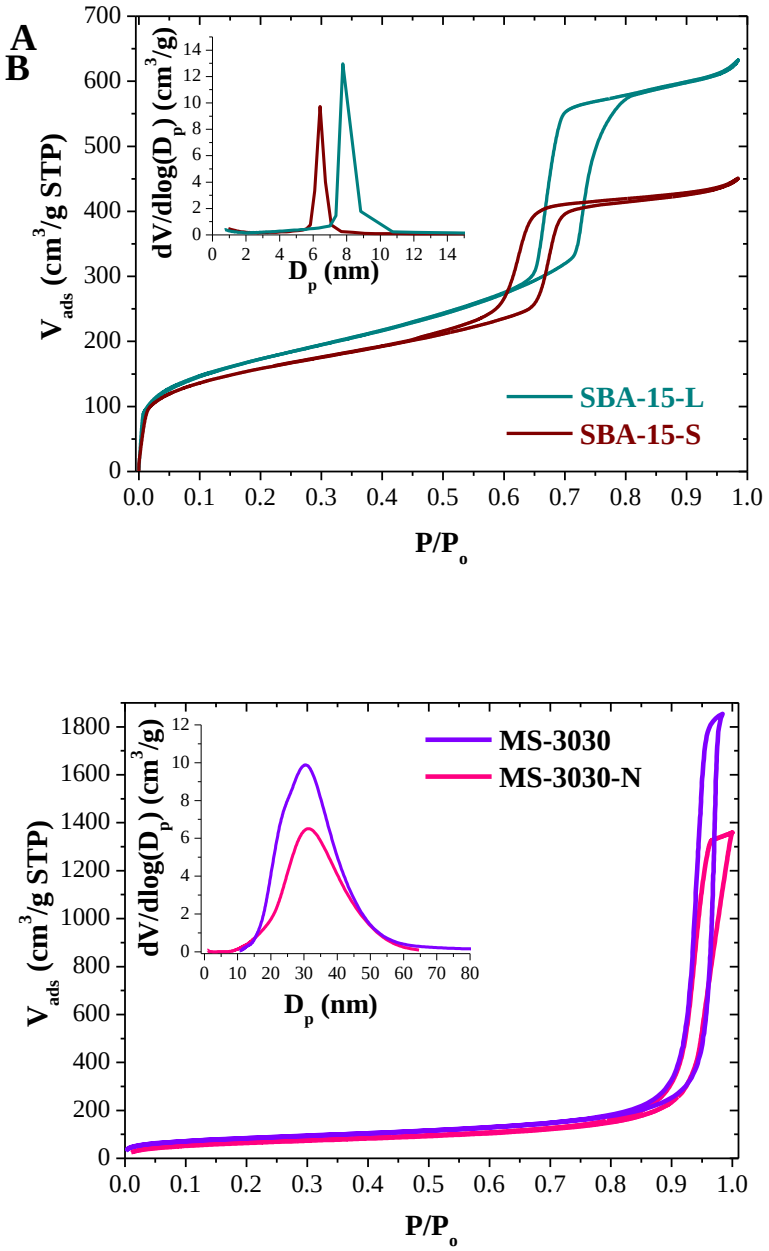

Figure 4. N_2 adsorption-desorption isotherms and pore size distributions: (**A**) SBA-15-L and SBA-15-S; (**B**) MS-3030 and MS-3030-N.

3.2. Immobilization of laccase and specific activity

The laccase used in this work was manufactured by pure culture fermentation of a genetically modified strain of *Aspergillus oryzae* that contains the laccase gene derived from *Myceliophthora thermophila*. Bioinformatics analysis was used to determine the aminoacid sequence and 3D structure of this commercial laccase because the crystal structure is not solved yet and its dimensions have not been reported. An image of the laccase has been reconstructed and visualized using the software package PyMOL [35]. With the use of PyMOL and repeated rotations of the enzyme molecule, the average molecular size of laccase was found to be approximately 6.1 nm × 5.0 nm × 4.9 nm (Figure 5 A).

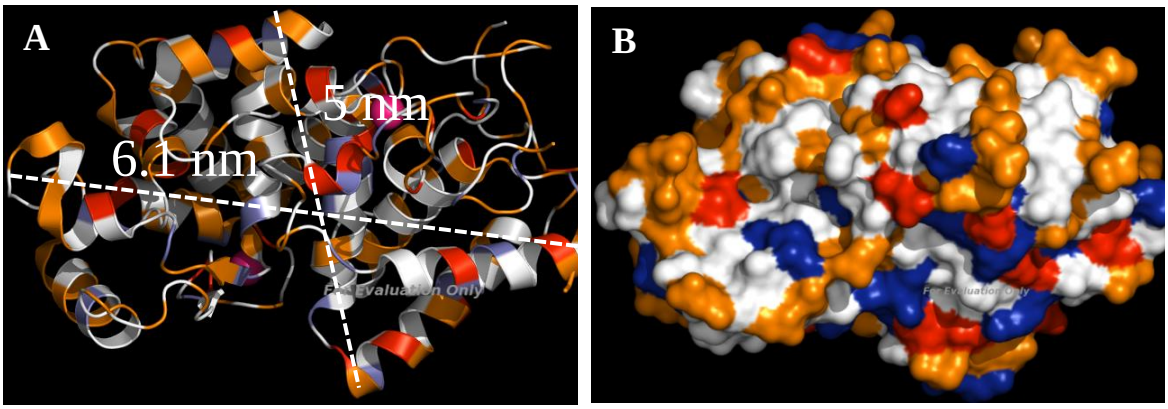

Figure 5. (**A**) Average dimensions of laccase measured in PyMOL (~6.1 nm × 5.0 nm × 4.9 nm). (**B**) Surface distribution of amino acids in laccase constructed in PyMOL (blue, basic amino acids; red, acidic amino acids; orange, polar amino acids; white, nonpolar amino acids; pink, copper atoms).

The molecular weight estimates for the laccase obtained from SDS-PAGE gel electrophoresis is around 80 kDa, consistent with other authors [36]. According to the enzyme dimensions and to the modelling studies and the textural properties of the supports, adsorption inside the pores of SBA-15 materials should be enabled. The surface distribution of amino acids in laccase is displayed in Figure 5 B.

Electrostatic interactions between laccase molecules and the inner mesopore wall were considered for enzyme immobilization. Immobilization of laccase was achieved by suspending purely siliceous materials (SBA-15-L, SBA-15-S and MS-3030) in laccase solution at pH 3.5. In these conditions, laccase molecules bear a positive net

charge (isoelectric point (pI) of laccase is 4.2). The silanol groups inside the mesopores are deprotonated at pH 3.5 bearing a negatively charged surface, because their isoelectric point is about 2.0.

Both ordered materials are similar in textural properties. However, despite the moderately lower surface area and pore diameter of SBA-15-S, this support exhibited moderately higher adsorption capacity compared to SBA-15-L (38.41 mg/g *vs.* 31.28 mg/g). The main difference comes from the different support morphology highlighting the influence of this parameter on laccase immobilization. A schematic illustration is proposed (Figure 6) showing the immobilization of laccase on the two different supports. Laccase dimensions are of similar magnitude than channels pore size, so the presence of an enzyme molecule inside may prevent the access of another one, acting as a stopper or at least making enzyme diffusion more difficult. Therefore, despite the smaller pore diameter of SBA-15-S, its shorter channels (of about 170 nm) can accommodate more enzyme molecules per unit length than the longer ones of SBA-15-L (1,000 nm length) where a part of the inner surface of the channel is not accessible to laccase molecules. This also explains why this material having a higher surface area does not result in a higher immobilization yield. This behavior has also been observed by other authors. According to Fan and coworkers [37], a SBA-15 sample with rod-like macromorphology displays faster loading kinetics and a higher loading capacity for lysozyme than an SBA-15 sample with fiber-like morphology. So, the morphology of OMM particles plays a significant role in the efficiency of enzyme immobilization.

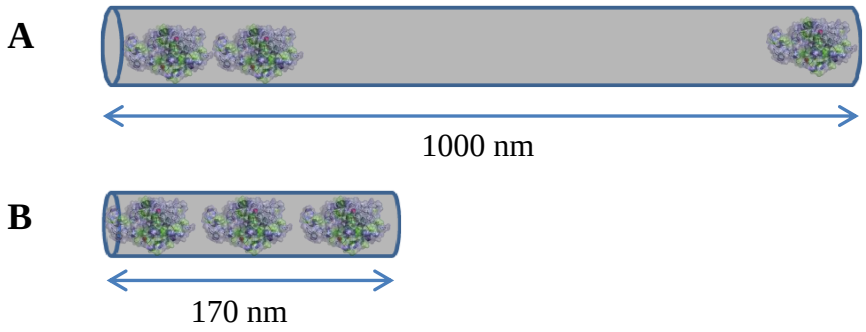

Figure 6. Schematic illustration of the laccase immobilization on SBA-15-L mesochannels (**A**) and SBA-15-S mesochannels (**B**).

Regarding specific activity, the longer channels seem to challenge the diffusion of substrates and products more than the shorter ones, as suggested by the lower value in the long-channel SBA-15-L.

The isoelectric points of the support and the enzyme are close, so the charge densities at pH 3.5 are low. Grafting the support with amine groups shifts its pI to higher value, so the interval becomes larger. Protonated terminal amine groups can interact with deprotonated residues of aspartic acid and glutamic acid (pKa 4) at pH 5.5 which is an intermediate value between isoelectric points of enzyme and amino-modified support, and it is far from these values. Therefore the respective densities of charge should be higher than in the systems enzyme-siliceous supports at pH 3.5. These high charge densities should drive stronger electrostatic interactions and favor the immobilization of laccase. However, the close sizes of enzyme and pore diameter does not enable to functionalize SBA-15 materials while leaving enough room for enzyme diffusion, therefore a commercial siliceous material, MS-3030, with wider pores was used for comparison. The 30 nm average pore size of this amorphous material permits functionalization without compromising the access or diffusion of enzyme molecules. Figure 7 and Table 1 displays the adsorption of laccase on purely siliceous materials (SBA-15-L, SBA-15-S and MS-3030 at pH 3.5) and amine grafted amorphous silica (MS-3030-N at pH 3.5 and pH 5.5) for initial amount of enzyme solution of 50 mg/g support.

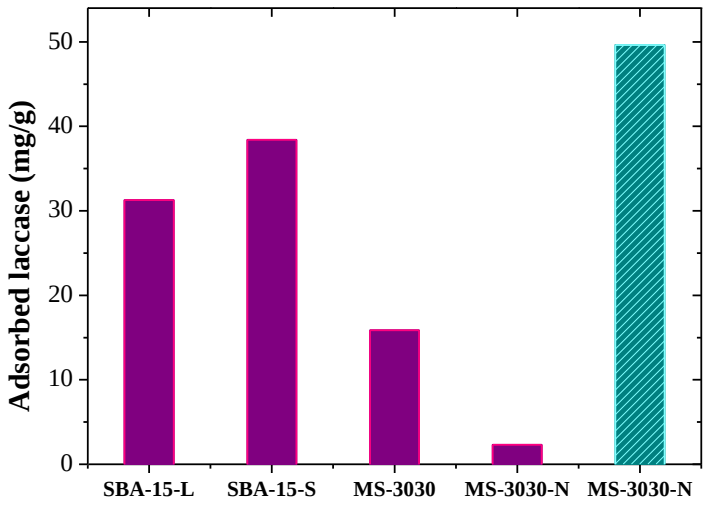

Figure 7. Adsorption capacity of different supports. Solid bars: immobilization at pH 3.5. Dashed bar: immobilization at pH 5.5.

Laccase was also adsorbed on purely siliceous MS-3030 at pH 3.5 with poor results: 15.88 mg/g in the same immobilization time of 3 h. The pore tortuosity and large particle size of this material may result in a slower diffusion of enzyme through the pore network despite the wider average pore size of 30 nm. Immobilization on MS-3030-N at pH 3.5 was negligible (2.32 mg/g, *results not shown*) because of electrostatic repulsion between the positively charged enzyme and the protonated amino groups of the support. However, immobilization on MS-3030-N performed at pH 5.5 gave a 99 % yield despite the surface area is only 296 m^2/g. At this pH, enzyme and support surfaces have opposite charges and high charge densities, which favors strong electrostatic interactions. This phenomenon indicates that amino groups are appropriate for laccase immobilization at a suitable pH.

Table 1. Laccase immobilization characteristics and catalytic results for initial amount of enzyme solution of 50 mg/g support.

Support	pH immob.[a]	t_c (h)[b]	% Immob.[c]	Enzyme loading (mg/g)[d]	Specific activity (*U*/mg)[e]
SBA-15-L	3.5	3	62.56	31.28	0.134
SBA-15-S	3.5	3	76.82	38.41	0.159
MS-3030	3.5	3	31.76	15.88	0.014
MS-3030-N	5.5	3	99.28	49.64	0.981

[*a*] pH of immobilization; [*b*] The time contact (t_c) is the time required to reach a constant activity of the supernatant towards the oxidation of syringaldazine, indicative of maximum loading in the solid; [*c*] percent yield of immobilization; [*d*] The enzyme loading is expressed in milligrams of enzyme per gram of material; [*e*] The specific activity is expressed in units of syringaldazine converted per milligram of enzyme inside the material. Specific activity of soluble laccase: 5.68 *U*/mg.

The activity of the biocatalysts was tested in the oxidation of syringaldazine. Table 1 shows that the presence of the amine moieties in MS-3030-N also improves the specific activity of the laccase. SBA-15-L and SBA-15-S display higher activity than MS-3030, probably due to slower diffusion of substrate and product through the tortuous porous network and the larger particle size of this latter material. In contrast,

SBA-15 materials offer an ordered structure with high pore connectivity and they are assembled with smaller particles than amorphous silica, which should favor a shorter diffusion course [38]. Other authors have also shown that materials with pore sizes much larger than the enzyme size have an adverse effect on enzyme activity [39].

3.3. Leaching test of immobilized laccase

The extent of leaching of laccase from the inner structure of supports in aqueous media and the presence of laccase inside the porous network of the materials after the leaching tests have been studied due to the non-covalent nature of the enzyme-support binding through electrostatic interactions. Biocatalysts were incubated in aqueous solution of low ionic strength buffer and high dilution at pH 4.5. In these conditions, weak repulsion is established between negatively charged SBA-15-L or SBA-15-S and laccase, and weak attraction is still maintained between the positively charged MS-3030-N support and negatively charged laccase. In both cases low ionic strength buffered solution is used just to preserve pH without forcing enzyme leaching due to ionic competition anion-enzyme. These conditions are expected to favor enzyme desorption from the siliceous materials more than from the amino-modified one. Figure 8 summarizes these results, plotting the percentage of the initial enzyme loading leached with time.

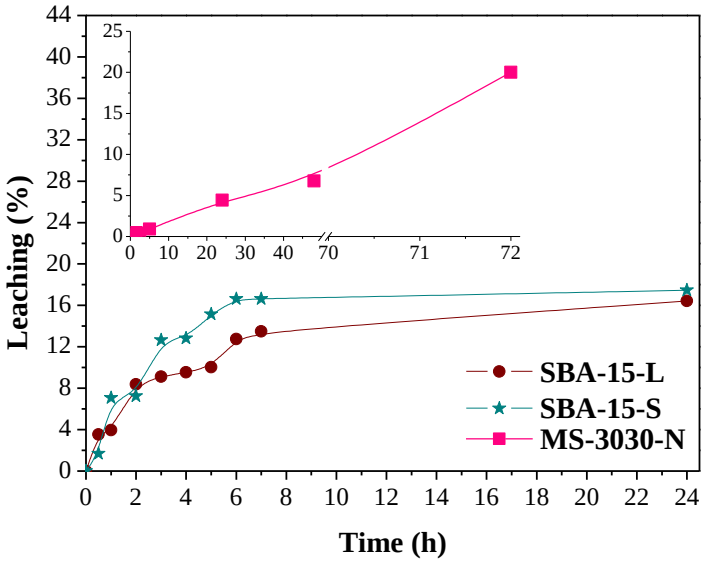

Figure 8. Leaching of enzyme from materials, expressed as percent of the initial enzyme loading released as a function of time.

Two different kinds of patterns can be distinguished. Leaching profile in SBA-15-L and SBA-15-S showed fast initial desorption values and a plateau suggesting that the narrow pore size and confinement of the laccase minimize leaching of the enzyme from the inner surfaces. The first initial slope is probably due to enzyme molecules immobilized on external surfaces or close to the pore edges of the OMM particles.

Despite the electrostatic attraction between the enzyme molecules and functional groups on the surface remaining at pH 4.5, amine amorphous silica (MS-3030-N) shows a continuous and fast release of enzyme, without reaching an equilibrium point in the range of time studied (up to 72 h). This material with much larger pore diameter offers no restriction to enzyme diffusion and is highly susceptible to leaching during the operation. The confinement of the enzyme inside pores seems to be more efficient to prevent leaching than the intensity of interaction with support.

From leaching tests, some laccase molecules seem to be adsorbed on the external surface of SBA-15 particles. In order to check the presence of enzyme inside particles, the biocatalysts previously incubated under the leaching conditions described above were treated in denaturing conditions of SDS-PAGE and their supernatants were assayed for electrophoresis. Linear polypeptide chain should easily exit the pores after this treatment and be detected in the supernatants. Bands were observed for all the samples which confirm that the enzyme is adsorbed inside the pores of amorphous silica and both SBA-15 materials (Figure 9). Leaching profile of MS-3030 is not displayed because laccase molecules were released from the support during biocatalyst washing due to wide pores and weak attraction; moreover the protein band obtained by electrophoresis is very thin (Figure 9, lane 5).

Figure 9. Electrophoresis in standard conditions. **1**: Protein standard (high range SDS-Page standard stained with coomassie G-250 stain; **2**: Soluble laccase; **3**: SBA-15-L; **4**: SBA-15-S; **5**: MS-3030; **6**: MS-3030-N.

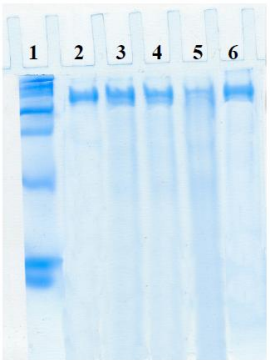

4. CONCLUSIONS

Two similar ordered mesoporous materials with well-defined morphologies and highly uniform particle sizes synthesized using surfactant templates in acidic solutions were tested as supports for laccase immobilization. The morphology of SBA-15 demonstrated to play a significant role in the efficiency of enzyme immobilization. Short SBA-15-S channels proved to be more efficient to carry higher enzyme loading whereas restriction to enzyme diffusion in the longer SBA-15-L channels resulted in lower enzyme loading and higher retention (or less leaching). Also, some restriction to the diffusion of substrate or product may drive a lower specific activity.

The relevance of the pore and particle features was also demonstrated by the comparison with an amorphous meso-macroporous siliceous material, where electrostatic interactions were strengthen by the presence of amine groups. Despite immobilization yield was higher in this material, leaching of the enzyme had no restriction. However, the confinement in SBA-15 channels was more efficient to retain enzyme.

Our results on the immobilization of laccase on ordered mesoporous materials (SBA-15-L and SBA-15-S) demonstrate the importance of matching pore diameter and enzyme dimensions and chemical affinity (MS-3030-N). Efficient immobilization of laccase can be improved when a detailed understanding of the enzyme properties is combined with a tailored design of mesoporous supports. The aim should be now to synthesize ordered mesoporous materials with larger pore diameter and to incorporate amine groups.

5. SUPPLEMENTARY INFORMATION

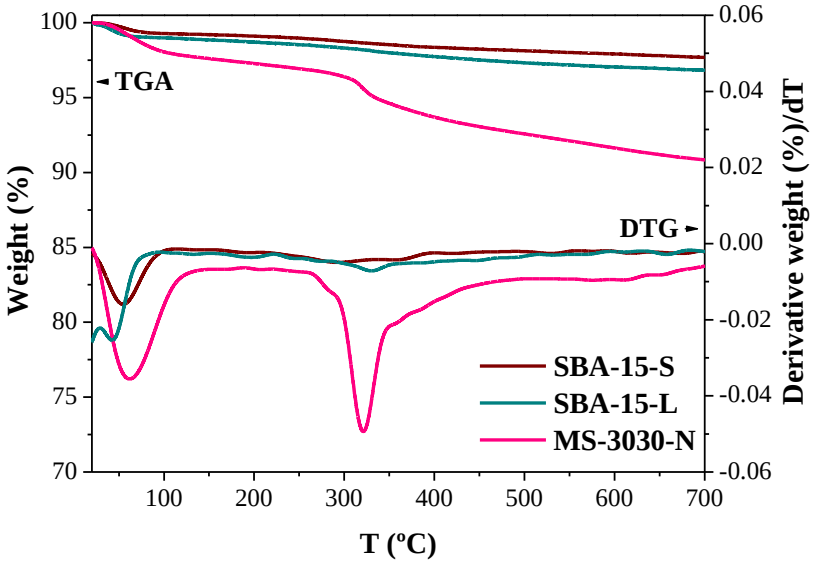

Figure SI 1. TGA and DTG of SBA-15-S, SBA-15-L and MS-3030-N

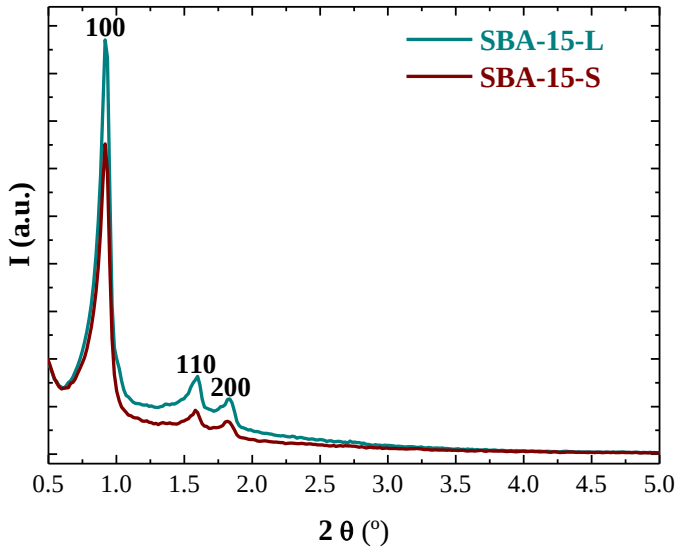

Figure SI 2. Low-angle XRD patterns of SBA-15-L and SBA-15-S supports.

6. REFERENCES

[1] M. Hartmann, Ordered mesoporous materials for bioadsorption and biocatalysis, *Chem. Mater.*, 17 (**2005**) 4577-4593.

[2] S. Hudson, E. Magner, J. Cooney, B.K. Hodnett, Methodology for the immobilization of enzymes onto mesoporous materials, *J. Phys. Chem. B*, 109 (**2005**) 19496-19506.

[3] E. Serra, A. Mayoral, Y. Sakamoto, R.M. Blanco, I. Diaz, Immobilization of lipase in ordered mesoporous materials: Effect of textural and structural parameters, *Microporous Mesoporous Mater.*, 114 (**2008**) 201-213.

[4] M. Hartmann, X. Kostrov, Immobilization of enzymes on porous silicas--benefits and challenges, *Chem. Soc. Rev.*, 42 (**2013**) 6277-6289.

[5] Z. Zhou, M. Hartmann, Progress in enzyme immobilization in ordered mesoporous materials and related applications, *Chem. Soc. Rev.*, 42 (**2013**) 3894-3912.

[6] A.S.M. Chong, X.S. Zhao, Functionalization of SBA-15 with APTES and characterization of functionalized materials, *J. Phys. Chem. B*, 107 (**2003**) 12650-12657.

[7] R.M. Blanco, P. Terreros, M. Fernandez-Perez, C. Otero, G. Diaz-Gonzalez, Functionalization of mesoporous silica for lipase immobilization - Characterization of the support and the catalysts, *J. Mol. Catal. B: Enzym.*, 30 (**2004**) 83-93.

[8] A. Vinu, K.Z. Hossain, K. Ariga, Recent advances in functionalization of mesoporous silica, *J. Nanosci. Nanotechnol.*, 5 (**2005**) 347-371.

[9] J. Aguado, J.M. Arsuaga, A. Arencibia, M. Lindo, V. Gascon, Aqueous heavy metals removal by adsorption on amine-functionalized mesoporous silica, *J. Hazard. Mater.*, 163 (**2009**) 213-221.

[10] G.L. Athens, R.M. Shayib, B.F. Chmelka, Functionalization of mesostructured inorganic–organic and porous inorganic materials, *Curr. Opin. Colloid Interface Sci.*, 14 (**2009**) 281-292.

[11] X.S. Zhao, X.Y. Bao, W. Guo, F.Y. Lee, Immobilizing catalysts on porous materials, *Mater. Today*, 9 (**2006**) 32-39.

[12] D.N. Tran, K.J. Balkus, Perspective of Recent Progress in Immobilization of Enzymes, *ACS Catal.*, 1 (**2011**) 956-968.

[13] Y. Zhou, M.M. Wan, L. Gao, N. Lin, W.G. Lin, J.H. Zhu, One-pot synthesis of a hierarchical PMO monolith with superior performance in enzyme immobilization, *J. Mater. Chem. B*, 1 (**2013**) 1738-1748.

[14] A. Leonowicz, N.S. Cho, J. Luterek, A. Wilkolazka, M. Wojtas-Wasilewska, A. Matuszewska, M. Hofrichter, D. Wesenberg, J. Rogalski, Fungal laccase: properties and activity on lignin, *J. Basic Microbiol.*, 41 (**2001**) 185-227.

[15] A.M. Mayer, R.C. Staples, Laccase: new functions for an old enzyme, *Phytochem. Rev.*, 60 (**2002**) 551-565.

[16] P. Baldrian, Fungal laccases - occurrence and properties, *FEMS Microbiol. Rev.*, 30 (**2006**) 215-242.

[17] A. Kunamneni, F.J. Plou, A. Ballesteros, M. Alcalde, Laccases and their applications: a patent review, *Recent Pat. Biotechnol.*, 2 (**2008**) 10-24.

[18] K. Brijwani, A. Rigdon, P.V. Vadlani, Fungal laccases: production, function, and applications in food processing, *Enzyme Res.*, 2010 (**2010**) 149748.

[19] R.C. Minussi, G.M. Pastore, N. Duran, Potential applications of laccase in the food industry, *Trends Food Sci. Tech.*, 13 (**2002**) 205-216.

[20] S. Rodriguez Couto, J.L. Toca Herrera, Industrial and biotechnological applications of laccases: a review, *Biotechnol Adv*, 24 (**2006**) 500-513.

[21] S. Riva, Laccases: blue enzymes for green chemistry, *Trends Biotechnol.*, 24 (**2006**) 219-226.

[22] O.V. Morozova, G.P. Shumakovich, S.V. Shleev, Y.I. Yaropolov, Laccase-mediator systems and their applications: A review, *Appl. Biochem. Microbiol.*, 43 (**2007**) 523-535.

[23] Y. Li, G. Jiang, J. Niu, Y. Wang, L. Hu, Laccase-Catalyzed Oxidation of Organic Pollutants in Water, *Prog. Chem.* 21 (**2009**) 2028-2036.

[24] J.F. Osma, J.L. Toca-Herrera, S. Rodriguez-Couto, Uses of laccases in the food industry, *Enzyme Res.*, 2010 (**2010**) 918761.

[25] T. Kudanga, G.S. Nyanhongo, G.M. Guebitz, S. Burton, Potential applications of laccase-mediated coupling and grafting reactions: a review, *Enzyme Microb. Technol.*, 48 (**2011**) 195-208.

[26] M. Fernandez-Fernandez, M.A. Sanroman, D. Moldes, Recent developments and applications of immobilized laccase, *Biotechnol Adv*, 31 (**2013**) 1808-1825.

[27] D.Y. Zhao, J.L. Feng, Q.S. Huo, N. Melosh, G.H. Fredrickson, B.F. Chmelka, G.D. Stucky, Triblock copolymer syntheses of mesoporous silica with periodic 50 to 300 angstrom pores, *Science*, 279 (**1998**) 548-552.

[28] P. Linton, V. Alfredsson, Growth and Morphology of Mesoporous SBA-15 Particles, *Chem. Mater.*, 20 (**2008**) 2878-2880.

[29] P. Linton, A.R. Rennie, M. Zackrisson, V. Alfredsson, In situ observation of the genesis of mesoporous silica SBA-15: dynamics on length scales from 1 nm to 1 microm, *Langmuir*, 25 (**2009**) 4685-4691.

[30] A. Stein, B.J. Melde, R.C. Schroden, Hybrid inorganic-organic mesoporous silicates - Nanoscopic reactors coming of age, *Adv. Mater.*, 12 (**2000**) 1403-1419.

[31] M.M. Bradford, A rapid and sensitive method for the quantitation of microgram quantities of protein utilizing the principle of protein-dye binding, *Anal. Biochem.*, 72 (**1976**) 248-254.

[32] A. Leonowicz, K. Grzywnowicz, Quantitative estimation of laccase forms in some white-rot fungi using syringaldazine as a substrate, *Enzyme Microb. Technol.*, 3 (**1981**) 55-58.

[33] A. Sanchez-Amat, F. Solano, A pluripotent polyphenol oxidase from the melanogenic marine Alteromonas sp shares catalytic capabilities of tyrosinases and laccases, *Biochem. Biophys. Res. Commun.*, 240 (**1997**) 787-792.

[34] U.K. Laemmli, Cleavage of structural proteins during the assembly of the head of bacteriophage T4, *Nature*, 227 (**1970**) 680-685.

[35] The PyMOL Molecular Graphics System, http://www.pymol.org/, 14/01/14

[36] R.M. Berka, P. Schneider, E.J. Golightly, S.H. Brown, M. Madden, K.M. Brown, T. Halkier, K. Mondorf, F. Xu, Characterization of the gene encoding an extracellular laccase of Myceliophthora thermophila and analysis of the recombinant enzyme expressed in Aspergillus oryzae, *Appl. Environ. Microbiol.*, 63 (**1997**) 3151-3157.

[37] J. Fan, J. Lei, L.M. Wang, C.Z. Yu, B. Tu, D.Y. Zhao, Rapid and high-capacity immobilization of enzymes based on mesoporous silicas with controlled morphologies, *Chem. Commun.*, (**2003**) 2140-2141.

[38] O. Fernandez, I. Diaz, C.F. Torres, M. Tobajas, V. Tejedor, R.M. Blanco, Hybrid composites octyl-silica-methacrylate agglomerates as enzyme supports, *Appl. Catal., A*, 450 (**2013**) 204-210.

[39] E. Weber, D. Sirim, T. Schreiber, B. Thomas, J. Pleiss, M. Hunger, R. Glaser, V.B. Urlacher, Immobilization of P450 BM-3 monooxygenase on mesoporous molecular sieves with different pore diameters, *J. Mol. Catal. B: Enzym.*, 64 (**2010**) 29-37.

CAPÍTULO 2

Efficient retention of laccase by non-covalent immobilization on amino-functionalized ordered mesoporous silica

Victoria Gascón, Carlos Márquez-Álvarez and Rosa M. Blanco

Published in *Applied Catalysis A: General*, 2014, vol. 482, pp. 116-126.

DOI: 10.1016/j.apcata.2014.05.035

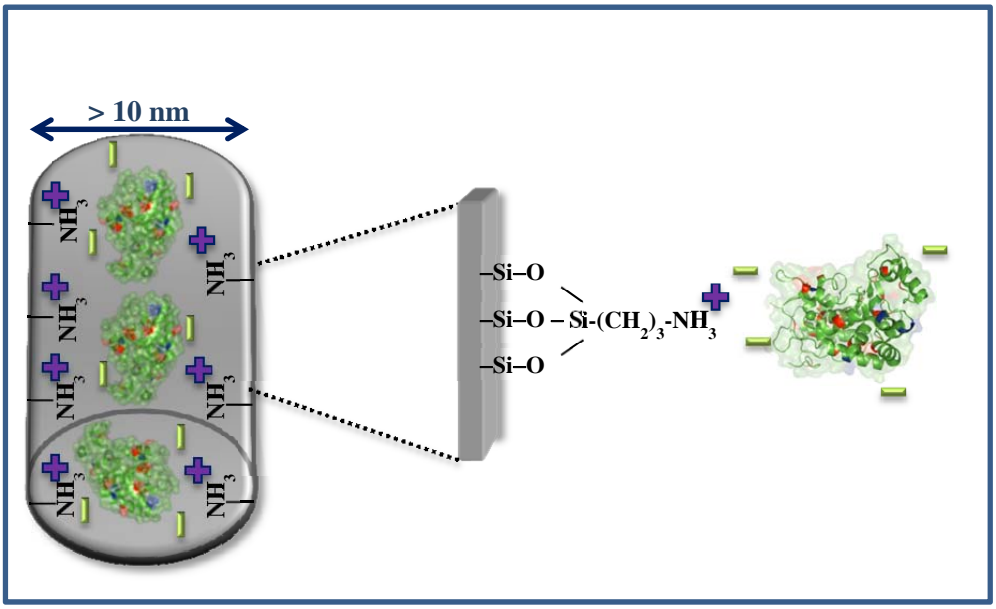

ABSTRACT

The present work aims to be a step forward in the synthesis of siliceous ordered mesoporous materials (OMM) as tailor made matrices to optimize the immobilization and stabilization of enzymes. Based on a classic non-covalent adsorption by electrostatic interactions we have developed the syntheses of materials especially designed for this enzyme, in order to optimize the properties of the final biocatalyst. Siliceous materials with a hexagonal arrangement of parallel mesoporous channels (SBA-15 type of structure) have been synthesized, whose pore diameter has been tuned according to the molecular dimensions of laccase. The synthesis conditions used allowed to obtain pore sizes large enough to permit laccase entrance and diffusion through the pore channels. Diffusion of the enzyme is crucial to obtain high immobilization yield since most of the surface area of the particles is the internal surface of the pores. A poor diffusion would involve retention of enzyme molecules in the pore mouths preventing new ones to access the channel and leading to a low enzyme loading of the catalyst. A micelle swelling agent has been used to expand the supramolecular aggregates that generate the pore architecture of SBA-15 silica. The surfaces of the supports were functionalized with amino groups aiming to strengthen electrostatic interactions between support and enzyme at a suitable pH. Two strategies of surface functionalization of the large-pore ordered mesoporous silica materials were followed: 1) anchoring of an amino-functional alkoxysilane on mesoporous silica and 2) direct co-condensation of a silicon alkoxide and an amino-functional alkoxysilane to obtain the functionalized material in one step. The possibility to prepare carriers where each characteristic has been separately studied and optimized has allowed to obtain biocatalysts with optimal properties. Enzyme loading up to 187 mg per gram of catalyst and high activities were achieved with the amino-functionalized large-pore supports. Furthermore, immobilization improved enzyme stability in ethanol. Strong binding forces were capable of housing and retaining the enzyme irreversibly, fully preventing leaching in aqueous medium. Through the careful design of the support material, the biocatalysts obtained share the advantages of enzyme-support covalent attachment regarding absence of leaching and stability, while avoiding drawbacks like loss of activity and enabling the reuse of the support.

KEYWORDS. Biocatalysts; enzyme immobilization; laccase; large pore; ordered mesoporous materials.

1. INTRODUCTION

The field of ordered mesoporous materials (OMMs) has been progressively growing in the last two decades, and a wide variety of new different types of materials and structures have been obtained [1]. These mesostructured materials have rapidly acquired significant attention in the field of materials science and in many areas of chemistry and biotechnology [2-5]. Using cationic surfactants to template the pore architecture, mesoporous silica materials with well-ordered pore networks were first obtained by Mobil Corporation in 1991 [6, 7]. The possibility to obtain silica with different pore network topologies and the ability to tailor pore size boosted the rapid growth of research activity in this field of materials science. Pore size control in OMMs can be achieved by modifying surfactant type and chain length or by adding a swelling agent [8]. Silica with a pore size of approximately 3 nm can be made using cationic surfactants, with reasonably short alkyl chains [6]. By replacing the cationic head group by a larger non-ionic group, the size of the surfactant micelles can be increased and materials with pore sizes in the range of 5-6 nm are obtained [9]. Even larger surfactants like *polyethyleneoxide-polypropyleneoxide-polyethyleneoxide* triblock copolymers can produce materials with pore sizes of 7 nm and higher such as SBA-15 silica, which possesses a two-dimensional hexagonal structure of cylindrical mesopores [10]. These pore diameters are however not sufficient for the immobilization of large enzymes with high molecular weight. On the other hand, the synthesis of mesoporous silica with large pore size tends to lead to less ordered structures. Making use of this approach, the size of mesopores is limited by the dimensions of the micelle templates, and well-ordered SBA-15 materials with pore size up to 10 nm have been obtained [11]. Other mesostructures, named foam-like (MCF) or worm-like mesoporous molecular sieves, have also been reported showing disordered mesoporous structures with a pore size up to 10 nm, (HMS (D_p = 2-10 nm) [12]; MSU-J (D_p = 2.5-10 nm) [13-15]).

The addition of swelling agents which are dissolved inside the hydrophobic regions of the surfactant micelles allows to further increase the pore diameter of the solid [9, 16]. Hydrophobic swelling agents such as substituted aromatic hydrocarbons (1,3,5-trimethylbenzene, 1,3,5-triisopropylbenzene) or other organic compounds like alcohols (butanol, pentanol, hexanol), aliphatic hydrocarbons (dodecane), tertiary amines, poly(propylene glycol), etc., have been used to expand the pore size of SBA-15 silica up

to 12-15 nm [8, 17, 18]. However, the pore diameter of these materials has to be primarily controlled through the selection of the initial synthesis temperature, and further adjusted through the selection of the hydrothermal treatment temperature and time, as well as the type and amount of the swelling agent [18]. Otherwise, an increase in the amount of the swelling agent causes the formation of a different structure, called a mesocellular foam (foamlike), which is poorly ordered or disordered and features spherical mesopores of large diameter (20–40 nm) [19, 20]. In most cases it results in disordered mesostructures with the loss of the 2D hexagonal ordering [4].

Mesostructured materials offer versatile features, such as high specific surface area, large specific pore volume, narrow pore size distribution, mesopores interconnected by micropores, tunable chemical properties and high chemical and mechanical stability. These unique properties have been previously reported in our group for lipases [21-23]. The aim on this work is to go further in the synthesis of OMM with larger pore sizes which open new possibilities for immobilization of molecules too large to fit into the pores of standard OMM. This is the case of laccase from *Myceliophthora thermophila* (*Mt*L), an enzyme with larger dimensions than lipase.

Laccases (benzenediol:oxygen oxidoreductase, E.C. 1.10.3.2) belong to the group of blue multicopper oxidases, an important class of enzymes found in many organisms, including plants, insects, fungi and bacteria [24-27]. These enzymes catalyse the reduction of molecular oxygen to water by oxidation of various phenolic compounds. The fact that they only require molecular oxygen for catalysis makes them suitable for different applications [26].

In last years, laccases have been used for many different biotechnological processes, such as pulp delignification, oxidation of organic pollutants, textile and petrochemical industries [28], development of biosensors [29], or wine and beverage stabilization [30-34] among other uses [33, 35-37]. Some attempts to use laccase in wine and beer industries have been done [30, 33, 34, 38] and this seems to be an interesting application to study. However, the use of soluble laccase is not allowed in these industries, which highlights the relevance of immobilized enzyme with optimized properties.

Furthermore, the industrial application of free laccases is limited since their stability and catalytic activity are considerably affected by a variety of environmental conditions

[35]. In fact, immobilization allows easy separation from the reaction medium by simple filtration, potential reuse of the biocatalyst and sometimes more resistance of the enzyme to a thermal or chemical inactivation [39].

In this work, a classic enzyme immobilization method on amino-containing surfaces is used. Particularly, the design of ordered mesoporous materials with the exact pore size required by laccase, and the synthesis conditions of this kind of materials also containing amino groups are studied and presented. Pore size is maybe the most relevant parameter; it must be wide enough to enable the enzyme to enter and diffuse along the channels, leaving room for new molecules to enter as well. In the opposite situation, if the enzyme does not diffuse, then the molecules would be stacked in the pore mouths, acting as a stopper and preventing new laccase molecules to enter the pore. As a consequence, most of the inner pore surface would not be occupied by enzyme and the immobilization yield would be low.

Immobilization of laccases on OMM have been reported in the literature with varying degrees of success, mainly due to denaturation processes and restricted diffusion of the substrate [40-42]. We have chosen electrostatic interactions as the driving forces for laccase immobilization. *Mt*L has a low isoelectric point, so we propose in this work the functionalization of the siliceous supports with high pK_a groups (amine) [4, 43] to interact with negative charges of the enzyme [44].

Many research efforts have focused on surface functionalization of mesoporous silica materials with organic groups (such as amine) by the direct incorporation of these functionalities through co-condensation of siloxane and organosiloxane precursors [45, 46] or by post-synthesis grafting of organic groups onto the surface of the mesoporous silica [2, 47]. The presence of these groups in mesoporous materials additionally decreases pore sizes which again makes necessary wider channels [48, 49].

In the present study, we extend the use of the swelling agent 1,3,5-triisopropylbenzene (TIPB) to synthesize large pore ordered materials bearing amine groups. We use the principle of large pore sizes in combination with surface functionalization of mesoporous silicas with amino groups for improving the non-covalent immobilization of laccase.

2. EXPERIMENTAL SECTION

2.1 Materials and Reagents

Chemicals. Triblock co-polymer poly(ethylene oxide)-poly(propylene oxide)-poly(ethylene oxide) Pluronic P123 ($PEO_{20}PPO_{70}PEO_{20}$), from Aldrich (USA), was used as structure directing agent. Tetraethoxysilane (TEOS) (Merck, Germany) and 3-aminopropyltriethoxysilane (APTS) were provided by TCI (Belgium). Ammonium fluoride (NH_4F) and 1,3,5-triisopropylbenzene (TIPB) were from Alfa Aesar (Germany). 2'-azino-bis-(3-ethylbenzothiazoline-6-sulfonic acid) diammonium salt (ABTS) was from Sigma (USA). Amorphous silica MS-3030 was kindly donated by Silica PQ Corporation (USA).

The extract of soluble laccase (Suberase) from *Myceliophthora thermophila* expressed in *Aspergillus oryzae* was kindly donated by Novozymes (Denmark). Bovine serum albumin (BSA, Sigma-Aldrich, USA) was used as protein standard for protein content determination by the Bradford method [50]. The reagents for electrophoresis (SDS-PAGE) and broad molecular weight standards were from Bio-Rad (USA).

Potassium chloride, phosphoric acid, citric acid and toluene were purchased from Sigma-Aldrich (USA). Sodium acetate was purchased from Scharlau (Spain). Sodium di-hydrogen phosphate 1-hydrate, hydrochloric acid, ethanol, acetic acid and acetone were purchased from Panreac (Spain). Tri-sodium citrate dehydrate was from Analyticals Carlo Erba (Italy). Solvents were all analytical or HPLC grade and salts were of high purity. All materials were used as obtained without further purification. Water was grade Milli-Q.

2.2 Synthesis of supports

2.2.1 Synthesis of large-pore SBA-15 silica

The synthesis of ordered mesoporous silica with two-dimensional hexagonal arrangement of pore channels (SBA-15) was carried out using 1,3,5-triisopropylbenzene as micelle expander to obtain a large-pore material. The procedure was based on a previously reported method [8, 18], which was slightly modified. NH_4F was used to facilitate hydrolysis and condensation of the silica source [51]. Typically, 2.4 g of triblock co-polymer Pluronic P123 and 0.027 g of NH_4F were dissolved at room temperature in

84.0 mL of 1.30 M aqueous HCl solution, in a closed container made of Teflon, using a magnetic stirrer. The container was then transferred to a water bath kept at a temperature of 20 ºC and the solution gently stirred for 1 hour to allow for temperature equilibration. Then, a mixture of 5.5 mL of TEOS and 1.2 mL of micelle expander TIPB was added. The white gel obtained was vigorously stirred for 24 h at 20 ºC and subsequently heated at 100 ºC in the closed container under static conditions for 2 days. The mixture was then filtered and the solid product was washed with water and dried at room temperature. Finally, the sample was calcined in a furnace for 5 h at 550 ºC (heating ramp: 2 ºC/min). Complete surfactant removal was verified by thermogravimetric analysis (TGA). This material was labelled as OES (Ordered Expanded Silica).

2.2.2 Synthesis of aminopropyl-functionalized supports by grafting

Large-pore silica (OES) and commercial mesoporous amorphous silica MS-3030 (AS) were functionalized with aminopropyl groups by reaction of surface hydroxyls with APTS. The silica powder (1.1 g) was introduced in a round bottom flask and degassed at 80 ºC under vacuum for 18 h to remove adsorbed water. The dried material was dispersed in 100 mL of dry toluene, then 0.96 mL of 3-aminopropyltriethoxysilane were added and the mixture was refluxed at atmospheric pressure under N_2 for 24 h. The suspension was then filtered, washed twice with dry toluene and three times with acetone and finally dried at room temperature for 24 h. The functionalized nitrogen-bearing supports obtained were designated NGOES (N Grafted Ordered Expanded Silica) and NAS (N Amorphous Silica).

2.2.3 Synthesis of aminopropyl-functionalized silica SBA-15 by co-condensation

Amine-functionalized mesoporous SBA-15 silica obtained by a one-pot synthesis method (co-condensation) was synthesized following the procedure previously reported to incorporate other functional groups into mesostructured silica [23, 46, 52]. The synthesis was performed with the addition of the micelle expander TIPB.

Pluronic P123 (4 g) was dissolved at room temperature in 125 mL of 1.9 M HCl aqueous solution. After cooling to 18 ºC, 8.21 mL of TEOS and 2 mL of TIPB were added to the solution, and the mixture kept under stirring for 45 min. Then, 0.96 mL of APTS were slowly added. The resulting mixture was stirred at 18 ºC for 20 h and then aged at 100 ºC under static conditions for 24 h. The solid product was recovered by filtration and dried at room temperature for 24 h. The surfactant and TIPB were removed

from the material by solvent extraction: 1 g of solid was added to 140 mL of ethanol and refluxed for 24 h, followed by filtration, washing several times with ethanol and drying at room temperature for 24 h. The resultant sample is denoted as NCOES (Nitrogen-bearing Co-condensed Ordered Expanded Silica).

2.3 Characterization

Mesoscopic order was investigated by Low-angle X-Ray Diffraction (XRD). Patterns of the samples were obtained with a Philips X´PERT diffractometer using Cu K_α radiation.

Nitrogen adsorption-desorption isotherms were measured at -196 ºC using the Micromeritics ASAP 2020 and ASAP 2420 sorptometers to determine textural properties. Pure silicas were pretreated at 350 ºC for 16 h and the functionalized supports, at 120 ºC for 16 h. The total pore volume, V_p, was determined from the amount of nitrogen adsorbed at a relative pressure of 0.97. Pore size distributions were determined from the adsorption branches of isotherms using the Barrett-Joyner-Halenda (BJH) model with cylindrical geometry of the pores [53]. The BJH pore diameter, $D_{p\ BJH}$, is defined as the position of the maximum of the pore size distribution.

Quantitative determination of the nitrogen content of organo-functionalized supports was performed using a LECO CHNS-932 Elemental Analyser with a Perkin Elmer AD-4 autobalance.

Thermogravimetric analyses were carried out using a Perkin Elmer TGA 7 instrument Samples were heated in air atmosphere from 25 to 900 ºC at a rate of 20 ºC/min.

Transmission electron micrographs (TEM) were taken using a JEOL 2100 electron microscope operating at 200 kV. The samples for TEM analysis were prepared by suspending a small amount of solid in acetone using sonication in an ultrasonication water bath for 5 min. A drop of this suspension was then dispersed onto a holey carbon film on a copper grid, followed by drying at room temperature.

Scanning electron microscopy (SEM) micrographs were collected with a FE-SEM FEI Nova Nanosem 230 microscope with vCD detector. The samples were prepared by placing material powder on double-sided graphite adhesive tape mounted on the sample holder.

2.4 Laccase activity assay

Laccase activity was determined spectrophotometrically by measuring the increase in absorbance at 405 nm caused by the oxidation of ABTS [36, 54, 55] at 25 ºC, using an Agilent 8453 UV-Vis spectrophotometer equipped with a stirring device and temperature control. The reaction mixture consisted of a 1.6 mM ABTS solution in 100 mM acetic acid/sodium acetate buffer at pH 4.5. To 1.9 mL of this solution in the cuvette, 50 µL of enzyme solution or suspension were added under stirring and the reaction was monitored continuously for 30 min by measuring the absorption at 405 nm. One unit of Laccase (*U*) was defined as the amount of enzyme required to oxidize 1 µmol of ABTS per minute at 25 ºC ($\varepsilon_{405\ nm} = 35{,}000\ M^{-1}\cdot cm^{-1}$).

2.5 Protein determination

Protein content of solutions was determined with the Bio-Rad Protein Assay (Bio-Rad, USA), based on the Bradford assay [50], using bovine serum albumin (BSA) as protein standard. The Suberase commercial extract was found to contain a protein concentration of 3.283 mg/mL.

SDS-polyacrylamide gel electrophoresis (SDS-PAGE) was performed for identification of the enzyme and the purity of the commercial extract [56].

Bioinformatics analysis was used to determine the aminoacid sequence and 3D structure of *Myceliophthora thermophila* laccase (*Mt*L) because the crystal structure is not resolved yet and its dimensions have not been reported. An existing aminoacid sequence from *Mt*L in the NCBI Protein Database [57] (accession number AEO 58496.1) was used as a template to identify homologous sequences of the laccase in BLASTP algorithm [58]. The protein BLAST analysis for *Mt*L showed that it shares high identity (73 %) and high query coverage (99 %) with *Melanocarpus albomyces* laccase (PDB: 1GWO-A) [59, 60].

The 3D structure of *Mt*L was modeled applying the alignment mode on the Swiss model server [58, 61-64] using the three-dimensional structure of the *Melanocarpus albomyces* laccase. The modeled *Mt*L structure has been visualized using Pymol software [65].

The molecular analysis of the whole protein using the tools ProtParam [66], UniProt KB (G2QFD0 and G2Q560) [67, 68] and Brenda [69] showed that it has a molecular weight between 63 and 85 kDa. The predicted isoelectric point (pI) was found to be 4.2. These data do not differ significantly from other authors [70], who reported a molecular weight of 80 kDa for the glycosylated protein and 73 kDa upon deglycosilation, and a pI of 4.2.

Laccase from *Melanocarpus albomyces* (1GWO) has been used to perform an estimation of the molecular dimensions of *Mt* laccase used in this work. These dimensions were calculated from the composition of the peptide chain by simulation using the program PyMOL. From these data, approximate dimensions have been estimated as 6.3 x 7.2 x 8.9 nm.

2.6 Immobilization of laccase on mesoporous silicates

Immobilization of laccase on purely siliceous supports, namely OES and AS, was performed by suspending the materials in enzyme solutions at pH 3.5 (50 mM citric acid/trisodium citrate buffer). Hybrid amino-silica materials NAS, NGOES and NCOES were suspended in laccase solutions in 50 mM acetic acid/sodium acetate buffer at pH 5.5.

To 10 mL enzyme solutions, 50 mg of the respective mesoporous material were added and left in suspension under mild stirring at room temperature to permit immobilization to occur by adsorption. Aliquots were withdrawn at given times, and the enzymatic activity of the suspension and supernatant were analyzed by the ABTS oxidation assay. The decrease in activity of the supernatant to a minimum and constant value indicated the end point of the immobilization process. Protein content of the supernatant was measured to calculate the immobilization yield. At this point, the solid was separated by vacuum filtration using a quartz fritted disk and washed with acetate buffer (50 mM, at the same pH as used for immobilization, 3.5 or 5.5). No protein was detected in these washings. The solid samples were then dried under vacuum and afterwards under dry nitrogen stream, and were stored at 4 ºC for later analysis. For the determination of immobilized enzyme activity, 10 mg of the respective biocatalysts were resuspended in 1 mL 50 mM acetate buffer (pH 3.5 for biocatalysts prepared with purely siliceous supports or pH 5.5

for those on amino-silica supports) and analyzed for remaining laccase activity by the ABTS oxidation assay.

In order to determine the maximum enzyme loading attainable for each support, adsorption isotherms were obtained by carrying out the same immobilization procedure described above with various enzyme to support ratios in the range from 25 to 400 mg/g. Enzyme concentration in the solutions was changed but the final volume was always 10 mL in order to keep a constant solution to support ratio.

2.7 Effect of pH on laccase activity

The activity assays of the free and immobilized laccases were performed as a function of pH at 25 ^{o}C, following the procedure described in section 2.4. ABTS solutions were prepared at pH ranging between 2.5 and 6.0 in 0.05 M phosphoric acid/sodium dihydrogenphosphate (pH 2.0) and 0.05 M citric acid/trisodium citrate (pH 3.0, 3.5, 4.0, 4.5, 5.0, 6.0) at 25 ºC (triplicated). In order to perform enzyme spectrophotometric assays at different pH values, the isosbestic point of oxidized ABTS (ABTS*) was determined. This value was found to be 430 nm. The molar absorption coefficient of ABTS* measured at these wavelength was $\varepsilon_{430\ nm} = 20{,}700\ M^{-1}\ cm^{-1}$, independent of the pH.

2.8 Leaching

The resistance of the enzyme to leach from the support was studied under conditions that presumably favor the release of the protein, namely high dilution and low ionic strength. The catalysts were incubated in 50 mM acetic acid/sodium acetate buffer at pH 4.5 and the solid/total volume ratio was 1.25 mg of solid per mL of buffer. Enzyme-support interactions at this pH are weak and the effect of support structure on leaching prevention can be observed. Enzyme leaching was calculated by monitoring the appearance of enzyme in the supernatant with the Bradford assay [50].

Enzyme molecules immobilized on the external surface of the particles or in the mouths of the pore channels are released more easily than those supposedly immobilized deep inside the pores. It is interesting to check if most of the enzyme is located inside pore channels. Since solid samples are not suitable for electrophoresis, the enzyme was forced to exit the pores. First, the laccase immobilized on different materials (NGOES and NCOES) was suspended in buffered solutions as described above to desorb as much

enzyme as possible, especially to eliminate all protein molecules adsorbed on the external surface of support particles. The supernatants containing the released protein were separated, and the filtered solids were suspended in electrophoresis sample buffer (containing Sodium Dodecyl Sulfate, mercaptoethanol, bromophenol blue, Tris buffer pH 6.8 and glycerol) in the same amounts as in electrophoresis samples, and boiled for 5 min. In such denaturing conditions including the split of disulfide bonds favored by the presence of mercaptoethanol, the tertiary structure of the protein should be lost and the random coil chain should then be easily released from the pores. The supernatants of these suspensions were withdrawn and analyzed by SDS-PAGE electrophoresis. The solids corresponding to samples that did not show bands were again boiled in electrophoresis buffer and filtrated and then additionally suspended for one to two hours in a NaOH solution at pH 11.0. All amino groups from support and enzyme should be deprotonated in these alkaline solution and repulsive forces should be driving the release of protein from pore channels. These new supernatants were also analyzed by SDS-PAGE electrophoresis.

2.9 Thermal stability test

Thermal stability was determined by incubating free or immobilized laccases in 50 mM acetic acid/sodium acetate buffer at pH 3.5 (for biocatalysts supported on purely siliceous materials) or pH 5.5 (for amino-silica supported biocatalysts and free laccase) at 50 ºC for different time periods. Incubations were performed in individual vials for each aliquot to prevent evaporation. The pH values were selected to avoid or minimize enzyme leaching and ensure that the measured activity corresponded only to the immobilized enzyme. Aliquots of the suspensions of the catalysts were withdrawn, cooled and immediately assayed spectrophotometrically in the oxidation of ABTS (λ = 405 nm).

2.10 Evaluation of enzyme stability in the presence of ethanol

The organic medium was selected on the basis of a possible application of the laccase biocatalysts in controlled oxidation of wine polyphenols. Therefore the stability of the enzyme was studied by incubating free and immobilized enzyme at 25 ºC for variable time periods in conditions similar to those of wine, i.e., 10 % v/v ethanol/water solution at

pH 3.5 (50 mM citric acid/trisodium citrate). Incubations were performed in individual vials for each aliquot, thereby preventing evaporation. Then the remaining laccase activity of the suspensions was assayed at 25 ºC in standard conditions with ABTS (λ = 405 nm).

3. RESULTS AND DISCUSSION

Various mesoporous silica and amino-functionalized silica materials with pore diameter larger than 10 nm were synthesized to host the laccase. The pore size of these mesoporous materials was tailored by the addition of a swelling agent (1,3,5-triisopropylbenzene) to expand the Pluronic P123 micelles as described in the experimental section [9, 20, 71, 72]. Commercial amorphous silica (AS) was also used as support for comparison purposes.

3.1 Characterization of the supports

Figure 1 shows the XRD patterns of samples OES, NCOES and NGOES. The diffractogram of sample OES shows three well-resolved peaks corresponding to the 100, 110 and 200 reflections characteristic of the *p6mm* hexagonal symmetry, which confirms that this silica sample possesses a highly ordered SBA-15 type of structure [10, 17]. The diffractogram of sample NGOES indicates that it also possesses a highly ordered 2D hexagonal structure, indicating that grafting of aminopropyl groups on sample OES do not affect the pore ordering. This is also supported by TEM images of sample NGOES that evidence the well-ordered hexagonal arrangement of mesopore channels (Figure 2 *a, b*). In the case of the amino-functionalized silica obtained by co-condensation (sample NCOES), the diffractogram (Figure 1) shows an intense peak at low angle that indicates that this sample is mesostructured. Weak shoulders can also be observed at 2θ angles around 1.5°, which might be assigned to the 110 and 200 reflections of the *p6mm* space group, although the fact that these reflections are not well resolved suggests that pore ordering in sample NCOES might be restricted to smaller domains compared to samples OES and NGOES. Nevertheless, TEM images (Figure 2 *c*, *d*) show that sample NCOES possesses an ordered arrangement of uniform pore channels corresponding to the SBA-15 structure. In contrast to the former samples, the diffractogram of the commercial amorphous silica sample (AS) (not shown) does not exhibit any diffraction peak at low angle, due the lack of pore ordering in this sample [73].

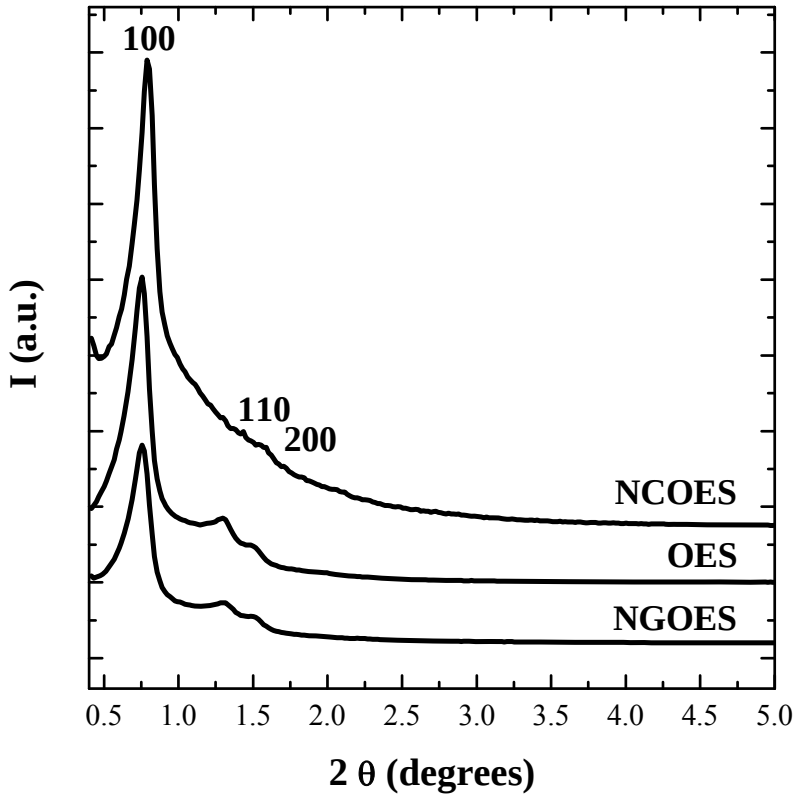

Figure 1. Low-angle XRD patterns of ordered mesoporous silica and amino-functionalized silica supports.

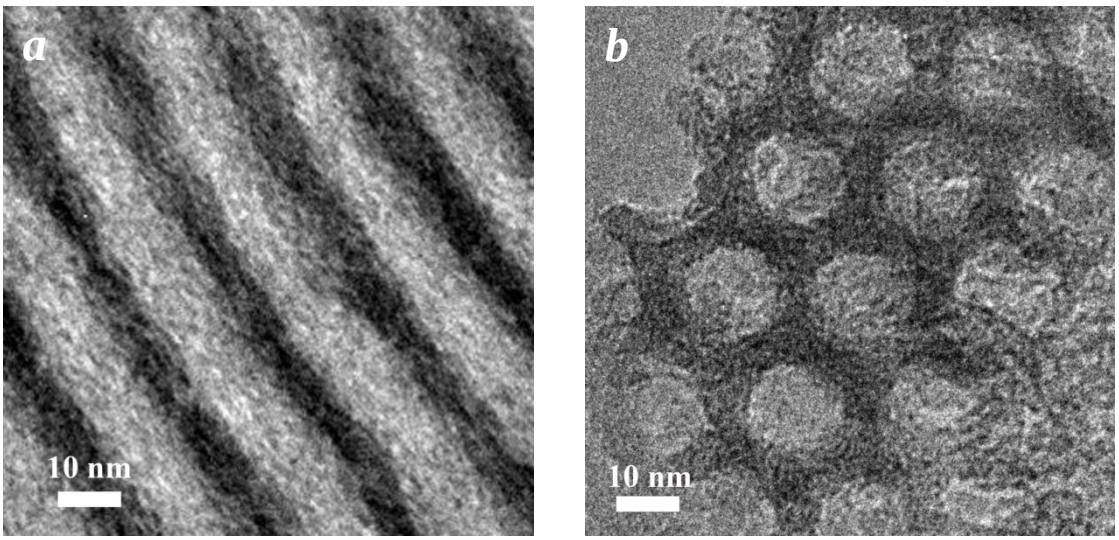

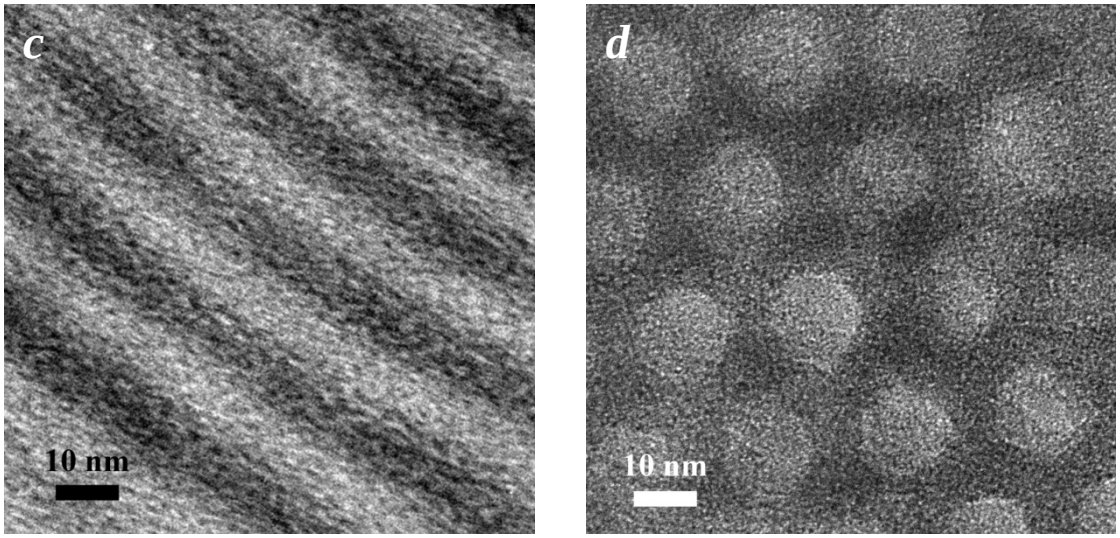

Figure 2. TEM micrographs of samples NGOES (*a*, *b*) and NCOES (*c, d*).

Nitrogen adsorption-desorption isotherms at -196 ºC of the supports are plotted in Figure 3, and their corresponding pore size distributions calculated by the Barrett-Joyner-Halenda (BJH) method are shown in the inset. The isotherms of samples OES, NGOES and NCOES (Fig. 3 *A*) show a steep adsorption step at high relative pressure values and a hysteresis loop corresponding to the capillary condensation in large mesopores [53]. The corresponding BJH plots show narrow pore size distributions as expected for samples having uniform pore size. On the other hand, the isotherms of sample AS and its amino-grafted counterpart (Fig. 3 *B*) show that adsorption in mesopores takes place at higher relative pressure, indicating that these samples contain larger mesopores. Furthermore, their BJH pore size distributions are also much broader than those of the ordered mesoporous supports. Textural properties obtained from the experimental isotherms are collected in Table 1. Nitrogen content of amino-functionalized samples determined by elemental analysis is also reported in Table 1. These values are given as mmol of nitrogen per gram of silicon dioxide, which corresponds to the residual weight determined from the thermogravimetric analyses. The pore diameter determined for sample OES was 15.0 nm, which represents a significant increase respect to the size obtained under similar conditions in the absence of the swelling agent (7.8 nm [74]). Taking into account the estimated dimensions of the enzyme, it is clear that only expanded materials could be used to ensure efficient laccase diffusion inside the pore channels. This is especially the case if pore surfaces of the support have to be functionalized to improve enzyme immobilization, as grafting of the alkoxysilane precursor would additionally decrease the

pore opening. Indeed, the textural data of sample NGOES (Table 1) show that grafting of the OES material with aminopropyl groups led to a decrease of pore size close to 4 nm, along with a small decrease in total pore volume. The decrease of both pore size and total pore volume are consistent with the relatively high loading of aminopropyl moieties obtained, calculated in 1.2 mmol of amine groups per gram of silica, according to the nitrogen content determined by chemical analysis (Table 1).

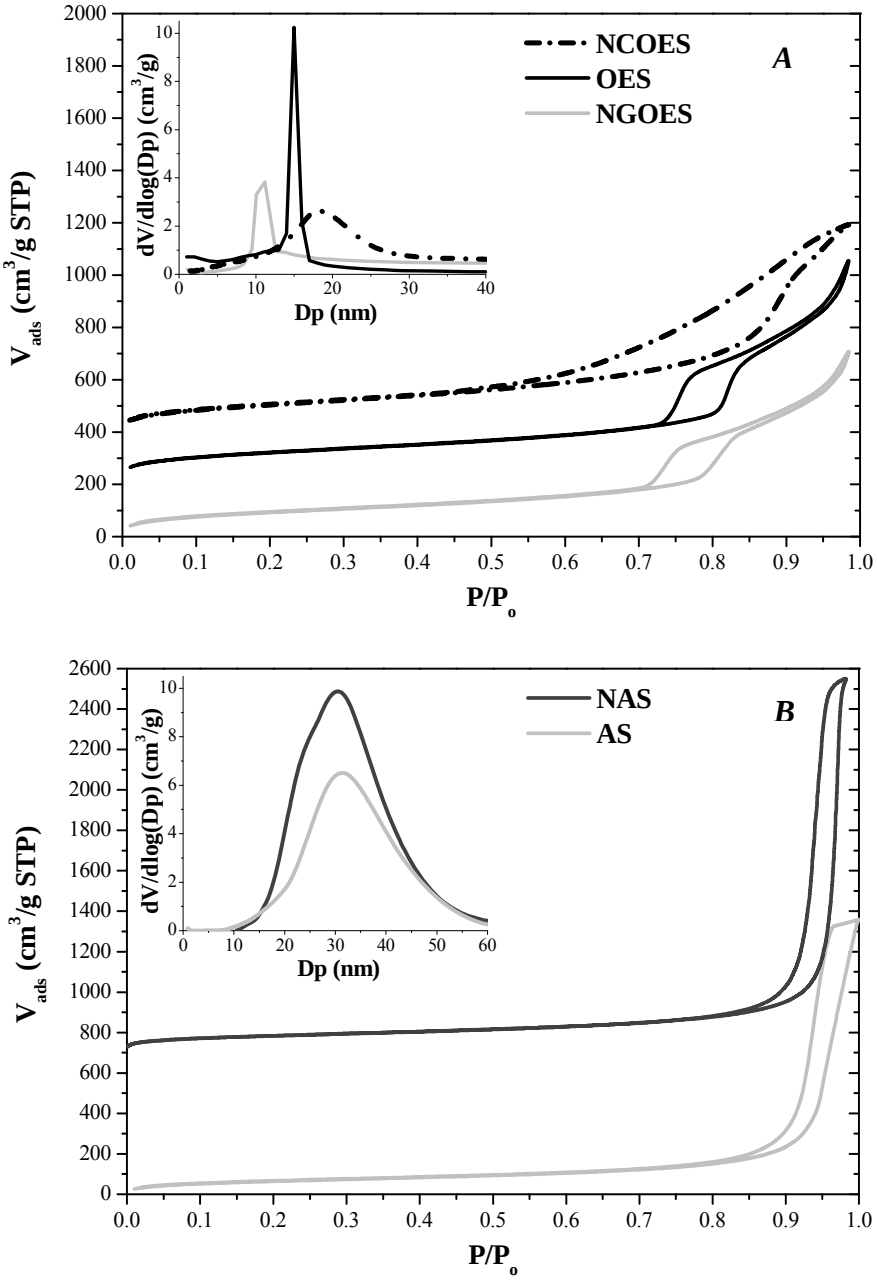

Figure 3. Nitrogen adsorption-desorption isotherms and pore size distributions of mesoporous silica and amino-silica supports. The isotherms have been shifted vertically for clarity (***A)*** NCOES +400; OES +200; NGOES +0. ***B)*** AS +700).

Compared to the two-steps grafting method, the synthesis of the amino-functionalized silica sample by co-condensation allowed to obtain a support with larger pore size and higher pore volume, and with a higher loading of amine groups (Table 1). However, this material exhibits a broader pore size distribution (Figure 3 *A*), which is in agreement with its poorer pore ordering. The amorphous silica sample (AS) exhibits textural properties notably different from those of the ordered mesoporous supports. The BJH pore size distribution (Figure 3 *B*) shows that the former sample possesses pores in the range of 10-60 nm, with the maximum of the distribution around 30 nm. Therefore, it contains larger and less uniform pores. The pore volume of sample AS is also much higher, reaching 2.5 cm^3/g. This sample allows for a large amount of aminopropyl species to be anchored on its surface by grafting, as indicated by the nitrogen content determined for sample NAS (Table 1), equivalent to 1.8 amine groups per gram of silica. As expected, this high level of surface modification produces a substantial decrease of pore volume, which nevertheless remains close to twice the pore volume of the amino-functionalized ordered silica supports. However, the effect on pore size is negligible due to the large pore dimensions.

Table 1. Textural properties and degree of functionalization of the supports, laccase immobilization characteristics and catalytic performance.

Material	$D_{p\ BJH}$[a] (nm)	V_p[b] (cm^3/g)	S_{BET}[c] (cm^3/g)	mmol N/g SiO_2[d]	t_c[e] (h)	Max. loading [f] (mg/g)	Biocatalyst activity [g] (U/g)	Cat. Eff [h] (U/mg)
OES	15.0	1.2	427	-	24	14.2	0.56	0.04
NGOES	11.2	1.0	339	1.2	2.0	170.0	50.7	0.30
NCOES	17.6	1.2	385	1.5	3.5	173.8	56.0	0.32
AS	~30	2.5	296	-	24	15.8	0.52	0.03
NAS	~30	2.1	236	1.8	24	187.1	169.5	0.91

[*a*] BJH pore diameter (nm) calculated from adsorption branch.

[*b*] Pore volume (cm^3/g) estimated at a relative pressure of 0.97.

[*c*] BET surface area (m^2/g).

[*d*] Amine groups incorporated in the silica framework = mmol N/g SiO_2 = (mmol N/g material) / %final weight (TGA)

[*e*] Time at which the maximum enzyme loading is achieved

[*f*] Maximum enzyme loading, expressed in milligrams of enzyme per gram of biocatalysts.

[*g*] Biocatalyst activity (Units/g biocatalysts) in ABTS test.

[*h*] Catalytic efficiency = Activity versus loading (Units/mg enzyme). The activity of enzyme in solution was 1.25 U/mg.

SEM images of samples OES (Fig. S1 *a*) and NGOES (Fig. S1 *b*) show particles with a fiberlike morphology, which consist of small agglomerated rod shaped primary particles of several tens of microns in length and a thickness of about 1 μm. This morphology is characteristic of the material SBA-15 [17]. In contrast, the SEM image of NCOES (Fig. S1 *c*) displays predominantly agglomerated fibrous particles and that of NAS (Fig. S1 *d*) shows fragmented spherical particles several tens of microns in size.

3.2 Laccase immobilization

To carry out the immobilization of the enzyme on the supports by electrostatic interactions, the solids should be suspended in an enzyme solution at a pH intermediate between the isoelectric point of the support and that of the laccase. The pI of purely siliceous supports is 2.0, while that of laccase is 4.2, therefore, the selection of pH 3.5 may allow to establish electrostatic interaction between the positively charged enzyme and the negatively charged support (Figure 4 *A*). However, this pH is very close to pI of both the support and the enzyme, leading to a weak driving force for adsorption, which in turn produces low enzyme loadings, around 14-16 mg per gram of support for samples OES and AS (Table 1).

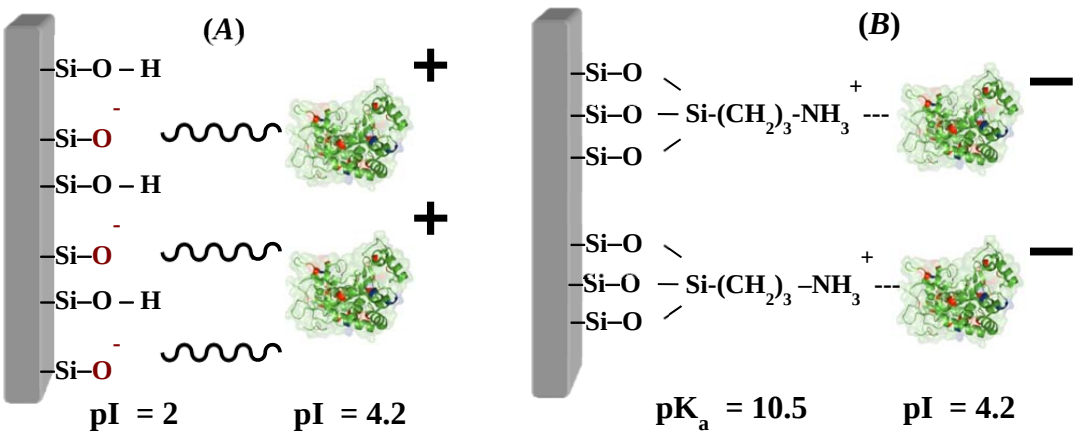

Figure 4. Laccase immobilization on (*A*) siliceous materials without amino groups and (*B*) supports with amino groups.

By introduction of primary amine groups (with pK_a around 10) on the surface of the support, the balance of charges can be reversed and immobilization may be driven in a wider pH range, between 4 and 10, which allows to work at pH values far from the pI of both the support and the enzyme, and thus higher charge density on both species can be established and drive a stronger interaction (Figure 4 *B*).

Immobilization on amino-modified supports was therefore performed at pH 5.5, at which the amino groups of the support are positively charged and the net charge of the enzyme is negative as seen in Figure 4 *B*. Despite this is not the optimal pH for laccase (as further shown), the weak nature of the chemical bonding ensures non or minimal distortion of the enzyme molecule upon immobilization. The different supports were suspended in solutions with increasing enzyme concentrations for immobilization. Figure 5 shows the relationship between the initial amount of enzyme in solution per gram of support in suspension and the actual enzyme loading achieved at adsorption equilibrium.

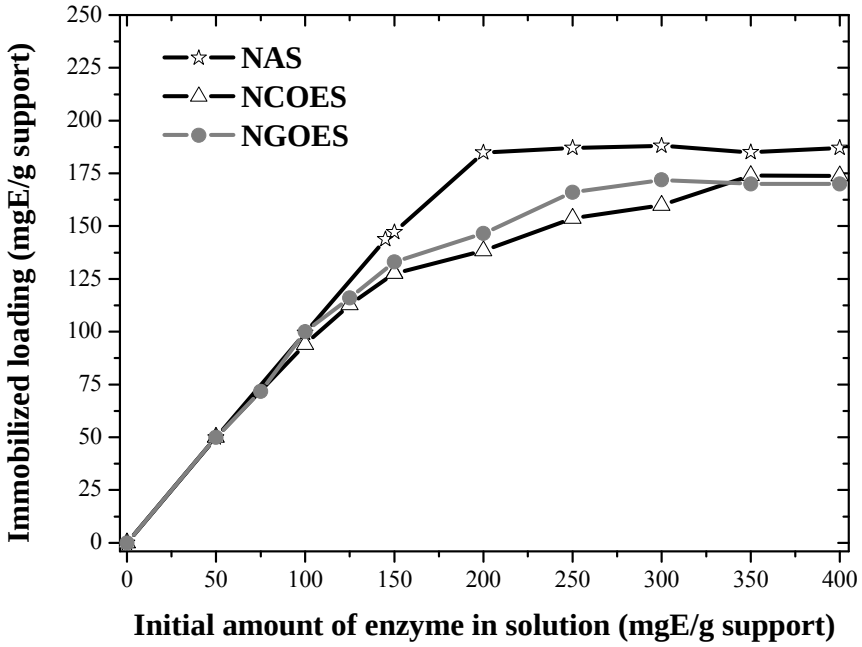

Figure 5. Equilibrium loading of immobilized enzyme versus initial enzyme content in solution at pH 5.5 for amino-modified supports.

For all the supports, the enzyme loading showed a continuous increase with the total enzyme to support mass ratio until a plateau is reached, which means that the maximum

capacity of the support has been reached. The maximum adsorption amounts determined were 187 mg/g for NAS and around 170 mg/g for NGOES and NCOES (Table 1). These adsorption curves follow a Langmuir model, that is, their shape indicates that immobilization takes place forming an enzyme monolayer. This behavior is expected for the confinement of enzyme in the narrow pores of the two ordered mesoporous supports, which does not permit the formation of a multilayer. However, multilayer adsorption would be possible on the external surface of the particles or within the large pores of the NAS support. The lack of multilayer adsorption also in these cases can be attributed to electrostatic repulsion among enzyme molecules, as the enzyme surface should possess a significant net negative charge at the pH used for immobilization, well above the isoelectric point of the enzyme.

The adsorption isotherm obtained for sample NAS shows a constant slope in the low enzyme concentration region and an abrupt change of slope at the enzyme concentration at which the plateau is reached. On the contrary, the isotherms of the two OMM supports show a progressive decrease of slope with the increase of enzyme concentration until the plateau is reached. This different behavior suggests that diffusion of enzyme inside the narrow pore channels of the OMM supports is progressively more restricted as the loading of enzyme increases, while the large pores of the NAS support would allow enzyme diffusion to be independent of surface coverage. Taking into account these considerations, it is worth determining whether the maximum loading of enzyme obtained for the OMM supports corresponds to a complete filling of pores by enzyme molecules. The estimated dimensions of the enzyme are 6.3 x 7.2 x 8.9 nm, and its approximate volume is 402 nm^3. Hence, the maximum enzyme loading can be estimated in $2.5 \cdot 10^{18}$ molecules per cm^3 of pore volume. According to its amino acid sequence, the molecular weight of the enzyme would be around 73 kDa. Thus, the maximum loading achieved for the OMM supports (around 170 mg of enzyme per cm^3 of pore volume) would be equivalent to 60% of the theoretical maximum laccase loading. Indeed, the actual filling of pore volume must be higher than 60%, as this calculation does not consider the glycosylation of the protein [70]. Glycosylation explains that the band determined by electrophoresis of the Suberase extract shows a molecular weight higher than 73 kDa, since the presence of covalently attached carbohydrates often results in incorrect molecular weight values using the SDS-PAGE technique [70, 75-77] (Figure S3).

The purely siliceous materials AS and OES yielded similar low enzyme loading and catalytic efficiency values (Table 1), despite their large differences in pore sizes and structures. The incorporation of amino groups on the surface of these materials leads to a tenfold increase in enzyme loading on both, amorphous and ordered materials. This indicates that the chemical affinity of the enzyme for the surface of the materials is crucial for success in the immobilization of enzymes. Catalytic efficiencies of biocatalysts based on purely siliceous materials OES and AS are some 10 times lower than their respective amine-functionalized analogues. In the case of amorphous materials the difference is even more marked, maybe suggesting a better substrate diffusion in this wider pore network.

The pores of the OES support are wide enough to accommodate the laccase molecules even after anchoring propylamine groups on the silica surface as confirmed by the high enzyme loading achieved on the NGOES support, very close to that obtained with the NAS support, which possesses wider pores. Similar loading capacity has been obtained with the amino-functionalized ordered mesoporous silica obtained by co-condensation (NCOES). These results confirm that the tailored pore dimension of the large-pore OMM materials (OES, NGOES and NCOES) allows for diffusion of enzyme through the pore channels.

These results are especially encouraging considering that the *Myceliophthora thermophila* laccase expressed in *Aspergillus oryzae* is hyper-glycosylated by eukaryotic host so steric hindrances might prevent interactions between the surface of the enzyme and the functionalized materials [78].

Immobilization of laccase on amine-containing supports is also faster than in purely siliceous materials, as seen by the contact time required to reach the respective maximum loadings (see Table 1). So, by controlling the affinity between enzyme and ordered mesoporous silica, the uptake rate and the maximum loading achieved can be drastically improved.

The orientation of the enzyme with regard to support surface is not an issue with these materials, since confinement of the enzyme in the sufficiently narrow pore channels ensures the same surrounding environment to all enzyme molecules.

3.3 Effect of pH on the activity of laccase

Once immobilized at pH 5.5, the biocatalysts can be suspended in solutions of different pH values. Figure 6 shows relative activity of the laccase at different pH values in the range 2.5-6.0 determined for the enzyme in solution and immobilized in the different supports.

The activity of laccase shows very similar trend with pH for the enzyme in solution and immobilized on amorphous silica (AS). In both cases, the maximum activity is obtained at pH 3.0 and there is a strong decrease of activity at both higher and lower pH values. On the other hand, for the enzyme immobilized on amino-functionalized supports, the maximum activity is obtained at a higher pH (3.5). This shift of the optimum pH might be attributed to the existence of a pH gradient between the solution and the pores of the support due to the presence of anchored amino groups. It can be also observed that, at higher pH, there is a strong decrease of activity for the enzyme supported on the amino-functionalized amorphous silica (NAS), in a similar way as it occurs for the enzyme supported on the unmodified silica (AS). However, the pH increase has lower effect on activity for the enzyme supported on NCOES and especially on NGOES, where the activity remains constant. Pore size of NGOES is smaller than NCOES and much smaller than NAS. This suggests that the microenvironment generated by amine groups in the enzyme vicinity is more efficient as these groups are closer to the laccase. In the extreme situations, the wide pore of NAS is not sufficient to maintain the effect over pH 3.5 whereas the effect of the presence of positive charges close to the enzyme in NGOES remains even at pH 6.0. These results show that confinement in narrow pore sizes permits to take advantage of the properties of the support.

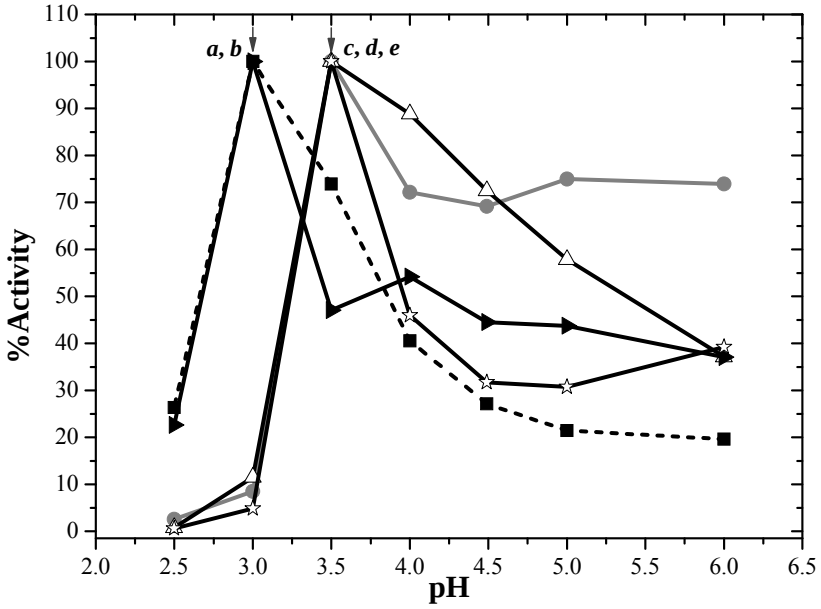

Figure 6 Effect of pH on the activity of *a*) free enzyme (■) and enzyme immobilized on *b*) AS (▶), *c*) NGOES (●), *d*) NCOES (△), *e*) NAS (☆). Oxidation of ABTS at 25 °C in 0.05 M phosphoric acid/sodium dihydrogenphosphate or 0.05 M citric acid/trisodium citrate buffer solutions.

3.4 Enzyme leaching

The non-covalent nature of the enzyme bonding to support makes necessary an evaluation of the potential enzyme leaching. Therefore, all the biocatalysts were subjected to leaching experiments, in order to determine whether the confinement in the pores and the enzyme-support electrostatic interaction allow to efficiently and irreversibly entrap the laccase.

Figure 7 shows the relative amount of enzyme that was removed from the different supports along the leaching experiment. Amorphous silica AS and its corresponding amine functionalized form NAS showed a continuous release of enzyme at a nearly constant rate during the whole leaching treatment (48 h). It can be concluded that the wide pore size of these materials does not offer any restriction for enzyme diffusion and, therefore, leaching can not be prevented under the conditions used (high dilution and low ionic strength).

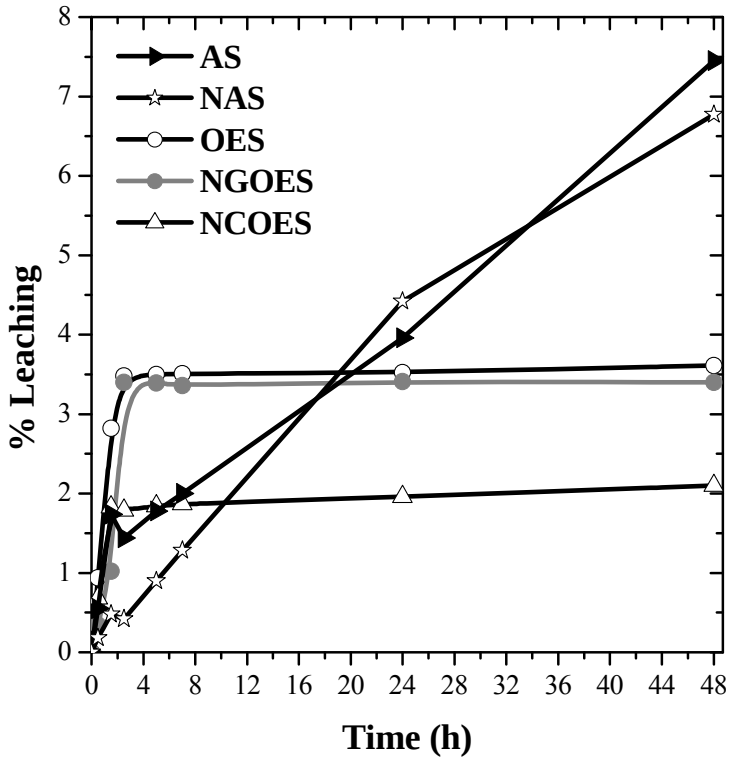

Figure 7. Leaching of enzyme from channel-like materials and amorphous mesoporous silica, expressed as percent of the initial enzyme loading leached as a function of time.

In contrast the leaching profiles of OMM-supported samples, both purely siliceous and amino-functionalized materials, show an initial desorption during the first two hours of treatment, after which the profiles reach a plateau. Longer incubation times showed no further increase of protein content in the supernatants indicating that no more leaching occurred. These results suggest that confinement of enzyme in narrow pores contributes to prevent leaching of the enzyme, even from the support that was not modified with amino groups to increase its affinity with the enzyme. The initial desorption observed is probably due mainly to removal of enzyme molecules immobilized on the external surface of the OMM particles, which is consistent with the maximum leaching level observed of only 4% of the enzyme loading or lower. The density of amino groups seems to be less relevant than pore size to determine resistance to leaching, although a lower enzyme leaching was detected with NCOES, the material having the highest amine content (1.5 mmol/g) among the OMM. Laccase was hardly desorbed (only 2%) from this material with pore size slightly larger than enzyme dimensions, and a high density of amine groups that should promote a strong interaction with laccase. It is worth

emphasizing that this strong retention of the enzyme inside the channels of OMM supports is comparable to a situation of covalently bound enzymes, despite the nature of the linkage is non-covalent.

In order to check the presence of enzyme inside particles, the catalysts previously incubated under the conditions of leaching described above, were treated for SDS-PAGE (polyacrylamide gel electrophoresis with Sodium Dodecyl Sulfate) in standard conditions and their supernatants were assayed for electrophoresis (EF). The incubation in 2-mercaptoethanol and SDS at 100 ºC should be severe enough to fully denature the protein and thus enable its release from inner surfaces as a random coil. Thus, a protein band was expected in the corresponding electrophoresis gels. However, these bands were observed (Figure S2) only for the samples corresponding to purely siliceous supports (OES and AS) and the amino-functionalized amorphous silica (NAS). The lack of band in the lanes corresponding to the amine-containing OMM supports (NGOES and NCOES) seems to suggest that laccase was fully retained inside these supports, even as a linear aminoacid chain. The high density of protonated amine groups seems to exert a strong electrostatic interaction also on the denatured protein. In order to confirm the presence of the enzyme inside these materials, the biocatalysts submitted to the leaching treatment followed by the SDS-PAGE denaturing conditions were centrifuged and the supernatant was replaced by the same volume of a NaOH solution at pH 11.0 to ensure deprotonation of amine groups and, therefore, remove electrostatic interaction between enzyme and support. The samples were incubated for 1-2 hours and then the corresponding supernatants were assayed in EF. As seen in Figure S3 a band corresponding to the same MW as laccase appeared in the electrophoresis gel in the lanes corresponding to NCOES (lane 2) and NGOES (lane 3) supports.

These results confirm the immobilization of the enzyme inside pores and also explain the absence of leaching of the enzyme. The adsorption process of the laccase indicates a very strong interaction between the functionalized surface and the enzyme, which remains when the protein is in the random coil conformation thus preventing also the desorption of the denatured protein. Only when these interactions disappear at high pH the leaching occurs.

The total absence of enzyme leaching from a non-covalent immobilization is a promising result since advantages from both kind of bonding can be found in these catalysts, and very interestingly, it permits support reutilization after enzyme inactivation.

3.5 Thermal stability

Despite the strong interaction with the support, thermostability was not significantly increased by immobilization. Suspension of the catalysts in aqueous solutions at high temperature (50 ºC) did not show significant effects regarding stability. All samples showed similar activity decay with time, comparable to that of the enzyme in solution (Figure 8). Maybe the explanation is related to the fact that laccase from *Myceliophthora thermophila* is thermoresistant in native state [68, 70]. Nonetheless it is also likely that partially unfolded and inactive conformation may be stabilized by the proximity of the amino groups of the support.

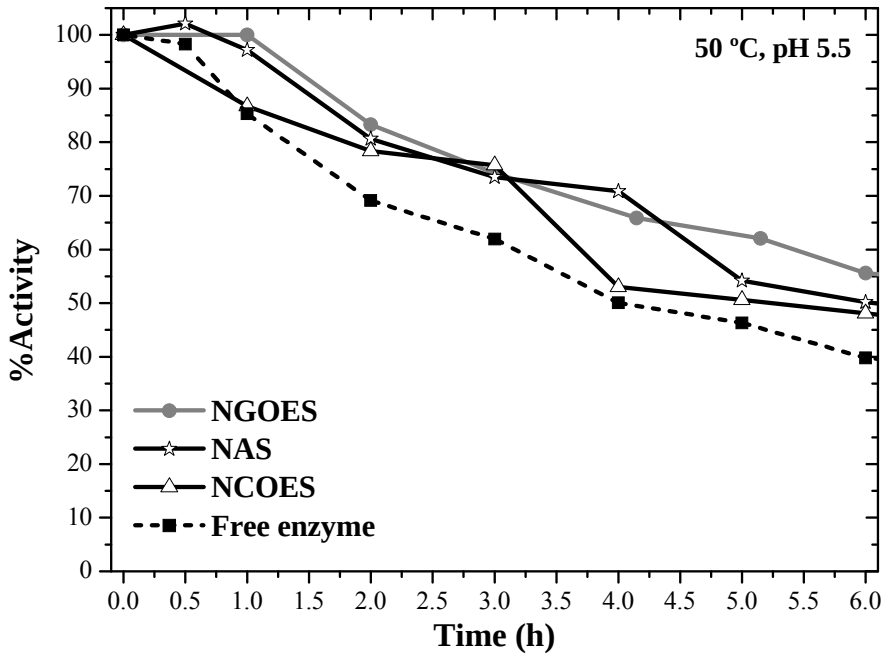

Figure 8. Thermostability profiles of free and immobilized laccase. Oxidation of ABTS at 50 ºC in 50 mM acetic acid/sodium acetate buffer at pH 5.5

3.6 Stability in ethanol-containing solution

Stability in organic solvent was also tested. Organic cosolvents are known to interfere the hydrogen bonds and thus promote protein unfolding [79]. The solvent of choice was

ethanol because one of the possible applications of this enzyme is the partial oxidation of wine polyphenols. Catalysts were incubated in a medium similar to wine: 10% ethanol and acidic pH. Catalytic activity was assayed in ABTS oxidation.

In all cases the immobilization protects from inactivation due to the distortion of the protein structure driven by the organic medium (Figure 9).

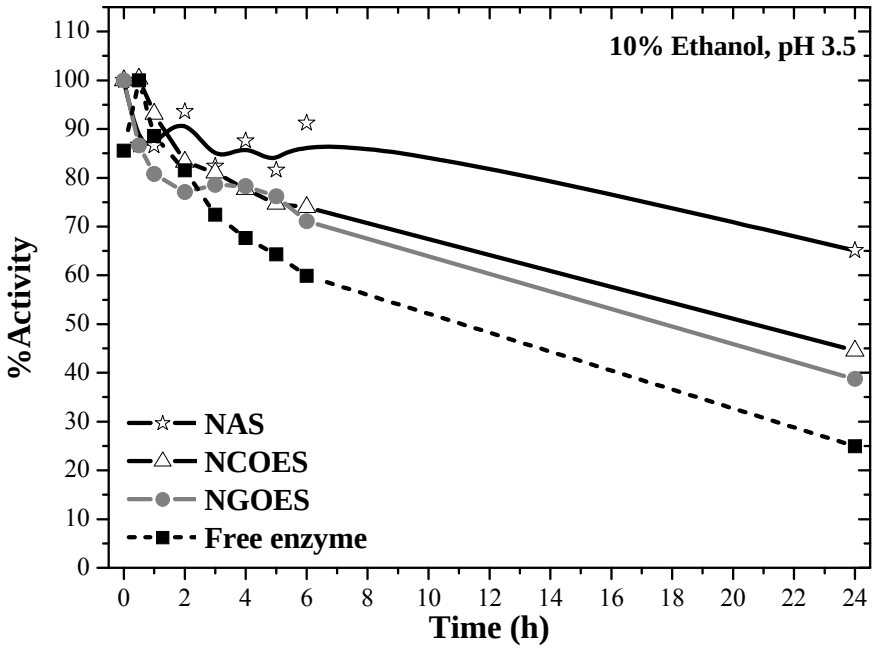

Figure 9. Stability tests of free and immobilized laccase in acidic aqueous solution containing ethanol (10 vol% ethanol in 50 mM citric acid/trisodium citrate buffer at pH 3.5). Oxidation of ABTS was performed at 25 ºC.

Confinement of the enzyme within narrow pores and strong interaction with the surface contribute to prevent enzyme unfolding and thus activity can be preserved for longer periods. In all cases, immobilized enzyme showed higher stability than native one. The amorphous and wide pore NAS showed the highest stability the catalysts. NGOES and NCOES showed the same deactivation rate, with half-lives around double than free laccase.

4. CONCLUSION

Laccase from *Myceliophthora thermophile* (*Mt*L) was readily and efficiently immobilized in expanded-pore mesoporous silica supports functionalized with amino

groups by means of electrostatic interaction. The summary of the advantages of this immobilization strategy are the following:

- Pore size is wide enough to permit access and diffusion of the enzyme.
- Pore size is narrow enough to prevent enzyme leaching and provide stabilization against unfolding.
- Chemical affinity is efficient to increase enzyme loading.
- Chemical affinity, along with uniform pore size, is efficient to prevent enzyme leaching.
- Ordered structure is efficient to limit diffusional restrictions of the substrates and products.

Enzymes with large molecular dimensions are difficult to immobilize inside pores of ordered mesoporous materials. The use of micelle expanders like TIPB has been applied to overcome this handicap. Based on this methodology, a strategy of synthesis of expanded pore ordered mesoporous materials (OMM) at low temperature and surface functionalization with amine groups was successfully developed. Laccase was transported through the channels and was effectively immobilized on the inner surfaces with hardly any diffusional restriction. The relatively large diameter of the pores also enabled to anchor functional groups to increase the affinity between the silica support and the enzyme without compromising the diffusion of the enzyme. The good pore connectivity common to OMM facilitates diffusion of substrates and products throughout the porous network. These features of the support materials enabled to obtain nanostructured biocatalysts having high enzyme loading and high catalytic activity in terms of catalytic efficiency, that is, minor loses of activity upon immobilization.

Confinement of enzyme molecules within pores having only slightly larger diameter than enzyme dimension prevents unfolding of protein structure which increases the stability of the biocatalyst in organic medium. The strong interaction with the functional groups of the support contributes to additionally increase enzyme stabilization.

As a result of the tuned pore size and high affinity provided by these materials, the leaching of non-covalently anchored enzyme can be fully prevented.

Laccase immobilized on NGOES and NCOES displayed high enzyme loading, good activity, good stability and no leaching which are promising properties for industrial application in subsequent reaction cycles. Even after enzyme inactivation, the non-covalent nature of the link may also permit to recover and reutilization of supports, so their advantages can be further exploited with no additional cost.

5. SUPPLEMENTARY INFORMATION

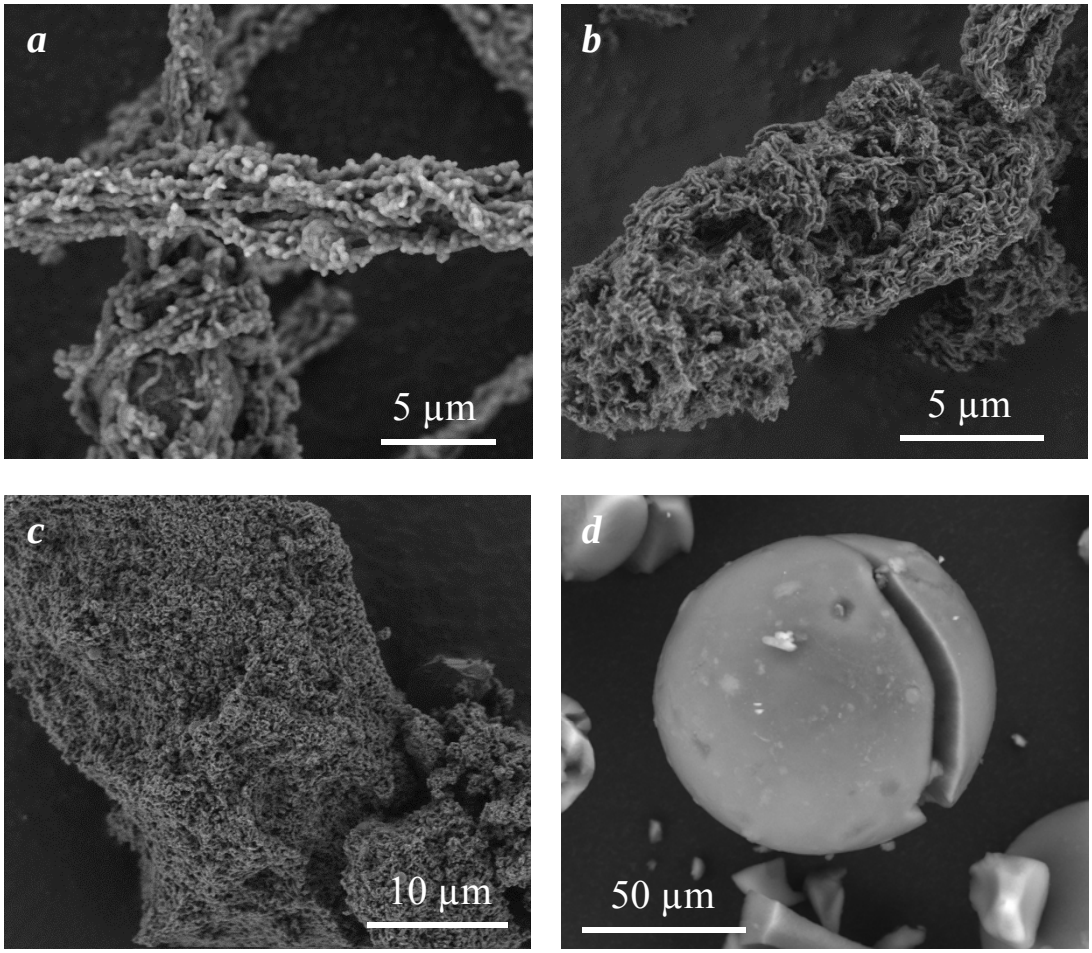

Figure S1. SEM micrograph of OES (*a*), NGOES (*b*), NCOES (*c*) and NAS (*d*).

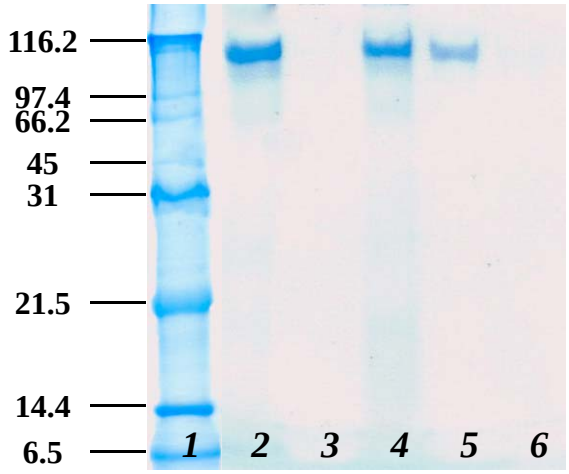

Figure S2. Electrophoresis in standard conditions. 1: Protein standard (Broad range SDS-Page standard stained with Coomassie G-250 stain), 2: OES, 3: NGOES, 4: AS, 5: NAS, 6: NCOES.

*Due to the high glycosylation the band of the laccase do not correspond to the molecular weight of the broad range molecular weight standard.

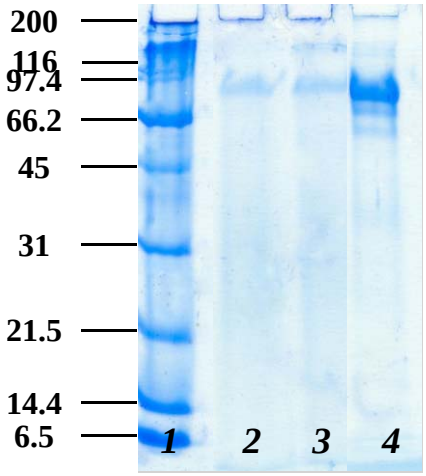

Figure S3. Electrophoresis at pH 11.0. 1: Protein standard; 2: NGOES, 3: NCOES, 4: Soluble laccase.

6. REFERENCES

[1] Y. Han, D. Zhang, Ordered mesoporous silica materials with complicated structures, *Curr. Opin. Chem. Eng.*, 1 (**2012**) 129-137.

[2] A. Stein, B.J. Melde, R.C. Schroden, Hybrid inorganic-organic mesoporous silicates - Nanoscopic reactors coming of age, *Adv. Mater.*, 12 (**2000**) 1403-1419.

[3] M. Hartmann, Ordered mesoporous materials for bioadsorption and biocatalysis, *Chem. Mater.*, 17 (**2005**) 4577-4593.

[4] H.H.P. Yiu, P.A. Wright, Enzymes supported on ordered mesoporous solids: a special case of an inorganic-organic hybrid, *J. Mater. Chem.*, 15 (**2005**) 3690-3700.

[5] X.S. Zhao, X.Y. Bao, W. Guo, F.Y. Lee, Immobilizing catalysts on porous materials, *Mater. Today*, 9 (**2006**) 32-39.

[6] J.S. Beck, J.C. Vartuli, W.J. Roth, M.E. Leonowicz, C.T. Kresge, K.D. Schmitt, C.T.W. Chu, D.H. Olson, E.W. Sheppard, A new family of mesoporous molecular sieves prepared with liquid crystal templates, *J. Am. Chem. Soc.*, 114 (**1992**) 10834-10843.

[7] C.T. Kresge, M.E. Leonowicz, W.J. Roth, J.C. Vartuli, J.S. Beck, Ordered mesoporous molecular sieves synthesized by a liquid-crystal template mechanism, *Nature*, 359 (**1992**) 710-712.

[8] L. Cao, T. Man, M. Kruk, Synthesis of Ultra-Large-Pore SBA-15 Silica with Two-Dimensional Hexagonal Structure Using Triisopropylbenzene As Micelle Expander, *Chem. Mater.*, 21 (**2009**) 1144-1153.

[9] Y. Wan, D. Zhao, On the controllable soft-templating approach to mesoporous silicates, *Chem. Rev.*, 107 (**2007**) 2821-2860.

[10] D.Y. Zhao, Q.S. Huo, J.L. Feng, B.F. Chmelka, G.D. Stucky, Nonionic triblock and star diblock copolymer and oligomeric surfactant syntheses of highly ordered, hydrothermally stable, mesoporous silica structures, *J. Am. Chem. Soc.*, 120 (**1998**) 6024-6036.

[11] M. Kruk, M. Jaroniec, V. Antochshuk, A. Sayari, Mesoporous silicate - Surfactant composites with hydrophobic surfaces and tailored pore sizes, *J. Phys. Chem. B*, 106 (**2002**) 10096-10101.

[12] P.T. Tanev, T.J. Pinnavaia, A neutral templating route to mesoporous molecular sieves, *Science*, 267 (**1995**) 865-867.

[13] J.L. Blin, A. Léonard, B.L. Su, Synthesis of Large Pore Disordered MSU-Type Mesoporous Silicas through the Assembly of C16(EO)10Surfactant and TMOS Silica Source: Effect of the Hydrothermal Treatment and Thermal Stability of Materials, *J. Phys. Chem. B*, 105 (**2001**) 6070-6079.

[14] G. Herrier, J.L. Blin, B.L. Su, MSU-type mesoporous silicas with well-tailored pore sizes synthesized via an assembly of deca(ethylene oxide) oleyl ether surfactant and tetramethoxysilane silica precursor, *Langmuir*, 17 (**2001**) 4422-4430.

[15] K. Cassiers, P. Van der Voort, T. Linssen, E.F. Vansant, O. Lebedev, J. Van Landuyt, A counterion-catalyzed ((SH+)-H-0)(X-I+) pathway toward heat- and steam-stable mesostructured silica assembled from amines in acidic conditions, *J. Phys. Chem. B*, 107 (**2003**) 3690-3696.

[16] J.L. Ruggles, E.P. Gilbert, S.A. Holt, P.A. Reynolds, J.W. White, Expanded mesoporous silicate films grown at the air-water interface by addition of hydrocarbons, *Langmuir*, 19 (**2003**) 793-800.

[17] D.Y. Zhao, J.L. Feng, Q.S. Huo, N. Melosh, G.H. Fredrickson, B.F. Chmelka, G.D. Stucky, Triblock copolymer syntheses of mesoporous silica with periodic 50 to 300 angstrom pores, *Science*, 279 (**1998**) 548-552.

[18] L. Cao, M. Kruk, Synthesis of large-pore SBA-15 silica from tetramethyl orthosilicate using triisopropylbenzene as micelle expander, *Colloids Surf., A*, 357 (**2010**) 91-96.

[19] P. Schmidt-Winkel, W.W. Lukens, D.Y. Zhao, P.D. Yang, B.F. Chmelka, G.D. Stucky, Mesocellular siliceous foams with uniformly sized cells and windows, *J. Am. Chem. Soc.*, 121 (**1999**) 254-255.

[20] J.S. Lettow, Y.J. Han, P. Schmidt-Winkel, P.D. Yang, D.Y. Zhao, G.D. Stucky, J.Y. Ying, Hexagonal to mesocellular foam phase transition in polymer-templated mesoporous silicas, *Langmuir*, 16 (**2000**) 8291-8295.

[21] E. Serra, V. Alfredsson, R.M. Blanco, I. Diaz, A comprehensive strategy for the immobilization of lipase in ordered mesoporous materials, in: A. Gedeon, P. Massiani, F. Babonneau (Eds.) *Zeolites and Related Materials: Trends, Targets and Challenges, Proceedings of the 4th International Feza Conference* (**2008**), pp. 369-372.

[22] E. Serra, A. Mayoral, Y. Sakamoto, R.M. Blanco, I. Diaz, Immobilization of lipase in ordered mesoporous materials: Effect of textural and structural parameters, *Microporous Mesoporous Mater.*, 114 (**2008**) 201-213.

[23] E. Serra, E. Diez, I. Diaz, R.M. Blanco, A comparative study of periodic mesoporous organosilica and different hydrophobic mesoporous silicas for lipase immobilization, *Microporous Mesoporous Mater.*, 132 (**2010**) 487-493.

[24] A. Leonowicz, N.S. Cho, J. Luterek, A. Wilkolazka, M. Wojtas-Wasilewska, A. Matuszewska, M. Hofrichter, D. Wesenberg, J. Rogalski, Fungal laccase: properties and activity on lignin, *J. Basic Microbiol.*, 41 (**2001**) 185-227.

[25] A.M. Mayer, R.C. Staples, Laccase: new functions for an old enzyme, *Phytochem. Rev.*, 60 (**2002**) 551-565.

[26] P. Baldrian, Fungal laccases - occurrence and properties, *FEMS Microbiol. Rev.*, 30 (**2006**) 215-242.

[27] M. Fernandez-Fernandez, M.A. Sanroman, D. Moldes, Recent developments and applications of immobilized laccase, *Biotechnol Adv*, 31 (**2013**) 1808-1825.

[28] T. Kudanga, G.S. Nyanhongo, G.M. Guebitz, S. Burton, Potential applications of laccase-mediated coupling and grafting reactions: a review, *Enzyme Microb. Technol.*, 48 (**2011**) 195-208.

[29] M. Pita, C. Gutierrez-Sanchez, D. Olea, M. Velez, C. Garcia-Diego, S. Shleev, V.M. Fernandez, A.L. De Lacey, High Redox Potential Cathode Based on Laccase Covalently Attached to Gold Electrode, *J. Phys. Chem. C*, 115 (**2011**) 13420-13428.

[30] R.C. Minussi, G.M. Pastore, N. Duran, Potential applications of laccase in the food industry, *Trends Food Sci. Tech.*, 13 (**2002**) 205-216.

[31] R.C. Minussi, M. Rossi, L. Bologna, L. Cordi, D. Rotilio, G.M. Pastore, N. Duran, Phenolic compounds and total antioxidant potential of commercial wines, *Food Chem.*, 82 (**2003**) 409-416.

[32] R.C. Minussi, M. Rossi, L. Bologna, D. Rotilio, G.M. Pastore, N. Duran, Phenols removal in musts: Strategy for wine stabilization by laccase, *J. Mol. Catal. B: Enzym.*, 45 (**2007**) 102-107.

[33] A. Kunamneni, F.J. Plou, A. Ballesteros, M. Alcalde, Laccases and their applications: a patent review, *Recent Pat. Biotechnol.*, 2 (**2008**) 10-24.

[34] J.F. Osma, J.L. Toca-Herrera, S. Rodriguez-Couto, Uses of laccases in the food industry, *Enzyme Res.*, 2010 (**2010**) 1-8.

[35] S. Rodriguez Couto, J.L. Toca Herrera, Industrial and biotechnological applications of laccases: a review, *Biotechnol. Adv.*, 24 (**2006**) 500-513.

[36] O.V. Morozova, G.P. Shumakovich, S.V. Shleev, Y.I. Yaropolov, Laccase-mediator systems and their applications: A review, *Appl. Biochem. Microbiol.*, 43 (**2007**) 523-535.

[37] L. Betancor, G.R. Johnson, H.R. Luckarift, Stabilized Laccases as Heterogeneous Bioelectrocatalysts, *ChemCatchem*, 5 (**2013**) 46-60.

[38] K. Brijwani, A. Rigdon, P.V. Vadlani, Fungal laccases: production, function, and applications in food processing, *Enzyme Res.*, 2010 (**2010**) 149748.

[39] N. Duran, M.A. Rosa, A. D'Annibale, L. Gianfreda, Applications of laccases and tyrosinases (phenoloxidases) immobilized on different supports: a review, *Enzyme Microb. Technol.*, 31 (**2002**) 907-931.

[40] A. Salis, M. Pisano, M. Monduzzi, V. Solinas, E. Sanjust, Laccase from Pleurotus sajor-caju on functionalised SBA-15 mesoporous silica: Immobilisation and use for the oxidation of phenolic compounds, *J. Mol. Catal. B: Enzym.*, 58 (**2009**) 175-180.

[41] L. Fernando Bautista, G. Morales, R. Sanz, Immobilization strategies for laccase from Trametes versicolor on mesostructured silica materials and the application to the degradation of naphthalene, *Bioresour. Technol.*, 101 (**2010**) 8541-8548.

[42] J. Forde, E. Tully, A. Vakurov, T.D. Gibson, P. Millner, C. Ó'Fágáin, Chemical modification and immobilisation of laccase from Trametes hirsuta and from Myceliophthora thermophila, *Enzyme Microb. Technol.*, 46 (**2010**) 430-437.

[43] D.N. Tran, K.J. Balkus, Perspective of Recent Progress in Immobilization of Enzymes, *ACS Catal.*, 1 (**2011**) 956-968.

[44] A. Mayoral, R. Arenal, V. Gascon, C. Marquez-Alvarez, R.M. Blanco, I. Diaz, Designing Functionalized Mesoporous Materials for Enzyme Immobilization: Locating Enzymes by Using Advanced TEM Techniques, *ChemCatChem*, 5 (**2013**) 903-909.

[45] A.S.M. Chong, X.S. Zhao, Functionalization of SBA-15 with APTES and characterization of functionalized materials, *J. Phys. Chem. B*, 107 (**2003**) 12650-12657.

[46] X. Wang, K.S. Lin, J.C. Chan, S. Cheng, Preparation of ordered large pore SBA-15 silica functionalized with aminopropyl groups through one-pot synthesis, *Chem. Commun.*, (**2004**) 2762-2763.

[47] J. Aguado, J.M. Arsuaga, A. Arencibia, M. Lindo, V. Gascon, Aqueous heavy metals removal by adsorption on amine-functionalized mesoporous silica, *J. Hazard. Mater.*, 163 (**2009**) 213-221.

[48] Y. Han, S.S. Lee, J.Y. Ying, Pressure-Driven Enzyme Entrapment in Siliceous Mesocellular Foam, *Chem. Mater.*, 18 (**2006**) 643-649.

[49] H.G. Manyar, E. Gianotti, Y. Sakamoto, O. Terasaki, S. Coluccia, S. Tumbiolo, Active Biocatalysts Based on Pepsin Immobilized in Mesoporous SBA-15, *J. Phys. Chem. C*, 112 (**2008**) 18110-18116.

[50] M.M. Bradford, A rapid and sensitive method for the quantitation of microgram quantities of protein utilizing the principle of protein-dye binding, *Anal. Biochem.*, 72 (**1976**) 248-254.

[51] Z. Jin, X. Wang, X. Cui, Acidity-dependent mesostructure transformation of highly ordered mesoporous silica materials during a two-step synthesis, *J NON-CRYST SOLIDS*, 353 (**2007**) 2507-2514.

[52] D. Margolese, J.A. Melero, S.C. Christiansen, B.F. Chmelka, G.D. Stucky, Direct syntheses of ordered SBA-15 mesoporous silica containing sulfonic acid groups, *Chem. Mater.*, 12 (**2000**) 2448-2459.

[53] K.S.W. Sing, Reporting physisorption data for gas/solid systems with special reference to the determination of surface area and porosity (Recommendations 1984), *Pure Appl. Chem.*, 57 (**1985**) 603-619.

[54] S. Rodríguez Couto, J.F. Osma, V. Saravia, G.M. Gübitz, J.L. Toca Herrera, Coating of immobilised laccase for stability enhancement: A novel approach, *Appl. Catal., A.*, 329 (**2007**) 156-160.

[55] C. Crestini, R. Perazzini, R. Saladino, Oxidative functionalisation of lignin by layer-by-layer immobilised laccases and laccase microcapsules, *Appl. Catal., A.*, 372 (**2010**) 115-123.

[56] U.K. Laemmli, Cleavage of structural proteins during the assembly of the head of bacteriophage T4, *Nature*, 227 (**1970**) 680-685.

[57] NCBI Protein Database.

[58] Standard Protein BLAST.

[59] Rutgers, UCSD, RCSB Protein Data Bank.

[60] N. Hakulinen, L.L. Kiiskinen, K. Kruus, M. Saloheimo, A. Koivula, J. Rouvinen, Crystal structure of a laccase from Melanocarpus albomyces with an intact trinuclear copper site, *Nat. Struct. Biol.*, 9 (**2002**) 601-605.

[61] E. Gasteiger, A. Gattiker, C. Hoogland, I. Ivanyi, R.D. Appel, A. Bairoch, ExPASy: the proteomics server for in-depth protein knowledge and analysis, *Nucleic Acids Res.*, 31 (**2003**) 3784-3788.

[62] K. Arnold, L. Bordoli, J. Kopp, T. Schwede, The SWISS-MODEL workspace: a web-based environment for protein structure homology modelling, *Bioinformatics*, 22 (**2006**) 195-201.

[63] L. Bordoli, F. Kiefer, K. Arnold, P. Benkert, J. Battey, T. Schwede, Protein structure homology modeling using SWISS-MODEL workspace, *Nat. Protoc.*, 4 (**2009**) 1-13.

[64] F. Kiefer, K. Arnold, M. Kunzli, L. Bordoli, T. Schwede, The SWISS-MODEL Repository and associated resources, *Nucleic Acids Res.*, 37 (**2009**) 387-392.

[65] W.L. DeLano, The PyMOL Molecular Graphics System, DeLano Scientific, California, USA, **2008**.

[66] ExPASy - ProtParamtool.

[67] UniProt KB.

[68] R.M. Berka, I.V. Grigoriev, R. Otillar, A. Salamov, J. Grimwood, I. Reid, N. Ishmael, T. John, C. Darmond, M.C. Moisan, B. Henrissat, P.M. Coutinho, V. Lombard, D.O. Natvig, E. Lindquist, J. Schmutz, S. Lucas, P. Harris, J. Powlowski, A. Bellemare, D. Taylor, G. Butler, R.P. de Vries, I.E. Allijn, J. van den Brink, S. Ushinsky, R. Storms, A.J. Powell, I.T. Paulsen, L.D. Elbourne, S.E. Baker, J. Magnuson, S. Laboissiere, A.J. Clutterbuck, D. Martinez, M. Wogulis, A.L. de Leon, M.W. Rey, A. Tsang, Comparative genomic analysis of the thermophilic biomass-degrading fungi Myceliophthora thermophila and Thielavia terrestris, *Nat. Biotechnol.*, 29 (**2011**) 922-929.

[69] B.T.C.E.I. System., BRENDA: The Comprehensive Enzyme Information System.

[70] R.M. Berka, P. Schneider, E.J. Golightly, S.H. Brown, M. Madden, K.M. Brown, T. Halkier, K. Mondorf, F. Xu, Characterization of the gene encoding an extracellular laccase of Myceliophthora thermophila and analysis of the recombinant enzyme expressed in Aspergillus oryzae, *Appl. Environ. Microbiol.*, 63 (**1997**) 3151-3157.

[71] D.Y. Zhao, J.Y. Sun, Q.Z. Li, G.D. Stucky, Morphological control of highly ordered mesoporous silica SBA-15, *Chem. Mater.*, 12 (**2000**) 275-279.

[72] M. Mandal, M. Kruk, Versatile approach to synthesis of 2-D hexagonal ultra-large-pore periodic mesoporous organosilicas, *J. Mater. Chem.*, 20 (**2010**) 7506-7516.

[73] V. Meynen, P. Cool, E.F. Vansant, Verified syntheses of mesoporous materials, *Microporous Mesoporous Mater.*, 125 (**2009**) 170-223.

[74] V. Gascón, I. Díaz, C. Márquez-Alvarez, R.M. Blanco, Mesoporous silica with tunable morphology for the immobilization of lacase, *Molecules*, 19 (**2014**) 7057-7071.

[75] C. Hart, B. Schulenberg, T.H. Steinberg, W.Y. Leung, W.F. Patton, Detection of glycoproteins in polyacrylamide gels and on electroblots using Pro-Q Emerald 488 dye, a fluorescent periodate Schiff-base stain, *Electrophoresis*, 24 (**2003**) 588-598.

[76] J. Wu, N.J. Lenchik, M.J. Pabst, S.S. Solomon, J. Shull, I.C. Gerling, Functional characterization of two-dimensional gel-separated proteins using sequential staining, *Electrophoresis*, 26 (**2005**) 225-237.

[77] J.I. Lopez-Cruz, G. Viniegra-Gonzalez, A. Hernandez-Arana, Thermostability of native and pegylated Myceliophthora thermophila laccase in aqueous and mixed solvents, *Bioconjug. Chem.*, 17 (**2006**) 1093-1098.

[78] A. Kunamneni, B. Cutino-Avila, D.F. Gil, A. Del Monte, M. Alcalde, A. Ballesteros, F.J. Plou, Modelling the covalent immobilization of Myceliophthora thermophila laccase in Sepabeads (R) EC-EP3: application of RSM and novel computational analysis, *New Biotechnol.*, 25 (**2009**) S135-S135.

[79] V.V. Mozhaev, Y.L. Khmelnitsky, M.V. Sergeeva, A.B. Belova, N.L. Klyachko, A.V. Levashov, K. Martinek, Catalytic activity and denaturation of enzymes in water/organic cosolvent mixtures. Alpha-chymotrypsin and laccase in mixed water/alcohol, water/glycol and water/formamide solvents, *Eur. J. Biochem.*, 184 (**1989**) 597-602.

CAPÍTULO 3

Hybrid periodic mesoporous organosilica designed to improve properties of immobilized enzymes

V. Gascón, I. Díaz, R. M. Blanco, C. Márquez-Álvarez

Published in *RSC Advances*, 2014, vol. 4, pp. 34356-34368.
DOI: 10.1039/c4ra05362a

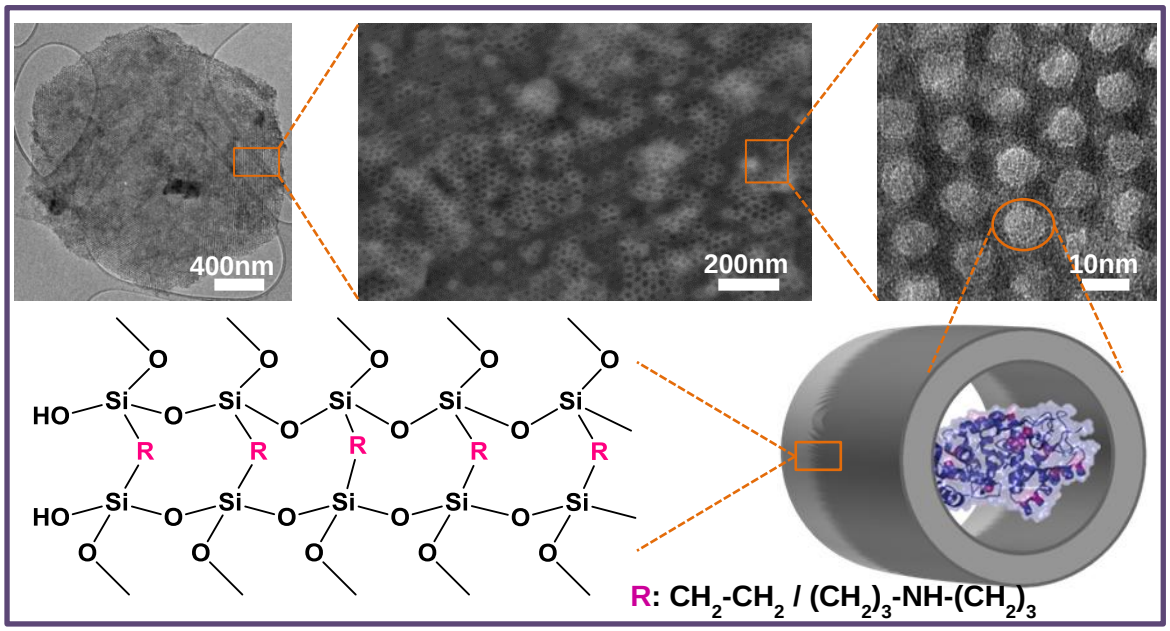

ABSTRACT

Two types of highly ordered periodic mesoporous organosilicas have been synthesized as tailor-made supports to immobilize two different enzymes, lipase and laccase. These materials provide an environment where abundant organic groups in close vicinity of the enzyme surface generates a high chemical affinity, which results in high values of enzyme loading, catalytic activity and stabilization. A hydrophobic periodic mesoporous organosilica support (PMO) with a highly ordered hexagonal arrangement of parallel pore channels with diameter around 7 nm, containing framework hydrocarbon groups (ethylene), was used for lipase immobilization. A novel periodic mesoporous aminosilica (PMA), containing secondary amine groups in its framework and having expanded pores was synthesized and studied for immobilization of a larger enzyme, namely laccase. The synthesis conditions were adjusted, using bis[(3-trimethoxysilyl)propyl]amine and 1,2-bis(trimethoxysilyl)ethane as framework co-precursors and 1,3,5-triisopropylbenzene as micelle expander for producing large pores (> 10 nm). The properties of this multifunctional PMA having hydrophilic amino groups and hydrophobic ethylene/propylene groups within the framework were studied. This work compares the confinement of lipase and laccase enzymes in the pores of these hybrid organosilica materials and its effect on immobilization and stabilization parameters. Laccase immobilized on PMA and lipase immobilized on PMO exhibited higher stability in solvents (ethanol and methanol, respectively) compared to enzymes supported on functionalized silica materials with pending organic groups on the surface. High retention of enzymes inside the pores of these materials has been achieved and leaching has been fully prevented. These results can be attributed to the different interactions (hydrophobic, electrostatic and hydrogen bonding) established between the surfaces of enzyme and the PMO/PMA support, which are enhanced by an optimum pore size adjusted to the enzyme dimensions.

Keywords: Periodic mesoporous organosilica; periodic mesoporous aminosilica; ordered mesoporous materials; expanded pores; enzyme immobilization.

1. INTRODUCTION

Siliceous ordered mesoporous materials (OMM) have burst into the field of enzyme immobilization as excellent supports to obtain nanostructured biocatalysts with improved properties [1]. Three main parameters of these materials can be controlled by adjusting the synthesis conditions: (a) pore connectivity through regular porous network, (b) pore size, which can be fine-tuned to accommodate to dimensions of the enzyme for optimal confinement, and (c) surface chemical functionalization to enhance enzyme-support affinity. This control enables to obtain biocatalysts with improved properties regarding enzyme loading, catalytic efficiency, stability, and leaching prevention [2].

The development of hybrid periodic organo-bridged silicas with ordered mesopores and large pore diameter is a breakthrough in the field of ordered mesoporous materials. In these periodic mesoporous organosilicas (PMO), the organic groups are not anchored to the surface but become part of the framework. Using such hybrid supports allows to avoid the pore size reduction that occurs upon grafting of the organic functionality on the surface of purely inorganic supports, which might hinder diffusion of enzyme molecules [3]. However, literature regarding bulky enzyme immobilization on these materials is rather scarce.

The synthesis of PMO materials is carried out using bridged alkoxysilane molecules ((**R′**O)$_3$Si-**R**-Si(O**R′**)$_3$; **R**: bridging hydrocarbon group, **R′**: methyl or ethyl) as precursors [4-6]. New hybrid organic-inorganic OMM offer more possibilities for application, particularly in enzyme immobilization [4, 7, 8]. The porous structures, surface, and framework properties of PMO materials can be finely tuned by changing the bridging organic groups incorporated and the synthesis conditions employed [9-13]. However, the lack of structural rigidity of the organic moiety of the silsesquioxane may result in a disordered material, especially when attempting to synthesize materials with large pore size.

Initially, research on PMOs had been focused on the incorporation of small aliphatic moieties (methylene [14], ethylene [12, 15], ethenylene [16]) into the walls of the channel-like structures, obtaining different morphologies [17, 18]. Later, organic bridges in the framework were extended to more functional species ranging from hydrocarbons and heteroaromatics to metal complexes. Recent developments in novel PMO involve innovation in their components and structural designs. Multifunctional PMO can be easily

obtained by co-condensation of a mixture of bridged organosilane precursors with different surface properties of the pore walls [19-23]. For example, Morell et al., 2006 [24] incorporated aromatic bridging groups (phenylene and thiophene) and obtained PMO materials with pore sizes in the range of 4.8–5.4 nm employing the triblock copolymer Pluronic P123 as structure-directing agent.

The limited pore size of PMO materials may restrict their applications in some areas where large pores are essential for adsorption and immobilization of large biomolecules [25], and only a few works have been published regarding the immobilization of bulky enzymes, for which large pores are required [26, 27]. In comparison with their purely siliceous counterparts, pore size is more difficult to adjust in PMO [16, 28].

We have formerly described the immobilization of *Candida antarctica* lipase B (*Ca*LB) on a PMO material containing ethylene groups [29]. Lipases are known to have a hydrophobic domain, which often constitutes a lid responsible for their interfacial activation [30]. *Ca*LB lacks this lid [31, 32], but still has the hydrophobic domain on its surface. Supports with hydrophobic surfaces can interact with this domain to drive lipase immobilization, therefore, PMO containing ethylene bridges were obtained and tested as supports in our group.

Laccase is a larger enzyme than CaLB, therefore two challenges are to be faced. One is the increase of chemical affinity and the other is obtaining a support with pore size large enough to accommodate the enzyme. We have recently reported [33] the immobilization of laccase on OMM with expanded pore size functionalized with amine groups anchored on the silica surface. The large difference between the pI of laccase (around 4) and the pKa value of these groups (close to 10) enabled strong electrostatic interactions in a broad pH range. Based on these results we report here the synthesis of large-pore periodic mesoporous organosilica materials containing amino groups within the framework as supports for immobilization of laccase. Few attempts to introduce nitrogen-containing groups into the walls of hybrid organosilica materials have been reported. Asefa et al, 2003 [34] prepared periodic mesoporous aminosilica (PMA) materials that contained amine functional groups within the framework via thermal ammonolysis of PMOs under a flow of ammonia gas. The pore diameter of these materials was around 3-4 nm. It has also been reported the synthesis of PMA using silane precursors with amine groups. However, it has to be noticed that the order of the structure is an issue. The increase in concentration of the bridged alkoxysilane with non-rigid organic bridges may lead to a decrease in the

order of the material, as reported by Wahab et al., 2004 [4] even for materials with pore size as small as 3.5 nm. An interesting transition of the mesostructure of this system was observed with increasing content of bis[(3-trimethoxysilyl)propyl]-amine (BTMSPA) in the starting mixture for the co-condensation of BTMSPA and 1,2-bis(trimethoxysilyl)ethane (BTME) in the presence of octadecyltrimethylammonnium chloride [35]. When the ratio of BTME/BTMSPA was changed from 90:10 to 55:45, a change from a 2D hexagonal (*p*6*mm*) to a cubic mesophase took place. Higher BTMSPA concentrations in the reaction mixture led to the collapse of the structure. Tan et al., 2006 [36] obtained uniform mesopores in a material made with BTMSPA using hexadecyltrimethylammonium bromide (CTAB) as template. When BTMSPA was used, the hydrophilic chain helped to promote co-assembly of the precursor with CTAB micelles, limiting bulk condensation. The reported material had relatively low pore volume and specific surface area, as well as a reduced pore diameter (3.1 nm) but it had a combination of uniform pore size and amine groups integrated in the pore walls. In all these reported works, the pore sizes obtained were always smaller than those attainable for pure silica and did not exceed 6 nm. This factor limits the potential applications of PMAs as supports for the immobilization of large enzymes.

On the basis of previous works with laccase immobilized on OMM with SBA-15 structure and expanded pores, functionalized with primary amine groups anchored to the siliceous surface, we report here the synthesis of a novel hybrid material: periodic mesoporous aminosilica with large pore size. The aim of this work is to study and compare the behaviour of two model enzymes, laccase and lipase confined within the pores of two different periodic mesoporous organosilica supports.

2. EXPERIMENTAL

2.1. Materials and Reagents

Triblock copolymer $PEO_{20}PPO_{70}PEO_{20}$ (Pluronic P123) and 1,2-bis(trimethoxysilyl)ethane (BTME) were from Aldrich (USA). 3-aminopropyltriethoxysilane (APTES) and bis[3-(trimethoxysilyl)propyl]amine (BTMSPA) were purchased from TCI (Belgium). 1,3,5-triisopropylbenzene (TIPB) and n-octyltriethoxysilane (OTES) were from Alfa Aesar (Germany). Amorphous silica MS-3030 was kindly donated by Silica PQ Corporation (USA).

The extracts of soluble laccase from *Myceliophthora thermophila* (Suberase) and lipase from *Candida antarctica B* (Lipozyme *Ca*LB L) both expressed in *Aspergillus oryzae* were kindly donated by Novozymes (Denmark). 2'-azino-bis-(3-ethylbenzothiazoline-6-sulfonic acid) diammonium salt (ABTS), p-nitrophenyl acetate (p-NPA), tributyrin (TB), mercaptoethanol, bromophenol blue and glycerol were from Sigma (USA). Bovine serum albumin (BSA, Sigma-Aldrich, USA) was used as protein standard for protein content determination by the Bradford method [37]. The reagents for electrophoresis SDS-PAGE (sodium dodecyl sulfate (SDS), ammonium persulfate, N,N,N',N'-tetramethylethylenediamine (TEMED), 40 % acrylamide/bis solution, 10x Tris base/glycine/SDS buffer and bio-safeTM coomasie G-250 stain) and broad molecular weight standards were from Bio-Rad (USA).

Citric acid, potassium chloride, phosphoric acid, sodium carbonate, sodium bicarbonate and toluene were purchased from Sigma-Aldrich (USA). Acetonitrile and sodium acetate were purchased from Scharlau (Spain). Sodium dihydrogen phosphate 1-hydrate, hydrochloric acid, ethanol, acetic acid, potassium dihydrogen phosphate, disodium hydrogen phosphate, sodium hydroxide, potassium phosphate and acetone were purchased from Panreac (Spain). Trisodium citrate dehydrate was from Analyticals Carlo Erba (Italy). Tris(hydroxymethyl)aminomethane (Tris base) was purchased from Fluka Analytical (USA). Solvents were all analytical or HPLC grade, salts were of high purity and water was Milli-Q grade. All materials were used as obtained without further purification.

2.2. Synthesis of hybrid periodic mesoporous materials

Ethylene-bridged periodic mesoporous organosilica (PMO) was synthesized as previously reported [29, 38] with few modifications. 3.19 g of Pluronic P123 were dissolved at room temperature in 126.84 mL of 0.174 M HCl aqueous solution in a flask with slow stirring. Once the surfactant was dissolved, 9.38 g of KCl were added. Both, the low acid concentration and the presence of inorganic salts play an important role in the formation of highly ordered materials [12, 18, 38-40]. When the resulting solution was homogenized, it was heated in a thermostated water bath to a constant temperature of 40 ºC. Then, 3.97 mL of bis-functional alkoxysilane, BTME, were added at once with rapid stirring. The resulting mixture was stirred at 40 ºC for 24 h and then aged at 100 ºC under static conditions for 24 h. Subsequently, the solid product was recovered by

filtration, washed with ethanol and dried at room temperature for 24 h. The surfactant was removed from the material by two successive reflux extractions in ethanol/HCl (1.5 g of as-made PMO in a solution made with 20 mL of 35 wt % HCl and 205 mL of ethanol) for 24 h. The resulting solid was recovered by filtration, washed with ethanol, and dried in air.

2.3. Aminodipropyl-bridged periodic mesoporous aminosilica (PMA)

Materials synthesized using only the highly flexible aminodipropyl-bridged silane collapsed upon surfactant extraction due to the lack of structural rigidity of the framework [4, 34]. Therefore, in order to obtain well-ordered pore structures PMA materials were synthesized by co-condensation of ethylene- and aminodipropyl- bridged silanes.

For the *standard synthesis* of periodic mesoporous aminosilica (PMA), 3.19 g of P123 were dissolved in 126.8 mL of a 0.17 M HCl aqueous solution. To this homogeneous mixture, 9.38 g KCl were added. The mixture was slowly stirred for 24 h. Then, 3.49 g of 1,2-bis(trimethoxysilyl)ethane (BTME) and 0.95 g of bis(3-trimethoxysilyl)propylamine (BTMSPA) were added, and the solution was stirred at 40 ºC for 24 h. The mixture was aged at 100 ºC under static conditions for 24 h. The solution was filtered and the solid product was washed with ethanol and air-dried at room temperature. The surfactant was extracted from the sample by two successive reflux extractions in ethanol/HCl, as indicated above for the PMO sample. The solution was filtered, and the solid product was washed with ethanol and dried under ambient conditions.

The synthesis *of pore-expanded PMA* (E-PMA) followed similar procedure with some modifications. 1.595 mL of the micelle expander agent TIPB were added to the surfactant solution and the mixture cooled down to 18 ºC prior to addition of BTME and BTMSPA. The suspension was kept under stirring at 18 ºC for 24 h. The obtained solid was suspended in 200 mL toluene and refluxed for 24 hours before being filtered and washed with ethanol. The solid was then submitted to reflux extraction in ethanol/HCl and dried in the same way as PMA.

2.4. Functionalization of mesoporous materials by grafting

For comparative purposes, commercial mesoporous amorphous silica (AS) was functionalized with both amine [33] and hydrophobic groups [41] to immobilize laccase and lipase, respectively.

The parent material (1.1 g) was degassed at 80 ºC under vacuum for 18 h and then dispersed in a solution containing the organoalkoxysilane selected for the functionalization process (22 mmol of 3-aminopropyltriethoxysilane (APTES) or 29 mmol of n-octyltriethoxysilane (OTES)) in 100 mL of toluene. The mixture was refluxed under N_2 stream for 24 h. The suspension was filtered, washed twice with dry toluene, three times with acetone and finally was dried at room temperature for 24 h. These supports are named NAS (amine-functionalized amorphous silica) and OAS (octyl-functionalized amorphous silica).

2.5. Characterization of supports

Mesoscopic order was investigated by low-angle X-ray diffraction (XRD) using a PANalytical X´Pert diffractometer with Cu K_α radiation.

Nitrogen adsorption-desorption isotherms were measured at -196 ºC using two Micromeritics sorptometers (ASAP 2020 and ASAP 2420) to determine textural properties. Pure silicas were pretreated at 350 ºC for 16 h and the functionalized supports, at 120 ºC for 16 h. The specific surface area, S_{BET}, was calculated from nitrogen adsorption data in the relative pressure range from 0.04 to 0.2 using the Brunauer-Emmet-Teller (BET) method [42]. The total pore volume, V_p, was determined from the amount adsorbed at a relative pressure P/P_o of 0.97 [42]. Pore size distributions were determined from the adsorption branch of the isotherms using the Barrett-Joyner-Halenda (BJH) model with cylindrical geometry of pores. The BJH pore diameter, $D_{p\ BJH}$, is defined as the position of the maximum in the pore size distribution.

Quantitative determination of the nitrogen content of amino-functionalized supports (NAS, PMA and E-PMA) was performed using a LECO CHNS-932 Elemental Analyser with a Perkin Elmer AD-4 autobalance.

Thermogravimetric analyses of the supports were carried out using a Perkin Elmer TGA 7 instrument. Samples were heated under synthetic air flow (60 mL/min) from 25 to 900 ºC at a rate of 20 ºC/min.

Transmission electron micrographs (TEM) were taken using a JEOL 2100 electron microscope operating at 200 kV. The samples for TEM analysis were prepared by suspending a small amount of solid in acetone by sonication in an ultrasonic water bath for 10 min. A drop of this suspension was then poured onto a copper grid coated with a holey carbon film and the solvent allowed to evaporate at room temperature.

2.6.Protein determination

The crystal structure of *Candida antarctica* lipase B, *Ca*LB (PDB: 1TCA) [43] was taken from the Protein Data Bank [44]. *Ca*LB has a molecular weight of 33 KDa and an isoelectric point (pI) of 6.0. *Ca*LB is a globular α/β type protein with approximate dimensions of 3 nm x 4 nm x 5 nm.

Bioinformatic analysis was used to determine the aminoacid sequence and 3D structure of *Myceliophthora thermophila* laccase (*Mt*L) because the crystal structure is not resolved. The amino acid sequence of MtL was taken from the NCBI Protein Database (accession number AEO 58496.1) [45]. This amino acid sequence was used as a template to identify homologous sequences of the laccase in BLASTP algorithm [46]. The protein BLAST analysis for *Mt*L showed that it shares high identity (73 %) and query coverage (99 %) with the *Melanocarpus albomyces* laccase (PDB: 1GWO-A) [44, 47].

The 3D structure of *Mt*L was modelled applying the alignment mode on the Swiss model server [46, 48-50] using the three-dimensional structure of the *Melanocarpus albomyces* laccase. The modelled *Mt*L structure has been visualized using Pymol software [51]. The molecular analysis of the whole protein using the tools ProtParam [52], UniProt KB (G2QFD0 and G2Q560) [53] and Brenda [54] showed that it has a molecular weight between 63 and 80 KDa. The predicted isoelectric point (pI) was found to be 4.2. These data are in agreement with those reported by other authors [55, 56]. *Mt*L has approximate dimensions of 6.3 nm x 7.2 nm x 8.9 nm.

Protein content of solutions was determined with the Bio-Rad Protein Assay (Bio-Rad, USA), based on the Bradford assay [37], using bovine serum albumin (BSA) as protein

standard. The commercial extracts of laccase and lipase were found to contain a protein concentration of 3.3 mg/mL and 3.0 mg/mL, respectively.

SDS-polyacrylamide gel electrophoresis (SDS-PAGE) was performed for identification of the enzymes and determination of the purity of the commercial extracts [57].

Proteins structural changes by organic solvents were evaluated spectrophotometrically by the changes in the UV-Vis spectra of enzyme solutions with different solvent concentration: laccase in 10 % ethanol and 50 mM sodium dihydrogenphosphate/disodium hydrogenphosphate buffer pH 7.0, and lipase in 50 % methanol and 50 mM sodium dihydrogenphosphate/disodium hydrogenphosphate buffer pH 7.0 compared to the spectra registered by identical enzyme concentrations in their respective buffers.

2.7. Enzymes immobilization

Lipase immobilization was carried out according to a protocol previously reported [41, 58, 59]. Enzyme solutions of different concentrations were prepared in buffered solutions to carry out immobilization at selected pH values. The buffer solutions used and their corresponding pH were: 50 mM glycine/hydrochloric acid (pH 3.5), 50 mM sodium acetate/acetic acid (pH 5.0), 50 mM potassium dihydrogen phosphate/disodium hydrogen phosphate (pH 7.0) and 50 mM sodium carbonate/sodium bicarbonate (pH 9.0). To carry out the immobilization, 100 mg of the support were impregnated with 0.5 mL ethanol (to facilitate its dispersion in aqueous solutions, due to the hydrophobic character of supports), and added to 10 mL enzyme solution. The suspension was kept under gentle stirring at room temperature. Aliquots of the suspension and supernatant were withdrawn at different times and assayed for catalytic activity measurement (pNPA test). The activity of a control enzyme solution was used as reference to evaluate the degree of enzyme immobilization with time. The time at which the residual activity of the supernatant reached a constant value was taken as the end of the immobilization process. The suspensions were then filtered, washed with 200 mM of the respective buffer at the same pH as used for immobilization and subsequently with acetone and allowed to dry at room temperature. High concentration of buffers was preferred for washing in order to preserve hydrophobic interactions and thus preventing enzyme leaching in this step. Dried biocatalysts were stored at 4 ºC. Activity of the supported biocatalysts was determined by

tributyrin hydrolysis assay. Suspensions with a lipase to support weight ratio between 20 and 600 mg/g were used to obtain adsorption isotherms (see Supplementary Information Figure S1 *a*) and determine the maximum enzyme loading capacity of the support under the best conditions of immobilization.

Laccase immobilization on the different supports was carried out at pH 5.5 (and also pH 6.0 for E-PMA) in 50 mM acetic acid/sodium acetate buffer solutions containing different enzyme concentrations. To the enzyme solution, 50 mg of the support were added and kept in suspension under mild stirring at room temperature. Aliquots were withdrawn at given times and the enzymatic activities of suspension and supernatant were assayed (ABTS assay). The decrease of the supernatant activity to a minimum and constant value indicated the end point of the immobilization process. At this point, the solids were filtered off and washed with acetate buffer (50 mM at the same pH as used for immobilization). The solid samples were first dried under vacuum and then under nitrogen stream and stored at 4 ºC for later analysis. Immobilizations were performed using different enzyme to support weight ratios in the range between 25 and 350 mg/g in order to determine adsorption isotherms and the maximum loading capacity for all supports (see Figure S1 *b* for enzyme adsorption isotherms). To determine the catalytic activity of the supported biocatalysts, 10 mg of the solid were suspended in 1 mL of 50 mM acetate buffer (at the same pH as used for immobilization) and assayed in the ABTS oxidation test.

2.8. Enzyme leaching study

The resistance to enzyme leakage from the supports was studied under conditions that presumably favour the release of the protein, namely high dilution and low ionic strength. Lipase catalysts were suspended in 50 mM potassium dihydrogen phosphate/disodium hydrogen phosphate at pH 7.0. The laccase catalysts were incubated in 50 mM acetic acid/sodium acetate buffer at pH 4.5. Suspensions were prepared with 1.25 mg of solid per mL of buffer solution and were incubated at 25 ºC. Enzyme leaching was calculated at different incubation times by measuring the amount of enzyme present in the supernatant using the Bradford assay [37]. After the leaching treatment, the solids were separated by filtration, suspended in electrophoresis sample buffer (containing SDS, mercaptoethanol, bromophenol blue, Tris buffer pH 6.8 and glycerol) and boiled for 5 min. After this treatment, proteins trapped in the solids would be denatured and the lineal

polypeptide chains should be easily released from the pores. The supernatants of these suspensions were withdrawn and analysed by SDS-PAGE electrophoresis.

2.9. Enzyme activity assays

Routine laccase activity tests were carried out spectrophotometrically by measuring the increase in absorbance at 405 nm caused by the oxidation of ABTS [60]. The reaction mixture consisted of a 1.6 mM ABTS solution in 100 mM acetic acid/sodium acetate buffer at pH 4.5. To 1.9 mL of this solution in the cuvette, 50 µL of enzyme solution or suspension were added under stirring and the reaction was monitored continuously at 25 ºC for 30 min. One unit of laccase activity (U_{ABTS}) was defined as the amount of enzyme required to oxidize 1 µmol of ABTS per minute at 25 ºC (the molar absorption coefficient of oxidized ABTS at 405 nm was taken as $\varepsilon_{405\ nm}$ = 35,000 $M^{-1} \cdot cm^{-1}$).

In order to perform enzyme spectrophotometric assays at different pH values, the isosbestic point of oxidized ABTS (ABTS*) was determined and established at 430 nm, and the molar absorption coefficient of ABTS* was calculated ($\varepsilon_{430\ nm}$ = 20,700 $M^{-1} \cdot cm^{-1}$). The activities of the free and immobilized laccases (on PMA and NAS) were determined at this wavelength as a function of pH, in 50 mM phosphoric acid/sodium dihydrogenphosphate (pH 2.5) and 50 mM citric acid/trisodium citrate (pH 3.0 to 6.0) buffer solutions at 25 ºC (triplicated).

Hydrolysis of p-NPA was used as a routine test to measure the nonspecific esterase activity for monitoring the immobilization of lipase. An aliquot of 50 µL of enzyme solution (control or supernatant) or immobilized enzyme suspension was added to a cuvette with 1.9 mL of 0.4 mM p-NPA aqueous solution (pH 7.0). The activity was determined at 25 ºC by measuring the rate of increase of absorbance at 348 nm due to the release of p-nitrophenol (the molar absorption coefficient was taken as $\varepsilon_{348\ nm}$ = 5,150 $M^{-1} \cdot cm^{-1}$).

Spectrophotometric assays of free enzyme and immobilized enzyme suspensions were performed using an Agilent 8453 UV-Vis spectrophotometer equipped with a stirring device and temperature control.

Lipase biocatalysts stability tests were performed using the hydrolysis of tributyrin as test reaction to evaluate hydrolytic activity of lipase. The activity was determined by titration of the butyric acid released by the hydrolysis of tributyrin. 1.47 mL of tributyrin

were added under stirring to 48.5 mL of 10 mM potassium phosphate buffer at pH 7.0 in a thermostated titration vessel at 25 °C. Once equilibrated at pH 7.0, a weighted amount of biocatalyst was added, and the rate of addition of a 0.1 M NaOH solution required to neutralize the acid product and maintain a constant pH of 7.0 was measured. One unit of activity (U_{TB}) was defined as the amount of lipase converting 1 µmol of tributyrin per minute.

Titrimetric determination of lipase activity was performed using a Mettler Toledo DL-50 pH-state.

2.10. Stability tests

The thermal stability of free and immobilized enzymes was determined by incubation at 55 ºC in 50 mM potassium dihydrogen phosphate/disodium hydrogen phosphate buffer at pH 7.0 (for lipase) and at 60 ºC in 50 mM acetic acid/sodium acetate buffer at pH 5.5 (for laccase).

Stability of free and immobilized enzymes in organic solvents was evaluated by incubating samples at 25 ºC in 50 % v/v methanol/water and pure methanol (lipase samples) or 10 % v/v ethanol at pH 3.5 (laccase samples).

Incubations were performed in different vials for each aliquot to prevent solvent evaporation during sampling. Aliquots were withdrawn at different times, cooled down and their activities were assayed in the hydrolysis of tributyrin (lipase) or in the oxidation of ABTS (laccase).

3. RESULTS

3.1. Characterization of the supports

TEM images of solvent-extracted hybrid organosilicas (Figure 1) show large domains with two-dimensional hexagonal arrangements of parallel channels of uniform size. This is consistent with X-ray diffraction (XRD) patterns (see Supplementary Information Figure S2), which exhibit an intense reflection and two relatively well resolved weak peaks in the low angle region (0.5-2º), that can be indexed as the 100, 110 and 200 reflections of p6mm hexagonal symmetry. These patterns indicate that the samples possess high degree of mesostructural order. In contrast with the hybrid organosilica supports, the XRD pattern of the commercial amorphous silica (not shown) does not exhibit any diffraction peak at low angle, evidencing the lack of mesoscopic order and, hence, the non-uniform pore structure of this material.

Figure 2 *a* shows nitrogen adsorption-desorption isotherms and the corresponding pore size distributions calculated by the BJH method for the solvent-extracted hybrid aminosilica samples. The isotherms are type IV, with H1 type hysteresis loop at high relative pressure, which is characteristic of mesoporous materials. The calculated pore size distributions (Figure 2 *a*, inset) indicate that the three samples possess uniform mesopores, in agreement with the regular pore structure shown by XRD and TEM.

The diameter of pore channels estimated by the BJH method is reported in Table 1. The pore size estimated for PMO and PMA supports is around 7 nm. This value increases up to more than 10 nm when the synthesis of hybrid aminosilica was carried out using the swelling agent (sample E-PMA). In the case of sample E-PMA the nitrogen isotherm (Figure 2 a) shows that, besides the main steep nitrogen uptake at a relative pressure around 0.8, corresponding to the regular mesopore channels, an additional increase of nitrogen adsorption occurs at relative pressures above 0.9. This is also apparent in the pore size distribution (Figure 2 a, inset) that evidences the presence of secondary mesoporosity, with a relatively broad pore size distribution ranging from 15 to 30 nm, which can be attributed to interparticle spaces. The three samples possess high surface area and pore volume (Table 1), although these parameters differ significantly among the three samples. Taking into account the unit cell parameters (a_0) calculated from the XRD patterns (11.6, 12.4 and 15.9 for PMO, PMA and E-PMA, respectively) and the diameter

of the pore channels determined from the nitrogen isotherms (Table 1), it can be estimated that the pore wall thickness of PMO, PMA and E-PMA is 4.5, 5.2 and 5.5 nm, respectively. Therefore, the differences in textural properties might be attributed to the different pore size and pore wall thickness of the three samples.

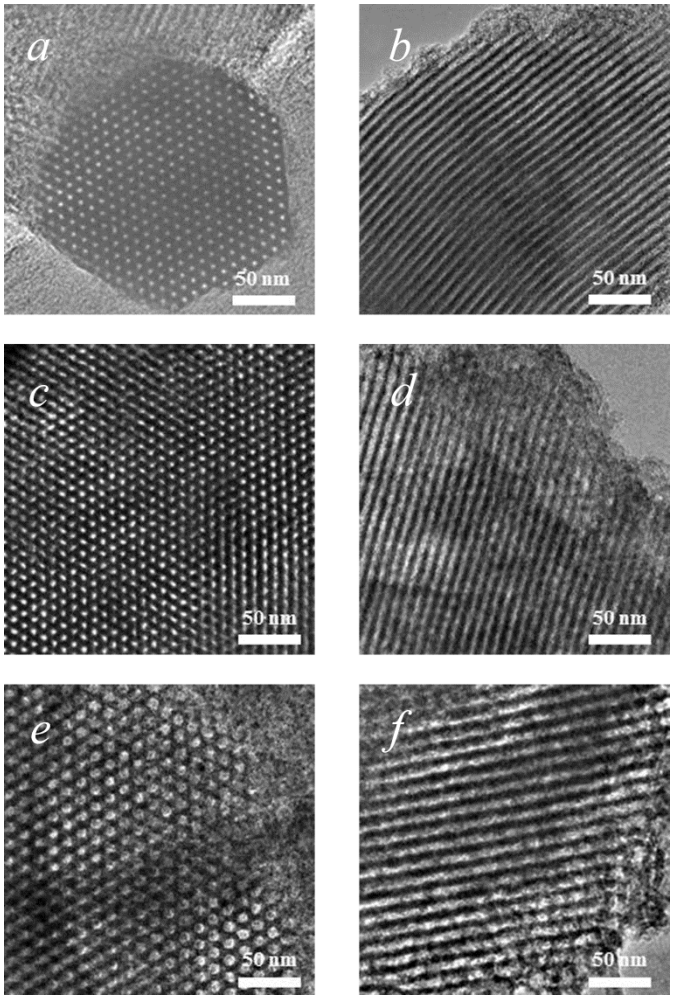

Fig. 1. TEM micrographs of PMO (a, b), PMA (c, d) and E-PMA (e, f).

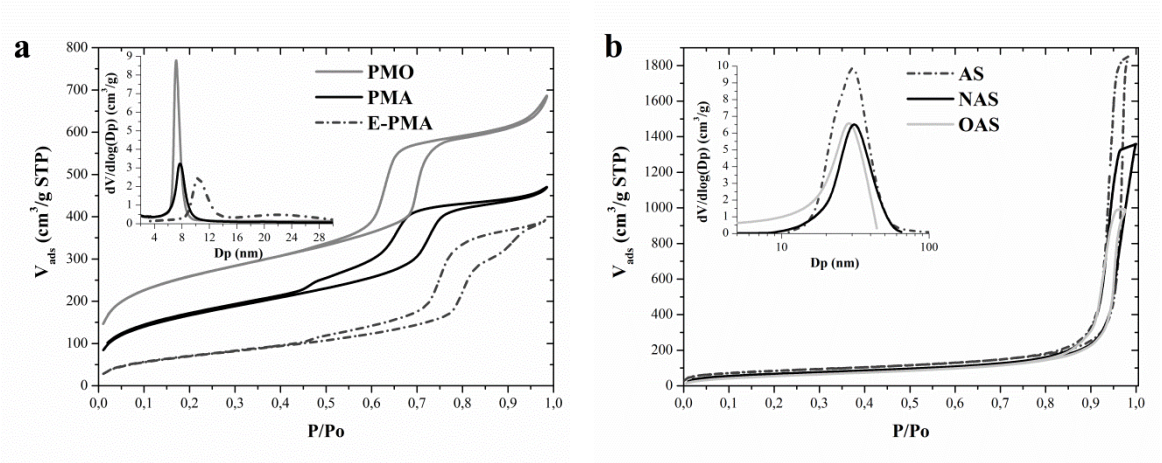

Fig. 2. Nitrogen adsorption isotherms and pore size distributions of: ***a***) hybrid organosilica supports and ***b***) parent and functionalized amorphous silica supports.

Figure 2 *b* shows the N_2 adsorption-desorption isotherms of the parent (AS) and functionalized amorphous silica supports (OAS and NAS). These supports show type IV isotherms corresponding to mesoporous materials [29, 41]. In contrast with hybrid organosilicas, the commercial amorphous silica has a wide pore size distribution, indicating heterogeneity in the porous structure, and larger pores, with the maximum of the pore size distribution around 30 nm (Figure 2 *b*, inset). Functionalization of the AS support has a negligible effect on pore size (Figure 2 *b*, inset and Table 1), as can be expected due to the large pore size. Nevertheless, grafting with aminopropyl or octyl groups on the silica surface produces a small decrease of both surface area and pore volume (Table 1).

Thermogravimetric analysis (TGA) profiles show the incorporation of organic groups in functionalized silica and hybrid organosilica supports (Figure S3). All materials show a small weight loss at temperatures below 150 ºC that can be attributed to desorption of water or residual organic solvents. The main weight loss occurs in the temperature range 150-600 ºC, which corresponds to decomposition and combustion of the organic groups. At temperatures higher than 600 ºC a further small weight loss is observed that that might be attributed to dehydroxylation of the silica surface. Therefore, the amount of hydrophobic groups (octyl chains in sample OAS and ethylene bridges in sample PMO) have been calculated from the weight loss in the temperature range 150-600 ºC. The results, expressed as mmol C per gram of silica are given in Table 1. It can be seen that the total amount of carbon of the hybrid organosilica material is around four times that of

the amorphous silica functionalized with octyl groups. In the case of supports containing amino groups (PMA and E-PMA), the weight loss assigned to removal of organic groups corresponds to both aminodipropyl and ethylene bridges. Therefore, the concentration of amino groups was determined by chemical analysis. All the supports obtained contain a relatively high amount of amine, ranging from 1 to 1.8 mmol per gram of silica (Table 1).

Table 1. Textural properties and organic groups content of supports.

Material	$D_{p\ BJH}$[a] (nm)	S_{BET}[b] (m^2/g)	V_p[c] (cm^3/g)	mmol C/g SiO_2[d]	mmol N/g SiO_2[e]
AS	30	285	2.2	-	-
OAS	30	212	1.6	4.2	-
NAS	30	236	2.1	-	1.8
PMO	7.1	882	1.0	16.1	-
PMA	7.2	594	0.7	-	1.5
E-PMA	10.4	264	0.6	-	1

[*a*] BJH pore diameter (nm).

[*b*] BET surface area (m^2/g).

[*c*] Total pore volume (cm^3/g).

[*d*] Hydrophobic (aliphatic carbon) groups content determined from TG analysis (weight loss in the temperature range 150-600 °C).

[*e*] Concentration of amine groups determined by chemical analysis.

3.2. Lipase immobilization on PMO at different pH values

The loading capacity of PMO for lipase immobilization was determined at pH 5.0 by the adsorption isotherm at room temperature (*Supplementary Information*, Figure S1). Maximum enzyme loading remained nearly constant (about 90 mg enzyme per gram of support) at a content of enzyme in the liquid phase over 100 mg/g. This can be attributed to the relatively small pore size that would prevent multilayer adsorption of enzyme. In contrast, on the octyl-functionalized amorphous silica support OAS, lipase loadings up to 400 mg enzyme per gram of support were obtained [29] due to its larger pore size.

However, this high enzyme loading leads to lower catalytic efficiency (90 U_{TB} per mg of enzyme, compared to 200 U_{TB}/mg for the PMO-supported catalyst [29]). This is probably due to the intense interaction with the highly hydrophobic octyl groups. Despite each single interaction is mild, the high content in ethylene groups and the high contact surface in PMO due to the confinement of enzyme within the pore, makes the overall interaction intense. But the mild interactions permit the catalyst to preserve high catalytic activity [29].

Suspensions with 90 mg enzyme per gram of support were prepared to evaluate the effect of pH on lipase immobilization on PMO. The maximum amount of lipase slightly decreased as the pH increased from 3.5 to 9.0 (Table 2). In the whole pH range used for lipase immobilization, silanol groups present on the support should be deprotonated, as the point of zero charge (pzc) of silica is around 2. Taking into account that the isoelectric point (pI) of lipase is around 6.0, electrostatic attractions or repulsions may also be established with the remaining siloxane groups on the surface of PMO [22] when the immobilization is performed at pH 3.5-5.0 or pH 7.0-9.0 respectively. Although maximal loading was achieved at pH 3.5 and 5.0, as expected, the values are rather close indicating that the driving forces of the immobilization are hydrophobic interactions.

Table 2. Immobilization of lipase on PMO at different pH values from suspensions containing 90 mg lipase per gram of support.

pH	t_c[a] (h)	Max. Load[b] (mg/g)	Biocatalyst activity[c] (U_{TB}/g)	Cat. Eff.[d] (U_{TB}/mg)
3.5	1.25	77.05	2377.8	30.9
5	1.25	70.18	4020	57.3
7	1.50	69.85	3958	56.7
9	1.75	49.14	1952.4	39.7

[*a*] Time at which the maximum loading is achieved.

[*b*] Maximum enzymatic loading, expressed in milligrams of lipase per gram of support.

[*c*] Biocatalyst activity expressed in U_{TB} per g of support.

[*d*] Catalytic efficiency expressed in U_{TB} per mg of lipase.

3.3. Laccase immobilization on PMA

The low isoelectric point of laccase (4.2) permits a wide pH range for electrostatic interactions between negatively charged enzyme and positively charged amine groups of the hybrid aminosilica supports (pKa around 11.0). Thus, immobilization was tested at pH 5.5. Because of the similar size between the dimensions of laccase (6.3 x 7.2 x 8.9) and the pore diameter of PMA (7.2 nm), maximal loading in this support is low, as well as activity and efficiency of the biocatalyst (Table 3). The enzyme molecules are probably absorbed only onto the external surface of PMA particles.

Loading capacity of our expanded pore material E-PMA with 10.2 nm pore diameter was tested. Table 3 shows the loading capacities of the three amine-coated supports. The rise in pore size enabled a twofold increase in the enzyme loading of E-PMA compared to PMA. Also, amine-functionalized amorphous silica was tested for comparative purposes. Similarly to lipase immobilization, the highest laccase loading was achieved in amorphous silica with much larger pore size. However, it is worth noting that adsorption equilibrium was reached more rapidly for the supports with uniform pore size.

It was also observed that increasing the pH of laccase solution to 6.0 led to a faster adsorption and higher enzyme loading on E-PMA: 119 mg/g vs 88.0 mg/g at pH 5.5. However the catalytic efficiency was significantly decreased at pH 6.0.

Table 3. Immobilization of laccase on different supports.

Support	pH[a]	t_c[b] (h)	Max. Load[c] (mg/g)	Biocatalyst activity[d] (U_{ABTS}/g)	Cat. Eff.[e] (U_{ABTS}/mg)
NAS	5.5	24	187	170	0.91
PMA	5.5	2.0	42	4.7	0.11
E-PMA	5.5	1.5	88	29	0.33
E-PMA	6.0	1.3	119	19	0.16

[*a*] pH of immobilization.

[b] Time at which the maximum loading is achieved.

[*c*] Maximum enzymatic loading, expressed in milligrams of laccase per gram of supported - biocatalyst.

[*d*] Biocatalyst activity expressed in U_{ABTS} per g.

[*e*] Catalytic efficiency expressed in U_{ABTS} per mg of lipase.

Figure 3 shows the pH/activity profiles of laccase in soluble and immobilized estates. It can be observed that for laccase supported on NAS, the optimum pH was 0.5 units higher than that of soluble laccase. This result might be explained assuming that amino groups incorporated into materials generate a new environment which may result in a pH gradient from inside the particle towards the external aqueous medium in which catalyst particles are suspended. This trend had been previously found with expanded-pore SBA-15 materials functionalized with primary amine groups, where optimum pH was shifted 0.5 pH units, as well as NAS [33]. The shift of optimum pH underwent by laccase immobilized on E-PMA was much more pronounced: from pH 3.0 to pH 5.0. As noted, laccase immobilized in the supports showed higher activity than the free enzyme in the pH range 4.0-6.0. This effect can be attributed to the microenviromental conditions [61] in this material, with secondary amines in the close vicinity of enzyme.

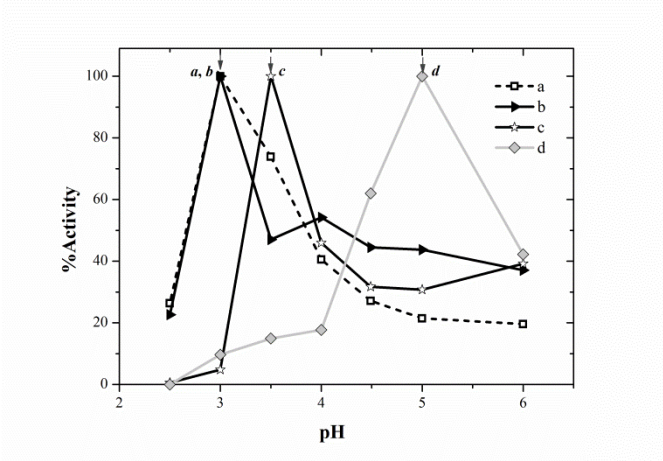

Fig. 3. Effect of pH on the activity of *a*) free enzyme, *b*) AS, *c*) NAS and *d*) E-PMA.

3.4. Leaching and electrophoresis

In former works we had determined the amount of lipase leached from OAS and PMO after two hour incubation under conditions of charge repulsion and high dilution, where the release of the enzyme is favoured and expected [29]. We present here a 24 h time course of enzyme leaching (Figure 4 *a*). Lipase in PMO only undergoes a 15 % initial leaching that may be due to removal of enzyme molecules immobilized on the outer

surface of PMO particles, and then no more leaching was detected. Leaching of lipase from OAS is higher and growing with incubation time.

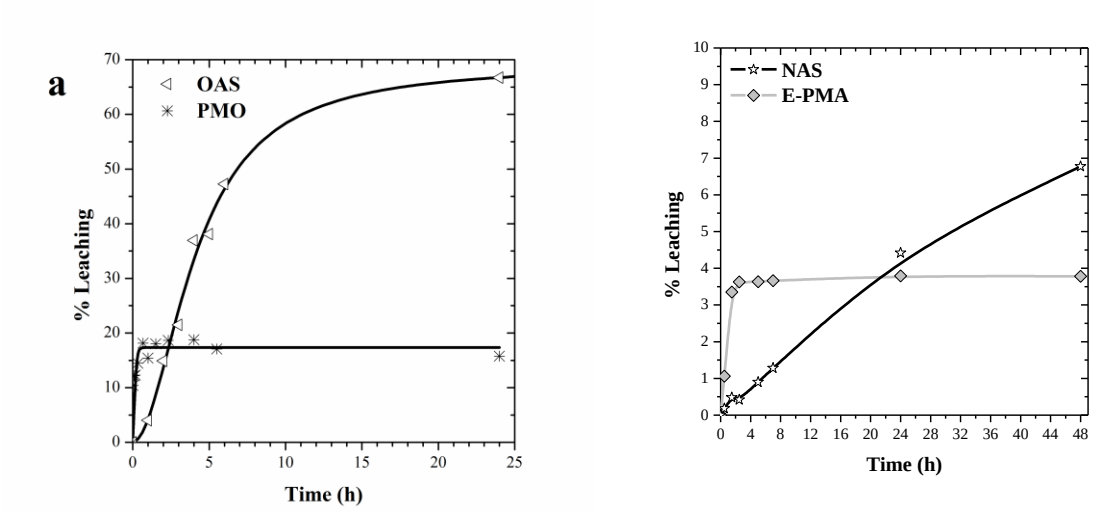

Fig. 4. ***a***) Leaching of lipase from ordered material (PMO) and amorphous mesoporous silica (OAS). ***b***) Leaching of laccase from ordered material (E-PMA) and amine amorphous silica (NAS). Expressed as percent of the initial enzyme leached on each material as a function of time.

Lipase tightly fitting into pores of PMO and fixed by ethylene groups is highly retained. In contrast, stronger interaction with octyl groups of OAS does not prevent enzyme from leaching through the 30 nm with pores of amorphous silica. These results seem to suggest that it both, chemical affinity and confinement in the pore contribute to minimize enzyme leaching.

The same trend is observed for laccase leaching from catalysts (Figure 4 *b*). NAS catalyst shows a continuous release of enzyme. Again, the affinity of laccase with amine groups is not enough to prevent leaching from pores with an average diameter of around 30 nm, with no diffusion restrictions. As shown in Figure 4 *b*, leaching profile in E-PMA showed also initial desorption, probably due to enzyme molecules immobilized on external surfaces. But percent values of laccase leached are much lower than in the case of lipase (4 %). The uniform pore size close to the enzyme dimensions along with the increased affinity of the laccase for secondary amine groups make this material more efficient to retain the enzyme inside the inner surfaces.

An attempt to verify the location of enzymes inside the porous network of the materials was made. Since solid samples of the biocatalysts are not suitable for electrophoresis, the enzymes were forced to exit the pores. First, biocatalysts were

suspended as described above for leaching tests to desorb as much enzyme as possible, especially to eliminate all protein molecules adsorbed on the external surface of support particles. Then the supernatants were removed and the filtered solids were boiled in sample electrophoresis buffer. In such denaturing conditions including the split of disulphide bonds, the tertiary structure of the protein should be lost and the random coil chain should then be easily released from the pores. However, no protein band could be seen from the E-PMA supernatant electrophoresis (Fig. S4 *a*). Then, E-PMA samples after the same SDS-PAGE treatment were centrifuged and suspended at pH 11 and 14 respectively and the supernatants were analysed again. Protein band only appeared in the supernatant of the sample suspended at pH 14.0. These results confirm the presence of the enzyme inside the pores, in agreement with previous results based on advanced TEM techniques [62] and evidence the strong binding of the enzyme to the inner surface of the support.

The results obtained with lipase catalysts are shown in Figure S4 *c*. In this case no further incubation was necessary, and the band corresponding to the immobilized lipase appeared from both, PMO and OAS.

3.5. Thermal stability

The thermal stability of enzymes catalysts is important for some industrial applications [63] because bioreactors are sometimes operated at elevated temperatures to improve productivity and to avoid microbial contamination.

Free and immobilized lipases were incubated in buffer at 55 ºC and their inactivation courses are shown in Figure 5. Lipase on PMO was inactivated at a faster rate than free enzyme, while maximal stabilization was achieved in OAS.

Thermal stabilities of free and immobilized laccase on NAS and E-PMA materials were evaluated at 60 ºC in the same way. Again, a faster inactivation rate was underwent by laccase in E-PMA and immobilization in NAS resulted in enzyme stabilization (Fig. 6).

3.6. Stability in organic solvents

Lipase can be used in the synthesis of biodiesel to catalyse both, the hydrolysis of triacylglycerols to release fatty acids and the methanolysis of these fatty acids [64-67].

The biocatalytic pathway is attractive due to the easier purification of products and environmental advantages [8, 68]. However, the necessary presence of methanol involves severe losses of enzymatic activity because of structural and inhibitory damages on the enzyme [66, 69]. This solvent was chosen to study the structural protection that PMO may provide.

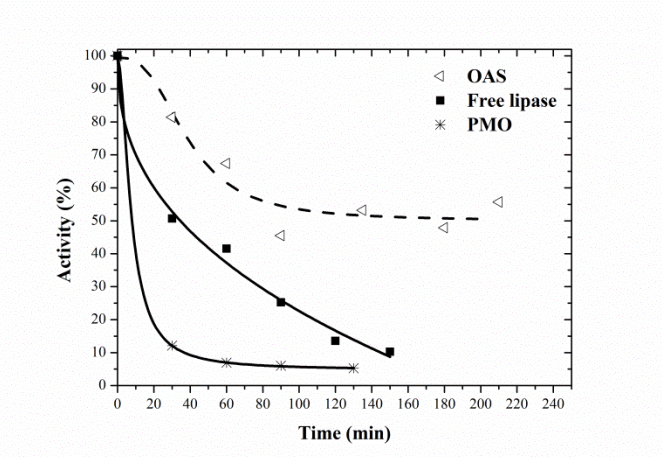

Fig. 5. Thermostability profiles at 55 ºC of free and immobilized lipase on PMO and octyl amorphous silica (OAS).

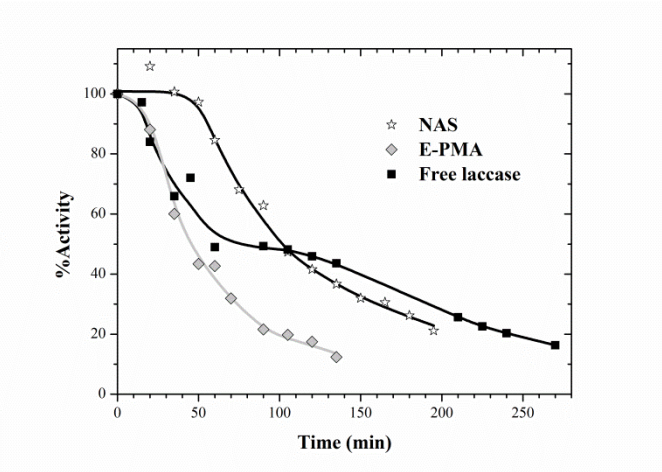

Fig. 6. Thermostability profiles at 60 ºC of free and immobilized laccase. Runs were performed at pH 5.5.

PMO-lipase incubated in 50 % methanol remained fully active after 24 hours, although the stability of the soluble enzyme was also high, as well as the one on OAS (Figure 7 *a*). Severe effects on the activity were registered by incubation in 100 % methanol, where soluble lipase and OAS-lipase kept only 25 % and 32 % residual activity after 1 hour respectively. In the same conditions PMO-lipase still kept 75 % activity (Figure 7 *b*). But

the activity was almost completely lost at longer incubation time for the three samples, probably because of inhibitory effect of methanol.

Laccase has been used to partially oxidize wine polyphenols [70-72]. Therefore, in order to evaluate the potential application of PMA-laccase biocatalysts in wine stabilization, the stability of biocatalysts was tested by incubation in a low ethanol concentration. Free laccase, NAS and E-PMA were incubated in a medium similar to wine: 10 % ethanol and acidic pH (Fig. 8). Inactivation was faster in the native enzyme, while NAS preserved around 85 % activity after 6 hours incubation and laccase immobilized on PMA remained fully active during the same period of time.

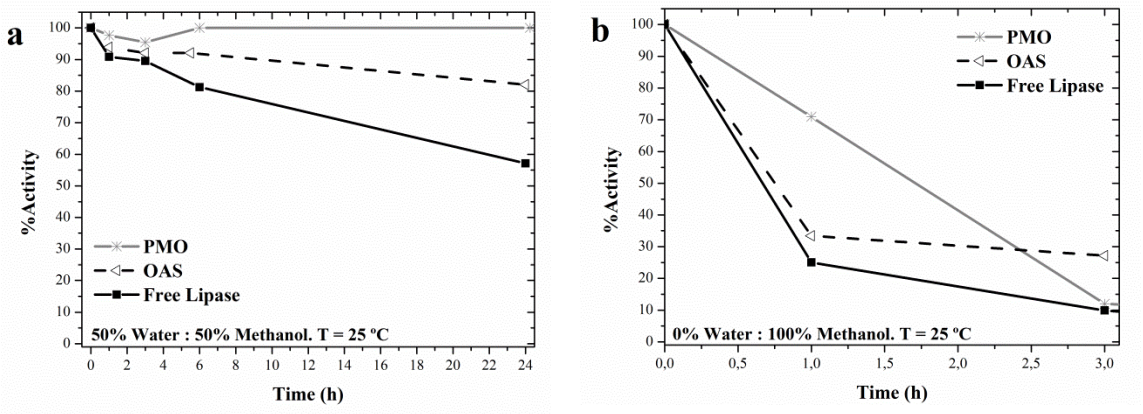

Fig. 7. Stability of lipase in solution and supported on OAS and PMO in: ***a***) 50 % aqueous solution: 50 % methanol; ***b***) 0 % aqueous solution: 100 % methanol. Runs were performed at 25 ºC.

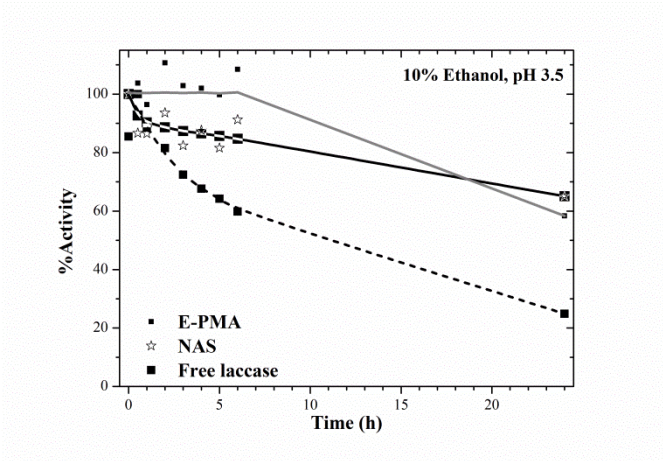

Fig. 8. Stability of free and immobilized laccase in ethanol : water solution at acidic pH. Runs were performed at 25 ºC

Figure 9 shows the UV-Vis spectra of soluble enzymes: lipase in buffer and 50 % methanol (*a*) and laccase in buffer and 10 % ethanol (*b*). Proteins absorbance at 280 nm is due to the presence of aromatic side chain of aminoacids, especially tryptophan. Spectra of the enzyme in the presence of cosolvents show higher peaks of absorbance at 280 nm, which suggests a higher amount of these aromatic aminoacids on the surface of the protein.

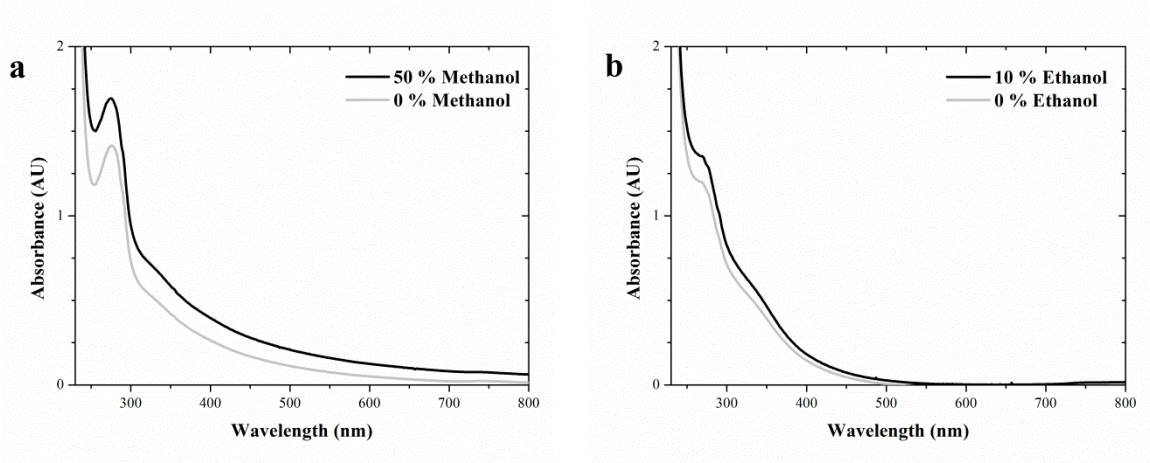

Fig. 9. UV-Vis spectra of lipase in aqueous buffer and 50 % methanol (***a***) and laccase in aqueous buffer and 10% ethanol (***b***).

4. DISCUSSION

The main characteristics of periodic mesoporous organosilica as support for enzyme immobilization are the confinement and the presence of chemical functionalities. These chemical groups are not anchored on the internal surface of pores but become part of it. These two features mean that there is close vicinity between the side chain groups of the enzyme and the functional groups of the support with no steric hindrances. Apart from the specific organic moieties introduced in the synthesis of the PMO (ethylene bridges) and PMA (dipropylamine and also ethylene bridges), silanol groups are present on the surface of silica that can also play their part.

The same loading of lipase on PMO was achieved at pH 5.0 and 7.0 despite repulsion should be established at the higher pH between negative charges on both, enzyme and support. What this probably means is that hydrophobic interactions are the driving forces of the process, over electrostatic ones. The only difference is found in the contact time: immobilization is faster at pH 5.0 than at pH 7.0. Also, the highest values of catalytic

efficiency were found at pH 5.0 and 7.0. At pH 3.5 higher loading was achieved as a result of the additional electrostatic attraction (the enzyme should have a net positive charge while the support is negatively charged). Nevertheless, the catalytic efficiency was lower probably because an excessive interaction is established with a distortional effect on the protein structure.

The immobilization of laccase showed higher values of enzyme loading and catalytic efficiency on the amorphous and wide pore support NAS. Although this amine-functionalized amorphous silica has lower surface area than E-PMA, the available surface in E-PMA is much lower because only one molecule of enzyme occupies the whole pore section, as the pore size is close to enzyme dimensions. Thus, the maximal capacity for enzyme immobilization determined for NAS was around four times higher than on E-PMA (Table 3). The intensity of the interaction with laccase is not identical for both supports since there are primary propylamine groups (pKa around 10) in NAS and secondary dipropylamine groups in E-PMA (pKa around 11). The interaction of negative charges of enzyme with these high pK_a should be more intense and this is probably the reason why the catalytic efficiency is lower. As discussed for lipase-PMO, the stonger interaction may distort protein structure. This may also explain that immobilization at pH 6.0 displays higher enzyme loading and lower catalytic efficiency than at pH 5.0, because of the higher density of negative charges on the enzyme.

This high pK_a in E-PMA is also responsible for a higher density of positive charges at the same pH, and consequently a higher pH gradient between the inner pores of the particles and the external medium. As a consequence, there is a large optimum pH shifting in the activity vs. pH profile, and it is likely that the immobilization inside the particle is occurring at a lower pH than measured in the bulk of the solution.

The absence of enzyme leaching from E-PMA samples can also be explained by this property. The protein unfolded under denaturing conditions does not leave the pores at pH below 11, probably because electrostatic attractions remain even in the random coil configuration. Only at pH extremely high (pH 14.0) all amino groups from support should be deprotonated and repulsive forces would be driving the release of protein from pore channels. These experiments reveal that leaching only occurs in very harsh conditions, showing that this non-covalent immobilization is nearly as irreversible as a covalent one.

Unfolding of the protein is promoted by both, high temperature and organic solvents. These conformational changes may drive the formation of new interactions of side chain amino acids with the support, but the processes do not occur identically.

At high temperature the close vicinity of amines (or ethylenes) and silanol groups promotes abundant new interactions with amino acids exposed upon partial unfolding of the peptide chain. In our experiments, incubation of the catalysts suspensions or enzyme solutions were performed at high temperatures, and cooled down to the assay temperature (25 ºC for lipase and laccase). The fact that in both cases: PMO-lipase and E-PMA-laccase resulted the least stable ones may be related to confinement. Probably the interactions established between the enzyme structure, partially unfolded upon heating and the "close-fitting-around" support, are preserved after cooling. Thus, refolding to a more active conformation is prevented and the activity would be irreversibly lost in PMO/E-PMA biocatalysts. Neither enzymes in the wide-pore amorphous silica (OAS, NAS) nor the free enzymes have this restriction from the support, and this absence of steric hindrance would still permit some margin for reversibility. As a consequence the enzymes can partially recover their native conformation at lower temperatures.

Only the lipases naturally contain a hydrophobic domain on their surface. With this exception, hydrophobic side chains of aminoacids are usually placed inside the protein globule, avoiding contact with aqueous medium. Cosolvents miscible in water are known to interfere hydrogen bonds and to unfold proteins, thus forcing some hydrophobic amino acids to arise to the external surface. Spectra in aqueous and organic media of both lipase and laccase (Figure 9) show a moderate higher absorbance at 280 nm in the organic solvents, which is usually attributed to tryptophan residues (hydrophobic) and confirm this effect of the solvents on both enzymes. PMO and E-PMA surfaces are contain ethylene bridges capable to establish new interactions with these arising hydrophobic groups. The stabilization results confirm that PMO and E-PMA are highly efficient to stabilize lipase and laccase versus methanol and ethanol respectively (Figures 7 and 8). This higher presence of hydrophobic aminoacids on the external protein surface increases the bonding intensity with the close support surface containing ethylene groups. In the case of E-PMA-laccase, new hydrophobic interactions are added to the former electrostatic ones.

Aminoacids involved in unfolding promoted by high temperature and solvents are different, thus the new interactions and the structure of the partially unfolded proteins are

also different. If the change does not lead to inactive conformations (as it happens by heating) the result is the stabilization of an active conformation, which becomes strengthened by abundant non-covalent bonds with the support.

The close match of sizes of enzyme and pore channels is the key to obtain this stabilization since the tertiary structure of the protein is physically prevented to keep on unfolding. However, laccase immobilized on ordered mesoporous materials (OMM) with similar structure and pore size bearing aminopropyl groups anchored on the surface had proven less stable than laccase-E-PMA catalyst in the same conditions [33]. The difference between both kinds of materials is that the organic moiety becomes part of the wall of the channel pores in the PMO/E-PMA materials, at the same level as silanols. Aminoacids can easily interact with either the negatively charged siloxanes or the ethylene bridges or dipropylamine groups. It is noticeable that in the case of E-PMA interactions can be established with the three of them. In the OMM materials where organic moieties are anchored to the siliceous surfaces, the silanol groups of the wall are not as accessible, as they are partially hindered by the propylamine or alkyl chains. Thus, additional interactions are not easily established.

5. CONCLUSIONS

We have synthetized a novel periodic mesoporous aminosilica with a pore size that matches with the dimensions of the enzyme laccase. The effects of presence of ethylene bridges and dipropylamine groups becoming part of the surface on laccase immobilization and the behaviour of the catalyst have been studied and compared to lipase immobilized on an ethylene-bridged PMO. The PMO materials display some specific properties which enable the immobilization with high enzyme loading while retaining high catalytic activity and providing protection against inactivation in organic solvents. This is possible because these materials integrate organic and inorganic components in a restricted space where the interaction with the enzyme takes place all around the enzyme molecules and the mobility is prevented. Interactions are also feasible with silanol (or siloxane) groups which are not hindered by organic groups since these are also part of the support framework. Moreover, the number of contact points increase in the presence of an organic cosolvent, where additional hydrophobic interactions are

established. The highly ordered structure contributes to keep high catalytic efficiency because it favours pore connectivity.

Laccase undergoes an especially strong interaction with secondary amines of E-PMA, which fully prevents leaching at pH below 14. This is a relevant result since the non-covalent nature of the linkage permits to recover the support after enzyme inactivation, namely by suspending it at elevated pH. Lipase immobilization on ethylene-bridged periodic mesoporous organosilica (PMO) appeared to be the most promising approach, since it occurred with high efficiency, maintained enzyme activity, and provided enzyme stability.

6. SUPPLEMENTARY INFORMATION

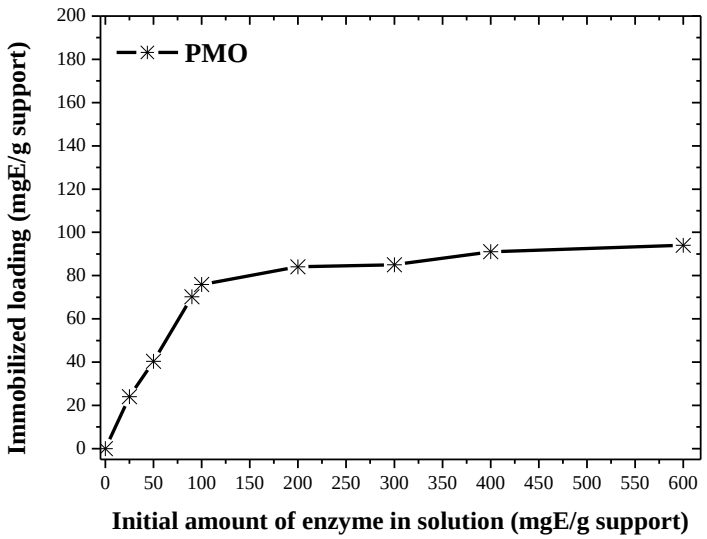

Figure S1 *a*. Immobilized loading versus initial enzyme loading at pH 5.0 for PMO.

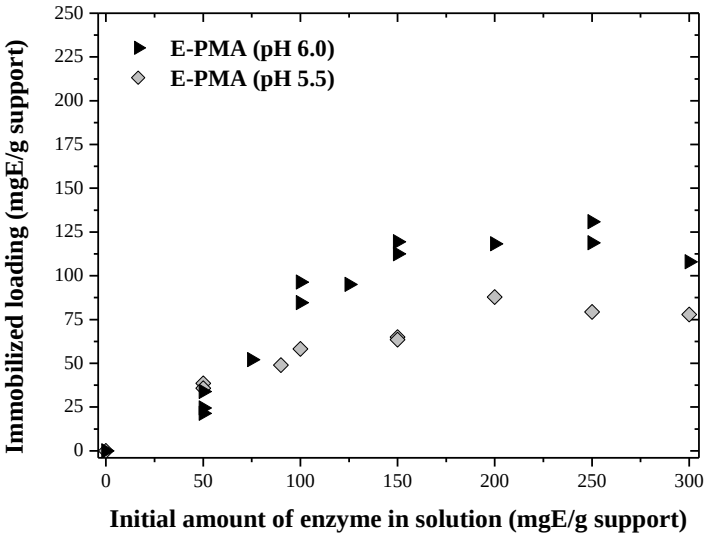

Figure S1 ***b***. Immobilized loading versus initial enzyme loading at pH 5.5 and 6.0 for E-PMA.

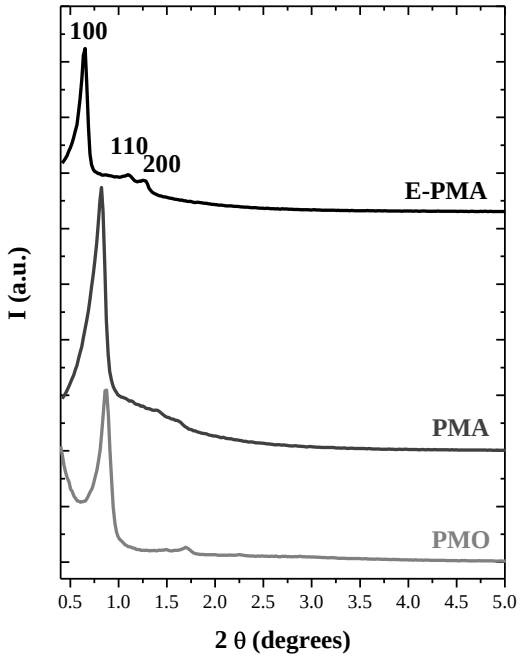

Figure S2. Low-angle XRD patterns of hybrid organosilica supports.

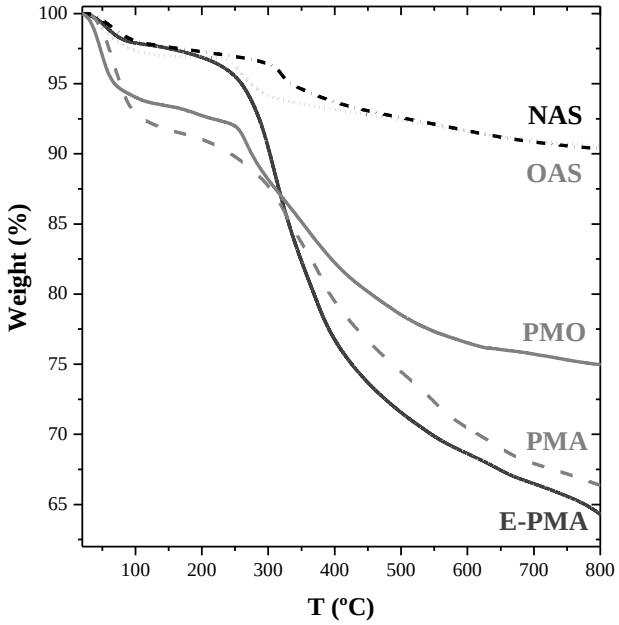

Figure S3. TGA profiles of hybrid organosilica and functionalized amorphous silica supports.

Figure S4. Electrophoresis.

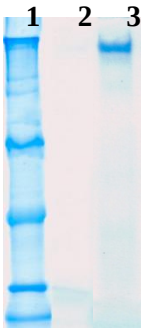

a) 1: Protein standard (high range SDS-Page standard stained with coomassie G-250 stain), 2: E-PMA at pH 6.5 and 3: NAS at pH 6.5.

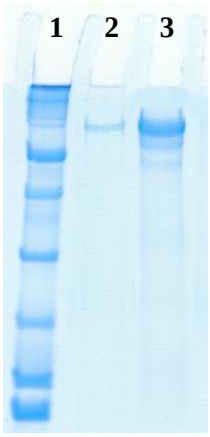

b) 1: Protein standard, 2: E-PMA at pH 14.0 and 3: soluble laccase.

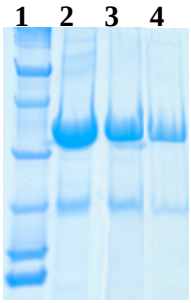

c) 1: Protein standard, 2: soluble lipase, 3: PMO, 4: OAS (all in standard conditions).

7. REFERENCES

[1] M. Hartmann, D. Jung, Biocatalysis with enzymes immobilized on mesoporous hosts: the status quo and future trends, *J. Mater. Chem.*, 20 (**2010**) 844.

[2] M. Hartmann, X. Kostrov, Immobilization of enzymes on porous silicas--benefits and challenges, *Chem. Soc. Rev.*, 42 (**2013**) 6277-6289.

[3] E. Serra, A. Mayoral, Y. Sakamoto, R.M. Blanco, I. Diaz, Immobilization of lipase in ordered mesoporous materials: Effect of textural and structural parameters, *Microporous Mesoporous Mater.*, 114 (**2008**) 201-213.

[4] M.A. Wahab, I. Kim, C.S. Ha, Bridged amine-functionalized mesoporous organosilica materials from 1,2-bis(triethoxysilyl)ethane and bis (3-trimethoxysilyl)propyl amine, *J. Solid State Chem.*, 177 (**2004**) 3439-3447.

[5] N. Mizoshita, T. Tani, S. Inagaki, Syntheses, properties and applications of periodic mesoporous organosilicas prepared from bridged organosilane precursors, *Chem. Soc. Rev.*, 40 (**2011**) 789-800.

[6] K. Ariga, A. Vinu, Y. Yamauchi, Q. Ji, J.P. Hill, Nanoarchitectonics for Mesoporous Materials, *Bull. Chem. Soc. Jpn.*, 85 (**2012**) 1-32.

[7] W.J. Hunks, G.A. Ozin, Challenges and advances in the chemistry of periodic mesoporous organosilicas (PMOs), *J. Mater. Chem.*, 15 (**2005**) 3716-3724.

[8] Z. Zhou, M. Hartmann, Progress in enzyme immobilization in ordered mesoporous materials and related applications, *Chem. Soc. Rev.*, 42 (**2013**) 3894-3912.

[9] T. Asefa, M.J. MacLachlan, N. Coombs, G.A. Ozin, Periodic mesoporous organosilicas with organic groups inside the channel walls, *Nature*, 402 (**1999**) 867-871.

[10] S. Inagaki, S. Guan, Y. Fukushima, T. Ohsuna, O. Terasaki, Novel mesoporous materials with a uniform distribution of organic groups and inorganic oxide in their frameworks, *J. Am. Chem. Soc.*, 121 (**1999**) 9611-9614.

[11] B.J. Melde, B.T. Holland, C.F. Blanford, A. Stein, Mesoporous sieves with unified hybrid inorganic/organic frameworks, *Chem. Mat.*, 11 (**1999**) 3302-3308.

[12] W.P. Guo, J.Y. Park, M.O. Oh, H.W. Jeong, W.J. Cho, I. Kim, C.S. Ha, Triblock copolymer synthesis of highly ordered large-pore periodic mesoporous organosilicas with the aid of inorganic salts, *Chem. Mat.*, 15 (**2003**) 2295-2298.

[13] P. Van der Voort, D. Esquivel, E. De Canck, F. Goethals, I. Van Driessche, F.J. Romero-Salguero, Periodic Mesoporous Organosilicas: from simple to complex bridges; a comprehensive overview of functions, morphologies and applications, *Chem. Soc. Rev.*, 42 (**2013**) 3913-3955.

[14] X.Y. Bao, X. Li, X.S. Zhao, Synthesis of large-pore methylene-bridged periodic mesoporous organosilicas and its implications, *J. Phys. Chem. B*, 110 (**2006**) 2656-2661.

[15] R.M. Grudzien, B.E. Grabicka, M. Jaroniec, Effect of organosilane/polymer ratio on adsorption properties of periodic mesoporous ethane-silica, *Colloids Surf., A*, 300 (**2007**) 235-244.

[16] M. Mandal, M. Kruk, Versatile approach to synthesis of 2-D hexagonal ultra-large-pore periodic mesoporous organosilicas, *J. Mater. Chem.*, 20 (**2010**) 7506-7516.

[17] C.H. Lee, S.S. Park, S.J. Choe, D.H. Park, Synthesis of periodic mesoporous organosilica with remarkable morphologies, *Microporous Mesoporous Mater.*, 46 (**2001**) 257-264.

[18] X.Y. Bao, X.S. Zhao, X. Li, P.A. Chia, J. Li, A novel route toward the synthesis of high-quality large-pore periodic mesoporous organosilicas, *J. Phys. Chem. B*, 108 (**2004**) 4684-4689.

[19] O. Olkhovyk, M. Jaroniec, Polymer-templated mesoporous organosilicas with two types of multifunctional organic groups, *Ind. Eng. Chem. Res.*, 46 (**2007**) 1745-1751.

[20] W.-H. Zhang, X. Zhang, L. Zhang, F. Schroeder, P. Harish, S. Hermes, J. Shi, R.A. Fischer, Synthesis of periodic mesoporous organosilicas with chemically active bridging groups and high loadings of thiol groups, *J. Mater. Chem.*, 17 (**2007**) 4320-4326.

[21] E.-B. Cho, D. Kim, M. Jaroniec, Bifunctional Periodic Mesoporous Organosilicas with Thiophene and Isocyanurate Bridging Groups, *Langmuir*, 25 (**2009**) 13258-13263.

[22] F. Goethals, B. Meeus, A. Verberckmoes, P. Van Der Voort, I. Van Driessche, Hydrophobic high quality ring PMOs with an extremely high stability, *J. Mater. Chem.*, 20 (**2010**) 1709-1716.

[23] L. Xia, Y. Hu, Y. Wu, M. Zhang, M. Rong, Manipulation of the phase structure of vinyl-functionalized phenylene bridging periodic mesoporous organosilica, *J. Sol-Gel Sci. Techn.*, 64 (**2012**) 718-727.

[24] J. Morell, M. Gungerich, G. Wolter, J. Jiao, M. Hunger, P.J. Klar, M. Froba, Synthesis and characterization of highly ordered bifunctional aromatic periodic mesoporous organosilicas with different pore sizes, *J. Mater. Chem.*, 16 (**2006**) 2809-2818.

[25] X. Zhou, S. Qiao, N. Hao, X. Wang, C. Yu, L. Wang, D. Zhao, G.Q. Lu, Synthesis of ordered cubic periodic mesoporous organosilicas with ultra-large pores, *Chem. Mater.*, 19 (**2007**) 1870-1876.

[26] S.Z. Qiao, H. Djojoputro, Q. Hu, G.Q. Lu, Synthesis and lysozyme adsorption of rod-like large-pore periodic mesoporous organosilica, *Prog. Solid State Chem.*, 34 (**2006**) 249-256.

[27] Z. Zhou, R.N. Klupp Taylor, S. Kullmann, H. Bao, M. Hartmann, Mesoporous organosilicas with large cage-like pores for high efficiency immobilization of enzymes, *Adv. Mater.*, 23 (**2011**) 2627-2632.

[28] M. Mandal, A.S. Manchanda, J. Zhuang, M. Kruk, Face-Centered-Cubic Large-Pore Periodic Mesoporous Organosilicas with Unsaturated and Aromatic Bridging Groups, *Langmuir*, 28 (**2012**) 8737-8745.

[29] E. Serra, E. Diez, I. Diaz, R.M. Blanco, A comparative study of periodic mesoporous organosilica and different hydrophobic mesoporous silicas for lipase immobilization, *Microporous Mesoporous Mater.*, 132 (**2010**) 487-493.

[30] S. Rehm, P. Trodler, J. Pleiss, Solvent-induced lid opening in lipases: A molecular dynamics study, *Protein Sci.* , 19 (**2010**) 2122-2130.

[31] M. Martinelle, M. Holmquist, K. Hult, On the interfacial activation of Candida antarctica lipase A and B as compared with Humicola lanuginosa lipase, *Biochim. Biophys. Acta, Lipids Lipid Metab.*, 1258 (**1995**) 272-276.

[32] P. Trodler, J. Pleiss, Modeling structure and flexibility of Candida antarctica lipase B in organic solvents, *BMC Struct. Biol.*, 8 (**2008**) 9.

[33] V. Gascón, C. Márquez-Álvarez, R.M. Blanco, Efficient retention of laccase by non-covalent immobilization on amino-functionalized ordered mesoporous silica, *Appl. Catal. A-Gen.*, 482 (**2014**) 116-126.

[34] T. Asefa, M. Kruk, N. Coombs, H. Grondey, M.J. MacLachlan, M. Jaroniec, G.A. Ozin, Novel route to periodic mesoporous aminosilicas, PMAs: ammonolysis of periodic mesoporous organosilicas, *J. Am. Chem. Soc.*, 125 (**2003**) 11662-11673.

[35] F. Hoffmann, M. Cornelius, J. Morell, M. Froba, Periodic mesoporous organosilicas (PMOs): Past, present, and future, *J. Nanosci. Nanotechnol.*, 6 (**2006**) 265-288.

[36] B. Tan, S.E. Rankin, Effects of progressive changes in organoalkoxysilane structure on the gelation and pore structure of templated and non-templated sol–gel materials, *J. Non-Cryst. Solids*, 352 (**2006**) 5453-5462.

[37] M.M. Bradford, A rapid and sensitive method for the quantitation of microgram quantities of protein utilizing the principle of protein-dye binding, *Anal. Biochem.*, 72 (**1976**) 248-254.

[38] S.Z. Qiao, C.Z. Yu, Q.H. Hu, Y.G. Jin, X.F. Zhou, X.S. Zhao, G.Q. Lu, Control of ordered structure and morphology of large-pore periodic mesoporous organosilicas by inorganic salt, *Microporous Mesoporous Mater.*, 91 (**2006**) 59-69.

[39] X.Y. Bao, X.S. Zhao, S.Z. Qiao, S.K. Bhatia, Comparative analysis of structural and morphological properties of large-pore periodic mesoporous organosilicas and pure silicas, *J. Phys. Chem. B*, 108 (**2004**) 16441-16450.

[40] S. Urrego, E. Serra, V. Alfredsson, R.M. Blanco, I. Díaz, Bottle-around-the-ship: A method to encapsulate enzymes in ordered mesoporous materials, *Microporous Mesoporous Mater.*, 129 (**2010**) 173-178.

[41] R.M. Blanco, P. Terreros, M. Fernandez-Perez, C. Otero, G. Diaz-Gonzalez, Functionalization of mesoporous silica for lipase immobilization - Characterization of the support and the catalysts, *J. Mol. Catal. B: Enzym.*, 30 (**2004**) 83-93.

[42] K.S.W. Sing, Reporting physisorption data for gas/solid systems with special reference to the determination of surface area and porosity (Recommendations 1984), *Pure Appl. Chem.*, 57 (**1985**) 603-619.

[43] J. Uppenberg, M.T. Hansen, S. Patkar, T.A. Jones, The sequence, crystal structure determination and refinement of two crystal forms of lipase B from Candida antarctica, *Structure*, 2 (**1994**) 293-308.

[44] RCSB Protein Data Bank, http://www.rcsb.org/pdb/home/home.do, 14/01/14

[45] NCBI Protein Database, http://www.ncbi.nlm.nih.gov/protein, 14/01/14

[46] Standard Protein BLAST, http://swissmodel.expasy.org/?pid=smd05, 14/01/14

[47] N. Hakulinen, L.L. Kiiskinen, K. Kruus, M. Saloheimo, A. Koivula, J. Rouvinen, Crystal structure of a laccase from Melanocarpus albomyces with an intact trinuclear copper site, *Nat. Struct. Biol.*, 9 (**2002**) 601-605.

[48] K. Arnold, L. Bordoli, J. Kopp, T. Schwede, The SWISS-MODEL workspace: a web-based environment for protein structure homology modelling, *Bioinformatics*, 22 (**2006**) 195-201.

[49] L. Bordoli, F. Kiefer, K. Arnold, P. Benkert, J. Battey, T. Schwede, Protein structure homology modeling using SWISS-MODEL workspace, *Nat. Protoc.*, 4 (**2009**) 1-13.

[50] F. Kiefer, K. Arnold, M. Kunzli, L. Bordoli, T. Schwede, The SWISS-MODEL Repository and associated resources, *Nucleic Acids Res.*, 37 (**2009**) 387-392.

[51] The PyMOL Molecular Graphics System, http://www.pymol.org/, 14/01/14

[52] ExPASy - ProtParamtool, http://web.expasy.org/protparam/, 14/01/14

[53] UniProt KB, http://www.uniprot.org/uniprot/G2QFD0, 14/01/14

[54] B. T. C. E. I. system., http://www.brenda-enzymes.org/php/result_flat.php4?ecno=1.10.3.2, 14/01/14

[55] R.M. Berka, P. Schneider, E.J. Golightly, S.H. Brown, M. Madden, K.M. Brown, T. Halkier, K. Mondorf, F. Xu, Characterization of the gene encoding an extracellular laccase of Myceliophthora thermophila and analysis of the recombinant enzyme expressed in Aspergillus oryzae, *Appl. Environ. Microbiol.*, 63 (**1997**) 3151-3157.

[56] R.M. Berka, I.V. Grigoriev, R. Otillar, A. Salamov, J. Grimwood, I. Reid, N. Ishmael, T. John, C. Darmond, M.C. Moisan, B. Henrissat, P.M. Coutinho, V. Lombard, D.O. Natvig, E. Lindquist, J. Schmutz, S. Lucas, P. Harris, J.

Powlowski, A. Bellemare, D. Taylor, G. Butler, R.P. de Vries, I.E. Allijn, J. van den Brink, S. Ushinsky, R. Storms, A.J. Powell, I.T. Paulsen, L.D. Elbourne, S.E. Baker, J. Magnuson, S. Laboissiere, A.J. Clutterbuck, D. Martinez, M. Wogulis, A.L. de Leon, M.W. Rey, A. Tsang, Comparative genomic analysis of the thermophilic biomass-degrading fungi Myceliophthora thermophila and Thielavia terrestris, *Nat. Biotechnol.*, 29 (**2011**) 922-929.

[57] U.K. Laemmli, Cleavage of structural proteins during the assembly of the head of bacteriophage T4, *Nature*, 227 (**1970**) 680-685.

[58] R.M. Blanco, P. Terreros, N. Munoz, E. Serra, Ethanol improves lipase immobilization on a hydrophobic support, *J. Mol. Catal. B: Enzym.*, 47 (**2007**) 13-20.

[59] E. Serra, V. Alfredsson, R.M. Blanco, I. Diaz, *in Zeolites and Related Materials: Trends, Targets and Challenges, Proceedings of the 4th International Feza Conference*, ed. A. Gedeon, P. Massiani, F. Babonneau, (**2008**), pp. 369-372.

[60] O.V. Morozova, G.P. Shumakovich, S.V. Shleev, Y.I. Yaropolov, Laccase-mediator systems and their applications: A review, *Appl. Biochem. Microbiol.*, 43 (**2007**) 523-535.

[61] M. Hartmann, Ordered mesoporous materials for bioadsorption and biocatalysis, *Chem. Mater.*, 17 (**2005**) 4577-4593.

[62] A. Mayoral, R. Arenal, V. Gascon, C. Marquez-Alvarez, R.M. Blanco, I. Diaz, Designing Functionalized Mesoporous Materials for Enzyme Immobilization: Locating Enzymes by Using Advanced TEM Techniques, *ChemCatChem*, 5 (**2013**) 903-909.

[63] A.S. Bommarius, M.F. Paye, Stabilizing biocatalysts, *Chem. Soc. Rev.*, 42 (**2013**) 6534-6565.

[64] K. Nie, F. Xie, F. Wang, T. Tan, Lipase catalyzed methanolysis to produce biodiesel: Optimization of the biodiesel production, *J. Mol. Catal. B: Enzym.*, 43 (**2006**) 142-147.

[65] C.-H. Kuo, L.-T. Peng, S.-C. Kan, Y.-C. Liu, C.-J. Shieh, Lipase-immobilized biocatalytic membranes for biodiesel production, *Bioresour. Technol.*, 145 (**2013**) 229-232.

[66] D.T. Tran, Y.J. Lin, C.L. Chen, J.S. Chang, Kinetics of transesterification of olive oil with methanol catalyzed by immobilized lipase derived from an isolated Burkholderia sp. strain, *Bioresour. Technol.*, 145 (**2013**) 193-203.

[67] P. Adlercreutz, Immobilisation and application of lipases in organic media, *Chem. Soc. Rev.*, 42 (**2013**) 6406-6436.

[68] B.D. Ribeiro, A.M. de Castro, M.A. Coelho, D.M. Freire, Production and use of lipases in bioenergy: a review from the feedstocks to biodiesel production, *Enzyme Res.*, 2011 (**2011**) 615803.

[69] C. Jose, G.B. Austic, R.D. Bonetto, R.M. Burton, L.E. Briand, Investigation of the stability of Novozym (R) 435 in the production of biodiesel, *Catal. Today*, 213 (**2013**) 73-80.

[70] R.C. Minussi, G.M. Pastore, N. Duran, Potential applications of laccase in the food industry, *Trends Food Sci. Tech.*, 13 (**2002**) 205-216.

[71] A. Kunamneni, F.J. Plou, A. Ballesteros, M. Alcalde, Laccases and their applications: a patent review, *Recent Pat. Biotechnol.*, 2 (**2008**) 10-24.

[72] J.F. Osma, J.L. Toca-Herrera, S. Rodriguez-Couto, Uses of laccases in the food industry, *Enzyme Res.*, 2010 (**2010**) 918761.

CAPÍTULO 4

Advanced Electron Microscopy applied to biocatalysts with enzymes immobilized on functionalized mesoporous materials

Álvaro Mayoral[a], Raúl Arenal[a, b], **Victoria Gascón**[c], Carlos Márquez-Álvarez[c], Rosa M. Blanco[c] and Isabel Díaz[c]

Published in *ChemCatChem*, 2013, vol. 5, pp. 903-909.
DOI: 10.1002/cctc.201200737

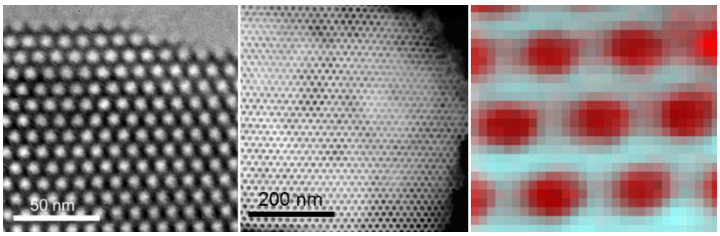

Ordered mesoporous materials can be customized for the desired applications, being the optimization of enzyme loading a real grounded scientific field with solid uses. Functionalized OMM have been produced for the immobilization of lipase and laccase and an exhaustive structural analysis has been performed by means of the most advanced electron microscopy techniques

ABSTRACT

One of the widely accepted uses of ordered mesoporous materials is as supports of enzymes for biotechnological applications. Enzymes have been trapped, anchored, or encapsulated in organized porous networks of the mesoporous range (2–50 nm). The reactivity of the surface of mesoporous materials has enabled the synthesis of various supports by using different forces for the immobilization process. To design catalysts for specific applications, we have developed functionalized mesoporous materials with tunable hydrophobicity for the immobilization of lipase. More recently, we moved to the immobilization of laccase with amino-functionalized ordered mesoporous materials. In this case, it is required to use pore expanders along with optimized functionalization techniques. Advanced TEM techniques have been applied to locate not only the functional groups but also the macromolecules inside the silica matrix.

Keywords: electron microscopy; enzymes; enzyme immobilization; functionalized mesoporous materials; laccase; lipase.

1. INTRODUCTION

Ordered mesoporous materials (OMMs) are no longer a new class of porous solids with great potential, but a grounded scientific field with solid uses. One of the widely accepted uses of OMMs is as supports of enzymes for biotechnological applications. Enzymes have been trapped, anchored, or encapsulated in organized porous networks of the mesoporous range (2–50 nm) [1]. The reactivity of silica and the introduction of organosilanes have allowed for a wide spectrum of supports using various forces for the immobilization process [2]. The incorporation of functional groups into OMMs for catalytic applications has yielded optimum materials in the past [3]. The porous space engineering however brings OMMs to a scenario in which material science, biotechnology, and engineering bind together in a multidisciplinary field [4]. This scenario fits perfectly with the aim of this issue "Chemical Functionalities on Mesoporous Materials: Methods and Catalytic Applications".

Herein, two cases are exemplified: immobilization of lipase by hydrophobic forces using alkyl functionalities on OMMs and immobilization of laccase by either hydrogen bonding or electrostatic interaction between amino groups and carboxylic acids on the surface of the enzyme. Interesting reviews can be found regarding enzyme immobilization [5] and particularly immobilization on mesoporous materials [6]. However, the location of enzymes inside the pores cannot be confirmed easily and usually a combination of indirect techniques is used for the characterization of these materials, such as nitrogen adsorption or thermogravimetry. The only direct and most complete method for the characterization of mesoporous solids is based on high-resolution TEM [7] combined with electron crystallography, [8] which allows solving all kinds of structures and gives a complete image of not only the pore distribution but also the pore connectivity. If the subject of interest is guest materials, scanning transmission electron microscopy (STEM) combined with high-angle annular dark field (HAADF) detector is more suitable because the contrast is related to the atomic number Z [9]. With the modern electron microscopes, which incorporate spherical aberration (C_s) correctors, probes down to sub-Angstrom resolution can be achieved, which facilitates an exhaustive analysis of the pores for OMMs. Herein, a detailed and conclusive analysis is performed on different functionalized OMMs loaded with lipase and laccase. From the ultrahigh- resolution images of perfectly oriented thin particles combined with electron energy loss

spectroscopy (EELS), the location of the enzymes inside the pores has been confirmed. All analyses were performed at an accelerating voltage of 80 kV, which proves a good stability of the mesoporous materials at this beam energy.

2. EXPERIMENTAL SECTION

2.1. Synthesis of pure silica SBA-15, expanded SBA-15, and functionalized OMM, PMO, and PMA

All samples were prepared in acid media with triblock copolymeric (Pluronic) surfactants and tetraethoxysilane as a silica source. Details of the synthesis of each material are available in the Refs. [10] and [11]. In addition, methylated analogues of the materials were synthesized through the co-condensation of tetraethoxysilane and methyltriethoxysilane. The amino-functionalized SBA-15 sample was prepared through grafting with aminopropyltrimethoxysilane (1 %). PMO was synthesized as described in the literature [11] with 1,2-bis(triethoxysilyl)ethane as a silica source; PMA was synthesized from 1,2-bis(trimethoxysilyl)ethane (82 % molar) and bis[3-(trimethoxysilyl) propyl]amine (18 % molar) [12]. The surfactant was removed through calcination at 550 ºC under consecutive N_2/air streams from pure silica samples and through extraction with ethanol/HCl from the methylated, amino-functionalized PMO and PMA.

2.2. Characterization of the OMM

All the samples were characterized extensively with a combination of several techniques. XRD was performed with a Seifert XRD 3000P diffractometer operating at a low angle. Nitrogen adsorption–desorption isotherms were determined at 77 K with a Micromeritics TriStar 3000 apparatus. Specific surface areas were calculated by using the BET method and the pore size distribution by applying the BJH protocol to the adsorption branch of the isotherm. Thermogravimetric analysis thermograms were recorded on a Perkin–Elmer TGA 7 equipment, scanning a temperature range of 20–900 ºC with a heating rate of 20 ºC/min. SEM images were recorded on a JEOL JSM-6400 Philips XL30 operating at 20 kV. TEM analyses of the enzyme-loaded OMM were performed in the bright-field mode of TEM coupled with selected area electron diffraction in an FEI

Tecnai G2 F30 FEG microscope by achieving a point-to-point resolution of 1.9 Å when operated at 300 kV. A more exhaustive analytical investigation was performed in an XFEG FEI Titan 60–300 kV microscope operated at 80 kV equipped with a monochromator (not excited for the current experiments), a C_s probe corrector from CEOS Company (which enables the formation of an electron probe of 0.08 nm mean size), and a Gatan Energy Filter Tridiem 866 ERS energy filter for the EELS experiments. The geometric aberrations of the probe-forming system were controlled so that a beam convergence of 24.9 mrad half-angle could be selected. The alignment of the microscope at 80 kV was verified through the CETCOR software. A focus/tilt tableau was acquired by measuring defocus and twofold astigmatism as a function of both radial and azimuthal tilt angles. For the EELS measurements, the collection semiangle was set to 145 mrad with an energy resolution of 1 eV.

2.3. Enzyme immobilization

Lipase from *Candida antarctica* fraction B (*Ca*LB) and laccase from Myceliphthora thermophila were kindly donated by Novozymes. Different amounts (between 0.25 and 2.5 mL) of the commercial extract of *Ca*LB with a protein content of 8 mg/mL determined by using Bradford assay were dissolved in phosphate buffer (50 mM) at pH 5 up to a total volume of 20 mL. To that solution the OMM (100 mg) was added and left in suspension with a helical stirrer. Aliquots were taken at given times, and the enzyme activity of the suspension and supernatant was determined spectrophotometrically by the increase of absorbance at 348 nm along with the hydrolysis of p-nitrophenyl acetate. The supernatant was obtained by centrifuging the aliquots for 2 min at 13,000 rpm. Once the enzyme activity of the supernatant was constant, the suspension was filtered off and washed twice with acetone. Finally, the solid was dried at room temperature, collected, and weighed.

Different amounts of the commercial extract of laccase with a protein content of 3.28 mg/mL were dissolved in acetate buffer (50 mM) at pH 5.5 up to a total volume of 15 mL. To that solution, the amino-containing mesoporous material (50 mg) was added and maintained in suspension with mild stirring. When the OMM was purely siliceous (SBA-15), the material was suspended in citrate buffer at pH 4.5. Aliquots of the suspension and supernatant were taken, and their catalytic activities were assayed spectrophotometrically by the increase of absorbance at 405 nm caused by 2,2’-azinobis-(3-ethylbenzthiazoline-

6-sulfonate) oxidation. When the constant values of supernatant activities were obtained, the suspension was filtered off, washed with distilled water, and dried in N_2 stream with use of molecular sieves.

In both cases, a control sample was also assayed to confirm that no enzyme inactivation occurred during immobilization. The immobilization yield was calculated from the difference between the initial catalytic activity of the respective enzyme solutions before suspension with supports and the final activity of the respective supernatants. Catalytic efficiency is defined as the ratio between the activity of the catalyst and its enzyme loading, which thus indicates the activity per milligram of immobilized enzyme.

2.4. Reproducibility

Catalytic activities of the obtained enzyme-immobilized samples were measured to determine catalytic efficiencies. Triplicate experiments were performed, and the results provided here are the average data of enzyme loading and activity.

2.5. Leaching and stability

Leaching tests with lipase were performed as published elsewhere [8, 13] by suspending soluble lipase and samples immobilized on SBA-15, Me-SBA-15, and PMO at pH 7 (at which the lipase presented negative net charge) as well as the silica surfaces. Therefore, electrostatic repulsions were established, and so the only forces keeping the enzyme linked to the support were hydrophobic interactions.

To measure the leaching of lipase from the supports, a sample of the solid containing the enzyme was suspended in phosphate buffer (50 mM) at pH 7. The solid/liquid ratio was 1.25 mg/mL. At different times, aliquots of the suspensions were taken and centrifuged and the protein content of the supernatants was determined by using Bradford assay [14].

A study of the leaching of some of the lipase catalysts in aqueous medium was described earlier [10, 11], which depended on the structure of the porous network: 10 and 15 % was leached from Me-SBA-15 and PMO, respectively. The possible contribution of the enzyme leached during the assay to the final activity measured was negligible. The

retention was also related to the hydrophobic interaction with the protein because leaching from SBA-15 increased linearly with time.

In contrast to lipase immobilization, laccase immobilization was driven only by electrostatic interactions; therefore, incubation could not be performed at pH values at which charge repulsions were established. Incubation was performed under the same conditions as for the reaction, but for longer time and in triplicate, to ensure that leaching occurred and the contribution of soluble enzyme to the activity measured. Laccase catalysts were incubated at pH 4.5 (NH_2-SBA-15exp and PMA) or pH 3.5 (SBA-15exp). The total reaction time was 30 min. To study laccase leaching from supports during the reaction, catalysts were incubated in the same buffers at a lower concentration (50 mM) for 1.5 h. After this time, suspensions were centrifuged and the protein content of the supernatants was determined by using Bradford assay. Leaching after 1.5 h was 1 % of laccase from NH_2-SBA-15exp, 2.8 % from SBA-15exp, and 3.35 % from PMA; therefore, the contribution of the leached enzyme to the catalytic activity measured in the assays could be neglected.

Leaching tests were performed at the same pH as that for the immobilization process (SBA-15exp), or at the same pH of the assay of catalytic activity (NH_2-SBA-15exp and PMA); thus, the results are reliable.

Preliminary studies on enzyme stability were performed through incubation in buffer at 50 ºC (laccase samples) and 65 ºC (lipase samples). Both are thermophile enzymes.

2.6. Laccases

Samples of soluble enzyme immobilized on SBA-15-exp and NH_2-SBA-15-exp and incubated at 50 ºC showed similar inactivation curves in which the time required to decrease activity by 50 % (t_{50}) was approximately 150 min in the three cases. However, this time was approximately 300 min for the PMA sample incubated under the same conditions (*data not shown*). The pore diameter of PMA is 1 nm smaller than that for both SBA-15 preparations, which means a higher confinement in this material that prevents unfolding of the enzyme and, therefore, contributes to increase its stability.

2.7. Lipases

Soluble enzyme maintained 50 % activity after 50 min of incubation at 65 ºC. Lipases immobilized on Me-SBA-15 and PMO were less stable with respective t_{50} values of 42 and 37 min. Only SBA-15 was more stable with a t_{50} value of 67 min. In the case of lipases, the stability depended not only on the pore size but also on the chemistry of the silica surface and the incubation medium.

Given the thermophile nature of the soluble enzymes, no increased stability was achieved under the conditions tested through immobilization, except for laccase-PMA and lipase-SBA-15 catalysts, which, together with low leaching during catalytic activity assays, means that a hypothetical contribution of the desorbed enzyme to the activity measured was negligible.

3. RESULTS AND DISCUSSION

3.1. Immobilization of lipase

The lipase from *Candida antarctica* fraction B (1TCA in Protein Data Bank 62 x 46 x 92 [13] can be immobilized easily on pure silica mesoporous materials of regular pore size (e.g., SBA-15 with 9 nm pore channel diameter) by electrostatic interactions. The isoelectric point of this enzyme is 6.2; thus, optimum immobilization is performed at pH 5, which is above the isoelectric point of silica, which is between 2 and 3. However, enzyme loading under these conditions is poor, and therefore, low activity is achieved [10]. In contrast, lipase is usually better immobilized on hydrophobic supports by using their property to possess a hydrophobic domain on the surface [15]. In this direction, several researchers have developed OMMs functionalized with hydrophobic groups. Han et al. functionalized SBA-15 with butyl groups; however, the decrease in pore size led to an immobilization process involving high pressure to facilitate the access of the enzyme in the framework [16]. We have managed to tune the surface properties of OMMs to an optimum hydrophobicity [11]. We have grafted the SBA-15 surface with methyl groups to increase hydrophobicity. Although the surface coverage with these small alkyl groups produced only a slight decrease in pore size (**Table 1**), the enzyme loading was not favored. However, the enzyme immobilized inside the channels was more active than that on the surface of pure silica SBA-15.

To achieve higher enzyme loading by gaining in affinity while maintaining the pore diameter, periodic mesoporous organosilica (PMO) was synthesized with ethanediyl

bridges as organic groups. On one hand, these ethanediyl radicals are more hydrophobic than methyl groups, and on the other hand, the PMO material contains a higher amount of organic groups (100 % vs. 6 %). Thus, the PMO material is more hydrophobic than methyl-SBA-15. The hydrophobic groups are not anchored but protrude on the siliceous surface and become part of it. This way the hydrophobic moiety could be a part of the material without decreasing the pore channel dimensions. The powder XRD patterns and nitrogen adsorption–desorption isotherms of the samples are shown in **Figure 1**. The symmetry of the materials is exactly the same in the three cases, which show the *p*6*mm* space group. In addition, the geometry of the mesopores is the same, given the type IV isotherms obtained in all the cases. Despite the smaller pore size shown by the PMO material, the enzyme loading was much higher (91 mg/g), which indicates the crucial role of the increase in affinity by the hydrophobic groups. Moreover, the catalytic efficiency was much higher in the PMO material, which indicates that the hydrophobic linkage does not involve significant conformational changes in the enzyme molecule and the catalytic activity is better preserved than in the case of electrostatic interaction.

Table 1. Textural and catalytic results of lipase immobilized on OMM.

Biocatalyst	**Pd[a] (nm)**	**Max. Load.[b] (mg/g)**	**Cat. Eff.[c] (U/mg)**	**% Hydroph.[d]**
SBA-15	8.8	44	60	-
CH_3-SBA-15	7.9	23	88	6
PMO	7.1	91	202	100

[*a*] Pore diameter; [*b*] Maximum enzyme loading; [*c*] Catalytic Efficiency = activity versus loading (Units/mg); [*d*] Percent of Si atoms linked to CH-chain.

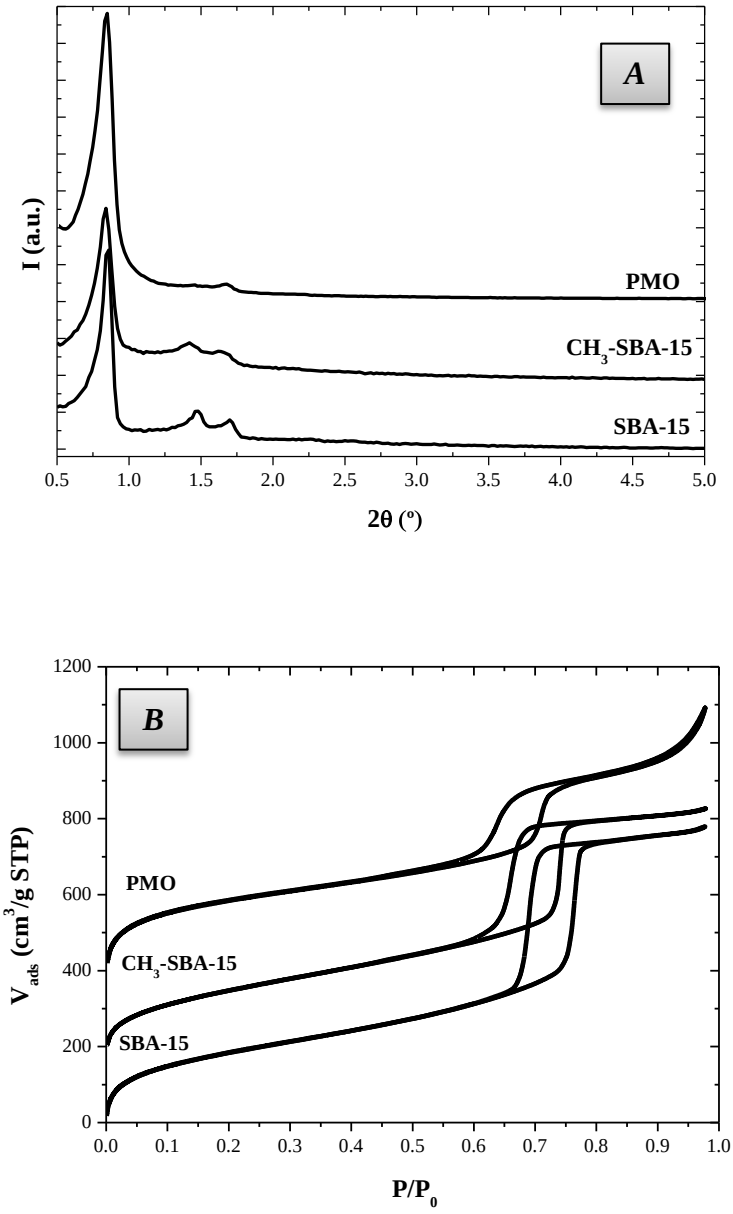

Figure 1. (***A***) Powder XRD patterns and (***B***) N_2 adsorption-desorption of functionalized ordered mesoporous materials with increasing hydrophobic surface properties.

3.2. Immobilization of laccase

To extend the method to other enzymes, the properties of each protein must be studied previously. Laccase (from *Myceliphthora thermophila*) has a potential use in the bioremediation field (wastewater treatment) as well as in many other fields [17]. The dimensions of this enzyme are 9.8 x 9.8 x 15 nm, which is too large to fit in the 9 nm

diameter channels of the SBA-15 support. Therefore, the first thing to do is to synthesize a material with larger pore size. However, in this expanded SBA-15, the immobilization of laccase by electrostatic interactions renders poor immobilization yields (**Table 2**). Because pore size is large enough (11.9 nm), the challenge must be the low affinity between the laccase and the pore surface of pure silica SBA-15. This protein has a low isoelectric point (pH 4). Therefore, the useful pH range for immobilization by electrostatic interaction is very narrow (ca. 3.0–3.5) and close to the isoelectric points of both the support and the enzyme. Under these circumstances, the introduction of positive charges on the OMM surface at a pH value high enough to ensure deprotonation of carboxylic groups on the enzyme surface would be the way to favor the interactions. Therefore, the functionalization with amine groups was performed on the SBA-15 support, with extended pores aiming to increase the affinity between the enzyme and the support. The large pores obtained with use of micelle expanders enable the introduction of propylamine groups without compromising the dimensions of the channels. The presence of amines (1.07 mmol N/g) led to a significant increase in enzyme loading, from 14 to as high as 170 mg/g (see **Table 2**).

To design an optimum OMM for the immobilization of laccase, periodic mesoporous aminosilica (PMA) was synthesized with the intention of increasing the affinity without decreasing the pore size. The XRD patterns with *p6mm* symmetry in the three cases are shown in **Figure 2**, which suggest that the expanded micelle method also works for the PMA materials [12, 18]. Furthermore, the isotherms correspond to those of functionalized mesoporous materials, with bulkier functional groups producing a broader hysteresis loop owing to a complex mechanism of adsorption and desorption given by a rougher surface. The PMA sample shows a second step at higher relative pressure owing to the small particle size obtained in this material, which leads to agglomerates as observed by using SEM (*data not shown*). Nevertheless, the textural properties of the samples enable the immobilization of laccase, even in the case of PMA for which a smaller pore size was obtained following the tendency observed in PMO. Despite a slightly smaller pore size of PMA (10.2 nm; **Table 2**), the dimensions are still wide enough to allocate laccase molecules in the proper orientation. The nitrogen concentration in PMA (0.58 mmol N/g) is 54 % smaller than in NH_2-SBA-15exp, and the enzyme loading achieved is 52 % lower. The higher affinity of laccase for NH_2-SBA-15exp can, therefore, be attributed to its higher nitrogen content. Thus, the chemical affinity of the enzyme for the OMM

surface is crucial for the success of enzyme immobilization if the pore size is at least large enough to let enzyme molecules fit inside.

Table 2. Textural and catalytic results of laccase immobilized on the ordered mesoporous material.

Biocatalyst	Pd[a] (nm)	Max. Load.[b] (mg/g)	Cat. Eff.[c] (U/mg)	mmol N/g[d]
SBA-15exp	11.9	14.2	0.04	-
NH_2-SBA-15exp	11.2	170	0.30	1.07
PMA	10.2	88	0.33	0.58

[*a*] Pore diameter; [*b*] Maximum enzyme loading; [*c*] Catalytic Efficiency = activity versus loading (Units/mg); [*d*] mmol of nitrogen per gram of the ordered mesoporous material.

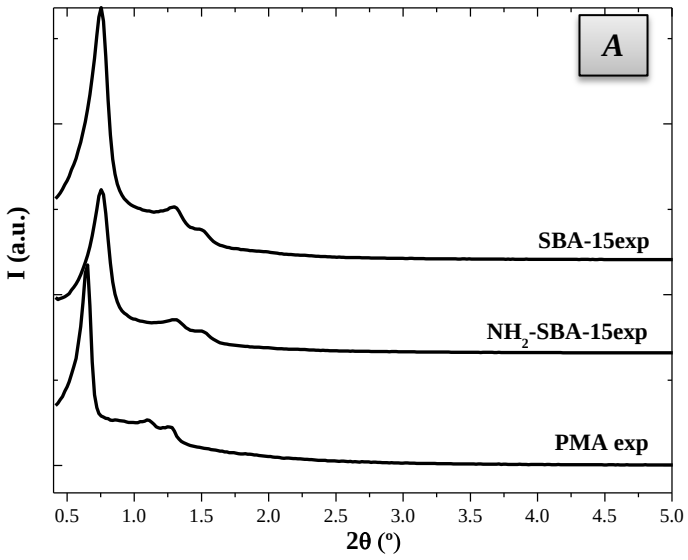

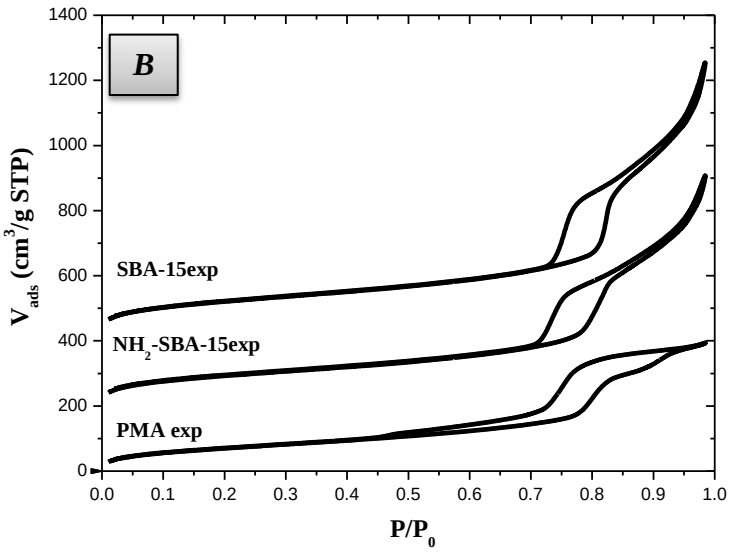

Figure 2. (***A***) Powder XRD patterns and (***B***) N_2 adsorption-desorption of functionalized ordered mesoporous materials with increasing amount of amine groups on the surface.

3.3. TEM studies

TEM is used conventionally to characterize mesoporous materials (ordered and nonordered) because it is the only technique that allows obtaining complete information of the materials [10]. From high-resolution TEM images, the pore distribution of purely siliceous SBA-15 can be observed easily, which confirms the good ordering of the material produced [19]. As previously described, a group of materials for enzyme immobilization is OMMs that contain HC groups in their frameworks.

These are novel materials, and a complete characterization before enzyme introduction must be undertaken to confirm good crystallinity and a nice pore distribution. The TEM images of the as-synthesized PMO material are shown in **Figure 3**. The hexagonal array of the channels that corresponds to the *p*6*mm* symmetry with a unit cell value of a = 104.49 Å is shown in **Figure 3** ***A***, whereas the perpendicular image of the pores is shown in **Figure 3** ***B***. The same preliminary analysis was performed for the PMA material. A typical image of the porous solid is shown in **Figure 3** ***C***, in which a large region with uniform pore distribution can be observed. In this case, a crystal of approximately 1 mm size is perfectly oriented, with its pores parallel to the electron beam. The ordering of this material with the pore arrangement extended over particles of several micrometers is

remarkable. The electron diffraction pattern (**Figure 3** ***C***, inset) can also be indexed as the *p*6*mm* space group with a unit cell value of a = 135.05 Å, which is 30 Å larger than that for the PMO material. A magnified image of the sample is shown in **Figure 3** ***D***, in which the last layer of pores is observed. This image clearly shows an "open-pore ending" with steps of one pore size, which are denoted by white arrows.

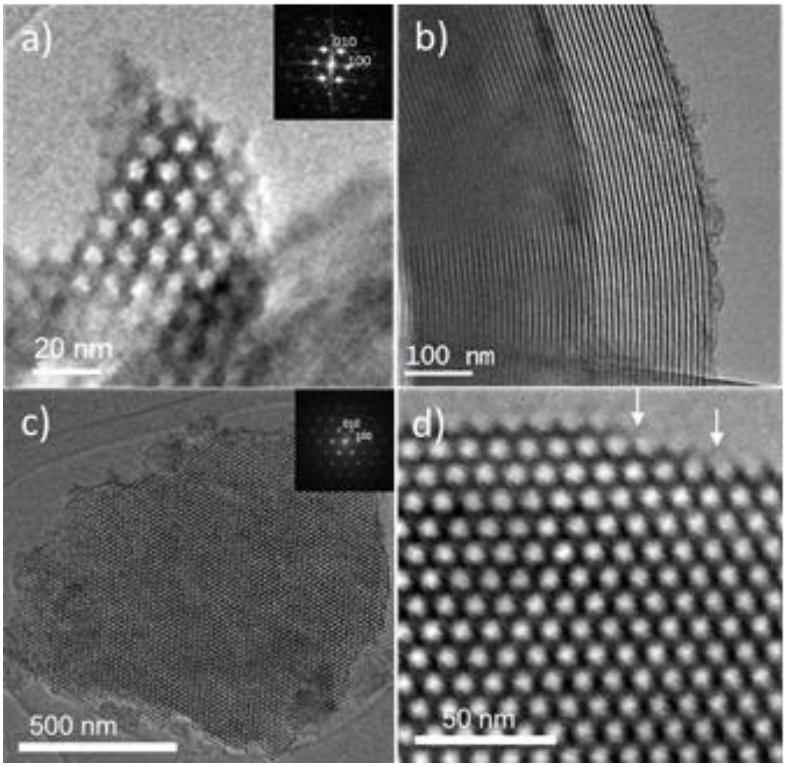

Figure 3. TEM micrographs (***A***) of periodic mesoporous organosilica (PMO) and (***B***) taken along the [001] and [110] orientations, respectively. (***C***) Periodic mesoporous aminosilica crystal oriented on the [001] and (***D***) magnified image of sample ***C*** in which steps of one pore size can be observed on the particle surface.

By using conventional TEM imaging (using a parallel illumination inside the microscope), the identification and location of guest solids, such as enzymes or metals, is unfortunately not possible in most cases. An in-depth study must be conducted by using a STEM-HAADF detector. In the STEM-HAADF detector, the beam is converged into a very fine probe that is scanned over the material and only the electrons that are scattered at very high angles are used to form the image. With these kinds of detectors, data can be interpreted easily because the contrast depends on the atomic number Z [9] and is less affected by multiple scattering or different defocus values, as commonly occurs in the TEM mode. For light elements introduced into the pores, a combination of STEM-

HAADF and EELS, with the spectrum-image acquisition mode [20, 21], is necessary to obtain a conclusive confirmation of the presence of enzymes inside the pores.

The [001] STEM-HAADF image is shown in **Figure 4**, which is parallel to the mesopores of the lipase–PMO sample. The organosiliceous matrix is shown in **Figure 4** ***A***, in which the cavities appearing in black represent a hexagonal array (*p*6*mm* symmetry). The fast Fourier transform (upper left corner of the inset) proves the good crystallinity of the material; a perfectly oriented six pore distribution (subject to analysis) with respect to the electron beam is shown in the upper right corner; crystals perfectly aligned with respect to the electron beam is an indispensable requirement for a reliable analysis of the pores and mesoporous walls. The STEM-HAADF image of the area in which a spectrum image was recorded is shown in **Figure 4** ***B***. The dimensions used were 30 x 26 pixels, which give a spatial resolution of 0.89 nm, and the time for analysis was 0.6 s/pixel. The relative carbon/oxygen composition is presented in **Figure 4** ***C***, which is the most crucial information for the enzyme location. As expected, the relation between carbon and oxygen is different irrespective of whether the beam illuminates the pore within the enzyme or the walls that contain SiO_2+(-CH_2-CH_2) groups; red areas correspond to the higher carbon content. This difference confirms the presence of lipase inside the pores. Because the nitrogen per molecule is very low, it is impossible to construct a map based on the nitrogen signal; however, a punctual analysis (black dashed square in **Figure 4** ***C***) of 3 s enabled the observation of the nitrogen K edge at 401 eV. The results of the EELS analysis of the pore is shown after background subtraction in **Figure 4** ***D***, in which oxygen and nitrogen edges can be seen clearly.

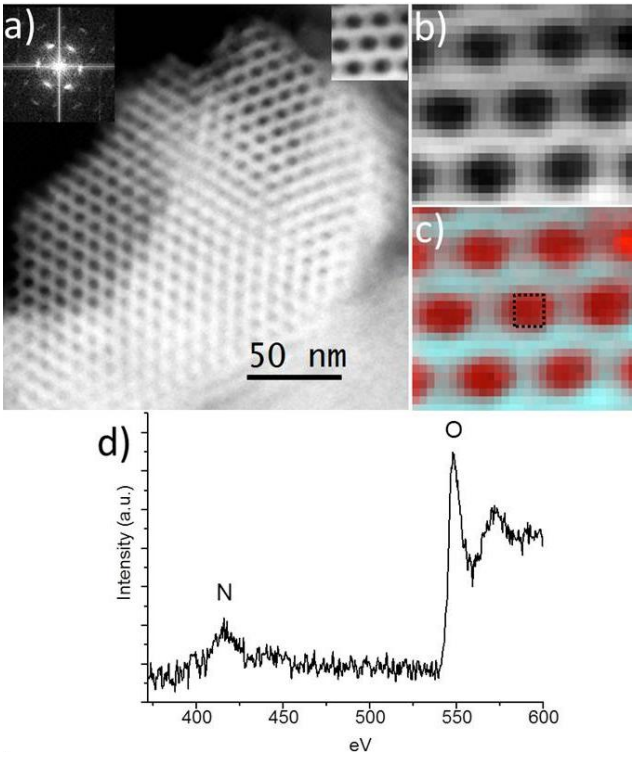

Figure 4. (***A***) Aberration-corrected scanning transmission electron microscopy combined with high-angle annular dark field (STEM-HAADF) image of a periodic mesoporous organosilica (PMO) crystal along the [001] orientation, showing the hexagonal array. The fast Fourier transform (upper left corner of the inset) confirms the sixfold axis. A magnified image of the pores is presented in the upper right corner. (***B***) STEM-HAADF signal of the area analyzed. (***C***) Map obtained from the EELS signal of the relative carbon/oxygen composition (in red). (***D***) Sum of the EEL spectra, after background subtraction, recorded in the dashed square marked in image ***C***.

Because of different particle morphologies of PMOs and PMAs, the latter allowed a better tilting of larger crystals. Therefore, although the enzyme loading is similar in both cases, it was easier to locate pores with higher enzyme content. A low-magnification image is shown in **Figure 5** ***A***. A magnified image of the pore system is shown in **Figure 5** ***B***, in which a spectrum image collection analysis was performed inside one of the pores (marked by green square) by analyzing 8 x 6 pixels with an exposure time of 2.5 s/pixel. The extracted spectrum profile (raw data; **Figure 5** ***C***) shows the oxygen and nitrogen edges corresponding to the enzyme.

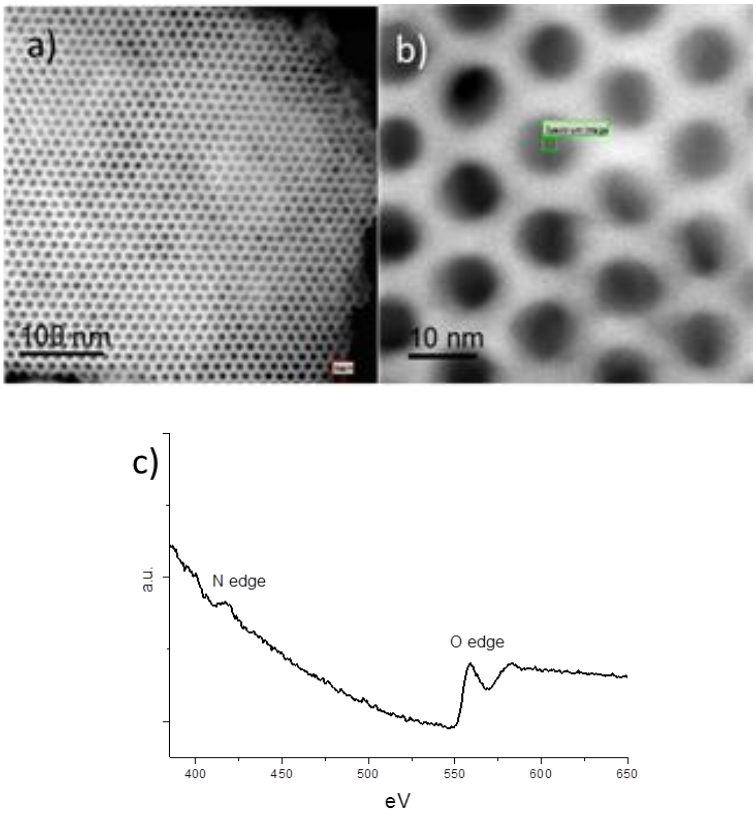

Figure 5. (***A***) C_s-corrected scanning transmission electron microscopy combined with high-angle annular dark field (STEM-HAADF) image of the periodic mesoporous aminosilica (PMA) loaded with laccase. (***B***) High-resolution image of the pores. The green rectangle represents the area in which the EELS analysis was performed. (***C***) EELS profile collected from image ***B***, showing the three edges that confirm the presence of laccase.

The nitrogen maps extracted from the spectra collected in areas perpendicular and parallel to the pores are depicted in **Figure 6**. The green square (**Figure 6** ***A*** and ***C***) represents the area in which the map was acquired by using 1.5 s/pixel in both cases. The nitrogen maps are shown in light blue color (**Figure 6** ***B*** and ***D***). As a consequence of the amino functionalization, nitrogen was detected in the framework and in certain pores, in which less contrast was observed (**Figure 6** ***A*** *and* ***B***); this confirms that some pores were not filled with laccase or that the nitrogen content was too low to be detected. In **Figure 6** ***C***, a different contrast, much "whiter", appears for which the analysis indicates higher nitrogen content attributed to the enzyme immobilized within the pores, as clearly observed in **Figure 6** ***D***.

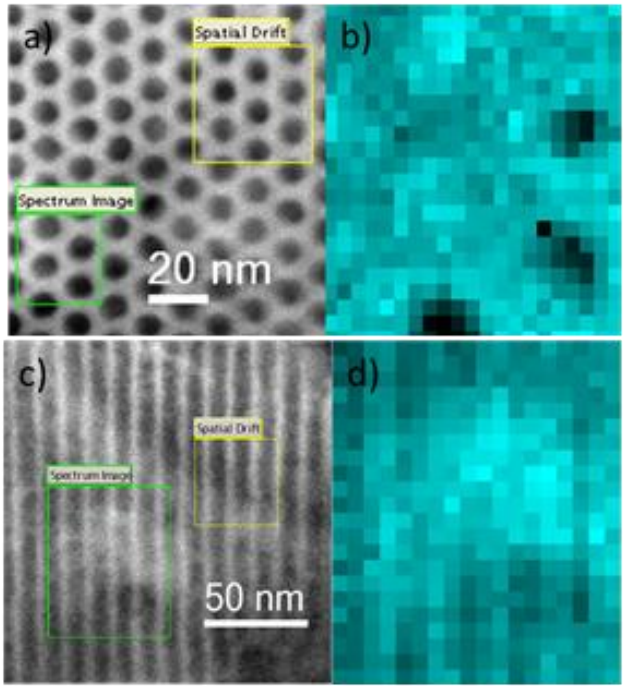

Figure 6. (***A***) C_s-corrected scanning transmission electron microscopy combined with high-angle annular dark field (STEM-HAADF) image of the pore system of periodic mesoporous aminosilica (PMA). (***B***) Nitrogen map extracted from the green square in image ***A***. (***C***) C_s-corrected STEM-HAADF image of the channels of PMA and (***D***) the corresponding nitrogen map.

A relatively strong electron beam was needed to gain enough counts for identifying the species. The total dose was 0.48 eA^{-12}/s, which remained on each pixel during data collection. The radiation damage is due to radiolysis if the energy from an electron of the beam is transferred to an electron of the specimen, which causes an increase in the electron energy and thus bond breakage [22, 23]. This effect depends directly on the beam energy, which makes the materials more stable if higher accelerating voltages (in kilovolts) are applied as the cross section is decreased and the temperature in the sample is also kept to lower values. However, "knock-on" damage (which occurs if an incoming electron from the beam interacts with the core of an atom and displaces it from its original position) cannot be discarded completely [24], especially in the current study in which carbon chains are present in the structure. For both PMOs and PMAs, knock-on damage could have increased its importance in the mesoporous decomposition as C-C bonds remained stable at 80 kV. On the contrary, working at this voltage can increase the temperature of the crystals analyzed, which is an important contributor to specimen damage [22]. For the case of analytical microscopes in which the beam is "converted" to a very fine spot of approximately 1 Å (as a result of the C_s corrector present in the

microscope), the temperature heating can be reduced significantly with respect to conventional TEM, which illuminates the entire crystal.

4. CONCLUSIONS

The current study proves the feasibility of designing functionalized ordered mesoporous materials for enzyme immobilization. A rational design of the surface properties, pore size, and connectivity of ordered mesoporous materials is nowadays straightforward. Furthermore, C_s-corrected scanning transmission electron microscopy combined with electron energy loss spectroscopy analysis allows imaging the functionalities of the mesopores of silica structures with ultra-high resolution as well as ambiguously determining the presence of enzyme molecules inside the channels of the material. The presence of lipase has been determined in periodic mesoporous organosilica (PMO) by observing the carbon/oxygen and nitrogen edges and by mapping the carbon/oxygen relative composition, which clearly differs from the wall to the pores because of the presence of organic molecules. Meanwhile, owing to the different morphologies of amino-functionalized periodic mesoporous aminosilica, nitrogen maps can be collected by locating enzymes inside the selected pores.

5. REFERENCES

[1] C. Ispas, I. Sokolov, S. Andreescu, Enzyme-functionalized mesoporous silica for bioanalytical applications, *Anal. Bioanal. Chem.*, 393 (**2009**) 543-554.

[2] H.H.P. Yiu, P.A. Wright, Enzymes supported on ordered mesoporous solids: a special case of an inorganic-organic hybrid, *J. Mater. Chem.*, 15 (**2005**) 3690-3700.

[3] I. Diaz, C. Marquez-Alvarez, F. Mohino, J. Perez-Pariente, E. Sastre, Combined alkyl and sulfonic acid functionalization of MCM-41-type silica - Part 1. Synthesis and characterization, *J. Catal.*, 193 (**2000**) 283-294.

[4] X.S. Zhao, X.Y. Bao, W. Guo, F.Y. Lee, Immobilizing catalysts on porous materials, *Mater. Today*, 9 (**2006**) 32-39.

[5] U. Hanefeld, L. Gardossi, E. Magner, Understanding enzyme immobilisation, *Chem. Soc. Rev.*, 38 (**2009**) 453-468.

[6] M. Hartmann, D. Jung, Biocatalysis with enzymes immobilized on mesoporous hosts: the status quo and future trends, *J. Mater. Chem.*, 20 (**2010**) 844.

[7] Y. Sakamoto, M. Kaneda, O. Terasaki, D.Y. Zhao, J.M. Kim, G. Stucky, H.J. Shim, R. Ryoo, Direct imaging of the pores and cages of three-dimensional mesoporous materials, *Nature*, 408 (**2000**) 449-453.

[8] M.W. Anderson, T. Ohsuna, Y. Sakamoto, Z. Liu, A. Carlsson, O. Terasaki, Modern microscopy methods for the structural study of porous materials, *Chem. Commun.*, (**2004**) 907-916.

[9] A. Mayoral, T. Carey, P.A. Anderson, A. Lubk, I. Diaz, Atomic Resolution Analysis of Silver Ion-Exchanged Zeolite A, *Angew.Chem. Int. Ed.*, 50 (**2011**) 11230-11233.

[10] E. Serra, A. Mayoral, Y. Sakamoto, R.M. Blanco, I. Diaz, Immobilization of lipase in ordered mesoporous materials: Effect of textural and structural parameters, *Microporous Mesoporous Mater.*, 114 (**2008**) 201-213.

[11] E. Serra, E. Diez, I. Diaz, R.M. Blanco, A comparative study of periodic mesoporous organosilica and different hydrophobic mesoporous silicas for lipase immobilization, *Microporous Mesoporous Mater.*, 132 (**2010**) 487-493.

[12] V. Gascón, I. Díaz, R.M. Blanco, C. Márquez-Alvarez, Hybrid periodic mesoporous organosilica designed to improve properties of immobilized enzymes, *RCS Adv.*, 4 (**2014**) 34356-34368.

[13] J. Uppenberg, M.T. Hansen, S. Patkar, T.A. Jones, The sequence, crystal structure determination and refinement of two crystal forms of lipase B from Candida antarctica, *Structure*, 2 (**1994**) 293-308.

[14] M.M. Bradford, A rapid and sensitive method for the quantitation of microgram quantities of protein utilizing the principle of protein-dye binding, *Anal. Biochem.*, 72 (**1976**) 248-254.

[15] R.M. Blanco, P. Terreros, N. Munoz, E. Serra, Ethanol improves lipase immobilization on a hydrophobic support, *J. Mol. Catal. B: Enzym.*, 47 (**2007**) 13-20.

[16] Y. Han, S.S. Lee, J.Y. Ying, Pressure-Driven Enzyme Entrapment in Siliceous Mesocellular Foam, *Chem. Mater.*, 18 (**2006**) 643-649.

[17] N. Duran, M.A. Rosa, A. D'Annibale, L. Gianfreda, Applications of laccases and tyrosinases (phenoloxidases) immobilized on different supports: a review, *Enzyme Microb. Technol.*, 31 (**2002**) 907-931.

[18] V. Gascón, C. Márquez-Álvarez, R.M. Blanco, Efficient retention of laccase by non-covalent immobilization on amino-functionalized ordered mesoporous silica, *Appl. Catal. A-Gen.*, 482 (**2014**) 116-126.

[19] F. Hoffmann, M. Cornelius, J. Morell, M. Froeba, Silica-based mesoporous organic-inorganic hybrid materials, *Angew. Chem. Int. Ed.*, 45 (**2006**) 3216-3251.

[20] C. Jeanguillaume, C. Colliex, Spectrum-image - The next step in EELS digital acquisition and processing, *Ultramicroscopy*, 28 (**1989**) 252-257.

[21] R. Arenal, F. de la Pena, O. Stephan, M. Walls, M. Tence, A. Loiseau, C. Colliex, Extending the analysis of EELS spectrum-imaging data, from elemental to bond mapping in complex nanostructures, *Ultramicroscopy*, 109 (**2008**) 32-38.

[22] C.F. Blanford, C.B. Carter, Electron radiation damage of MCM-41 and related materials, *Microsc. Microanal.*, 9 (**2003**) 245-263.

[23] O. Terasaki, T. Ohsuna, V. Alfredsson, J.O. Bovin, D. Watanabe, K. Tsuno, The study of zeolites by HVHREM, *Ultramicroscopy*, 39 (**1991**) 238-246.

[24] R. Csencsits, R. Gronsky, Damage of zeolite-Y in the TEM and its effects on TEM images, *Ultramicroscopy*, 23 (**1987**) 421-431.

a. Dr. A. Mayoral. Laboratorio de Microscopias Avanzadas, Instituto de Nanociencia de Aragon. Universidad de Zaragoza. Edificio I+D, Mariano Esquillor, 50018, Zaragoza, Spain.

b. Dr. Raul Arenal. Fundacion Araid, 50004, Zaragoza, Spain

c. V. Gascón, Dr. C. Márquez-Álvarez, Dra. R. M. Blanco, Dra. I. Diaz. Instituto de Catálisis y Petroleoquímica. ICP-CSIC. C/ Marie Curie 2, 28049 Madrid, Spain.

CAPÍTULO 5

Location of laccase in ordered mesoporous materials

Álvaro Mayoral[a], **Victoria Gascón**[b], Rosa M. Blanco[b], Carlos Márquez-Álvarez[b] and Isabel Díaz[b]

Accepted in *APL Materials*, 2014

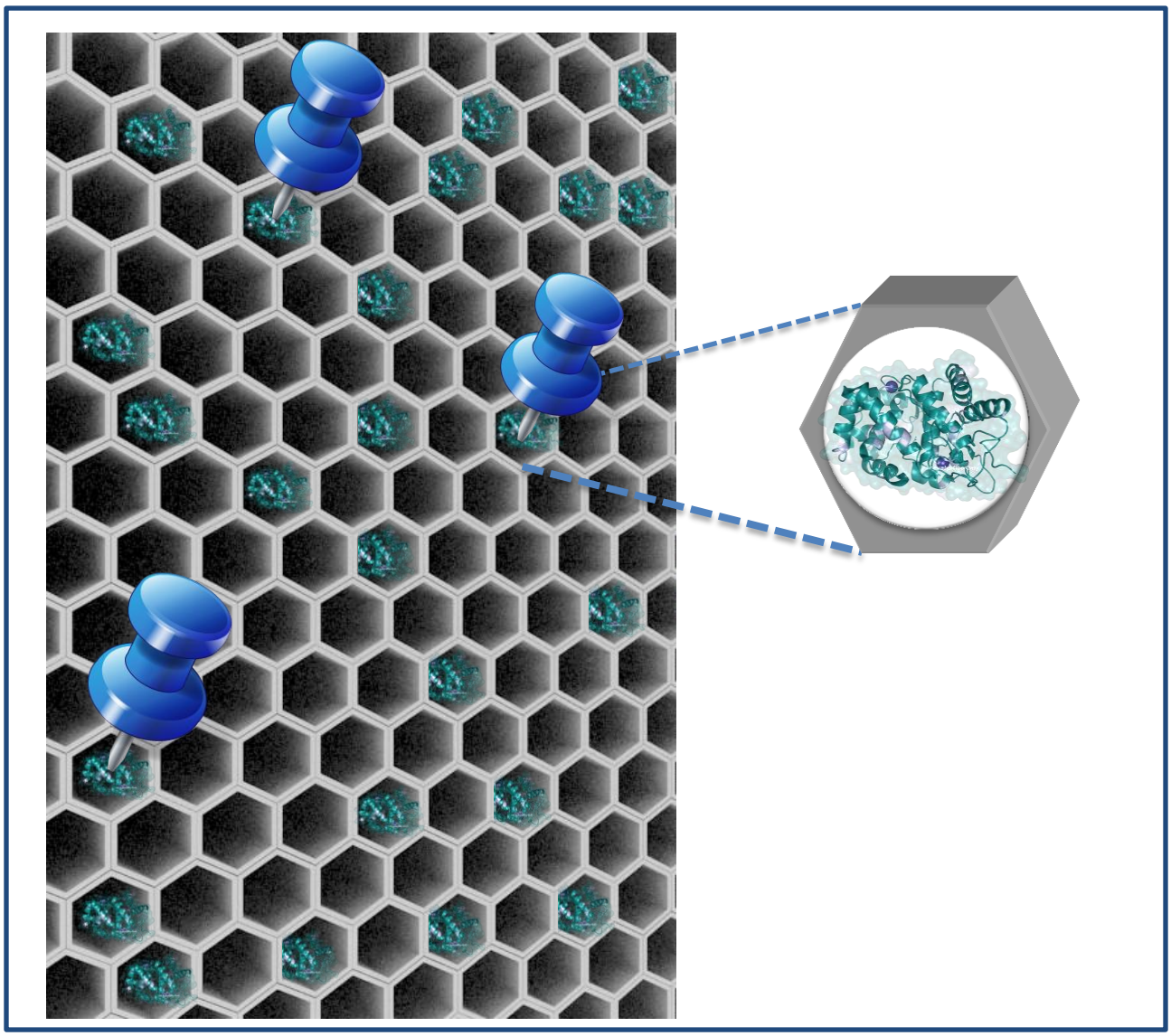

ABSTRACT

Laccase (from *Myceliphthora thermophila*) has an interesting potential applicability in the area of bioremediation (waste water treatment) as well as in many other fields. This protein has an isoelectric point rather low (pI=4). Therefore the useful pH range of immobilization via electrostatic interaction is very narrow (around 3.0-3.5) and close to the isoelectric points of both support and enzyme. The introduction of positive charges on the surface of the ordered mesoporous materials at a pH value high enough to ensure deprotonation of carboxylic groups on the surface of the enzyme would be the way to favor the interactions. Therefore, the functionalization with amine groups was developed on the SBA-15, and its effect in the enzyme immobilization is compared with that of a Periodic Mesoporous Aminosilica (PMA). Finally, a method to encapsulate the laccase *in situ* has been developed. The presence of butylamine in the gel is expected to protect the enzyme that would be surrounded by surfactant, and thus by silica in a "bottle around the ship" approach. In the current manuscript, spherical aberration (Cs) corrected scanning transmission electron microscopy (STEM) combined with a high angle annular dark field detector (HAADF) and electron energy loss spectroscopy (EELS) were employed for the location and the structural determination of the enzyme in the mentioned mesoporous solids.

1. INTRODUCTION

Mesoporous silica materials have received significant attention arising from the high surface areas together with the ability to encapsulate enzymes within the pores to provide a more stable environment in comparison to that at a soluble enzyme [1-3]. The advantage of using porous supports for immobilization of enzymes is evident, the large internal surface area can provide a safe haven for the enzyme [4, 5]. Implicit in this use is that the pore diameter must be sufficiently large to accommodate the enzyme [6, 7]. Recent progress has been achieved in the preparation of silica devices materials which can be used in enzyme nanoarchitectures with soft functions [8-10].

This work focusses on one particular type of enzyme, laccase from *Myceliophthora thermophila* (Figure 1).

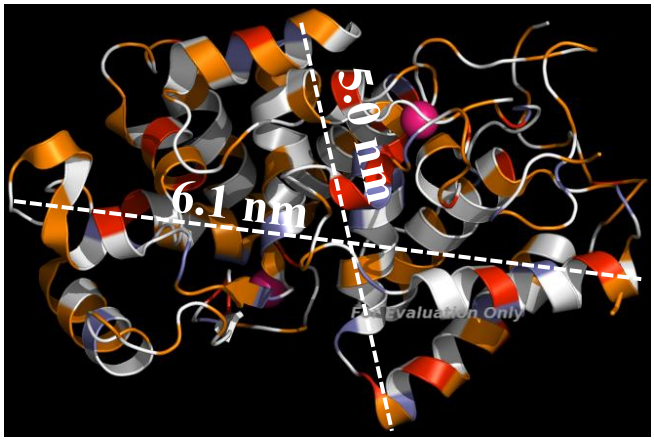

Figure. 1. Average dimensions of laccase measured in PyMOL (~6.1 nm × 5.0 nm × 4.9 nm).

Laccases are attractive biocatalysts for manufacturing pharmaceutical intermediates, specialty chemicals, and for bioremediation [11-20]. They exhibit excellent catalytic activity even with water-insoluble substrates such as lignin. One of the most important aspects of using these enzymes is the sensitivity to phenolic compounds that are considered very toxic [21-23]. In these reactions the oxygen is reduced directly to water without the intermediate formation of toxic hydrogen peroxide. In this direction, the immobilization of laccase in OMM provides the optimal control of the stabilization of the enzyme towards different media.

So far in our group we have successfully immobilized laccase in ordered mesoporous materials such as SBA-15 [24] via grafting approach and PMA [25]. Enzyme encapsulation is an attractive method among the different immobilization strategies to improve the reusability and stability of enzymes; however, current encapsulation methods have limitations including enzyme leakage. Silica based sol-gel encapsulation is the most used technique for enzyme encapsulation without the need of surfactants. OMM, which are prepared using surfactants, can provide a high specific surface area, controllable pore diameter, ordered porous network and large pore volume. Many of the classical OMM are formed using acidic pH, high temperature processes and hydrothermal synthesis reaction, which are severe conditions and are not compatible with the presence of enzymes. The goal in this work is to encapsulate laccase into a shell structure, with the silica shell serving as a robust and stable encapsulation layer to protect the enzymes where the encapsulated enzymes are physically confined inside the siliceous material. Until recently, it was impossible to corroborate the presence of the enzyme within the pores, only indirect method such as comparisons of XRD patterns and or pore volume before and after adsorption were applied [1, 3]. Evidences for the encapsulation of an enzyme in the pores of mesoporous silica were obtained in our group by combining spherical aberration (C_s) corrected scanning transmission electron microscopy (STEM) with a high angle annular dark field detector (HAADF) and electron energy loss spectroscopy (EELS) to show that lipase and laccase were present inside the pores of the host [26, 27]. In this work the presence of individual molecules of laccase within the pores could be directly observed.

The molecular weight estimated for the laccase is around 80 kDa, obtained from SDS-PAGE [28, 29] and the average molecular size was found to be approximately 6.1 nm high, 5.0 nm wide and 4.9 nm deep [29]. According to the modelling studies and the textural properties of the supports it is expected that the enzyme dimensions enable its adsorption inside the pores of OMM materials.

This protein has an isoelectric point rather low (pI 4). Hence, the useful pH range of immobilization via electrostatic interaction is very narrow (around 3.0-3.5) and close to the isoelectric points of both support and enzyme. Under these circumstances, the introduction of positive charges on the surface of the ordered mesoporous materials at a pH value high enough to ensure deprotonation of carboxylic groups on the surface of the enzyme would be

the way to favor the interactions. Therefore, the functionalization with amine groups was developed on the SBA-15 with extended pore aiming to increase the affinity between the enzyme and the support [24]. Figure 2, right side, shows a scheme of the functionalization process and location of the amino groups protruding the walls in SBA-15 and incorporated in the walls in PMA. Following, the materials are put in contact with the enzyme solution for immobilization via *grafting* method or *post-synthesis* approach. The large pores obtained with the use of micelle expanders allow introducing propylamine groups without compromising too much the dimensions of the channels (SBA-15-NH_2).

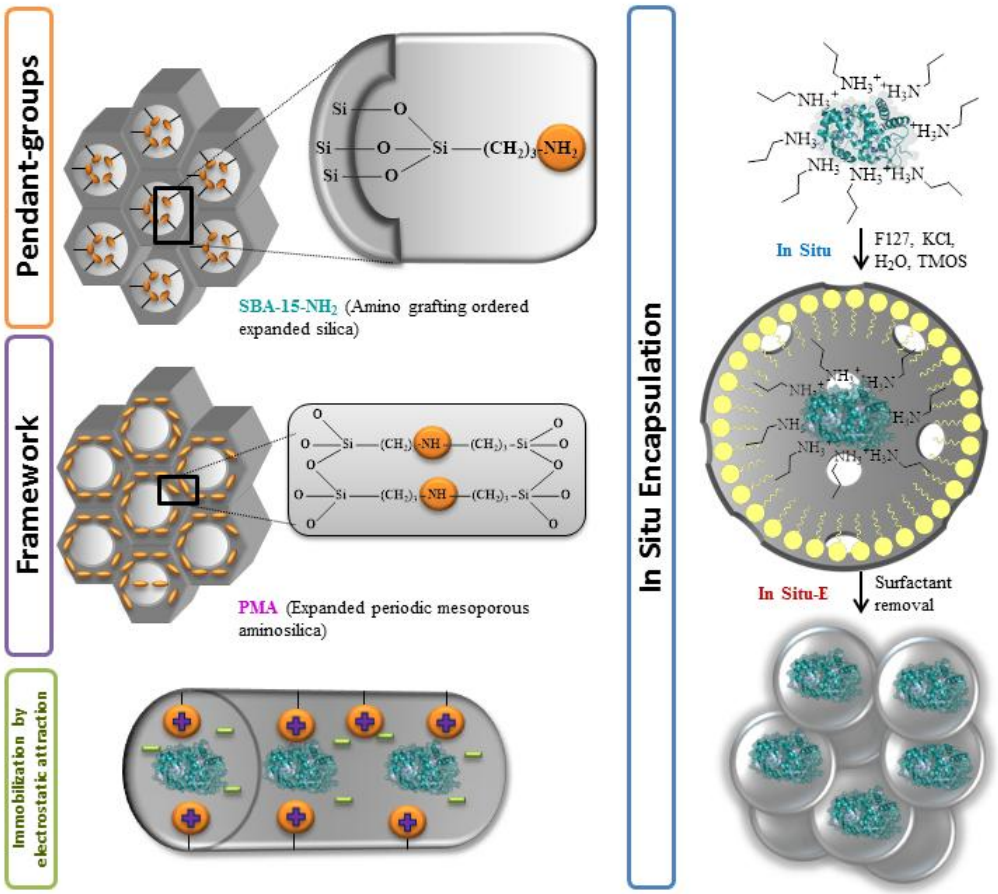

Figure. 2. Left: Incorporation of amine groups in SBA-15 and PMA materials and laccase immobilization post-synthesis. Right: Scheme of the in situ laccase encapsulation.

2. METHODOLOGY AND RESULTS

As seen in Table 1, the presence of amines (1.07 mmol N/g) leads to a significant increase in enzyme loading, as high as 170 mg/g. Following with our aim of designing an optimum ordered mesoporous material for the immobilization of laccase, a Periodic Mesoporous Aminosilica (PMA) was synthesized with the intention of increasing the affinity without decreasing the pore size [25]. Figure 3 shows the XRD patterns corresponding to *p*6*mm* symmetry in the case of SBA-15-NH_2 and PMA suggesting that the expanded-micelles method is also working for the PMA materials [24, 25]. Furthermore, the isotherms correspond to those of functionalized mesoporous materials with bulkier functional groups giving broader hysteresis loop due to a complex mechanism of adsorption and desorption given by a rougher surface. PMA sample shows a second step at higher relative pressure due to the small particle size obtained in this material leading to agglomerates as observed by SEM (*data not shown*). Nevertheless, the textural properties of the samples allow for immobilization of laccase (Table 1). Despite of its slightly smaller pore size (10.2 nm) the dimensions are still wide enough to allocate laccase molecules in the proper orientation. The concentration of N in PMA (0.58 mmol/g) is 54 % smaller than in SBA-15-NH_2, and the enzyme loading achieved is 52 % lower. The higher affinity of laccase for SBA-15-NH_2 can therefore be attributed to its higher N content. This leads again to the conclusion that the chemical affinity of the enzyme for the surface of the OMM is crucial to succeed in enzyme immobilization, when the pore size is at least large enough to let enzyme molecules fit inside.

Table 1. Textural properties, laccase immobilization and catalytic performance.

Material	$D_{p\ BJH}$ (nm)	S_{BET} (m^2/g)	V_p (cm^3/g)	Max. loading (mg/g)[a]	Biocatalyst activity (U/g)[b]	Catalytic Efficiency [c] (U/mg)
SBA-15-NH_2	11.2	339	1.0	170	50.7	0.30
PMA	10.4	264	0.6	88	29	0.33
In Situ	19.5	40	0.2	24.6	8.9	0.36
In Situ-E	20.8	465	1.1	24.6	3.6	0.15

[a] Maximum enzyme loading, expressed in milligrams of enzyme per gram of biocatalysts.
[b] Biocatalyst activity (Units/g biocatalysts) in ABTS test.
[c] Catalytic efficiency = Activity versus loading (Units/mg enzyme)

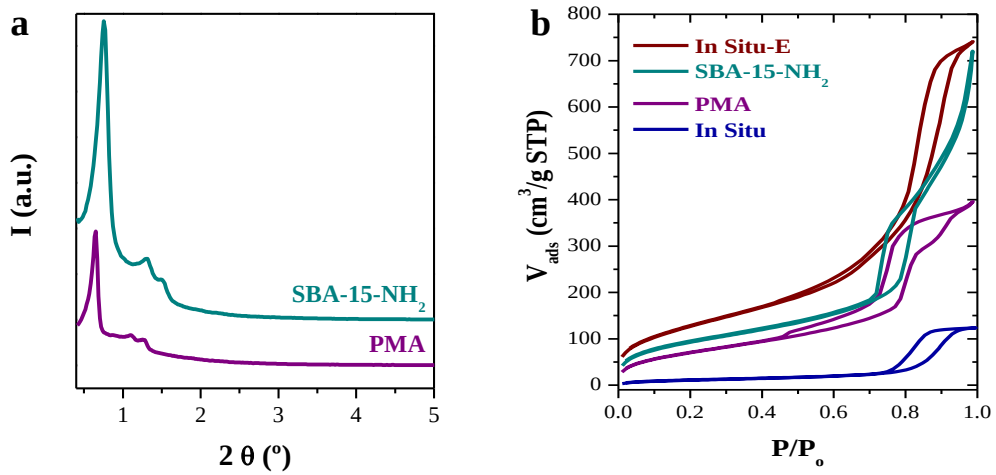

Figure. 3. a) Low angle XRD patterns of amino-functionalized silica supports; b) N_2 adsorption-desorption isotherms at -196 ºC.

On the other hand, the right hand side of Figure 2 shows an alternative path to encapsulate enzymes in ordered mesoporous materials [30], a novel route developed to provide the enzyme with hydrophobic moieties that may help to drive the encapsulation in only one step. At neutral pH carboxylic groups of laccase (with pI around 4) should be deprotonated, which in the presence of n-butylamine, it should interact through positively charged amino groups, so that the alkyl chains would be oriented outwards. In the end, the "protected" enzyme would be surrounded by surfactant, and thus by silica in a *bottle around the ship* approach. This synthesis, denoted as *in situ* (In Situ), was prepared using Pluronic F127 as template, tetramethoxysilane (TMOS) as silica source and mild conditions (neutral pH and 35 ºC). The capacity of these butyl chains on laccase surface to drive a correct arrangement of micelles to give rise to siliceous ordered structures is currently under study [31].

In the synthesis process, aliquots were taken at given times, and the laccase activity of the suspension and supernatant were determined spectrophotometrically towards the oxidation of 2,2′-Azino-bis(3-ethylbenzothiazoline-6-sulfonic acid) diammonium salt (ABTS). The activity of supernatant decreases as the enzyme molecules get encapsulated into the support. When the decrease in the activity reaches a minimum and constant value, it means that no more enzyme molecules can be immobilized. The suspension was then filtered off and washed. The solid sample was first dried under vacuum and then under nitrogen stream,

collected, weighted and finally stored at 4 ºC. Surfactant removal (In Situ-E for "extracted") was achieved by mild treatment with 10 % ethanol and acidic pH (3.5 in phosphoric acid solution).

The biocatalyst prepared in this manner, showed the maximum leaching of the laccase at 4 h and then remained constant proving that the remaining enzyme molecules are successfully encapsulated in the silica mesoporous material. The leaching observed before 4 h is probably due to the enzyme molecules loosely trapped in the material. As shown in Figure 4 and Table 1 only 10 % is lost in the leaching test. The biocatalyst activity and catalytic efficiency also decrease after the treatment for surfactant removal probably due to the above mentioned loss of active enzyme molecules. For the other two materials (PMA and SBA-15-NH_2) only 4 % of the enzyme is lost in the leaching test corroborating that the incorporation of amino groups enhances the affinity of the laccase for the mesoporous supports. Besides, in the case of the PMA, the pore size closer to the size of enzyme, results in a confinement effect that favors the versatility of this material as support. In summary, as observed from the data collected in Table 1, despite the lower loading of laccase in the In Situ material, it shows the highest catalytic efficiency regardless of the removal of the surfactant.

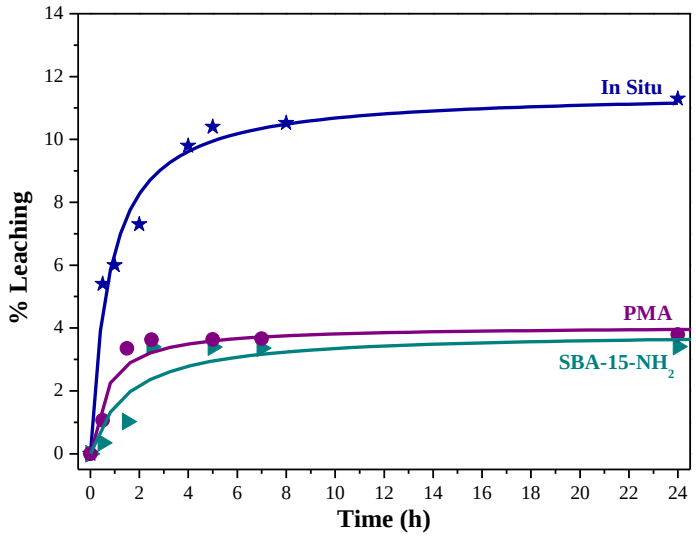

Figure 4. Leaching of enzyme from channel-like materials (SBA-15-NH_2 and PMA) and in situ mesoporous silica, expressed as percent of the initial enzyme loading leached as a function of time.

In order to corroborate the results discussed above, our aim in this work is to develop a reliable method to prove that the location of enzymes is actually inside the pores. The only direct and the most complete method for the characterization of mesoporous solids has been based on high-resolution transmission electron microscopy [32] combined with electron crystallography [33] which have allowed solving all kinds of structures, giving a complete image not only of the pore distribution but also the pore connectivity. When the subjects of interest are guest materials, scanning transmission electron microscopy (STEM) combined a HAADF detector is more suitable as the contrast is related to the atomic number Z. In the current manuscript C_s-corrected STEM-HAADF combined with electron energy loss spectroscopy (EELS) were the solely methods for the location and the structural determination of the enzyme and mesoporous solids. A FEI X-FEG Titan 60-300 kV, operated at 80 kV, equipped with a monochromator (not excited for the current experiments), a CEOS C_s-probe corrector (allowing forming an electron probe of 0.12 nm mean size at 80 kV) and a Gatan Energy Filter Tridiem 866 ERS was used for the experiments. The geometric aberrations of the probe-forming system were controlled to allow a beam convergence of 24.9 mrad half-angle to be selected. The alignment of the microscope at 80 kV was verified through the CETCOR software. A focus/tilt tableau was acquired measuring defocus and two-fold astigmatism as a function of both radial and azimuthal tilt angles. Concerning the EELS measurements, the collection semi-angle was of ~100 mrad, the energy resolution ~ 1.2 eV and the data were collected using the spectrum-imaging mode.

Figure 5 a shows an image of the pore system in the PMA-laccase system in which a spectrum image collection analysis was performed inside one of the pores (green square) analyzing 8 × 6 pixels with an exposure time of 2.5 seconds per pixel. The extracted spectrum profile (raw data), Figure 5 b, exhibits the O-K and N-K edges corresponding to the enzyme [26]. The nitrogen map, extracted from the spectrum-image collected from the green rectangle in Figure 5 c is also presented, using a pixel time of 1.5 seconds in an image formed by 26 × 26 pixels. In light blue the correspondent N map is shown. As a consequence of the amino functionalization N was detected in the framework and in certain pores, evidencing that some pores where not filled with laccase or that its content was too low to be detected. A relatively strong electron beam was necessary in order to gain enough counts to

identify the species. The total dose was 0.48 e/A^{2}s which stayed on each pixel during the data collection.

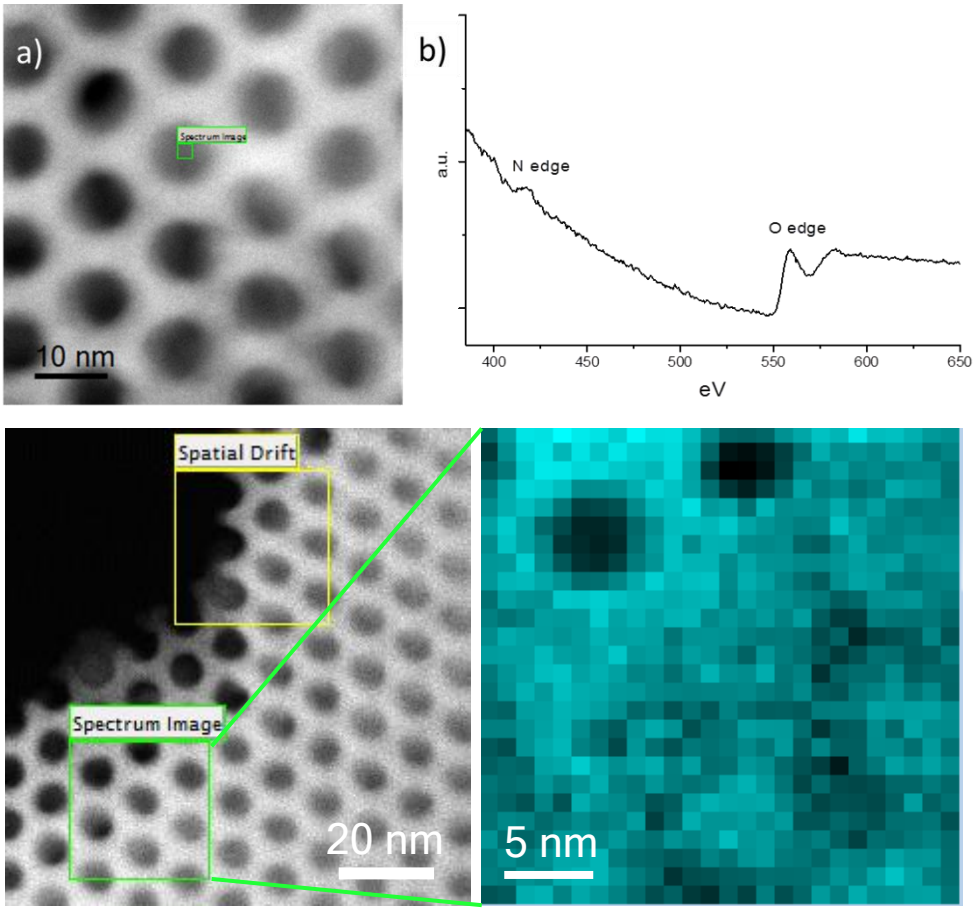

Figure 5. a) C_s-corrected STEM-HAADF image of the pore system. The green rectangle represents the area in which the EELS analysis was performed. b) EELS profile collected from image b, showing the N-K and O-K edges that confirm the presence of laccase. c) C_s-corrected STEM-HAADF image showing the hexagonal pore arrangement, the green square denoted as spectrum image corresponds to the area of analysis; the correspondent extracted N signal (blue color) is also displayed. Figure adapted from reference 26.

In the case of the material prepared *in situ* (In Situ-E-laccase), the presence of butylamine together with the surfactant yielded to a cage-type of materials although no ordered structure could be identified (Figure 6 a). Nevertheless, the presence of enzymes inside the cages was proven by the N and C content [27]. Figure 6 b shows the C_s-corrected HAADF image of certain pores, taken at 80 kV, where the spectrum image was acquired. The compositional map formed by Si-L_1 signal in green and N-K signal in red corroborates the presence of the

enzyme in some of these cavities (Figure 6 c). The EEL spectrum is depicted in Figure 6 d, after background subtraction, proving the presence of all elements coming from the mesoporous silica and the enzyme.

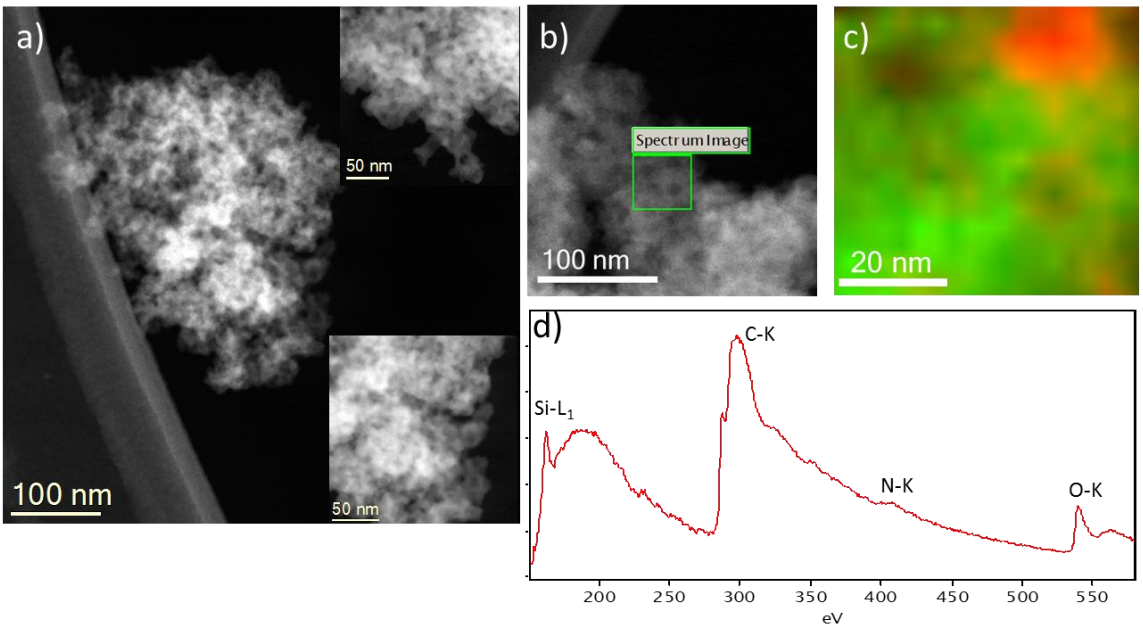

Figure 6. a) Cs-corrected STEM-HAADF images of the IS-laccase, a closer observation of the pores is shown inset. b) Area of EELS analysis, green rectangle. c) EELS compositional map, formed by Si (green) and N (red). d) EEL spectrum profile of the area analyzed.

3. CONCLUSION

In summary, current studies in our laboratory prove the feasibility of designing functionalized ordered mesoporous materials for enzyme immobilization. A rational design of the synthesis conditions, surface properties, pore size and connectivity of ordered mesoporous material is nowadays straightforward. Furthermore Cs corrected STEM microscopy simultaneously combined with EELS analysis allows imaging the functionalities of the mesopores of silica structures with ultra-high resolution and to unambiguously determine the presence of enzyme molecules inside the mesopores of the hybrid biocatalysts.

4. REFERENCES

[1] E. Magner, Immobilisation of enzymes on mesoporous silicate materials, *Chem. Soc. Rev.*, 42 (**2013**) 6213-6222.

[2] Z. Zhou, M. Hartmann, Progress in enzyme immobilization in ordered mesoporous materials and related applications, *Chem. Soc. Rev.*, 42 (**2013**) 3894-3912.

[3] N. Carlsson, H. Gustafsson, C. Thorn, L. Olsson, K. Holmberg, B. Akerman, Enzymes immobilized in mesoporous silica: A physical-chemical perspective, *Adv. Colloid Interface Sci.*, 205 (**2014**) 339-360.

[4] R.A. Sheldon, Enzyme immobilization: The quest for optimum performance, *Adv. Synth. Catal.*, 349 (**2007**) 1289-1307.

[5] R.A. Sheldon, S. van Pelt, Enzyme immobilisation in biocatalysis: why, what and how, *Chem. Soc. Rev.*, 42 (**2013**) 6223-6235.

[6] L. Bayne, R.V. Ulijn, P.J. Halling, Effect of pore size on the performance of immobilised enzymes, *Chem. Soc. Rev.*, 42 (**2013**) 9000-9010.

[7] M. Hartmann, X. Kostrov, Immobilization of enzymes on porous silicas--benefits and challenges, *Chem. Soc. Rev.*, 42 (**2013**) 6277-6289.

[8] K. Ariga, A. Vinu, Y. Yamauchi, Q. Ji, J.P. Hill, Nanoarchitectonics for Mesoporous Materials, *Bull. Chem. Soc. Jpn.*, 85 (**2012**) 1-32.

[9] K. Ariga, Q. Ji, T. Mori, M. Naito, Y. Yamauchi, H. Abe, J.P. Hill, Enzyme nanoarchitectonics: organization and device application, *Chem. Soc. Rev.*, 42 (**2013**) 6322-6345.

[10] K. Ariga, Y. Yamauchi, G. Rydzek, Q. Ji, Y. Yonamine, K.C.W. Wu, J.P. Hill, Layer-by-layer Nanoarchitectonics: Invention, Innovation, and Evolution, *Chem. Lett.*, 43 (**2014**) 36-68.

[11] N. Duran, M.A. Rosa, A. D'Annibale, L. Gianfreda, Applications of laccases and tyrosinases (phenoloxidases) immobilized on different supports: a review, *Enzyme Microb. Technol.*, 31 (**2002**) 907-931.

[12] A.M. Mayer, R.C. Staples, Laccase: new functions for an old enzyme, *Phytochem. Rev.*, 60 (**2002**) 551-565.

[13] R.C. Minussi, G.M. Pastore, N. Duran, Potential applications of laccase in the food industry, *Trends Food Sci. Tech.*, 13 (**2002**) 205-216.

[14] P. Baldrian, Fungal laccases - occurrence and properties, *FEMS Microbiol. Rev.*, 30 (**2006**) 215-242.

[15] S. Riva, Laccases: blue enzymes for green chemistry, *Trends Biotechnol.*, 24 (**2006**) 219-226.

[16] S. Rodriguez Couto, J.L. Toca Herrera, Industrial and biotechnological applications of laccases: a review, *Biotechnol Adv*, 24 (**2006**) 500-513.

[17] O.V. Morozova, G.P. Shumakovich, S.V. Shleev, Y.I. Yaropolov, Laccase-mediator systems and their applications: A review, *Appl. Biochem. Microbiol.*, 43 (**2007**) 523-535.

[18] A. Kunamneni, F.J. Plou, A. Ballesteros, M. Alcalde, Laccases and their applications: a patent review, *Recent Pat. Biotechnol.*, 2 (**2008**) 10-24.

[19] K. Brijwani, A. Rigdon, P.V. Vadlani, Fungal laccases: production, function, and applications in food processing, *Enzyme Res.*, 2010 (**2010**) 149748.

[20] J.F. Osma, J.L. Toca-Herrera, S. Rodriguez-Couto, Uses of laccases in the food industry, *Enzyme Res.*, 2010 (**2010**) 1-8.

[21] Y. Li, G. Jiang, J. Niu, Y. Wang, L. Hu, Laccase-Catalyzed Oxidation of Organic Pollutants in Water, *PROG CHEM*, 21 (**2009**) 2028-2036.

[22] A. Salis, M. Pisano, M. Monduzzi, V. Solinas, E. Sanjust, Laccase from Pleurotus sajor-caju on functionalised SBA-15 mesoporous silica: Immobilisation and use for the oxidation of phenolic compounds, *J. Mol. Catal. B: Enzym.*, 58 (**2009**) 175-180.

[23] J.-R. Jeon, P. Baldrian, K. Murugesan, Y.-S. Chang, Laccase-catalysed oxidations of naturally occurring phenols: from in vivo biosynthetic pathways to green synthetic applications, *Microbial Biotech.*, 5 (**2012**) 318-332.

[24] V. Gascón, C. Márquez-Álvarez, R.M. Blanco, Efficient retention of laccase by non-covalent immobilization on amino-functionalized ordered mesoporous silica, *Appl. Catal. A-Gen.*, 482 (**2014**) 116-126.

[25] V. Gascón, I. Díaz, R.M. Blanco, C. Márquez-Alvarez, Hybrid periodic mesoporous organosilica designed to improve properties of immobilized enzymes, *RCS Adv.*, 4 (**2014**) 34356-34368.

[26] A. Mayoral, R. Arenal, V. Gascon, C. Marquez-Alvarez, R.M. Blanco, I. Diaz, Designing Functionalized Mesoporous Materials for Enzyme Immobilization: Locating Enzymes by Using Advanced TEM Techniques, *ChemCatChem*, 5 (**2013**) 903-909.

[27] A. Mayoral, R.M. Blanco, I. Diaz, Location of enzyme in lipase-SBA-12 hybrid biocatalyst, *J. Mol. Catal. B: Enzym.*, 90 (**2013**) 23-25.

[28] R.M. Berka, P. Schneider, E.J. Golightly, S.H. Brown, M. Madden, K.M. Brown, T. Halkier, K. Mondorf, F. Xu, Characterization of the gene encoding an extracellular laccase of Myceliophthora thermophila and analysis of the recombinant enzyme expressed in Aspergillus oryzae, *Appl. Environ. Microbiol.*, 63 (**1997**) 3151-3157.

[29] V. Gascón, I. Díaz, C. Márquez-Alvarez, R.M. Blanco, Mesoporous silica with tunable morphology for the immobilization of lacase, *Molecules*, 19 (**2014**) 7057-7071.

[30] S. Urrego, E. Serra, V. Alfredsson, R.M. Blanco, I. Díaz, Bottle-around-the-ship: A method to encapsulate enzymes in ordered mesoporous materials, *Microporous Mesoporous Mater.*, 129 (**2010**) 173-178.

[31] V. Gascón, C. Márquez-Álvarez, R.M. Blanco, In-Situ encapsulation of laccase and β-glucosidase in mesoporous silicas, *Paper under preparation*, (**2014**).

[32] Y. Sakamoto, M. Kaneda, O. Terasaki, D.Y. Zhao, J.M. Kim, G. Stucky, H.J. Shim, R. Ryoo, Direct imaging of the pores and cages of three-dimensional mesoporous materials, *Nature*, 408 (**2000**) 449-453.

[33] M.W. Anderson, T. Ohsuna, Y. Sakamoto, Z. Liu, A. Carlsson, O. Terasaki, Modern microscopy methods for the structural study of porous materials, *Chem. Commun. (Camb)*, (**2004**) 907-916.

a. Dr. A. Mayoral. Laboratorio de Microscopias Avanzadas, Instituto de Nanociencia de Aragon. Universidad de Zaragoza. Edificio I+D, Mariano Esquillor, 50018, Zaragoza, Spain.

b. V. Gascón, Dr. C. Márquez-Álvarez, Dra. R. M. Blanco, Dra. I. Diaz. Instituto de Catálisis y Petroleoquímica. ICP-CSIC. C/ Marie Curie 2, 28049 Madrid, Spain.

RESUMEN DE RESULTADOS

4. RESUMEN DE RESULTADOS

4.1. Antecedentes

Las enzimas poseen características de gran interés para su aplicación en catálisis. Destaca que son muy activas en condiciones suaves, con el consiguiente ahorro energético. Además, se pueden aprovechar sus propiedades intrínsecas como son la gran especificidad de sustrato, lo que hace reducir los productos secundarios indeseables. Sin embargo, son muy inestables si se utilizan de forma soluble, por ello, se requiere su inmovilización en un soporte adecuado que preserve sus propiedades. Entre las ventajas que presenta la inmovilización de enzimas, cabe destacar el aumento de la estabilidad de la misma: mediante una técnica de inmovilización apropiada se consigue que la enzima se encuentre unida a un soporte evitando que su estructura se desnaturalice y se inactive. Además, debido a su carácter insoluble, los biocatalizadores heterogéneos pueden recuperarse y separarse fácilmente de los productos de reacción. Sin embargo, a pesar de las claras ventajas que presentan, el empleo de estos biocatalizadores muestra limitaciones como son la disminución de actividad en condiciones extremas de pH, presencia de disolventes orgánicos y temperatura, o la liberación de la enzima por lixiviado. Para solventar estos problemas se requiere un diseño adecuado del soporte.

La inmovilización de enzimas en materiales mesoporosos ordenados (MMO) en un campo de investigación de gran interés, que enlaza la catálisis inorgánica y la biológica, y se beneficia de la interacción multidisciplinar entre las dos áreas. Los MMO poseen varias características ventajosas frente a otros soportes convencionales, convirtiéndolos en soportes de enzimas potencialmente ideales. Desde los trabajos pioneros de Balkus y col en 1996, se han incorporado numerosos tipos de enzimas en los MMO con diferente éxito; tanto *post-síntesis* (es decir, mediante la síntesis previa de soporte y posterior inmovilización de la enzima), como *in-situ* o encapsulación de la enzima en el interior de la estructura durante la propia síntesis del material. Resultados previos logrados en el grupo de investigación en el que se ha realizado la presente Tesis Doctoral, mostraban biocatalizadores de lipasa activa tanto cuando se realizaba la inmovilización post-

síntesis como in-situ. Dichos resultados previos han llevado a una investigación más exhaustiva con otro tipo de enzimas como las estudiadas en la presente tesis doctoral: lacasa y B-glucosidasa, así como un estudio más profundo del comportamiento de lipasa en soportes de tipo PMO.

4.2. Hilo conductor

Esta Tesis Doctoral ha abordado el diseño de soportes silíceos mesoporosos ordenados para la inmovilización de enzimas, principalmente lacasa (EC 1.10.3.2., bencenodiol:oxígeno oxidorreductasas), una enzima oxidoreductasa que cataliza la oxidación de diversos compuestos, principalmente aromáticos, utilizando el oxígeno molecular como aceptor final de electrones, lo cual es de gran interés para la preparación de biocatalizadores activos con potenciales aplicaciones.

Siguiendo metodologías descritas en bibliografía se han sintetizado con éxito dos soportes mesoporosos puramente silíceos con simetría hexagonal plana tipo SBA-15, con alta superficie específica, diámetros de poro similares al de la enzima lacasa y con diferente tamaño y morfología de partícula (**Capítulo 1**). Estos soportes se han utilizado para inmovilizar lacasa que interacciona de forma iónica con los grupos siloxano superficiales (Si-O-) mediante fuerzas electrostáticas atractivas a un determinado valor de pH.

En cuanto a las condiciones de inmovilización, se observó que a un pH de 3,5 queda anclada en el soporte SBA-15-L con un diámetro de poro de 7,8 nm, el 63 % de la proteína ofrecida y el 77 % para SBA-15-S (D_p = 6,4 nm). Las conclusiones que se desprenden es que a pesar de que estos materiales poseen alta superficie específica (≈ 600 m^2/g), el similar tamaño de poro de los materiales y la enzima genera posiblemente problemas difusionales de la enzima que dificultan la mayor carga inmovilizada. Aun así, la morfología de SBA-15 juega un papel significativo en la eficiencia del proceso de inmovilización de enzimas. El soporte SBA-15-S con un sistema de canales de poros de menor longitud ha demostrado ser más eficiente en cuanto a carga enzimática y actividad específica que la SBA-15-L, con canales más largos. Probablemente se deba a que se generan menores problemas difusionales de la enzima para acceder a las

cavidades del poro, lo que también se corrobora por la mayor actividad específica de la enzima, probablemente también porque el acceso de los sustratos al biocatalizador y la difusión de los productos hacia el medio externo sea más fácil, sin embargo, se produce una mayor retención de la enzima (o menor lixiviado) en el biocatalizador de canales más largos.

Asimismo, se ha funcionalizado con éxito un material puramente silíceo mesoporoso, MS-3030, que carece de una estructura de poros ordenada y presenta una distribución de tamaño de poro amplia, que incorpora grupos aminopropilo anclados covalentemente a la superficie mediante el método de anclaje. El mayor tamaño de poro de este material, MS-3030-N, permite la presencia de los grupos orgánicos sin que se resienta el acceso a la enzima, presentado un mayor diámetro de poro que los soportes de tipo SBA-15, aunque menor superficie específica. Este material funcionalizado se ha empleado para inmovilizar a la enzima lacasa mediante interacciones electrostáticas con los grupos amino superficiales, a valores de pH entre los puntos isoeléctricos de la enzima y del soporte. La interacción con estos grupos no sólo funciona para inmovilizar la enzima, sino también para limitar su desorción o lixiviado.

En cuanto a las condiciones de inmovilización, se observó que el pH al que mejor se inmoviliza la lacasa en este material es a pH 5,5 debido a los diferentes puntos isoeléctricos de la enzima y el soporte a este pH con cargas opuestas, quedando anclada en el soporte el 99,3 % de la proteína ofrecida tras 3 horas de inmovilización. Este material presenta la combinación óptima de química superficial y tamaño de poro, dándose el proceso de adsorción de la enzima de forma rápida y sencilla. Siendo la máxima capacidad de adsorción de lacasa de 200 mg/g.

Las conclusiones que derivaron de este trabajo llevaron a pensar en la necesidad de sintetizar materiales mesoporosos ordenados de mayor diámetro de poro, que permitieran la incorporación de grupos amino sin comprometer el tamaño de poro adecuado para la inmovilización de la enzima lacasa (**Capítulo 2**), de esta manera se emplearon agentes expansores de micelas (TIPB), sales (NH_4F) y bajas temperaturas durante la síntesis de los soportes para conseguir mayores diámetros de poro, y se incorporaron los grupos amino mediante el método de anclaje y el de cocondensación,

resultando en los materiales con estructura ordenada NGOES (D_p 11.2 nm, 1,2 mmol N/g SiO_2) y NCOES (D_p 17.6 nm, 1.5 mmol N/g SiO_2), respectivamente. Estos soportes tienen un diámetro de poro suficientemente amplio para inmovilizar a la enzima lacasa mediante interacciones electrostáticas. La buena conectividad de los poros permite una buena difusión de la enzima, y de los sustratos y productos. Así, se han obtenido biocatalizadores con altas cargas enzimáticas (~ 170 mg/g), altas actividades catalíticas (~ 50 U/g) y eficiencias catalíticas (0,30 U/mg en NGOES y 0,33 U/mg para NCOES). Además, y muy importante, al haber obtenido soportes con un tamaño de poro adaptado a las dimensiones moleculares de la enzima, y con alta afinidad química se consiguió que la enzima apenas lixiviara de los soportes (< 4 %), tras someterlos a condiciones que favorecen el lixiviado de la misma, a pesar de no existir una unión covalente entre la enzima y el soporte.

También el alto confinamiento de las moléculas de enzima dentro de los poros de estos materiales hace que se evite el desplegamiento de la estructura de la proteína lo que aumenta la estabilidad del biocatalizador en medio orgánico con respecto a la enzima libre.

Como resultado los biocatalizadores obtenidos de lacasa inmovilizada sobre NGOES y NCOES muestran propiedades prometedoras para futuras aplicaciones industriales en ciclos de reacción, lo que demuestra la importancia de un buen diseño del soporte. Incluso después de la inactivación de la enzima, la naturaleza no covalente del enlace también puede permitir la recuperación y reutilización de los soportes, con el consiguiente ahorro.

Se quiso llegar más allá en el diseño de los soportes y se diseñaron materiales híbridos orgánicos-inorgánicos donde el grupo orgánico forma parte de la propia pared de material (**Capítulo 3**). De esta manera, se desarrollaron soportes tanto para la inmovilización de lipasa, denominados PMO, donde el soporte incorpora grupos hidrófóbicos (grupos etileno) dentro de la propia pared que interaccionan con la superficie hidrofóbica de la enzima consiguiendo altas cargas de la enzima lipasa; como soportes para la enzima lacasa (PMA) que integran grupos amino en su estructura. Mediante un profundo estudio de las condiciones de síntesis se consiguió obtener un

novedoso material en el que los grupos amino se incorporan en la pared del soporte formando una red híbrida orgánica-inorgánica, y además, mediante el empleo de expansores de micelas, el diámetro de poro es suficiente para albergar y retener a la enzima lacasa en el interior de sus canales y prevenir su lixiviado hasta valores de pH inferiores de 14. Con estos materiales se han combinado las ventajas de un poro regular y de tamaño adecuado, con una composición química de la superficie del soporte que interacciona con la superficie de la enzima y, por tanto, influye favorablemente para alcanzar altos rendimientos de inmovilización. Mediante este estudio se ha demostrado de nuevo la importancia sobre la inmovilización de enzimas de los factores estudiados: tamaño de poro y química de la superficie.

Además, los biocatalizadores PMO-lipasa muestran propiedades específicas destacables, además de alta carga enzimática, alta actividad catalítica y alta eficiencia catalítica, como es la alta estabilidad que presentan frente a disolventes orgánicos. Esto es posible porque como se ha indicado estos materiales integran componentes orgánicos e inorgánicos en su estructura formando una red híbrida, de modo que el poro interacciona con las moléculas de enzima rodeándolas, creando un espacio restringido, y evitando su movilidad, su inactivación y el desplegamiento de la proteína. Si se someten estos biocatalizadores a un medio orgánico (metanol), al ser una pared híbrida orgánica-inorgánica el número de puntos de contacto con la enzima aumenta, y se establecen nuevas interacciones hidrófobicas adicionales, lo que explica la alta estabilidad de la enzima en presencia de metanol, que no se daría nunca sin la protección del soporte, ya la enzima libre sería prácticamente imposible de mantenerse activa en ese medio externo extremo.

En un intento de localizar directamente a la enzima dentro de las cavidades y canales del propio soporte se han utilizado técnicas de microscopía electrónica altamente novedosas (STEM-HAADF), y se ha conseguido algo nuevo en el campo de los biocatalizadores, y es la localización sin ambigüedades de la enzima en el interior de los poros del soporte (**Capítulo 4**). Este trabajo es muy novedoso en el campo de la inmovilización de enzimas en materiales mesoporosos ordenados, ya que hasta la fecha no se había conseguido detectar por métodos directos a la enzima dentro de los poros.

Utilizando la experiencia previa del grupo se han desarrollado biocatalizadores in-situ, en el que se sintetiza los materiales en presencia de la enzima. Para ello, se han utilizado condiciones de síntesis muy suaves para mantener la actividad de la enzima. Esta estrategia ha servido para obtener materiales no muy ordenados, ya que las condiciones de síntesis no son favorables al ordenamiento de la estructura, pero en el que se ha comprobado que la enzima está retenida y encapsulada de forma activa en su interior (**Capítulo 5**) mediante técnicas bioquímicas, de microscopía (STEM-HAADF), y en ensayos de actividad.

Además, los mejores biocatalizadores de lacasa se han utilizado en una reacción de oxidación de compuestos fenólicos presentes en vino, lo que abre una vía de aplicación prometedora. Para finalizar, se ha desarrollado una novedosa metodología in-situ para encapsular B-glucosidasa, una enzima de grandes dimensiones, en la que se han utilizado en presencia de la enzima y en el mismo medio de síntesis expansores de micelas. Esta metodología es altamente novedosa ya que permite retener físicamente a la enzima activa en su interior. Estos dos últimos trabajos están actualmente pendientes de publicar, por lo que no se han incluido en esta memoria que se presenta como compendio de publicaciones.

De forma global, se han diseñado y optimizado nuevos materiales silíceos mesoestructurados bioinorgánicos en los que se controla el tamaño de poro, la morfología de partícula y la funcionalización de la superficie para incorporar moléculas de enzima (lacasa, lipasa y β-glucosidasa) en su interior. Se han obtenido biocatalizadores con elevadas cargas enzimáticas, altas actividades y eficiencias catalíticas. El diámetro de poro diseñado a medida y la alta afinidad enzima-soporte producen alta retención de la enzima y un lixiviado mínimo. La inmovilización y/o encapsulación de la enzima protege de la inactivación frente a disolventes orgánicos y se mejora la estabilidad térmica. Por todo ello, estos biocatalizadores cumplen con los requisitos para ser utilizados industrialmente.

CONCLUSIONES

5. CONCLUSIONES

La presente Tesis Doctoral se ha desarrollado en un tema multidisciplinar que abarca los ámbitos de la Ciencia de Materiales y la Biocatálisis. Con el objeto de inmovilizar enzimas de diferentes características se han desarrollado materiales silíceos mesoporosos ordenados y materiales híbridos orgánico-silíceos diseñados a medida para cada enzima. Los resultados obtenidos han cumplido las expectativas planteadas al inicio de la Tesis. Se ha trabajado sobre las características del material: morfología de la partícula y tamaños de poro adaptados a las dimensiones de las enzimas. También sobre la afinidad química de la enzima por el material, sintetizando distintos materiales híbridos que contienen grupos orgánicos funcionales, bien por anclaje del grupo funcional, o por cocondensación, o bien sintetizando materiales híbridos organosilíceos periódicos mesoporosos (de tipo PMO) en los que el grupo funcional forma parte de la propia pared de soporte. También se han desarrollado estrategias para encapsular in-situ a las enzimas.

A continuación se describen brevemente las conclusiones más importantes conseguidas en cuanto a los resultados obtenidos en este trabajo.

El conjunto de propiedades tamaño de poro-afinidad química de estos soportes proporciona al **biocatalizador** (una vez inmovilizadas las enzimas) excelentes características:

- ✓ Elevada capacidad de carga, gracias a la alta superficie específica y a la adecuación del tamaño de poro que permite la difusión de las enzimas (lacasa y lipasa) y el aprovechamiento de la superficie interna de los poros; también está facilitada por la estructura ordenada de los poros, que favorece igualmente la difusión de la enzima. La afinidad química contribuye también a aumentar la carga, mientras que la naturaleza no covalente de las uniones permite cierta movilidad de las moléculas de enzima que favorece también un aumento de la carga; por el contrario si las uniones fueran covalentes, una molécula de enzima unida irreversiblemente a la superficie del soporte ejercería un efecto “tapón”, que impediría el acceso de nuevas moléculas al poro, limitando la capacidad de carga del soporte.

- ✓ Elevada actividad específica, gracias a la unión no covalente de la enzima (lacasa, lipasa, β-glucosidasa)-soporte, que no ejerce un efecto distorsionante sobre la estructura proteica.

- ✓ Minimización de las limitaciones difusionales en los biocatalizadores, gracias al pequeño tamaño de partícula y a la alta conectividad de los poros (facilitada por su estructura ordenada), que permite buena difusión de sustratos y productos.

- ✓ Eliminación del lixiviado a pesar de la naturaleza no covalente de la unión. Gracias al conjunto afinidad química-tamaño de poro ajustado a las dimensiones de la enzima (lacasa, lipasa y β-glucosidasa), las moléculas de enzima permanecen fuertemente retenidas en el interior de los poros, de modo prácticamente irreversible. En los PMA, la lacasa permanece en los poros incluso desnaturalizada, hasta valores de pH 14.

- ✓ Estabilidad frente a disolventes orgánicos, especialmente en los biocatalizadores de tipo PMO-lipasa y PMA-lacasa, donde la presencia de grupos hidrofóbicos del soporte refuerzan la estructura proteica de la enzima en presencia del medio orgánico, donde las cadenas laterales de aminoácidos hidrofóbicos se reorientan hacia el exterior de la molécula proteica.

- ✓ Se han obtenido por primera vez micrografías electrónicas de transmisión (STEM-HAADF) donde se puede observar directamente la presencia de la enzima (lacasa y lipasa) en el interior de los poros perfectamente ordenados de los materiales (PMO y PMA, respectivamente), y en las cavidades de los soportes de lacasa y β-glucosidasa sintetizados "*in situ*".

- ✓ También se han obtenido biocatalizadores "*in situ*", en los que el material ha sido sintetizado en presencia de la enzima, tras el estudio de las condiciones de síntesis compatibles con la actividad enzimática. Estos biocatalizadores de lacasa y β-glucosidasa presentan una estructura no totalmente ordenada, corresponden a MCF (*mesocellular foam*) y conservan altos valores de actividad catalítica.

- ✓ Todos los biocatalizadores de lacasa han sido evaluados en unos estudios preliminares sobre sus propiedades para catalizar la oxidación de polifenoles (ácido cafeico) presencia de 10 % de etanol, con el objetivo de evaluar su capacidad de actuar en mostos catalizando una oxidación controlada de polifenoles pudiendo evitar así una oxidación masiva, y limitando la adición de agentes químicos como sulfitos.